Andrey Khlystov

CLOUD FORMING PROPERTIES OF AMBIENT AEROSOL IN THE NETHERLANDS AND RESULTANT SHORTWAVE RADIATIVE FORCING OF CLIMATE

PROEFSCHRIFT

ter verkrijging van de graad van doctor
op gezag van de rector magnificus
van de Landbouwuniversiteit Wageningen
prof. dr. C.M. Karssen,
in het openbaar te verdedigen
op maandag 16 maart 1998
des namiddags te vier uur in de Aula

Promotor:	Dr. J. Slanina hoogleraar in de meetmethoden in atmospherisch onderzoek
Co-promotor:	Dr. H.M. ten Brink Energieonderzoek Centrum Nederland (ECN)

Stellingen behorende bij het proefschrift

"CLOUD FORMING PROPERTIES OF AMBIENT AEROSOL IN THE NETHERLANDS AND RESULTANT SHORTWAVE RADIATIVE FORCING OF CLIMATE"

A.Khlystov

1. The effective radius of cloud droplets deduced from satellite measurements should not be used to estimate the indirect aerosol forcing unless the liquid water content is simultaneously assessed.

2. A substantial effort has been made to characterize broken clouds. However it is over-optimistic to compare in-cloud measurements and satellite observations of reflective properties of such clouds.

3. The continuing use of instrumentation that has not been calibrated is a major impediment for aerosol research to be considered as a serious branch of science.

4. Contrary to common belief, considerable efforts are required to achieve a reasonable accuracy (of at least 20%) in measurement of aerosol number concentrations.

5. Due to the relatively low size resolution of cascade impactors it is always possible to fit the data to a multimodal distribution.

6. One should not use the observed changes in (global) temperature as proof that present climate models accurately predict the effects of anthropogenic pollution on the global climate.

7. The general misconception that nitrate is present only in super-micrometer aerosol particles appears to be very persistent.

8. Though the evaporation coefficient for ammonium nitrate is usually taken to be 0.04 [Harrison et al. (1990) *Atmos.Environ.*,

V24A, 1833-1888], increasing evidence suggests that it is close to unity [Bai et al. (1995) Atmos.Environ.,V29, 313-321; Khlystov et al. (1997) *J.Aerosol Sci.*, S59-S60].

9. Improved tests on the mobility of pollutants in soils indicate that much of the efforts, dedicated to clean up soils, have been at least partial waste of money and labor (Comans and Zevenbergen [1997] *ECN rapport nr. ECN-C--97-055*, pp.86).

10. Policy makers do not understand that, due to the complexity of the processes in which atmospheric aerosol is involved, measures to combat one environmental effect of aerosols may lead to an enhancement of other adverse effects.

11. Though a reasonable theoretical explanation can now be offered for the discrepancy between measured and predicted deposition velocities of sub-micrometer ambient aerosols (see Chapter 2 of this thesis), there is great reluctance to accept the measured values in transport models.

12. The much increased speed of personal computers has not speeded up the process of reporting scientific data, due to the persistent and malicious development of unnecessarily over-sophisticated software.

We gratefully acknowledge the financial support from the Dutch National Research Program on Global Air Pollution and Climate Change (NOP Project nr. 852066).

We are especially thankful for the substantial funding of this research by the department of Economic Affairs of the Netherlands, within Mefis-contract nr.53478.

We would also like to thank the European Union for the financial contribution within contract nr. EV-5V-CT92-0171 in the Climatology and Natural Hazards Program of the EC ENVIRONMENT Program 1991-1994.

Contents

Summary

This thesis discusses properties of ambient aerosols in the Netherlands which are controlling the magnitude of the local aerosol radiative forcing. Anthropogenic aerosols influence climate by changing the radiative transfer through the atmosphere via two effects, one is direct and a second is indirect. Due to the scattering of solar light on aerosol particles the Earth surface receives less radiation and thus cools, which is called the direct aerosol effect. The indirect effect includes processes by which aerosols influence the radiation balance indirectly - via clouds. The indirect effect includes mechanisms by which anthropogenic aerosol particles enhance the reflectivity and prolong the life time of marine stratoform clouds by increasing their droplet number concentration. Anthropogenic aerosols were demonstrated to have a considerable cooling effect on climate, comparable in magnitude to that of the greenhouse gases, but opposite in sign. However, calculation of the aerosol radiative forcing is much more complex than that for the green house gases. This results in high uncertainties in the estimates of the effects of anthropogenic aerosols on climate. Both types of the aerosol radiative forcing and their magnitude, as estimated by the Intergovernmental Panel on Climate Change (IPCC), are discussed in Chapter 1.

The aerosol radiative forcing is a regional phenomenon because of the limited life time of aerosols in the atmosphere. Thus, the aerosol effects should be assessed locally. In Chapter 2 chemical composition of local ambient aerosols in the size range relevant to the radiative forcing is discussed. It is shown that ammonium nitrate, which is omitted by the IPCC, is a major contributor to the direct, and perhaps to the indirect forcing. The contribution of this compound to the local direct forcing is equal to that of anthropogenic sulfate aerosols. Measurements of ammonium nitrate content in submicrometer aerosol

are subject to artifacts due to the volatility of this compound. Automated techniques which were developed for artifact-free measurements of chemical composition of ambient aerosols are described.

Aerosol particles composed of water-soluble salts increase their size at elevated relative humidities. The increase in size enhances light scattering by aerosol particles which in turn enhances the direct radiative forcing. Hygroscopic properties of aerosol particles also play a central role in cloud droplet formation and thus are also relevant for the indirect aerosol effect. Chapter 2 discusses the hygroscopic size changes and characteristic growth times. It is also demonstrated that hygroscopic growth may substantially enhance dry deposition of aerosol particles to forests.

According to the IPCC the indirect aerosol effect is the most uncertain factor in the anthropogenic perturbation of the climate, with an uncertainty of the same magnitude as the total radiative effect by the greenhouse gases. One of the major uncertainties in the indirect effect is the unknown relation between the concentration of anthropogenic aerosol particles and the increase in droplet number concentration in clouds. In Europe only few measurements of the relation between the number of particles and the number of cloud droplets have been performed. It should be also noted that those measurements were performed with instruments that did not span the full range of aerosol sizes that is relevant for cloud formation. For this reason, the major part of the thesis was devoted to an experimental assessment of the cloud forming properties of ambient aerosol in the Netherlands. The indirect effect as well as factors controlling cloud droplet formation are discussed in Chapter 3.

Chapter 4 describes the large flow-through cloud chamber in which cloud forming properties of ambient aerosol were studied. The advantage of a cloud chamber over in-situ measurements is the use of instrumentation which is too delicate for use in aircraft and the possibility to compare, simultaneously, the aerosol before and after cloud processing. The aerosol was characterized both in terms of its

number concentration and size as well as its chemical composition with the emphasis on the amount of soluble material. The unique feature of the cloud chamber is its reproducible stable low supersaturations (around 0.1%) common for marine clouds. Aerosol monitors were used that measure the concentration of particles in the full range of sizes relevant for cloud formation. The unique large size and the high throughput flow of the chamber allowed unperturbed use of conventional cloud instrumentation for sizing and counting of droplets. Also high-flow cascade impactors for chemical analysis of aerosol were used. The cloud chamber was calibrated with artificially generated ammonium sulfate aerosol. This aerosol was selected because in anthropogenically influenced air in Western Europe most particles should consist of this compound. Experiments were done at different total aerosol number concentrations to check its influence on the number of resulting cloud droplets. A sub-linear relation between the aerosol and the droplet number concentrations was observed. The results of the tests with the reference aerosol were used for the interpretation of experiments with ambient aerosols.

The cloud activation tests on ambient aerosol are discussed in Chapter 5. The cloud forming efficiency of the aerosols was assessed by comparing the number concentration of droplets formed in the cloud chamber with that found during the tests with the reference ammonium sulfate aerosol at the same number concentration. Similarly to the reference sulfate aerosol, a sub-linear relation between the aerosol and droplet number concentrations was observed. However, the deviation from a linear relation was stronger in the ambient aerosol. This suggested that about one third of the (anthropogenic) particles was water-insoluble. The measurements of the composition supported this hypothesis. This demonstrates the importance of hygroscopicity for cloud formation. It also shows that measurements of the solubility of (individual) particles should be done along with conventional measurements of aerosol size and number.

The results of experiments discussed in Chapter 5 were used for an estimate of the local indirect aerosol radiative effect (Chapter 6). The difference between the droplet number concentration in clean marine

air and the average droplet number concentration in polluted air was used to estimate the corresponding increase in cloud reflectivity which, in turn, was translated into local indirect aerosol effect. The data on the aerosol light scattering discussed in Chapter 2 are used to estimate the local direct radiative forcing. The estimated total (direct plus indirect) local aerosol radiative forcing is about 4 times higher than the forcing by the anthropogenic greenhouse gases but opposite in sign.

Samenvatting

Dit proefschrift behandelt de eigenschappen van buitenlucht aërosolen in Nederland, die voor de lokale aërosol forcering bepalend zijn. Antropogene aërosolen verminderen de transmissie van zonnestraling in de atmosfeer en oefenen zo een koelend effect uit op het klimaat. Dit effect wordt gewoonlijk opgedeeld in het "directe" en het "indirecte" aërosol-effect. De directe weerkaatsing van zonlicht heet het directe stralingseffect. Het indirecte effect omvat mechanismen waarbij aërosoldeeltjes de reflectie door wolken doen toenemen. De aërosol-forcering is ongeveer gelijk aan de forcering door de broeikas gassen, maar van tegengesteld teken is. Het effect van de aërosolen is veel complexer dan dat van de broeikasgassen, wat leidt tot een grote onzekerheid in het klimaateffect van aërosolen. Beide aërosol-effecten en zijn schatting door de Intergovernmental Panel on Climate Change (IPCC) worden bediscussieerd in Hoofdstuk 1.

Het aërosol-effect treedt op regionale schaal door de beperkte levensduur van de aërosolen in de atmosfeer. Door verschillen in aërosolkarakter kunnen resultaten buiten Europa slecht naar hier vertaald worden. Het aërosol-effect moet, dus, lokaal bepaald worden. Metingen van chemische samenstelling van lokaal buitenlucht aërosol worden gepresenteerd in Hoofdstuk 2. De IPCC neemt aan dat (ammonium) sulfaat de enige antropogene aërosol component is die verantwoordelijk is voor de klimaat forcering. Er wordt aangetoond dat ammonium nitraat een aanzienlijke bijdrage levert aan het directe en vellicht aan het indirecte aërosol effect. De bijdrage van ammonium nitraat aan de direct aërosol effect is ongeveer gelijk aan die van ammonium sulfaat. Metingen van vluchtige ammonium nitraat aërosol zijn gecompliceerd door artifacten. Geautomatiseerde instrumenten die zijn ontwikkeld voor metingen van buitenlucht aërosol zonder artifacts, worden beschreven in dit Hoofdstuk.

Aërosoldeeltjes met water-oplosbaar materiaal zijn hygroscopisch en trekken zelfs water aan bij lage relatieve vochtigheid en nemen daardoor toe in grootte. Deze groei maakt dat de aërosoldeeltjes sneller uit de atmosfeer verdwijnen en verder dat ze ook meer zonlicht weerkaatsen. Hygroscopiciteit is ook van grote belang voor de vorming van wolkendruppels en dus voor het indirecte aërosol-effect. Vandaar dat hygroscopiciteit een centrale aërosol-factor is. Hoofdstuk 2 beschrijft de fysisch-chemische principes van de interactie van waterdamp en hygroscopische deeltjes. Het effect van de hygroscopiciteit op deeltjesgrootte en de snelheid waarmee deeltjes groeien door wateropname worden behandeld. De rol van hygroscopiciteit op het directe aërosol-effect wordt ingeleid in dit Hoofdstuk. Aangegeven wordt ook hoe de aangroei de depositie van deeltjes in bossen versnelt.

Volgens de IPCC is het indirecte aërosol-effect de meest onzekere factor in de klimaat verandering. Eén van de grootste problemen in berekeningen van het effect is de relatie tussen de extra antropogene aërosoldeeltjes met de daaruit gevormde extra wolkendruppels. In Europa is slechts een beperkt aantal metingen uitgevoerd in wolken vanuit een meetvliegtuig, echter, met apparatuur waarmee niet alle aërosoldeeltjes konde worden gemeten. Daarom is in dit proefschrift speciale apparatuur gebuikt die dat wel kan. Er is aandacht gegeven aan een experimentele inschatting van de invloed van de mens op de regionale wolken, in concreto de marine wolken aan de kust van de Noordzee. Het indirecte effect en de factoren die het beënvloeden worden behandeld in Hoofdstuk 3.

Het onderzoek werd uitgevoerd in een unieke grote doorstroom wolkenkamer die in Hoofdstuk 4 wordt beschreven. Het voordeel van een wolkenkamer boven een meetvliegtuig is het feit dat de zeer kwetsbare apparatuur die nodig is voor meting van het volledige aërosolspectrum gebruikt kan worden. Verder werden twee identieke instrumenten ingezet die het deeltjesspectrum voor en na de wolkenkamer maten. De samenstelling van het aërosol, als functie van grootte-klasse werd gemeten, waarbij vooral werd onderzocht welk percentage hygroscopisch was. Het unieke van de kamer is de lage

oververzadiging die over een zeer lange periode stabiel is en die karakteristiek is voor de dunne marine wolken die worden nagebootst. De grootte van het systeem stond verder de inzet toe van monitoren waarmee wolkendruppels worden gemeten en instrumenten waarmee deeltjes in grootte-klassen worden gescheiden voor verdere chemische karakterisering (cascade-impactoren). Ammoniumsulfaat werd gebruikt voor het ijken van de wolkenkamer, omdat het vermoedelijk de meest voorkomende component is in de deeltjes die bij de wolkenvorming in West-Europa betrokken zijn. Experimenten werden uitgevoerd met verschillende aantallen om de relatie tussen het aantal deeltjes en het aantal gevormde wolkendruppels in de kamer te bepalen. Een niet-lineaire relatie tussen aantal deeltjes en aantal druppels werd gevonden. Deze resultaten dienden als referentie voor de tests met buitenlucht aërosol.

De experimenten met buitenlucht aërosol staan in Hoofdstuk 5. Het aantal wolkendruppels dat werd gevormd werd vergeleken met het aantal dat in de referentietests met dezelfde aantallen en grootte werd gevormd. Net zoals bij het referentie aërosol is er een niet-lineaire relatie tussen het aantal deeltjes dat in principe druppels moet vormen dienen en dat werkelijk wordt gevormd. De reden dat er minder wolkendruppels ontstonden was dezelfde als in de referentie tests. Het is het feit dat er onvoldoende water is om zoveel druppels te vormen. Maar de wolkenforming vermogen van buitenlucht aërosol was lager dan die van de referentie aërosol, omdat zo'n 30% van de antropogene deeltjes uit zo weinig hygroscopisch materiaal bestaat dat ze geen water aantrekken en daardoor niet als wolkenkern kunnen fungeren. Dit laat het belang zien van de meting van de samenstelling van de aërosolen.

De resultaten uit Hoofdstuk 5 zijn in Hoofdstuk 6 geëxtrapoleerd naar een schatting van het lokale indirecte aërosol-effect. Hierbij is het verschil in aantal druppels bij wind vanuit Engeland en vanaf de poolstreken toegeschreven aan de antropogene aërosolen. Met de daarvoor bestaande methode is het extra aantal druppels in toename van de reflectie vertaald. De gegevens uit Hoofdstuk 2 over lichtverstrooing door antropogeëne aërosolen werden gebruikt voor een

schatting van het lokale directe aërosol-effect. Zo is een stralingseffect gevonden dat ongeveer vier keer groter is dan de lokale opwarming door de broeikasgassen.

Chapter 1

Introduction and overview

INTRODUCTION

Ample evidence exists that human activities have affected chemical composition of the atmosphere. As we all live by the presence of air, it is obvious that there is an increasing interest among individuals and governments in the atmospheric composition and man's effect on it. Our perception of air pollution is usually due to the presence of microscopic airborne particles, so-called aerosols, which cause a reduction in visibility and thus are more readily noticed than the mostly invisible gaseous pollutants.

Aerosol particles are produced, in addition to natural sources (volcanoes, sea spray from the oceans, forest fires, etc.), in large quantities by industrial emissions, traffic and other human activities. These man-made (anthropogenic) aerosol particles have great effects on the environment, which range from adverse health effects, contributions to acid deposition and eutrophication, influence on oxidant formation, to cooling of the global climate by the reflection of sun light.

A great attention was devoted in resent years to the problem of global climate change, which is usually associated with global warming due to the increasing concentrations of the so-called greenhouse gases, like carbon dioxide, arising from fossil fuel burning and other industrial activities. The concern is caused by the seriousness of the consequences of the global warming. On the basis of present and projected

anthropogenic emissions the following consequences of increased concentrations of the greenhouse gases are predicted [*IPCC*, 1996]:

- The global mean surface air temperature in the year 2100 is estimated to be about 2°C higher than in the year 1990.
- As a result of higher temperatures the average sea level is expected to rise by about 50 cm from the present to 2100.
- Warmer temperatures will lead to more severe droughts and / or floods, more extreme rainfall events and changes in the occurrence of severe storms.
- The climate change could also shift the balance among biological species. Some models predict forest dieback, which would further increase concentration of carbon dioxide, thus enhancing the climate change.

The concern over the global warming was further deepened by observations that global mean surface air temperatures were rising during the past century (Fig.1.1). In order to assess available scientific information on climate change and to formulate response strategies the Intergovernmental Panel on Climate Change (IPCC) was established in 1988 by the United Nations Environment Program and the World Meteorological Organization. A very extensive scientific research, summarized in the latest IPCC report, has been directed in recent years in order to understand and quantify the effect of man activities on global climate. The concentrations and life times of the greenhouse gases as well as their effect on climate have been very well documented.

However, human influence on climate is more complex than just via increasing the concentration of carbon dioxide in the atmosphere. Utilization of fossil fuels results in a production of large quantities of aerosol particles. These anthropogenic (man-made) particles were only recently recognized to be an important part in the climatic system. Anthropogenic aerosols were demonstrated to have a considerable cooling effect on climate, comparable to that of the greenhouse gases, but opposite in sign [*Charlson et al.*, 1992]. However, their effect on

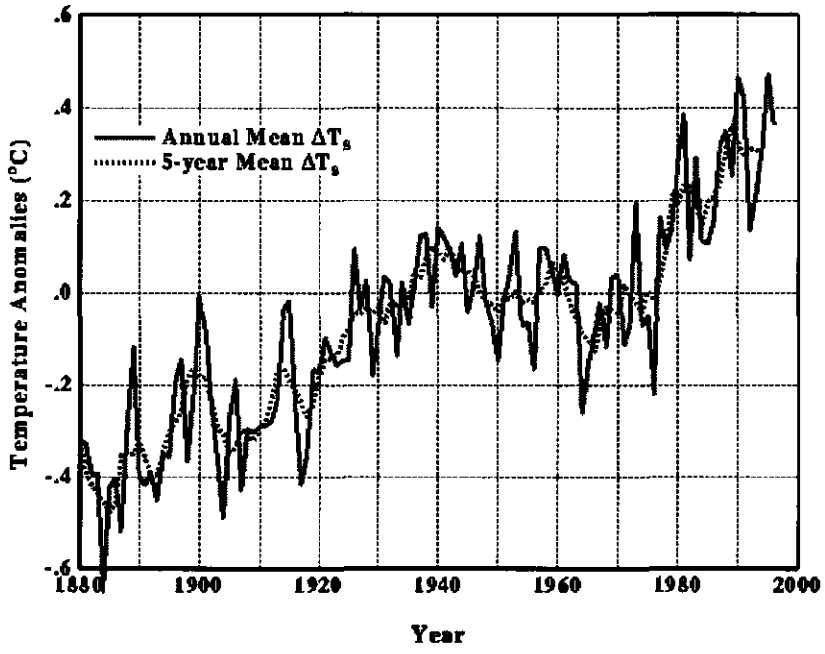

Figure 1.1. *Anomalies of global mean surface air temperature. (Source: NASA Goddard Institute for Space Studies. http://www.giss.nasa.gov/Data/GISTEMP/GLBann.gif).*

global climate is much more complex than that of the greenhouse gases and is very uncertain [*IPCC*, 1996].

The present thesis is aimed to contribute to a better understanding of the effects of anthropogenic aerosols on climate. A brief description of the climate system and the climatic effects of the greenhouse gases and aerosols is given below. Also the uncertainties in the magnitude of the aerosol effect, as given in the IPCC report are discussed and a set of problems is formulated for the present thesis.

THE CLIMATE SYSTEM

The global energy balance

"Climate" is usually defined as a long term (longer than 30 years) average over a large area of day-to-day weather, with the key quantities being average temperature and precipitation. Climate is established as a result of complex interactions between different components of the climate system: the atmosphere, the oceans, the cryosphere (glaciers, sea ice, and continental ice caps), the geosphere (the earth's solid surface) and the biosphere (living organisms in the oceans and on land).

The source of energy which drives the climate is the radiation from the Sun. Most of this energy is in the visible ("short-wave") part of electromagnetic spectrum. The energy flux at the top of the atmosphere is approximately 1370 W/m^2. Because the Earth has a spherical shape and because at any time half of the Earth is in night, the average energy flux on a horizontal surface outside the atmosphere is one quarter of this or 342 W/m^2. A part of this energy is scattered or reflected back to space by air molecules, aerosol particles and clouds or by the Earth's surface, which leaves about 235 W/m^2 to warm the Earth's surface and atmosphere.

To balance the incoming energy, the Earth radiates on average the same amount of energy as thermal (infrared or "long-wave") radiation back into space. Some of the infrared radiation from the Earth surface is transmitted through the atmosphere relatively unimpeded. The bulk of the radiation, however, is intercepted and absorbed by the atmosphere. The absorbed radiation is in turn re-emitted both up into the space and down to the surface. In this way a part of the thermal radiation becomes "trapped" in the atmosphere allowing the surface to be warmer than it would otherwise be. This is known as the greenhouse effect.

The (natural) greenhouse effect has the following physical basis. The amount of infrared energy emitted by a warm surface depends on its temperature. For the Earth surface to emit 235 W/m^2 it should have a temperature of about -19°C. This temperature is much lower than the actually observed global average surface temperature of about 15°C. This happens because the thermal energy, absorbed by clouds and gases that are active in the infrared, is re-emitted into space at much higher and colder levels of the atmosphere. A temperature of -19°C is found in mid-latitudes typically at about 5 km above the ground.

Most of the atmosphere (about 97 - 99%) does not contribute to the natural greenhouse effect, because it is composed of nitrogen and oxygen, that do not absorb infrared radiation. It is the water vapor, carbon dioxide, methane and some other minor gases, that absorb the infrared radiation emitted by the surface. These gases are known as the greenhouse gases, because they largely contribute to the natural greenhouse effect. The dominant natural greenhouse gases are water vapor, which amount in the atmosphere can be up to 2%, and carbon dioxide, which content in the atmosphere is about 0.03%, both gases being strong absorbers in the infrared.

Clouds also absorb thermal radiation and thus act similarly to the greenhouse gases. However, their contribution to the natural greenhouse effect depends on the altitude at which they are present. Low clouds contribute little to the effect, because their temperature does not significantly differ from that of the ground. In contrast, clouds present at a height of several kilometers above the ground re-emit the thermal radiation at a much colder levels, thus producing the greenhouse effect. However, clouds in general are also very effective reflectors of the short-wave radiation, that contains most of the incoming solar energy. The cooling influence of clouds, which results from their short-wave reflective power, dominates, on the global scale, the warming influence due to their greenhouse properties [*IPCC*, 1996].

To summarize, the radiative balance of the atmosphere is established as a result of complex interactions between its different components, the most important of which are:

- greenhouse gases due to their absorption of the outgoing thermal terrestrial radiation
- clouds due to their strong reflectivity, which reduces the amount of incoming solar energy
- aerosol particles which, similarly to clouds, reflect the incoming solar light.

The above components were always present in the atmosphere (except for the CFCs). However, the industrial activities of man have significantly changed amounts and properties of these components, thus affecting the global energy balance.

Radiative (climate) forcing

Climate can vary for many reasons, both natural and driven by man. However, the concept of climate change is usually referred only to variations due to human interference. A term radiative forcing is usually used to quantify a potential climate change mechanism. Radiative forcing is defined as the perturbation to the energy balance of the Earth (in W/m^2) following, for example, a change in concentration of carbon dioxide. A positive radiative forcing tends to warm the surface, while negative - to cool. Radiative forcing sometimes is called climate forcing.

Climate forcing arising from human activities can be divided into two major types: the greenhouse forcing due to increased concentrations of the greenhouse gases and the aerosol forcing. The greenhouse forcing is positive and thus has a warming influence on climate, while the aerosol forcing acts in the opposite way. Both the greenhouse and the aerosol forcing are discussed in the corresponding sections below.

THE ENHANCED (ANTHROPOGENIC) GREENHOUSE EFFECT

Since industrial revolution anthropogenic activity is considerably changing concentrations of some trace gases like carbon dioxide and methane. Due to their activity in the infrared these gases increase the heat trapping ability of the atmosphere, thus enhancing the natural greenhouse effect. The longest reliable direct record of atmospheric carbon dioxide concentrations from the Mauna Loa [*Keeling et al.,* 1982] shows a 14.3% increase in the mean annual concentration, from 315.83 parts per million by volume (ppmv) of dry air in 1959 to 360.90 ppmv in 1995 (Fig.1.2). Concentrations of CO_2 have been monitored for shorter periods of time at a large number of stations around the world. The globally averaged CO_2 concentration increased by approximately 1.53 ppmv a year over the period 1980 to 1989 and continue to rise [*IPCC,* 1996]. Several other greenhouse gases (methane, nitrous oxide and halogenated compounds) are also observed to be increasing in concentration in the atmosphere because of human activities (Table 1.1). These trends are attributed largely to fuel use, land use change and agriculture.

The observed increase in concentration of the greenhouse gases is expected to cause a global warming during the next decades [*Ramanathan et al.*, 1985]. The radiative forcing by the anthropogenic greenhouse gases since pre-industrial times is estimated to be 2.45 W/m^2 [*IPCC,* 1996] and is due primarily to increases in the concentrations of CO_2 (1.56 W/m^2), CH_4 (0.47 W/m^2) and N_2O (0.14 W/m^2). The IPCC estimates the uncertainty to be about 15%. Many greenhouse gases have very long life times (from tens to hundreds of years) and thus tend to accumulate in the atmosphere, exerting the radiative forcing on long time scales.

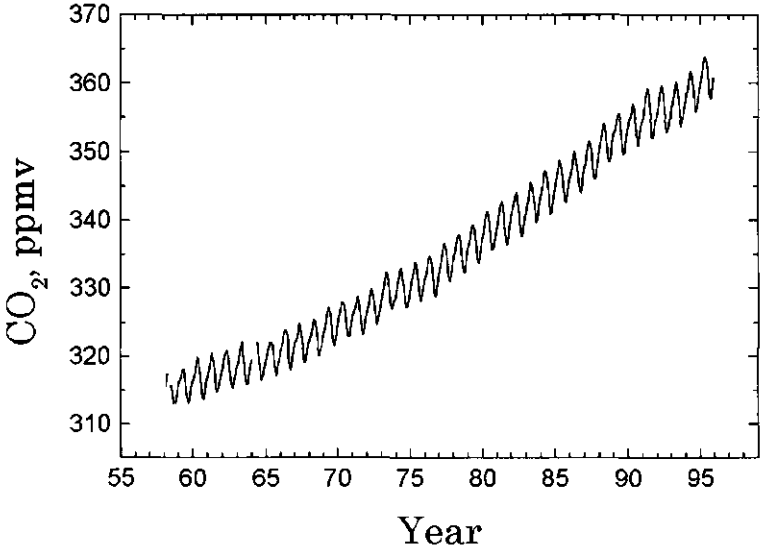

Figure 1.2. *The Mauna Loa record of atmospheric carbon dioxide concentrations. (Source: C.D. Keeling and T.P. Whorf, Scripps Institution of Oceanography, University of California. http://cdiac.esd.ornl.gov/ftp/trends/co2/mlosio.co2).*

Table 1.1. *Some of the greenhouse gases that are affected by human activities [IPCC, 1996].*

	CO_2	CH_4	N_2O	CFC-11	HCFS-22	CF_4
Pre-industrial concentration	~280 ppmv	~700 ppbv	~275 ppbv	0	0	0
Concentration in 1994	358 ppmv	1720 ppbv	312 ppbv	268 pptv	110 pptv	72 pptv
Rate of change	0.4 % / yr	0.6 % / yr	0.25 % / yr	0 % / yr	5 % / yr	2 % / yr

AEROSOL EFFECT ON CLIMATE

Aerosols, produced in large quantities by industrial emissions (mostly by gas-to-particle conversion of emitted gases), significantly influence both the transfer of solar light through the atmosphere and the atmospheric water cycle [*e.g., Twomey*, 1977a]. Atmospheric aerosols, thus, have a strong potential to exert a considerable climate forcing. The aerosol climate forcing is usually divided into a direct and an indirect forcing (or effects). The direct reflection and absorption of solar radiation by aerosol particles is associated with the direct aerosol effect. The indirect effect includes mechanisms by which aerosol particles affect the amount or radiative properties of clouds, thereby indirectly influencing the radiation balance.

Anthropogenic aerosols exert radiative forcing differently than the greenhouse gases. Aerosol particles have shorter life times in the troposphere, in the order of a few days [*Rodhe*, 1978, *Andreae*, 1995], than the greenhouse gases. This results in spatial and temporal non-uniformity of the aerosol distribution and, consequently, of the forcing. The aerosol forcing is largely a short-wave forcing dependent on sunlight and thus unlike the greenhouse gases the aerosol forcing is greatest only in daytime. Optical properties of aerosol particles and aerosol interactions with clouds depend on particle size and composition. Such differences make a description of the aerosol forcing much more complex than that for the greenhouse gases, which in turn results in high uncertainties in estimating the aerosol effects on climate [*Charlson and Heintzenberg,* 1995].

Direct forcing

Aerosol particles influence the Earth's radiative balance directly by back-scattering and absorption of short-wave radiation. Because of the back-scattering the surface receives less radiation and consequently cools. The forcing is strongest on clear sky days and above a low reflecting surface [*e.g. Charlson et al.,* 1992], like oceans which have a very low surface albedo (5% - 10%). On the other hand, aerosols can

exert a positive forcing above a bright surface, like snow, because the aerosol layer then reduces the local albedo [*Blanchet,* 1995]. However, such a positive forcing is much smaller than the negative forcing by anthropogenic aerosols [*IPCC*, 1996].

The particle scattering efficiency is strongly dependent on the size of the particles [*e.g. Twomey*, 1977a]. Particles with diameters between approximately 0.2 and 1 μm in diameter are the most effective in scattering the solar light [*Twomey,* 1977a; *Nemesure et al.,* 1995]. The scattering efficiency of aerosol, and thus its radiative forcing, is proportional to its concentration in this size range.

Most of the atmospheric aerosol particles are hygroscopic and thus increase their size in humid conditions [*e.g. Twomey*, 1977a]. This, in turn, affects the particle scattering efficiency both due to change in size and in refractive index of the particle, with the first effect being dominant [*Twomey*, 1977a]. *Nemesure et al.* [1995] have shown by performing Mie-scattering calculations for several model aerosol size distributions that the normalized forcing per unit mass strongly increases with increasing relative humidity, especially at relative humidities higher than 80%.

The influence of the relative humidity on the light scattering of ambient aerosol was recently studied in the Netherlands using the humidity controlled nephelometry [*Veefkind et al.*, 1996; *ten Brink et al.*, 1996a]. Humidity controlled nephelometry provides data of the light scattering of aerosol particles as a function of the relative humidity. It was shown that the light scattering of wet ambient aerosol at 60% RH is increased by 30-50% relative to the scattering at its dry state. At 90% relative humidity the light scattering is increased by approximately 2.5 times. This indicates the magnitude of the effect the hygroscopic growth has on the light scattering.

Estimates of the direct forcing *due to sulfate aerosol only* were made in resent years. *Charlson et al.* [1992] estimated the global annual mean direct forcing due to the sulfate aerosols to be around -1.3 W/m^2. *Kiehl and Rodhe* [1995] have computed the global direct forcing

to be -0.66 W/m^2. *Boucher and Anderson* [1995] gave an estimate of -0.29 W/m^2, which is similar to the estimate by *Kiehl and Briegleb* [1993]. *Chuang et al.* [1994] came to a direct forcing by sulfate aerosols of -0.45 W/m^2. *Taylor and Penner* [1994] using the same model obtained a forcing of -0.9 W/m^2, with the difference being due to a different treatment of the humidity dependence of the light scattering efficiency. It should be noted here that the mentioned models incorporate the effect of relative humidity on the particle size by taking into account an enhancement factor at some average relative humidity relative to a dry state. However, because of the exponential character of the particle growth and thus of the scattering efficiency with increasing relative humidity [*Nemesure et al.*, 1995; *Veefkind et al.*, 1996] the enhancement factor taken at an average relative humidity most probably represents a low-end estimate.

It should be stressed that the above mentioned estimates of the direct forcing were made assuming that sulfate is the only anthropogenic compound contributing to the light scattering. However, it was found that in the Netherlands ammonium nitrate aerosol has a larger contribution to the light scattering than (ammonium) sulfate aerosol [*ten Brink et al.*, 1996a]. Measurements of visibility reduction by sub-microne anthropogenic aerosols indicate a similar situation in some parts of the USA [*Trijonis et al.*, 1990]. Consequently, considering (ammonium) sulfate aerosol as the only contributor to the light scattering underestimates the aerosol climate forcing. Organic aerosol is also a possible strong contributor to the light scattering by the ambient aerosol [*Penner*, 1995]. It was shown that in the USA organic compounds contribute 20-50% to the mass of particles smaller than 2.5 μm [*White*, 1990] and, similarly, 20-50% to the total light scattering [*Trijonis et al.*, 1990]. The contribution of organic aerosol to the light scattering in Europe is yet to be quantified.

IPCC [1996] gives for the direct forcing by *sulfate only* aerosols a central estimate of -0.4 W/m^2 with a factor of 2 uncertainty. This estimate indicates that the direct effect of anthropogenic aerosol is comparable in magnitude to that of the greenhouse gases, but opposite in sign. The principal sources of uncertainty in these estimates are the

microphysical properties influencing optical and radiative properties of the aerosol and atmospheric chemistry properties, like residence time, etc. [*IPCC*, 1994; *Penner et al.*, 1994]. However, as discussed above, the radiative forcing by sulfate aerosols only is underestimating the total forcing by anthropogenic aerosols because of the omission of other important anthropogenic compounds like ammonium nitrate and organics. The radiative forcing by sulfate aerosols in itself is most probably underestimated because of the poor treatment of the relative humidity influence on the light scattering by the climate models.

The indirect effect

Apart from the cooling forcing due to direct scattering of the solar radiation, anthropogenic aerosols can also influence the radiation balance of the Earth indirectly by increasing the reflectivity of clouds and increasing their life time. Clouds cover vast areas of the globe and thus play a major role in the global radiation balance by controlling the amount of incoming short-wave solar radiation and outgoing terrestrial infrared radiation. Clouds form by condensation of water on preexisting water-soluble aerosol particles with sizes larger than 0.05-0.1 μm in diameter [*e.g. Twomey*, 1977a], the so-called cloud condensation nuclei (CCN). The concentration of aerosol particles thus governs the concentration of cloud droplets. Anthropogenic aerosols usually contain large quantities of water-soluble substances, like sulfate, and thus can also act as CCN.

It has been originally argued by *Twomey* [1977a,b; 1991] that tropospheric clouds formed in polluted regions have higher droplet number concentrations which leads to an increase in reflection power (albedo) of clouds in the visible (short-wave) part of the spectrum. In contrast to the effect on the short-wave albedo, an increase in droplet number concentration does not lead to higher absorption of infrared terrestrial radiation [*Grassl*, 1990] and thus does not increase the greenhouse action of clouds. Anthropogenic aerosols, thus, act (in an indirect way) as a radiative cooling factor in the atmospheric radiation balance.

Sensitivity studies show that the indirect aerosol radiative forcing should be most pronounced in marine stratus cloud fields close to polluted continents [*Wigley*, 1989; *Twomey*, 1991; *Charlson* et al., 1992; *Platnick and Twomey*, 1994; *Taylor and McHaffie*, 1994]. There are two reasons for this. The cloud albedo is sensitive to fractional changes in droplet number concentration [*Twomey*, 1991; *Schwartz and Slingo*, 1996]. Marine clouds are optically thin and have low droplet number concentrations, because the background concentrations of marine (natural) aerosols are low [*Hoppel et al.*, 1990; *Andreae et al.* 1995]. Consequently, even a small number of anthropogenic aerosol particles has the greatest (relative) influence. Also it was argued that a saturation occurs with respect to the numbers of cloud droplets in air with high aerosol loading which is usually observed over continents [*Jensen and Charlson*, 1984; *Leaitch et al.*, 1986; *Gillani et al.*, 1994]. Marine stratus and stratocumulus clouds cover approximately 30% of the oceanic surface [*Charlson et al.*, 1987], which has a very low surface albedo (5% - 10%). This in combination with the high sensitivity of their reflectance to anthropogenic pollution makes marine stratiform clouds the most important cloud type for the indirect aerosol climate forcing.

One of the striking experimental examples of how anthropogenic aerosols can (drastically) increase reflectance of marine clouds was found in satellite images of marine stratocumulus clouds modified by emissions from ships [*Coakley et al.*, 1987; *Albrecht*, 1989; *Radke et al.*, 1989; *King et al.*, 1993]. The so-called "ship tracks" are easily visible in satellite images as white lines against a gray background (Fig.1.3). Results from *in situ* studies of microphysical and optical properties of clouds modified by ship emissions agreed well with the physical principles underlying the indirect effect [*King et al.*, 1995].

Apart form their effect on the albedo of clouds increased droplet number concentrations are expected to result in smaller sizes of cloud droplets which inhibits the rain-out of these clouds by drizzle [*Albrecht*, 1989]. The persistence of clouds could be the reason for the increased cloudiness over the last decades in coastal regions in Europe [*Liepert et al.*, 1994; *Russak*, 1990]. An increase in life time of clouds would also disturb the atmospheric water vapor cycle. Because most of the

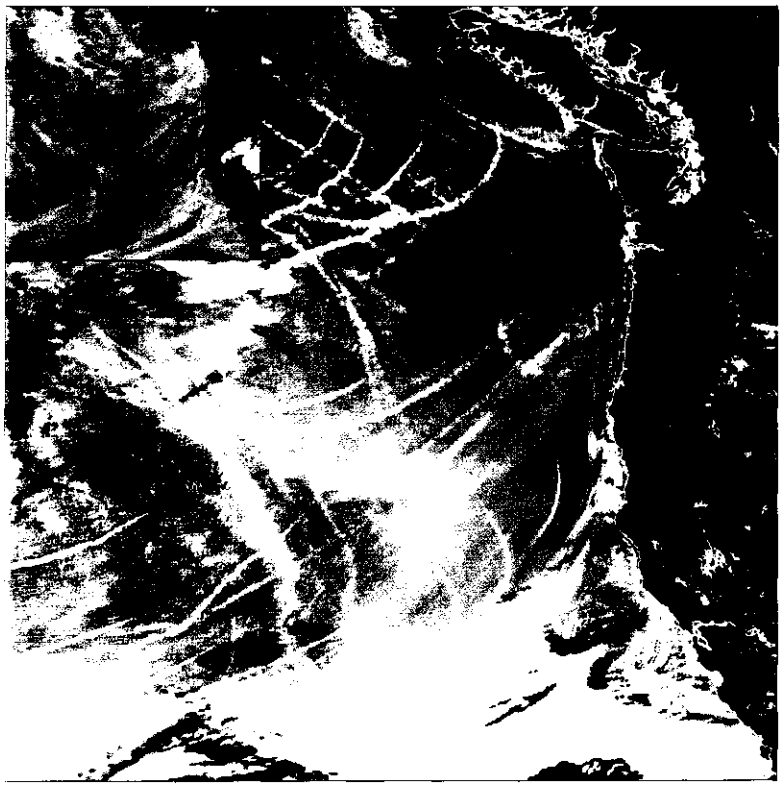

Figure 1.3. *Satellite images showing streaks of increased reflectivity ("ship tracks") on an extensive stratocumulus cloud system off the West Coast of the US (adopted from King et al., 1995).*

greenhouse warming is due to the (assumed) increase in atmospheric water vapor concentrations [*Twomey*, 1991], the increase in cloud life time may substantially change the magnitude of the warming. The combined result of these effects is very uncertain and requires a more accurate treatment of cloud processes in climate models [*Schwartz and Slingo*, 1996].

A simple analysis shows that a 30% increase in droplet number concentration in marine stratiform clouds due to anthropogenic aerosol, estimated for Northern hemisphere, corresponds to a 2.25% increase in cloud albedo [*Schwartz*, 1988; *Charlson et al.*, 1992]. This brightening of clouds translates into a hemispheric-mean forcing of -1.1 W/m^2. More sophisticated climate models give global mean indirect forcing of approximately the same magnitude. *Jones et al.* [1994] obtained mean indirect forcing of -1.3 W/m^2. *Boucher and Lohmann* [1995] estimated the indirect forcing to be between -0.5 and -1.5 W/m^2, dependent on different assumption on droplet number / sulfate concentration relationship. This value is comparable to the forcing by all greenhouse gases which is estimated to be about 2.5 W/m^2 [*Shine et al.*, 1990]. The combined direct and indirect aerosol forcing, thus, practically completely compensates the greenhouse forcing and, consequently, needs to be considered in evaluations of anthropogenic influence on global climate.

Though it was demonstrated that the magnitude of the indirect aerosol forcing is estimated to be comparable to that of the forcing by the greenhouse gases, the estimates of the indirect effect are very uncertain, with the main uncertainty arising from relating an increase in droplet number concentrations to an increase in concentration of cloud nuclei due to anthropogenic aerosol particles. Refering to the uncertainty in quantifying the indirect effect and despite the fact that all of the cited in the *IPCC* report studies give a mean indirect forcing substantially below zero (at least -0.5 W/m^2), the *IPCC* does not accept any midrange estimate and gives only a range between 0 and -1.5 W/m^2.

OVERVIEW OF THE CLIMATE FORCING

It has been shown that since industrialization man has considerably increased atmospheric concentrations of radiatively active

substances like the greenhouse gases (CO_2, CH_4, etc.) and aerosols, thus exerting a considerable radiative forcing [*IPCC*, 1996]. The anthropogenic climate forcing is mainly confined to the troposphere and may be divided into two major types: forcing by the greenhouse gases and forcing by anthropogenic aerosols. An overview of the climate forcing given by the *IPCC* [1996] is given in Fig.1.4 and Table 1.2.

Because of the differences in spatial distribution of the radiative forcing by the greenhouse gases and aerosols the *IPCC* does not provide any estimate of the overall net anthropogenic radiative forcing explaining it by difficulties in interpreting such a compound forcing. However, the *IPCC* does commit itself to attributing the observed rise in the global mean surface air temperature (see Fig.1.1) to the (compound) anthropogenic climate forcing: *"Most notable is that of the observed warming of about half a degree over the last century. This is about a factor of two smaller than conventional estimates according to*

Table 1.2. *Values for anthropogenic radiative forcing from the IPCC 1996 report.*

	Midrange estimate	**"Coldest" estimate**	**"Warmest" estimate**
Greenhouse gases	2.45	2.05	2.85
Tropospheric ozone	0.4	0.2	0.6
Stratospheric ozone	-0.1	-0.2	-0.05
Direct aerosol effect*	-0.5	-1	-0.25
Indirect aerosol effect*	0 (-0.75)**	-1.5	0
Total	*2.25 (1.5***)*	*-0.45*	*3.15*

* sulfate aerosol only

** no midrange estimate given by the IPCC, in parentheses: a midrange, estimated from the provided upper and lower estimates of the indirect effect.

*** total anthropogenic forcing if the midrange value for the indirect effect is taken into account.

A simple analysis shows that a 30% increase in droplet number concentration in marine stratiform clouds due to anthropogenic aerosol, estimated for Northern hemisphere, corresponds to a 2.25% increase in cloud albedo [*Schwartz*, 1988; *Charlson et al.*, 1992]. This brightening of clouds translates into a hemispheric-mean forcing of -1.1 W/m^2. More sophisticated climate models give global mean indirect forcing of approximately the same magnitude. *Jones et al.* [1994] obtained mean indirect forcing of -1.3 W/m^2. *Boucher and Lohmann* [1995] estimated the indirect forcing to be between -0.5 and -1.5 W/m^2, dependent on different assumption on droplet number / sulfate concentration relationship. This value is comparable to the forcing by all greenhouse gases which is estimated to be about 2.5 W/m^2 [*Shine et al.*, 1990]. The combined direct and indirect aerosol forcing, thus, practically completely compensates the greenhouse forcing and, consequently, needs to be considered in evaluations of anthropogenic influence on global climate.

Though it was demonstrated that the magnitude of the indirect aerosol forcing is estimated to be comparable to that of the forcing by the greenhouse gases, the estimates of the indirect effect are very uncertain, with the main uncertainty arising from relating an increase in droplet number concentrations to an increase in concentration of cloud nuclei due to anthropogenic aerosol particles. Refering to the uncertainty in quantifying the indirect effect and despite the fact that all of the cited in the *IPCC* report studies give a mean indirect forcing substantially below zero (at least -0.5 W/m^2), the *IPCC* does not accept any midrange estimate and gives only a range between 0 and -1.5 W/m^2.

OVERVIEW OF THE CLIMATE FORCING

It has been shown that since industrialization man has considerably increased atmospheric concentrations of radiatively active

substances like the greenhouse gases (CO_2, CH_4, etc.) and aerosols, thus exerting a considerable radiative forcing [*IPCC*, 1996]. The anthropogenic climate forcing is mainly confined to the troposphere and may be divided into two major types: forcing by the greenhouse gases and forcing by anthropogenic aerosols. An overview of the climate forcing given by the *IPCC* [1996] is given in Fig.1.4 and Table 1.2.

Because of the differences in spatial distribution of the radiative forcing by the greenhouse gases and aerosols the *IPCC* does not provide any estimate of the overall net anthropogenic radiative forcing explaining it by difficulties in interpreting such a compound forcing. However, the *IPCC* does commit itself to attributing the observed rise in the global mean surface air temperature (see Fig.1.1) to the (compound) anthropogenic climate forcing: *"Most notable is that of the observed warming of about half a degree over the last century. This is about a factor of two smaller than conventional estimates according to*

Table 1.2. *Values for anthropogenic radiative forcing from the IPCC 1996 report.*

	Midrange estimate	**"Coldest" estimate**	**"Warmest" estimate**
Greenhouse gases	2.45	2.05	2.85
Tropospheric ozone	0.4	0.2	0.6
Stratospheric ozone	-0.1	-0.2	-0.05
Direct aerosol effect*	-0.5	-1	-0.25
Indirect aerosol effect*	0 (-0.75)**	-1.5	0
Total	*2.25 (1.5***)*	*-0.45*	*3.15*

* sulfate aerosol only

** no midrange estimate given by the IPCC, in parentheses: a midrange, estimated from the provided upper and lower estimates of the indirect effect.

*** total anthropogenic forcing if the midrange value for the indirect effect is taken into account.

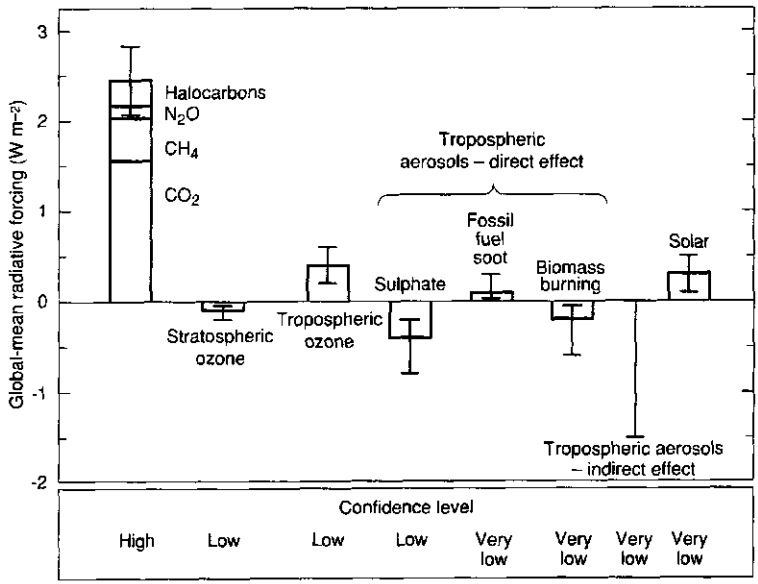

Figure 1.4. *Estimates of the global annual-mean radiative forcing (W/m^2) from 1850 to 1990 for a number of potential climate change mechanisms. The height of the column indicates a midrange estimate of the forcing whilst the error bars show an estimate of the uncertainty range. (Source: IPCC 1995 report).*

models including only trace gas increases but is consistent with the inclusion of the expected effects of sulfate aerosols." [*IPCC*, 1996, p.199]. However, according to the IPCC's estimations (see Table 1.2) the net anthropogenic climate forcing over the industrial period may very well be negative: -0.45 W/m^2. Moreover, as was discussed in the previous section, the accepted by the *IPCC* values for the aerosol radiative forcing most probably represent a low-end estimate because of the omission of other important anthropogenic aerosol compounds like

ammonium nitrate and organics together with a poor treatment of the effect of relative humidity on optical properties of aerosols.

Due to the overall uncertainty, arising largely from the uncertainty in the aerosol radiative forcing, the net forcing is actually estimated to be between -0.45 and 3.15 W/m^2. A more strict treatment of the individual uncertainties does not provide a net forcing that is confidently different from zero [*Schwartz and Andreae*, 1995]. If the uncertainty in aerosol forcing and the resultant uncertainty in the net forcing over industrial period is as great as stated in the *IPCC report* [1996], then it is impossible to attribute warming over the industrial period to anthropogenic forcing over this period and likewise impossible to say that climate observations substantiate global warming models [*Schwartz*, 1995].

The implications of the uncertainty in aerosol forcing should be recognized in the broader issue of global climate change, which has been dominated by consideration of the greenhouse forcing. If aerosols indeed are offsetting much of the effect of greenhouse gases, which is consistent with present uncertainties, than the observed 0.5°C increase in the global temperature is due to a small net forcing. This would imply that the planetary temperature is much more sensitive to the anthropogenic forcing, than when the aerosol forcing is small [*Schwartz and Andreae*, 1995]. Furthermore, if the aerosol forcing is offsetting a substantial fraction of the greenhouse forcing, then it is the forcing by a week's emission of aerosol precursors that is offsetting the forcing due to decades of past greenhouse gas emissions, that are continuously accumulating. If the temperature sensitivity is high, global warming may accelerate sharply in the future, especially if emissions of aerosols and their precursors are reduced in order to fight acid deposition, eutrification, adverse health effects, etc. Recognition of this means that the aerosol forcing is extremely important for understanding of man's influence on global climate and urgently necessitates a major research in order to substantially reduce the uncertainty in predictions of the aerosol radiative forcing, which is required for confident policy making.

SCOPE OF THIS WORK

The above discussion leads to the conclusion that in order to reduce the present uncertainty in the aerosol radiative forcing an extensive research is required to characterize tropospheric aerosols. Given the local nature of anthropogenic aerosols, which is due to their relatively short life time in the troposphere (a few days), ambient aerosols need to be characterized on the local basis. Most of the model estimates of the aerosol influence on climate were done using experimental data obtained in the USA [*IPCC*, 1995]. There are currently few data available from outside the USA to validate the extrapolation. This stresses the need in characterization of (anthropogenic) aerosol in other parts of the globe and Europe in particular.

The aim of the present thesis is to characterize the local ambient aerosol in relation to the aerosol radiative forcing. This is done on the basis of the local experimental data obtained at a coastal site in the Netherlands. The following aerosol parameters were investigated: (size dependent) chemical composition, relative contribution of different ambient aerosol components to the light scattering, effect of relative humidity on light scattering and cloud nucleating properties of ambient aerosols at conditions relevant for marine stratiform clouds (maximum supersaturation in the order of 0.1%).

The chemical composition of ambient aerosols as a function of size is discussed in Chapter 2. The relative contribution of different chemical constituents of the aerosol to the light scattering and thus to the local direct forcing is also discussed based on the study of *ten Brink et al.* [1996a]. It will be shown that, in contrast to the generally accepted view, (ammonium) nitrate aerosol has a contribution to the local direct radiative forcing which is equal to that of sulfate aerosol. On the basis of data available in the literature it will be shown that contribution of ammonium nitrate aerosol to the direct forcing on the global basis is most probably underestimated because concentrations of this volatile compound are underestimated due to evaporative losses during the sampling. It is concluded that new artifact-free sampling

techniques are required in order to assess the man's impact on climate and environment as a whole. Two novel automated instruments are described which are artifact-free and can be used in monitoring networks.

Hygroscopicity (or water attracting ability) of ambient aerosol is the property that is crucial for estimating both the direct and the indirect aerosol effects. The basic thermodynamics and kinetics of the hygroscopic growth of aerosols is considered in Chapter 2 in order to demonstrate the extent to which this property may effect the aerosol light scattering and thus the magnitude of the direct forcing.

The relation between the number concentration of cloud droplets and the number concentration of the aerosol particles is one of the largest sources of uncertainty in estimations of the indirect aerosol effect, which is discussed in Chapter 3. Experimental data on this relationship are scares and in Europe in particular. In this thesis an effort is made to provide experimental data on the cloud forming properties of ambient aerosols in the Netherlands as measured in a unique cloud chamber that operates under low supersaturations (in the order of 0.1%), common for marine stratiform clouds. The cloud chamber and its characterization are described in Chapter 4. In Chapter 5 the results of cloud activation experiments on ambient aerosols are given. It will be shown that the (expected from the cloud chamber measurements) droplet number concentration in polluted air is increased by about a factor of 6 relatively to clean marine air.

In order to demonstrate the magnitude of the local aerosol forcing, Chapter 6 gives a simple estimate of the forcing based of the measured local aerosol characteristics, which are discussed in the preceding chapters. The local annual-mean direct radiative forcing is estimated to be -3 ±1.1 W/m^2. The main source of uncertainty in this estimate arises from the absence of statistically significant meteorological data like the height of the atmospheric boundary layer and the relative humidity distribution with height within the boundary layer. The annual mean indirect radiative forcing by anthropogenic aerosols is estimated to be about -6.5 ±2.5 W/m^2, with the uncertainty mostly coming from the

uncertainty in the value for the pre-industrial "clean" droplet number concentration. The total annual-mean local radiative forcing by anthropogenic aerosols is estimated to be about -9.5 ±3 W/m^2, which is about 4 times higher than the (positive) forcing by all anthropogenic greenhouse gases.

Chapter 2.

Factors influencing the local direct radiative aerosol forcing

2.1 INTRODUCTION

Aerosol particles are effective scatterers of solar light. By scattering part of the incoming solar radiation back into space atmospheric aerosols play an important role in the radiative balance of the atmosphere. Because of the back-scattering the surface of the Earth receives less radiation and consequently cools. Industrial activities, traffic emissions and biomass burning produce (directly and indirectly) large amounts of aerosol particles. At present, global anthropogenic aerosol emissions are estimated to be comparable in magnitude to aerosol emissions from natural sources [*Charlson et al.*, 1992; *Andrea,* 1995]. As a consequence, aerosol concentration in the troposphere has increased over the industrial era. Due to higher aerosol concentrations the light reflecting efficiency of the atmosphere increases, which can be readily observed by the appearance of haze or smog in polluted air. The amount of the back-scattered light by the atmosphere is also higher at higher aerosol concentrations. Thus, anthropogenic aerosols exert a negative (cooling) radiative forcing. This radiative forcing is usually referred to as the direct aerosol effect, because anthropogenic aerosols alter the radiative balance by scattering solar light directly, as opposed to the indirect effect in which aerosols do it indirectly via clouds.

According to the so-called box models, representing a well-mixed column of air from the Earth's surface to the top of the planetary boundary layer (most of the anthropogenic aerosols are concentrated

there), the areal mean direct forcing ΔF_R can be estimated as [*Charlson et al.*, 1992]:

$$\Delta F_R = -\frac{1}{2} F_T T^2 (1-A_c)(1-R_s)^2 \beta \alpha f(RH) C \qquad 2.1$$

in which F_T is the global mean top-of-the-atmosphere radiative flux, T is the fraction of incident light that is transmitted by the atmospheric layer above the aerosol layer, A_c is the fractional cloud cover, R_s is the mean surface albedo, β is the upward fraction of scattered light by the aerosol, α is the light scattering efficiency per unit aerosol mass, and *f(RH)* is the effect of ambient relative humidity on the light scattering efficiency which will be discussed further in this chapter. C is the column burden of the aerosol, which is equal to the aerosol concentration multiplied by the height of the aerosol layer (which may be well approximated by the height of the atmospheric boundary layer). The negative sign denotes the cooling tendency. This equation shows that the forcing depends linearly on the aerosol concentration and that the forcing is maximum on clear sky days.

As discussed in the previous chapter, model estimates of the global average direct forcing by anthropogenic sulfate aerosols are at about -0.4 W/m^2 with a factor of 2 uncertainty [*IPCC*, 1996]. For Europe, *Charlson et al.* [1991] and *Kiehl and Briegleb* [1993] estimate that the aerosol direct radiative forcing may be of equal magnitude to or even exceed the warming by the greenhouse gases. These estimates of the amount of solar energy reflected by the man-made aerosols were not based on data but on calculated aerosol-sulfate concentration fields and under the assumption that sulfate is the only dominant light-scattering aerosol species of anthropogenic origin. Compounds like organic substances, that have been shown to contribute 20 - 50% to the total light scattering in the USA [*Trijonis et al.*, 1990] were not included into the IPCC's estimates of the direct forcing. Ammonium nitrate was assumed to be present only in large (above 1 μm in diameter) particles and was neglected as a very weak light scattering compound as compared to ammonium sulfate, that is present mostly in submicrometer particles. Moreover, data obtained in the USA were extrapolated to other places of the globe and were used to estimate the

direct forcing, though, as is correctly stated in the *IPCC report* [1995] "there is very few data available to justify such extrapolation and thus more research is required in other parts of the globe".

Recent measurements in the Western Europe [ten Brink et al., 1996a,b,c] indicate that the assumption that sulfate is the only man-made compound responsible for the direct aerosol forcing is not justified, at least not for the West-European region. It was found that in the Netherlands in continental air flows which, unlike marine air flows, are usually associated with clear sky conditions and thus provide the maximum radiative forcing by aerosols, another major anthropogenic compound - ammonium nitrate - contributes 30% or more to the total aerosol light scattering. The size distribution of this compound is approximately equal to that of ammonium sulfate, as will be shown further in this chapter. Data from some parts of the USA [*Trijonis et al.*, 1990] show a similar situation. It is well documented in literature that measurements of chemical composition of ambient aerosols are usually underestimating the amount of ammonium nitrate due to its volatility [*Appel et al.*, 1981]. Recent measurements by *Simon and Dasgupta* [1995], who applied a sampling instrument which avoids evaporative losses during the sampling to measurements of ambient aerosols in Lubbock, Texas, USA, indicate concentrations of nitrate in the aerosol phase to be higher than the sulfate concentrations. If the size distribution of nitrate is the same as that of sulfate and if nitrate is present in aerosol in larger mass than hitherto assumed, it is clear that the current estimates by the IPCC of the direct radiative forcing by anthropogenic aerosols are too low.

This chapter will discuss mass size distributions of ammonium nitrate in ambient aerosol as measured with cascade impactors in Petten, the Netherlands. The contribution of ammonium nitrate to the light scattering in the Netherlands will be also discussed using the data from a study by *ten Brink et al.* [1996a]. It will be shown that in continental air flows (ammonium) nitrate has practically the same size distribution as (ammonium) sulfate. The implications of the volatility of ammonium nitrate for measurements of size distributions and total concentrations of this compound are also discussed. It will be shown

that the present techniques (filter packs and impactors) are poorly suited to answer the present requirements of the environmental research. There is a need for automated systems that can measure aerosol composition on-line with a time resolution of about an hour. To answer this need automated systems like thermodenuders [*Slanina et al.*, 1985; *Keuken et al.*, 1988] and samplers of the SJAC type [*Khlystov et al.*, 1995] have been recently developed. These systems are briefly described in this chapter to demonstrate the possibility of performing artifact-free measurements needed for many areas of investigation including the climate research.

Another shortcoming of the modeling efforts made up to now and included into the evaluations by the IPCC is the treatment of the effect of the hygroscopicity (water-attraction ability) of aerosol particles on the light scattering. Both ammonium sulfate and ammonium nitrate are hygroscopic compounds [*e.g. Twomey*, 1977a] and attract water vapor in humid air. The condensation of water vapor onto particles results in an increase in the particle size and consequently in the optical cross-section, thus increasing the light scattering. Using the data from a study by *ten Brink et al.* [1996a] and *Veefkind et al.* [1996] the effect of hygroscopic growth on the light scattering by ambient aerosols is discussed along with its implications for the direct radiative forcing. Because hygroscopicity plays a central role in the cloud formation by (anthropogenic) aerosols, which is subject of the following chapters of this thesis, it is treated in more detail in this chapter.

NITRATE

Contribution to light-scattering

Up to now most of the efforts to assess the direct forcing by anthropogenic aerosols, including the IPCC, failed to consider ammonium nitrate as a major factor in the direct aerosol effect. This is

largely explained by a general perception that ammonium nitrate is present only in supermicrometer particles and thus has a very poor light scattering efficiency. This perception, in turn, is largely based on impactor measurements done in the seventies in the USA [*e.g. Milford and Davidson*, 1987]. However, *Harrison and Pio* [1983] in a study performed in the northwest of England in 1980-1981 found that in continental and polluted marine air flows the major part of nitrate is found in submicrometer particles. Moreover, the general pollution situation has changed considerably during the past decades. In order to fight acid deposition and other adverse effects of air pollution, industrial emissions of SO_2 (the gaseous precursor of sulfate aerosols) have been reduced considerably [*Arends et al.*, 1996], while emissions of NO_x and NH_3 (the gaseous precursors of ammonium nitrate) have not [*EMEP*, 1996]. Such a change in the emission rates should have resulted in a change in the relative amounts of sulfate and nitrate in the aerosol phase in total and per size class. Furthermore, it is well documented in the literature [*Wall et al.*, 1987; *Wang and John*, 1988; *ten Brink et al.*, 1996b,c] that ammonium nitrate size distributions measured with impactors are most probably distorted due to evaporative losses from impactor stages, mostly with the lower cutoff diameters.

Already in the eighties it was found that in the Netherlands other aerosol components were as important for the light-scattering as sulfate. During that study, performed in the period 1979 to 1981 [*Diederen et al.*, 1985], the aerosol light-scattering was factorized according to aerosol composition. In particular, nitrate, while present in lower quantities than sulfate, appeared to have an equal contribution to the aerosol light-scattering. The nitrate was present in the form of ammonium nitrate. The results of that study are particularly remarkable, because later it has been established that the method used for the collection of nitrate at the time, filter packs, was not quantitative. In filter packs the first filter is used to collect the aerosol-nitrate and the second to collect the gaseous nitric acid. However, because of evaporation of the ammonium nitrate from the first (aerosol) filter its concentration is underestimated and that of nitric acid overestimated [*Appel et al.*, 1981].

In a number of campaigns in 1982 and 1983 in the Netherlands [*van der Meulen*, 1986] denuders were used for stripping gaseous HNO_3 (nitric acid) before the aerosol entered the filter packs. With the gaseous HNO_3 removed, the sum of the amounts of nitrate in the two filters in the filter pack represents the accurate amount of aerosol-nitrate, since it is certain that the gaseous nitrate in the second filter is the result of the evaporation of the nitrate from the first filter. This study showed that virtually all aerosol-nitrate was present as ammonium nitrate in concentrations similar to those of ammonium sulfate and contributing to the same extent to the aerosol light-scattering.

A very recent study by *ten Brink et al.* [1996a] has shown (again) that ammonium nitrate is the dominant light-scattering compound in the Netherlands. Because this study was more detailed and performed with greater care than the previous studies, it is discussed here in more detail.

Similarly to the above mentioned study by *Diederen et al.* [1985] the light-scattering by aerosols was correlated with the concentration of sulfate and nitrate. Automated thermodenuders (see further in this chapter) were used for hourly measurements of ammonium nitrate and ammonium sulfate concentrations. As will be shown further in this chapter, thermodenuders are free of sampling artifacts and thus provide accurate concentration values with a very good time resolution. The hourly measurements were performed for the following reason. In the mentioned studies by *Diederen et al.* [1985] and *van der Meulen* [1986] only the 24-hour aerosol concentrations were available. *Janssen et al.* [1987] showed that the daytime (12-hour) concentration of sulfate in the Netherlands is on average a factor of two higher than the 24-hour concentration. Use of the 24-hour values thus leads to underestimation by a factor of two in the aerosol light-scattering and consequently in the direct forcing, because it occurs during daytime, especially at midday. This example stresses the fact that in order to assess the contribution of different aerosol components to the direct forcing one needs to perform measurements of the chemical composition at the relevant time (during sunshine hours) with the time

resolution of about one hour. Automated instruments capable of performing such measurements will be discussed further in this chapter.

The hourly measurements in the study by *ten Brink et al.* [1996a] allowed a further quantification of the diurnal variation in ammonium sulfate concentration. The diurnal variation of sulfate was analyzed for those days on which the concentration after 24 hours was less than 30% different from that on the previous day at the same time. This was done to exclude the days on which meteorological changes like frontal passages could have been the cause of the observed change in concentration. It was found that in the summer the concentration of sulfate at midday was 30% higher than the 24-hour average concentration, while in the winter season such a difference was absent. Unfortunately, insufficient data were available for a proper assessment of the diurnal variation of ammonium nitrate.

Concentrations of ammonium nitrate and sulfate as measured with the thermodenuders were related to the aerosol light scattering which was simultaneously measured with an integrating nephelometer (MRI 1562). The nephelometer measured the light-scattering under dry conditions (relative humidity below 30%) to avoid the influence of humidity on the light scattering (see further in this chapter). The relation between aerosol concentration/composition and light-scattering was evaluated for the relevant time of the day only (at 14:00 local time). The ratio of light-scattering coefficient to sulfate or nitrate mass concentration (proportionality factor), usually denoted as a (see Eq.2.1), was expressed in units m^2/g [*IPCC*, 1995]. This unit derives from the fact that light-scattering is expressed in m^{-1} and the concentration of sulfate in g/m^3. As an example: $\alpha = 1$ m^2/g corresponds to an aerosol light-scattering of $1 \cdot 10^{-6}$ m^{-1} per $\mu g/m^3$ of (sulfate) mass.

On physical grounds a has a maximum value of 6 m^2/g for pure sulfate [*Waggoner et al.*, 1981]. When a is larger, other aerosol components contribute to the light-scattering. For instance in the 1984 study, the ratio of the aerosol light-scattering to sulfate was 16 m^2/g. This indicates that the minimum contribution of other aerosol

components to the light-scattering is about 60%. The factorization of the light-scattering according to components showed that, indeed, sulfate contributed approximately 35% to the aerosol light-scattering.

In the study of *ten Brink et al.* [1996a] it was found that in arctic marine air the aerosol light-scattering attains its lowest value, as low as $5 \cdot 10^{-6}$ m^{-1}, which is more than an order of magnitude less than the average value of $7.1 \cdot 10^{-5}$ m^{-1}, found during about a year of measurements. Similar values were found in a study in the period 1979 - 1981 [*Diederen et al.*, 1985]. In polluted continental air it could be almost an order of magnitude higher than the average value. This increase in the light-scattering is a measure of the anthropogenic influence on the light-scattering and thus of the magnitude of the direct aerosol forcing.

The ratio of light-scattering coefficient and sulfate concentration in the study of *ten Brink et al.* [1996a] was 20 m^2/g, but with a rather large uncertainty. The ratio of light-scattering coefficient to the concentration of nitrate showed large day-to-day variations. A much better correlation existed between light-scattering and the sum of the nitrate and sulfate concentration, which was 7 m^2/g in the winter. This value, compared to a ratio of light-scattering coefficient to sulfate of 20 m^2/g, is a strong indication of a larger contribution of nitrate than sulfate to the aerosol light-scattering. In the summer season, the ratio of light-scattering coefficient to the concentration of sulfate plus nitrate was 9 m^2/g, which shows a comparable contribution of nitrate and sulfate.

It should be noted that the observed high light scattering efficiency of nitrate is that of ammonium nitrate, because thermodenuders, as will be shown further in this chapter, measure only ammonium nitrate concentrations. By deduction, one may conclude that most of submicrometer aerosol nitrate is present in the form of its ammonium salt. This conclusion is supported by the impactor measurements which are discussed below.

Size distribution

Mass size distributions of ambient aerosols in continental and marine air flows were measured with cascade impactors in Petten, The Netherlands in relation to both the direct and the indirect (see Chapter 3) effects. Because continental air flows, unlike marine flows, are usually associated with clear sky conditions, they contribute most to the direct radiative forcing. For this reason, impactor measurements of continental aerosols were mostly done to assess the direct effect and were triggered by clear sky conditions. Measurements of marine aerosols were done mostly for the indirect effect study. However, marine aerosols in "clean" arctic air flows were also used as the "background" reference to estimate the direct aerosol effect.

Mass size distributions of sulfate and nitrate in ambient aerosol as measured in Petten are given in Appendix 1. Sulfate and nitrate are the dominant compounds in the submicrometer continental aerosol. Analysis of the ionic balance shows that sulfate and nitrate in submicrometer aerosol are fully neutralized by ammonium. Hence, both sulfate and nitrate in continental aerosol are present in the form of their ammonium salts. This should be kept in mind when modeling optical properties of sulfate and, especially, nitrate particles.

Only small differences in size distribution exist for sulfate and nitrate. Remarkably, both sulfate and nitrate mass distributions are centered at around 0.5 μm in diameter. This size coincides with the wave length region where the solar light has its maximum power, which renders maximum light scattering efficiency to (anthropogenic) sulfate and nitrate aerosols. This also explains the observed high light scattering efficiency per unit mass of nitrate [*ten Brink et al.*, 1996a], which would not be expected if nitrate is present only in supermicrometer particles, as is usually assumed. Thus, for continental aerosol in the Netherlands (by deduction from the measurements in Petten) the preposition that nitrate is concentrated in the supermicrometer particle is not valid. Taking into account that continental air flows are dominating the direct effect, it is clear that

ammonium nitrate is a major factor in the direct radiative forcing in the Netherlands.

The similarity of size distributions of nitrate and sulfate also implies that nitrate particles have a comparable to sulfate contribution to the number of anthropogenic cloud condensation nuclei (CCN) and thus to the indirect aerosol effect, which will be discussed in the following chapters of this thesis. The fact that nitrate is present not in supermicrometer, but mostly in submicrometer sized particles has serious environmental implications, not only for the calculation of the radiative forcing by aerosols but also for estimating the contribution of nitrate aerosol to acid deposition, eutrophication and long range transport of pollutants.

As mentioned before, it is usuallly assumed that nitrate is present only in supermicrometer particles. Such a distribution of nitrate is mostly observed in the presence of (large) sea-salt aerosol [*Savoie and Prospero*, 1982; *Harrison and Pio*, 1983; *Khemani et al.*, 1985], or in the presence of (coarse) carbonate particles over arid areas [*Wolff*, 1984]. In such cases, nitric acid formed by photochemical reactions in the atmosphere substitutes more volatile acids from the salts composing the coarse particles forming sodium or calcium nitrates. These compounds are relatively stable and do not evaporate from impactor stages. Indeed, in air of (mostly) marine origin nitrate was mostly found in large particles (Appendix 1).

Another argument in favor of the supermicrometer nitrate concept was that nitrate is driven out from small particles by condensing sulfuric acid [*Wolff*, 1984]. However, the pollution situation has changed considerably during the last decades. As a result of reduction in SO_2 emissions the concentration of sulfate in the Netherlands has decreased by approximately 50% [*Arends et al.*, 1996, *EMEP*, 1996] in the last fifteen years. Meanwhile, emissions of NO_x, the gaseous precursors of aerosols nitrate, stayed on the same level [*EMEP*, 1996]. In the presence of high concentrations of gaseous ammonia, resulting mostly from agricultural activities, all of the acidic sulfate is neutralized by ammonia (see Appendix 1), allowing for gaseous nitric

acid to form ammonium nitrate on the same particles on which sulfate condenses. This would explain the presence of ammonium nitrate in the submicrometer aerosol.

Ammonium nitrate, unlike sodium and calcium salts of nitric acid, is a very volatile compound [*e.g. Stelson and Seinfeld*, 1982]. For this reason, impactor measurements tend to underestimate concentration of ammonium nitrate, which will be demonstrated later in this chapter. The losses are especially pronounced at high ambient temperatures [*ten Brink et al.*, 1996b,c]. The losses are more pronounced at stages sampling smaller particles, because of the lower pressures above those stages [*Wang and John*, 1988]. Thus, the impactor measurements most probably provide distorted spectra, biased towards large sizes. It can not be ruled out that due to very low overall aerosol concentrations in marine air all the submicrometer ammonium nitrate (if present) evaporates from impactor stages.

The impactor data (Appendix 1) also show that up to half of the aerosol-mass is in the submicrometer size-range, the range which dominates the light-scattering [*Waggoner et al.*, 1981], was not identified as a water-soluble inorganic material. Most likely the "missing" material is of a carbonaceous (organics and elemental carbon) nature. An indication of the contribution of the missing material to the light-scattering is the fact that the average ratio of scattering coefficient to nitrate plus sulfate concentration is 8 m^2/g. A typical value of 4 m^2/g was found for the scattering by the total (submicrometer) aerosol in the Netherlands [*Diederen et al.*, 1985]. After correction for the ammonium, the contribution of the non-identified species to the aerosol light-scattering would amount to 40% in summer and to 20% in winter. This is a speculative number to be verified by further measurements of the concentration and size distribution of the missing material.

To summarize, the study by *ten Brink et al.* [1996a] has shown that the light scattering by aerosols in polluted continental air is increased by one to two orders of magnitude as compared to (relatively) clean arctic marine air flows, indicating the magnitude of the direct radiative

forcing by anthropogenic aerosols. It was found that other compounds, in addition to sulfate, which is usually considered as the sole man-made factor in the direct aerosol effect, are strongly contributing to the aerosol light scattering. The major contributor to the light scattering by anthropogenic aerosols in the Netherlands was found to be ammonium nitrate, being equal or stronger than ammonium sulfate contributor to the light scattering. Unidentified material, most probably of organic nature, was contributing 20 - 40% to the total light scattering by aerosols. These values compare to the identified contribution of organic material of 20 to 50% to the total light scattering in the USA [*Trijonis et al.*, 1990]. Thus, the discussed above measurements provide a very strong indication that, at least for the Western Europe, the current estimates by the IPCC of the direct radiative forcing are a factor of 2 to 3 too low, due to neglecting ammonium nitrate and organic aerosols.

Techniques which avoid artifacts in sampling aerosols.

From the above discussion it follows that ammonium nitrate plays a central role in aerosol radiative forcing. However, because of its high concentrations and abundance in the submicrometer aerosol, its role is not limited only to the aerosol radiative forcing, but is also important for other environmental issues, like acid deposition, eutrification, etc. Measurements of this compound, both of the total concentration and size segregated measurements, suffer from sampling artifacts [*Appel et al.*, 1981; *Wang and John*, 1988]. Thus, artifact-free methods for (size segregated) sampling of this compound are required.

As discussed in the previous sections, a good time resolution is required from the measuring instruments, for instance, to measure aerosol composition during the relevant time of the day. This requirement is not limited only to ammonium nitrate but is valid for other aerosol constituents as well. A good time resolution is also needed for other research areas, like studies of industrial process emission and health related studies. Furthermore, measurements of temporal and spatial changes in the relative concentrations of different species in aerosols can give considerable insight into the origin of particles.

To understand the anthropogenic influence on the environment and climate in particular, there is a need in large measuring networks, operated both in polluted and (relatively clean) remote locations. At present, aerosols are mostly sampled by filter packs, which are very labor intensive, and suffer from sampling artifacts, if used without pre-denuders [*Appel et al.*, 1981]. Denuders are used to trap gaseous components which could interfere in filter measurements [*Forrest et al.*, 1982; *Slanina et al.*, 1992]. Manual procedures for the application of denuders to measure a large number of components in the atmosphere were developed to measure short time series of concentrations generally in the process of comparing the results to other methods. However, the methods were not very easy to apply in monitoring networks [*Slanina and Wyers,* 1994]. In addition, at low ambient concentrations errors due to contamination during the handling of the filters pose serious problems. To avoid these problems there is a need for automated systems that can measure aerosol composition on-line, *i.e.* avoiding the handling.

To summarize: there is a need in instruments that would perform on-line measurements of chemical composition of aerosol particles with a time resolution of about one hour and be free of sampling artifacts. These systems should be automated and reliable. To be operated in remote locations they should have limits of detection in order of 0.1 $\mu g/m^3$ or lower. Because the size distribution of chemical compounds is important for understanding their environmental effects, these systems should also be able to perform at least a crude size segregation, for instance on sub- and supermicrometer fractions.

Thermodenuders

Thermodenuders provided the first successful means to automate chemical analysis of aerosol species. These devices can be operated automatically and have indeed been used as monitors. The operating principle of thermodenuder systems is that a species is trapped on a suitable, *i.e.* selective denuder coating and liberated by heating the denuder and converting this species into an easy to measure form. It is also possible to use the differences in thermal behavior of atmospheric

components for selective trapping on the denuder coating. The temperature of the coating determines in some cases which component is dissociated and the products adsorbed, eventually followed by sequential conversion by further heating.

As an example, thermodenuder systems used in the study by *ten Brink et al.* [1996a] for automated measurements of ammonium nitrate and ammonium sulfate are described here. Both ammonium nitrate and ammonium sulfate are thermally unstable and fully decompose at elevated temperatures into gaseous components. In the thermodenuders use is made of this property. The mentioned components are volatilized at the appropriate temperatures and treated as gases which can be much more easily analyzed with routine gas monitors.

These instruments have been described elsewhere [*Slanina et al.*, 1985; *Klockow et al.*, 1989] and will be discussed here at some length, using the denuder for ammonium nitrate as the prime example. In the instrument for ammonium nitrate the nitric acid resulting from the volatilisation / decomposition of ammonium nitrate from the aerosol at 135°C is sampled on a coating of $MgSO_4$. The coating is applied by flushing the inside with a solution which is afterwards dried. Fig.2.1 shows this thermodenuder with at its heart the heated section. The thermodenuder tube is of the annular type, consisting of two concentric quartz tubes with outside diameters of 25 and 32 mm. The resulting annular space in-between is 1.5 mm. The total length is 90 cm. This length includes the pre-separator tube for the removal of nitric acid gas, discussed below.

The heating of the thermodenuder is accomplished by an oven which consists of wires of Canthal wound around (quartz tubes). The "oven", with a length of 40 cm, can be moved over a micro switch (Fig. 2.1). After a given sampling time, which is typically thirty minutes, the collection is stopped and the adsorbed nitric acid is subsequently desorbed as nitrogen oxides in a high temperature ramp at 700°C in a flow of air. The desorbed gases (nitrogen oxides) are measured with a conventional NO_x-monitor, which is periodically calibrated with NO.

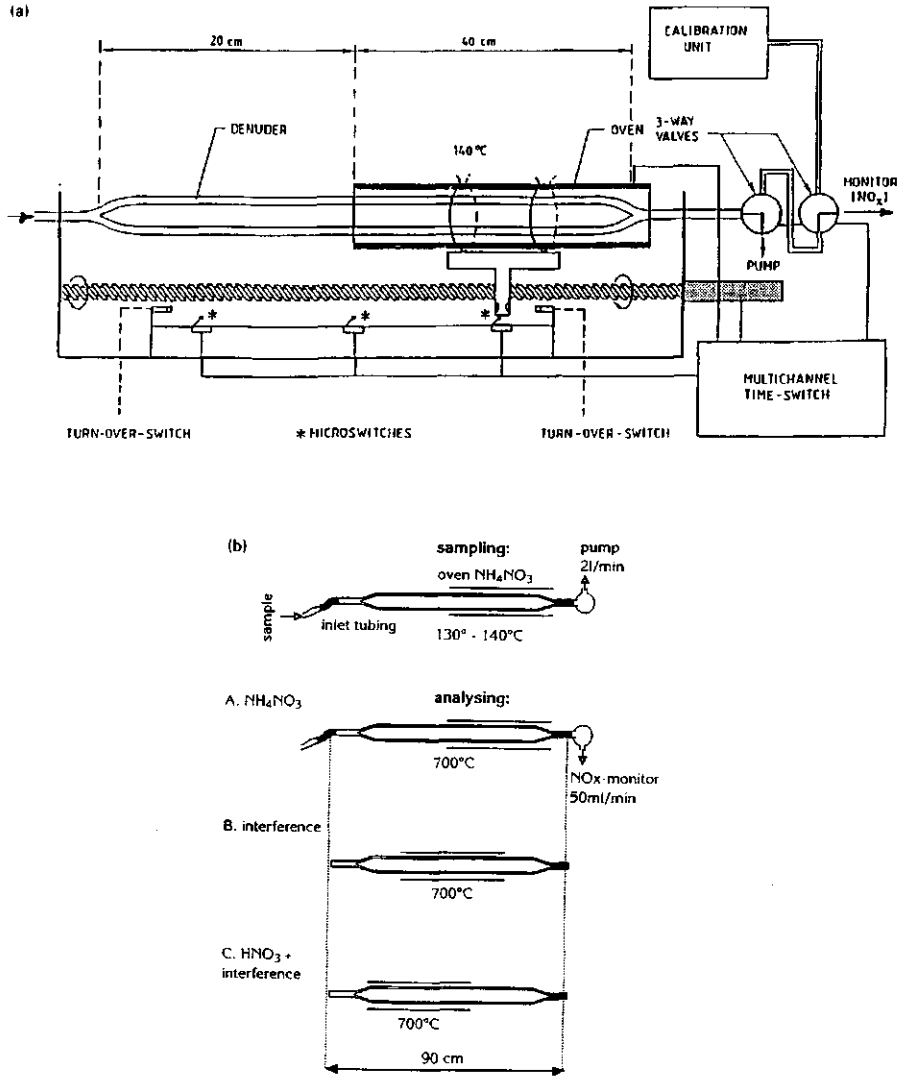

Figure 2.1. *Scheme of the thermodenuder for ammonium nitrate (a) and a schematic view of the measuring cycle (b).*

The integrated signal of the desorbed nitrogen oxides is the measure of the amount of nitric acid absorbed. The system was calibrated using HNO_3 gas from a permeation standard. After the desorption step the denuder is cooled down.

A measurement cycle takes one hour. It was established that both absorption and desorption of the nitric acid were complete for the conditions mentioned. It should be stressed that the part of the tube which serves as a denuder is preceded by an unheated part where gaseous nitric acid gas is removed which would otherwise also be collected and analyzed. This part of the denuder system, incidentally, can be used for determining the nitric acid concentration, as shown in Figure 2.1.

The detection limit of the thermodenuder for ammonium nitrate for the typical sampling time of 30 minutes is about 0.1 $\mu g/m^3$. The comparability of two identical thermodenuder systems was tested for 60 days and it was found that the differences between the two systems were random, with a standard deviation of less than 0.1 $\mu g/m^3$. The performance of the thermodenuder for ammonium nitrate was tested during comparison with other conventional techniques, like denuder - filter packs, which will be described further in this chapter.

The thermodenuder for ammonium sulfate is similar to that for ammonium nitrate, and has been extensively discussed elsewhere [*Klockow et al.*, 1985]. It is operated at the more elevated temperature of 270°C, because ammonium sulfate is less volatile. Also the coating of the thermodenuder tube is of a different material, *viz.* CuO. Sulfur dioxide (SO_2), released in the desorption step at 800°C, is measured with a conventional SO_2-monitor, which is periodically calibrated with sulfur dioxide from a permeation standard.

In the ammonium sulfate thermodenuder the thermodenuder section is preceded by two pre-denuders. In the first, activated carbon captures all gaseous organic sulfur containing components, in the second pre-denuder H_2S is captured on an acidic Ag_2SO_4-coating.

The thermodenuder section consists of two thermodenuder tubes. The first thermodenuder evaporates and captures sulfuric acid aerosol. The second thermodenuder decomposes ammonium sulfate aerosol. The cycle time for the sulfate thermodenuder is the same as that for the ammonium nitrate, one hour.

The thermodenuders were extensively tested by comparing the data averaged over a day with those of 24-hour (denuder) filter pack samples. The tests have shown a good comparability (within 10%) between the two methods for sulfate [*Klockow et al.* 1989].

Steam-Jet Aerosol Collector (SJAC)

The previous section has shown that thermodenuders considerably simplify the measurements of chemical composition of aerosol, providing automated measurement with low detection limits and a time resolution of about an hour, which makes them applicable for monitoring networks. These instruments however allow measurements only of some specific compounds like ammonium nitrate and ammonium sulfate.

Recently a new principle of sampling aerosol particles by means of steam injection with the consequent collection of grown droplets has been developed. This opened the way for artifact-free on-line analysis of practically all water-soluble aerosol species with a time resolution as low as a few minutes. A prototype of an aerosol sampler employing this principle was described previously [*Khlystov et al.*, 1995]. However, since that time the sampler was further improved and new features were added to its operation. For this reason, the instrument and its new features are described here at some length.

General description

A general scheme of the Steam-Jet Aerosol Collector (SJAC) is given in Fig.2.2. First, a wet denuder [*Keuken et al.*, 1988] removes interfering water-soluble gases from the sample air stream. Then the air stream is rapidly mixed with steam inside the mixing reservoir.

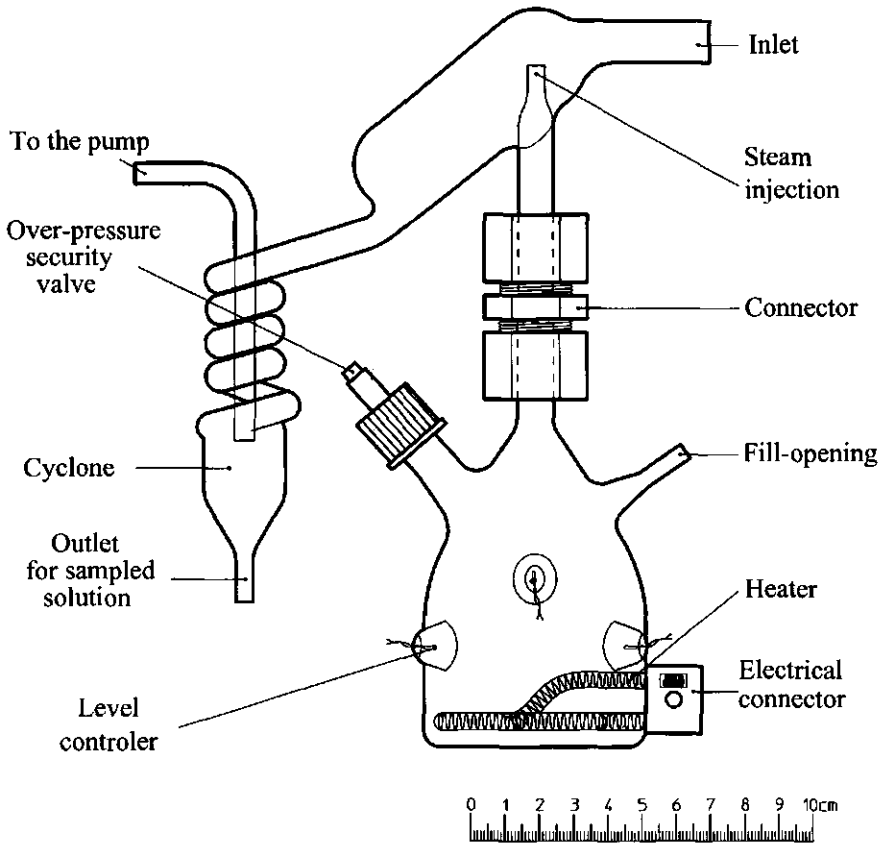

Figure 2.2. *General scheme of the Steam-Jet Aerosol Collector.*

Cooling results in a high supersaturation and causes aerosol particles to grow into large droplets of at least 1 μm in diameter. These droplets containing dissolved aerosol species are then collected in a cyclone with the cutoff diameter of less than 1 μm. The solution collected in the cyclone is constantly pumped out with a peristaltic pump and can be on- or off-line analyzed by means of ion chromatography (IC), flow-injection analysis (FIA) or any other suitable method. Such a system is expected to be free of the artifacts for the following reasons. The wet denuder removes water-soluble gases from the sample air stream, thus avoiding possible interference. Because the sampler collects aerosols by steam injection, any dissociation products (if dissociation ever occurs in the collector) are absorbed in the water, condensing in the collector, and are analyzed together with the collected aerosol solution. Thus evaporative losses common for filters and impactors are also avoided.

Air is drawn into the system by a pump equipped with a critical orifice for 30 *l*/min. The actual flow rate into the sampler is 22.5 *l*/min because of the addition of steam and thermal expansion. After the SJAC a condenser is used to reduce the amount of water entering the pump and to reduce the influence of ambient temperature fluctuations on the flow rate into the sampler.

The sampling efficiency of the sampler was determined with a back-up filter and with a DMPS (Differential Mobility Particle Sizer, TSI Model 3932). Ammonium sulfate aerosol was used as a model aerosol for these experiments. The number and the mass size distributions of the aerosol were measured with the DMPS. The number and mass distributions of the aerosol are given in Fig.2.3. The number geometrical mean diameter lies in the range 0.038 - 0.039 μm and the volume geometrical mean diameter is in the range 0.133 - 0.135 μm. The number concentration of the generated aerosol was rather high, approximately 60000 cm^{-3}, but for the purpose of testing it was not of importance, as the higher the number concentration is, the more difficult it is to induce growth of all droplets to the required size.

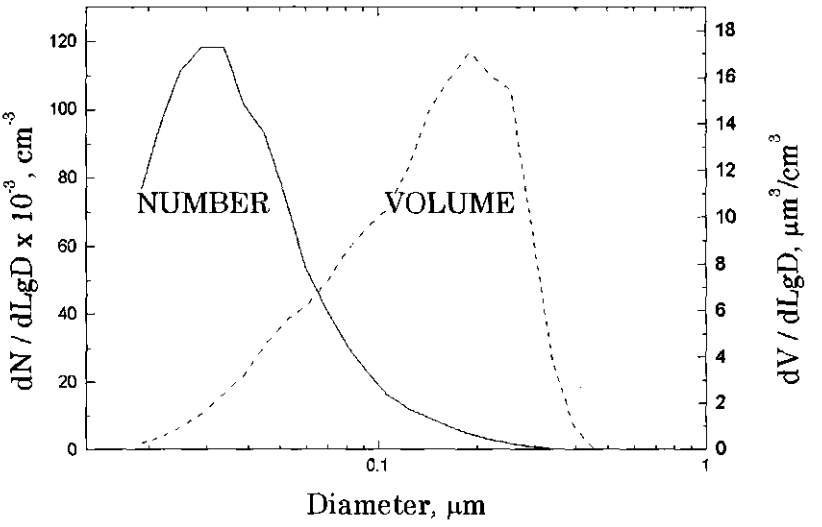

Figure 2.3. *Number and mass distributions of model ammonium sulfate aerosol used for testing the Steam-Jet Aerosol Collector.*

To determine the mass sampling efficiency of the instrument a filter was placed between the cyclone and the condenser. The sampling efficiency was determined as the ratio of the aerosol mass collected by the sampler to the mass collected both in the sampler and on the back-up filter. The efficiency was found to be better than 99%.

The DMPS was also used to determine the sampling efficiency and to find out to which size particles are sampled in the system. The sampling efficiency was determined from a comparison of dry size spectra of the aerosol found behind the cyclone with and without steam injection. To find the optimum steam injection rate, the spectra were recorded at different steam input rates. A comparison of size spectra is given in Figure 2.4. The steam injection rate of 3.5 g/min was found to

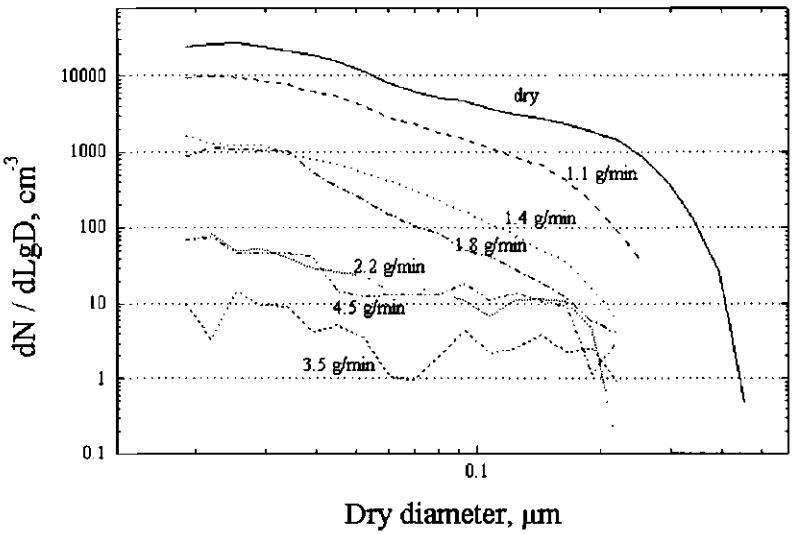

Figure 2.4. *Comparison of number size distributions of model ammonium sulfate aerosol found behind the SJAC at different steam injection rates.*

be optimal as the number concentration in any size class does not exceed 0.12% of the concentration without steam injection. Thus, it is concluded that the sampler collects more than 99% of the total aerosol number in the size range 0.019 through 0.886 µm, which is in good agreement with the filter measurements.

Because no handling of the samples is required, the blanks of the sampler are low and the detection limit for ammonium, sulfate, nitrate and chloride ions is around 10 ng/m^3. The sampler proved to be stable, working without any assistance for days, which makes it suitable for measurements in background locations. The next step in the development of the instrument was a construction and testing of a unit based on a SJAC sampler for on-line analysis of the aerosol species.

Combination with an on-line IC and FIA units

A combination of a SJAC sampler and an automated IC and an FIA-unit has been built and tested. The automated IC and FIA units have been developed especially to be coupled to samplers of the SJAC type with the aim to be operated in the field for long periods without much maintenance and are described elsewhere [*Wyers et al.*, 1993; *Oms et al.*, 1996]. The sample stream (*e.g.* produced by the SJAC at a rate of 1 to 2 ml per minute) is split into two lines. One is pumped to the IC and the other - to the FIA ammonium detector.

This instrument has the following characteristics:

- Time resolution is about 15 minutes.
- Accuracy depends on the measured concentrations and is between 1 and 5 % relative.
- An internal standard is used for calibration of the IC and FIA and provides quality assurance and quality control.
- Detection limits are in the order of a few ppb in the sample.
- The blanks of the system are at the level of a few ppb or less.
- The sensitivity of the analytical method in combination with a high sample flow of the SJAC (20 *l*/min), low blanks of the sampling and analytical procedures leads to detection limits below 20 ng/m^3 for ammonium, sulfate, nitrate and chloride in aerosols.

The system has been checked against a reference denuder - filter pack method with laboratory generated (stable) ammonium sulfate and (unstable) ammonium nitrate aerosols. These compounds were chosen because they are the most abundant species in the ambient aerosol. The comparison gave very good results for both of the compounds, which will be described further in this chapter.

It is obvious that this kind of rather complicated analytical machinery will always require regular attention and maintenance, but the system can be operated continuously on the basis of two checkups

per week and was successfully tested during a field campaign in the Netherlands.

Adaptation for size segregated measurements

During the discussion of size distribution of ammonium nitrate in ambient aerosol earlier in this chapter it was shown that artifact-free sampling methods for determination of the aerosol composition as a function of size are required for assessing environmental effects of air pollution. The usual method for size segregated chemical analysis - imactors - requires extensive manual handling, which results in high processing costs and contamination during the handling which makes their application for network measurements practically impossible. In addition, impactors suffer from losses of volatile aerosol components, like ammonium nitrate [*ten Brink et al.*, 1996b,c].

New, artifact-free sampling methods for determination of the aerosol composition as a function of size are urgently needed. A combination of a pre-separator (impactor) and a Steam-Jet Aerosol Collector (SJAC), is very promising in this respect. Such a system is expected to be free of the artifacts arising, for instance from evaporation of ammonium nitrate, for the following reasons. The wet denuder removes water - soluble gases from the sample air stream, thus avoiding a positive artifact. Because a SJAC sampler collects aerosols by steam injection, any dissociation products (if dissociation ever occurs in the collector) are absorbed in the water, condensing in the collector, and are analyzed together with the collected aerosol solution. Thus evaporative losses common for filters and impactors are also avoided. Dissociation products arising from evaporation in the impactor are also absorbed in the wet denuder together with other water-soluble gases. This avoids an under-sizing error.

A system, consisting of a Berner impactor [*Berner et al.*, 1979] followed by a wet denuder - SJAC system, was tested using laboratory generated ammonium sulfate and ammonium nitrate aerosols. Air sampled at a flow rate of 19 *l*/min passes the Berner impactor. The impactor removes particles that are larger than the cutoff diameter of

the lowest stage. Smaller particles pass the wet-denuder and are quantitatively collected in the SJAC. By changing the lowest cutoff diameter of the impactor a cumulative size distribution of water-soluble aerosol species can be obtained. Impactor stages with cutoff diameters of 0.25, 0.5 and 1 μm were tested. Operation using stages with cutoff diameters of 0.06 and 0.125 μm was not possible because of the very high pressure drop across these stages of up to 0.5 atm, which disturbed the operation of the wet denuder.

Because of the under-pressure after the impactor a possibility exists that the sampling efficiency of the impactor - SJAC combination is lower than at normal conditions. The collection efficiency of the impactor - SJAC was determined by measuring the particle number concentration behind the collector with a CPC 3010 (TSI Inc.). It was found that collection efficiency is not affected by the under-pressure and is 99.9% (in number) for particles down to a few nanometers in diameter.

To check the absence of a positive artifact resulting from evaporation of ammonium nitrate from the impactor the following test was done. The impactor plates were loaded with ammonium nitrate. The loaded plates were then installed into the impactor in front of the wet-denuder - SJAC system and a particle free air was sampled for a few hours. No signal was observed in the SJAC system, indicating that no gaseous compounds originating from the impactor plates were reaching the collector.

Comparison with filter pack and denuder measurements

An ammonium nitrate thermodenuder system and an online SJAC-IC system were checked against a reference denuder - filter pack method using laboratory generated (stable) ammonium sulfate and (unstable) ammonium nitrate aerosols. These compounds were chosen because they are the most abundant species in the ambient aerosol. Simultaneous measurements with a Berner cascade impactor [*Berner et al.*, 1979] were also performed.

The aerosol was produced by spraying a water solution of one of the salts using a Wiesbadener nebulizer. This nebulizer was chosen because of the remarkable stability of its output. The stability of the output was monitored with an integrating nephelometer (MRI 1562) and was stable during a day of measurements within about 15%. The output of the nebulizer was mixed with a ten-fold excess of dry (relative humidity below 10%) particle-free air to dry the aerosol. The dry aerosol mass size distribution was centered at 0.3 - 0.5 μm in diameter, depending on the concentration of the sprayed solution which was measured with an SMPS system (TSI Inc.). Then the aerosol-laden stream (about 100 *l*/min) was introduced into a tunnel where it was homogenically mixed with a 500 *l*/min ambient air stream from which the aerosols were removed by means of an absolute filter. The resulting relative humidity in the tunnel was about 50%. The instruments were sampling from the tunnel, with the inlets positioned close to each other.

A dry NaF-coated denuder was used in front of the filter packs to avoid interference by gaseous compounds. The filter-packs consisted of a Teflon filter, for aerosol collection, followed by NaF- and H_3PO_4 - impregnated filters, for collection of gaseous HNO_3 and NH_3 resulting from evaporation of the aerosol collected on the Teflon filter. After collection the filters were rinsed with a 7 ml of doubly demineralyzed water in an ultrasonic shaker. The obtained solutions were subsequently analyzed by means of ion chromatography (the NH_3-content was not analyzed).

The results for ammonium sulfate and ammonium nitrate aerosols are summarized in Figures 2.5 and 2.6, respectively. The concentrations obtained with the SJAC were on average identical to the results obtained with the filter-packs within the combined experimental error of the two methods which is estimated at 10%. Ammonium sulfate concentrations according to the impactor measurements were also identical to the concentrations obtained with the filter-packs within the experimental error. However, in case of ammonium nitrate the impactor shows larger deviations from the values obtained with the filter-packs, obviously due to losses of ammonium nitrate from the impactor stages. The ammonium nitrate

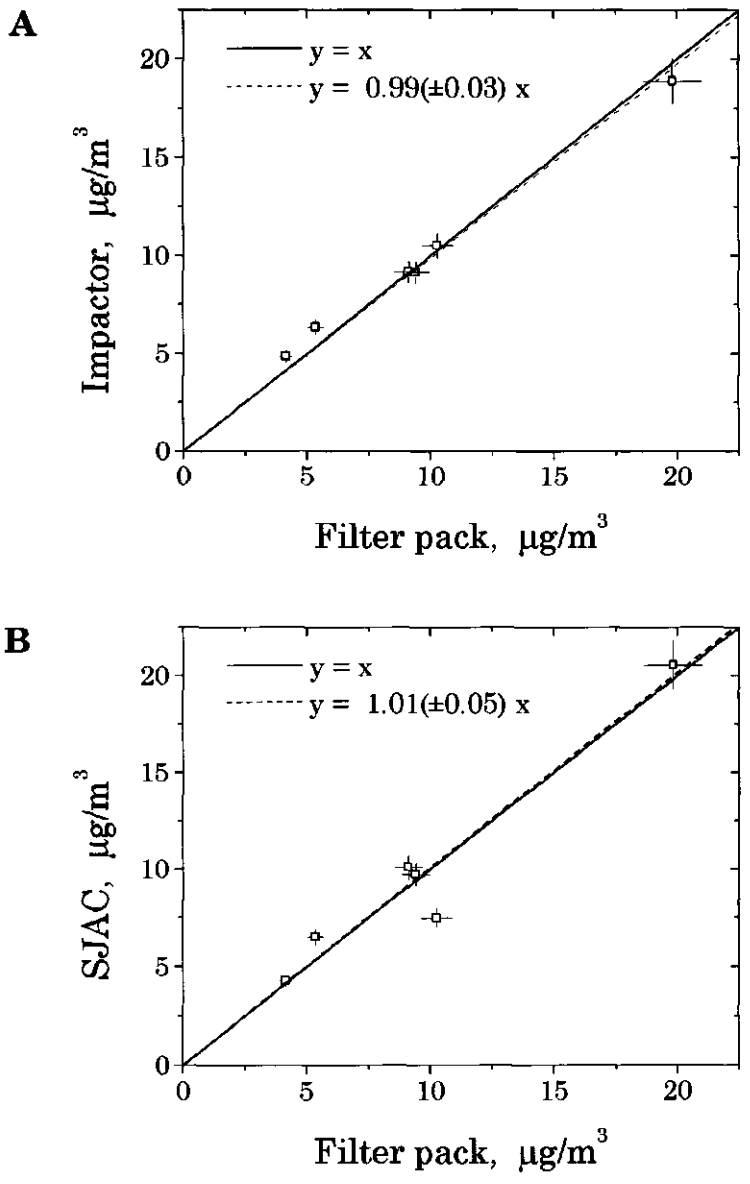

Figure 2.5. *Comparison of Berner impactor (a) and on-line SJAC sampler (b) with filter pack measurements of ammonium sulfate aerosol.*

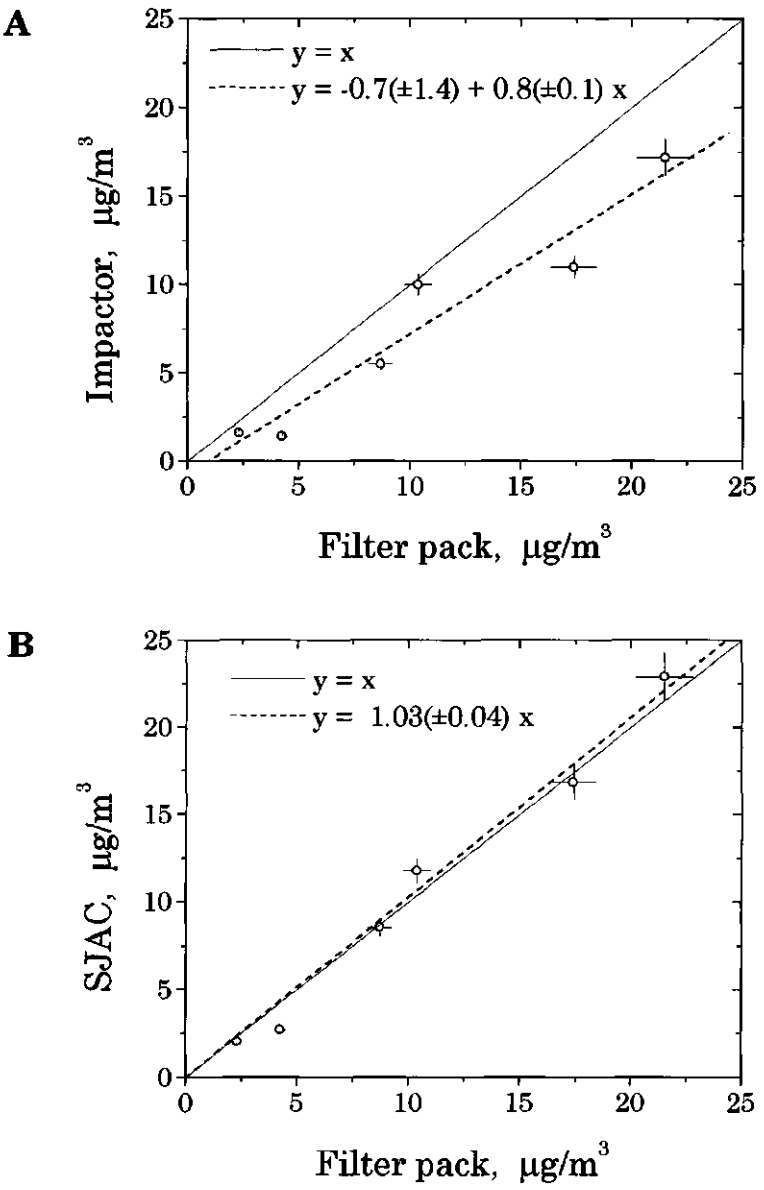

Figure 2.6. *Comparison of Berner impactor (a), on-line SJAC sampler (b) and thermodenuder (c) with filter pack measurements of ammonium nitrate aerosol.*

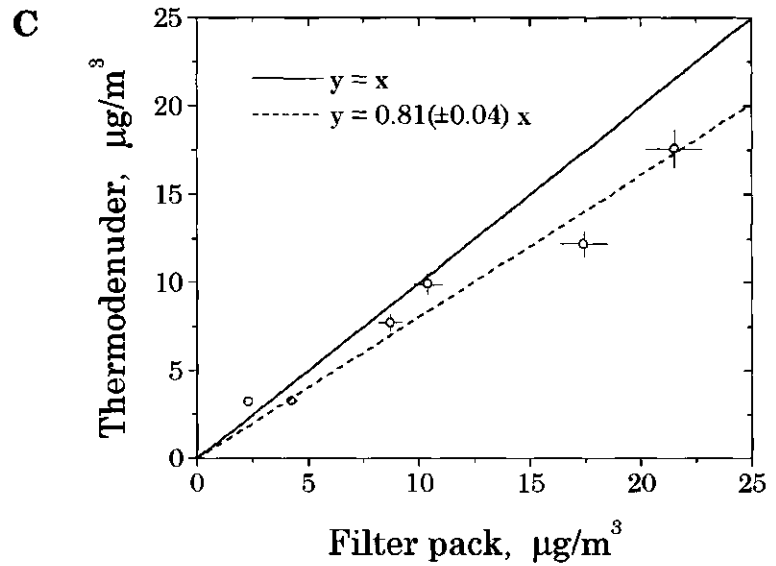

Figure 2.6. *(Continued) Comparison of Berner impactor (a), on-line SJAC sampler (b) and thermodenuder (c) with filter pack measurements of ammonium nitrate aerosol.*

thremodenuder shows a good comparison with the filter-pack at concentrations lower than about 15 µg/m^3. At higher concentrations, however, the thermodenuder indicates lower concentrations, which is due to the saturation of the denuder coating and the resulting lower retention efficiency. This was due to the sampling time of 1.5 hours which is used for low aerosol concentrations (below 10 µg/m^3). For higher aerosol concentrations a shorter sampling time should be used.

The SJAC sampler was compared with filter packs also during a number of measurements of ambient aerosol. Two wet denuders were placed in front of the sampler to remove water-soluble gases. The first was a denuder with a carbonate solution for sampling acidic species.

The second contained formic acid for sampling ammonia. The SJAC was operated in the off-line mode: the aerosol solution was collected in test tubes each 15 minutes and was subsequently analyzed by means of ion chromatography and flow-injection analysis. The filter packs consisted of a Teflon filter, NaF- and H_3PO_4 - coated filters. Two dry annular denuders (NaF- and H_3PO_4 -coated) were used in front of the filter packs to avoid interference by gaseous compounds. The filters sampled for 2 hours each. The inlets of both systems were put next to each other. The SJAC was sampling at a rate of one sample per 15 min. The samples were then off-line analyzed by means of IC and FIA. The data were averaged per 2 hours and then compared to the data from the simultaneous filter pack measurements.

The results of the measurements are summarized in Table 2.1 and Figure 2.7. The experiments gave very good comparison results. Except for an outlier on 10 September, the average difference between the two methods for ammonium was 9%, for sulfate - 5% and for nitrate - 11%. The difference in concentrations of NH_4^+ and NO_3^- on 10 September is most probably explained by losses of ammonium nitrate particles in the dry annular denuders. The comparison for chloride is problematic,

Table 2.1. *Comparison of SJAC with filter packs (FP) during ambient aerosol measurements.*

Date	NH_4^+		SO_4^{2-}		NO_3^-		Cl^-	
	SJAC	FP	SJAC	FP	SJAC	FP	SJAC	FP
10.09.92	4.7	3.0	4.3	4.6	9.1	5.7	0.4	0.1
11.09.92	4.7	4.3	4.7	4.7	7.9	7.1	0.6	0.7
11.09.92	1.9	2.0	3.1	3.2	2.6	2.3	2.0	3.0
17.09.92	2.2	2.3	1.7	1.7	5.7	5.2	2.4	1.7
17.09.92	6.3	6.0	5.0	5.5	10.7	10.8	0.7	0.8
18.09.92	7.5	7.1	5.8	6.3	14.6	13.3	0.8	1.1
18.09.92	10.3	10.1	8.4	8.2	18.9	21.1	1.7	2.4
27.09.92	1.8	2.2	4.1	3.8	1.8	2.1	1.9	3.1
27.09.92	1.8	2.3	3.1	3.0	2.1	2.6	1.1	2.7

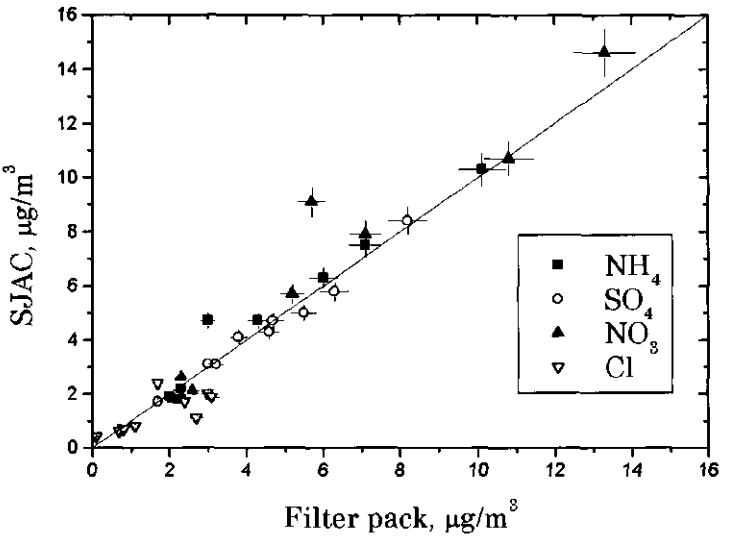

Figure 2.7. *Comparison of SJAC sampler with filter pack measurements of ambient aerosol.*

because of the low chloride concentrations on those days. Concentrations of chloride found with the filter packs were on average higher than found with the SJAC, most probably due to the contamination during the handling of the filters.

Environmental implications

The facts discussed in the previous sections have several major environmental implications.

It has been shown that in the Netherlands, and by deduction in the West Europe, the contribution of nitrate to the direct radiative forcing is of the same order as that of sulfate or even higher. There are indications that a similar situation is found in some parts of the USA

[*Trijonis et al.*, 1990]. Because nitrate was assumed to be present only in supermicrometer particles, and for this reason neglected in climate models, it is clear that the current estimates of the direct radiative forcing are too low.

In order to assess the radiative cooling by anthropogenic aerosols both the size and the chemical composition of the aerosols must be known. The chemical composition influences not only the optical properties of aerosols but also their hygroscopic properties (whether particles will grow by the uptake of water vapor by the hygroscopic compounds of the aerosol), which also has a major enhancing effect on the light scattering by aerosols (see further in this chapter). However, measurements of concentration and size distribution of ammonium nitrate are complicated by sampling artifacts due to volatility of this compound. Measurements of bulk compounds in aerosols in The Netherlands with new techniques that avoid artifacts (see previous sections) lead to the conclusion that the mass of nitrate in aerosol is about the same as sulfate or even slightly higher. *Simon and Dasgupta* [1995] have applied a sampling instrument, which is quite similar to the SJAC, to measurements of ambient aerosols in Lubbock, Texas. Their results indicate the same situation: concentrations of nitrate in aerosol are higher than the sulfate concentrations at that location in the USA. This suggests that nitrate concentrations reported in the literature are most probably underestimated. As only a very limited set of measurements, which are not influenced by the artifacts, is available, it is not possible to draw a general conclusion with certainty. However, the conclusion is warranted that artifact-free characterization of bulk elements in aerosol regarding total composition as well as size distribution should have a high priority.

The contribution of particulate nitrate to acid deposition and eutrophication is generally estimated to be low. If nitrate concentrations are higher than assumed and as indications exist that the deposition velocity of small particles is also higher than formerly reported [*BIATEX*, 1996], the contribution of particulate nitrate to deposition and eutrophication is probably much higher than generally assumed.

EFFECTS OF HYGROSCOPIC GROWTH

Another source of uncertainty in quantification of the aerosol radiative forcing is the influence of the relative humidity on the aerosol light-scattering [*Charlson et al.*, 1992; *Kiehl and Briegleb*, 1993]. In the previous sections it was demonstrated that ammonium sulfate and ammonium nitrate are the main aerosol constituents in the Netherlands responsible for the direct radiative forcing. Both ammonium sulfate and ammonium nitrate are hygroscopic salts. Aerosol particles containing hygroscopic salts absorb water in humid conditions [*e.g. Twomey,* 1977a] which results in considerable growth in size. The size changes induced by the hygroscopic growth result in a strong increase in the light scattering by the particles [*Rood et al.*, 1989; *Nemesure et al.*, 1995; *Pilinis et al.*, 1995; *Veefkind et al.*, 1996]. For this reason, hygroscopic behavior of aerosols is of major importance for the direct radiative forcing.

The importance of hygroscopicity, however, is not limited to the direct aerosol effect. Hygroscopicity of aerosol particles plays a major role in cloud droplet formation [*e.g. Twomey*, 1977a] and thus is relevant to the indirect aerosol effect also. The hygroscopic growth also effects deposition velocity of particles and, hence, their life time, because dry deposition and precipitation via uptake in clouds are the major sink mechanisms of aerosols. The effect of hygroscopic growth on dry deposition velocity will be briefly discussed further in this chapter. All this makes hygroscopicity of aerosol particles a very important environmental issue. Because a major part of the work covered in this thesis was devoted to an experimental assessment of cloud forming properties of ambient aerosols in the Netherlands in relation to the indirect aerosol radiative forcing, hygroscopic behavior of aerosols is discussed here at some length. The effect of the hygroscopic growth on the direct radiative forcing by anthropogenic aerosol in the Netherlands is demonstrated on the basis of the work done by *ten Brink et al.* [1996a] and *Veefkind et al.* [1996].

Deliquescence and hysteresis

Upon exposure to moist air aerosol particles composed of water-soluble substances exhibit the phenomenon of deliquescence [*Twomey*, 1977a; *Tang*, 1980]. Deliquescence is the fast phase transition from a solid particle into a liquid drop, which occurs only when the relative humidity reaches a certain value. The relative humidity of this transition (usually referred to as the relative humidity of deliquescence) is the relative humidity above the saturated solution of the substance composing the particle and is specific for every chemical compound. The relative humidity of deliquescence of inorganic salts, that are found in the local ambient aerosol, see Appendix 1, are given in Table 2.2. Because the solubility of a salt depends on temperature, so does the relative humidity of deliquescence. However for the range of ambient temperatures, this dependence usually may be neglected. A few electrolytes, which have infinite solubility in water (*i.e.* can be mixed with water in any proportions), such as sulfuric acid, tend to adsorb water at any relative humidity and, consequently, do not deliquescence.

Table 2.2. *Relative humidity of deliquescence of some inorganic salts found in ambient aerosols (at room temperature).*

Salt	*Twomey* [1977a]	*Pilinis et al.* [1989]
$(NH_4)_2SO_4$	80	80
NH_4NO_3*		62
Na_2SO_4	91	93
NaCl	76	76
$NaNO_3$		74

* It should be noted that deliquescence of ammonium nitrate aerosol was not observed experimentally [*Tang*, 1980]. The relative humidity above the saturated salt solution of NH_4NO_3 is given.

Aerosols composed of several salts (the so-called internally mixed aerosols) exhibit similar behavior to single component aerosols [*Tang*, 1976]. As the relative humidity (RH) increases, the salt mixture is a solid until the relative humidity reaches the deliquescence of one of the salts in the mixture. At this point the substance absorbs water until a saturated aqueous solution of that salt is formed. This aqueous solution causes the partial dissolution of the rest of the species, with their distribution between the solid and the liquid phases governed by thermodynamic equilibrium. As the relative humidity increases, the deliquescence point of the second salt is reached and additional water is added into the system. The deliquescence point of a salt in a multicomponent solution occurs at a relative humidity lower than its deliquescence point in a single component system [*Wexler and Seinfeld*, 1991]. As an example the relative humidity of deliquescence of atmospherically relevant salt pairs at their eutonic point are given in Table 2.3.

After deliquescence wet particles absorb water and grow to a certain equilibrium size. If the relative humidity of the environment is lowered, particles loose water and become smaller. The changes of size with relative humidity will be considered in the following sections.

Table 2.3. *Deliquescence relative humidity at eutonic point at 303°K of some salt mixtures [Tang, 1976].*

Mixture	RH, %
$NH_4NO_3 + (NH_4)_2SO_4$	62.3
$NH_4NO_3 + NaCl$	42.2
$NH_4NO_3 + NaNO_3$	46.3
$NaNO_3 + NaCl$	67.6

When the relative humidity is reduced below the deliquescence point, particles do not dry, but stay as droplets of a supersaturated salt solution. Only at a relative humidity well below the deliquescence point particles crystallize and become dry. This behavior is known as the hysteresis effect. The relative humidity at which crystallization occurs (also called efflorescence relative humidity) is specific for each compound. For $(NH_4)_2SO_4$ it is at about 39%, for NH_4HSO_4 it is at about 2% [*Tang and Munkelwitz*, 1994]. The crystallization relative humidity of NH_4NO_3 is below 10% [*ten Brink et al.*, 1996a]. Due to the hysteresis effect it is often difficult to tell whether particles are wet or dry, if the environment is at a relative humidity between that of deliquescence and that of crystallization. To do that, one should know the previous history of the environmental humidity. In the troposphere, especially its lowest part - the boundary layer, where most of the pollution is concentrated, particles can be expected to be most of the time in the wet state because the relative humidity rarely becomes sufficiently low to initiate crystallization of wet particles [*Rood et al.*, 1989].

The Köhler equation

A wet particle is in equilibrium with its environment, if the water vapor pressure at the particle surface is equal to the vapor pressure in the gas phase. The relation between the so-called saturation ratio (ratio of the environmental water vapor pressure to the saturation water vapor pressure above a plane surface) and the wet size of the particle is given by the Köhler equation [*e.g. Pruppacher and Klett*, 1978]:

$$S = \frac{p}{p_{sat}(T)} = \exp\left(\frac{2\,\sigma\,M_w}{\rho_w\,R\,T} - \frac{i\,\varepsilon\,\rho_{dry}\,r_{dry}^3\,M_w}{(\rho_{sol}\,r^3 - \rho_{dry}\,r_{dry}^3)\,M_s}\right) \qquad 2.2$$

in which S is the saturation ratio, p is the water vapor pressure above the particle surface, $p_{sat}(T)$ is the saturation vapor pressure above a flat surface of water at temperature T. r is the wet radius, r_{dry} is the dry radius. ε is the mass fraction of water-soluble salt in the particle. σ is the surface tension, M_w and M_s are, respectively, the molecular weights of water and water-soluble salt, comprising the particle. ρ_w, ρ_{dry} and ρ_{sol}

are, respectively, the density of water, salt and solution. R is the gas constant. i is the van't Hoff factor - the degree of ionic dissociation of the salt, which can be defined through the relation [*McDonald*, 1953]:

$$a_w = \frac{n_w}{n_w + i n_s} \qquad 2.3$$

in which a_w is the activity of water in the solution, n_w and n_s are the number of moles of water and salt, respectively.

The first term on the right side of Eq.2.2 represents the enhancing effect of the surface tension due to the curvature of the particle surface (the so-called Kelvin effect), while the second term corresponds to lowering of the vapor pressure due to the dissolved matter (the so-called Rault's effect).

The van't Hoff factor is not constant and decreases with increasing solute concentration [*McDonald*, 1953]. For this reason one is tempted to use the correct van't Hoff factor at every solute concentration and substitute it into Eq.2.2. However, *Young and Warren* [1992] have shown that more accurate results are obtained by using a constant value of the van't Hoff factor at infinite dilution, than using a variable van't Hoff factor.

The plot of the saturation ratio of water vapor at the particle surface versus the radius (or diameter) of the particle is called the Köhler curve. An example of the Köhler curve is given in Fig.2.8. One of the features of the Köhler curve is that the saturation ratio has a maximum value (Fig.2.8b). The saturation ratio increases with the droplet size first, until the so-called critical point is reached after which the saturation ratio gradually decreases. The saturation ratio and the size corresponding to the critical point are called the critical size (critical radius or diameter) and the critical supersaturation. The critical point can be found by differentiating the Köhler equation with respect to size and putting the differential equal to zero [*Twomey*, 1977a]:

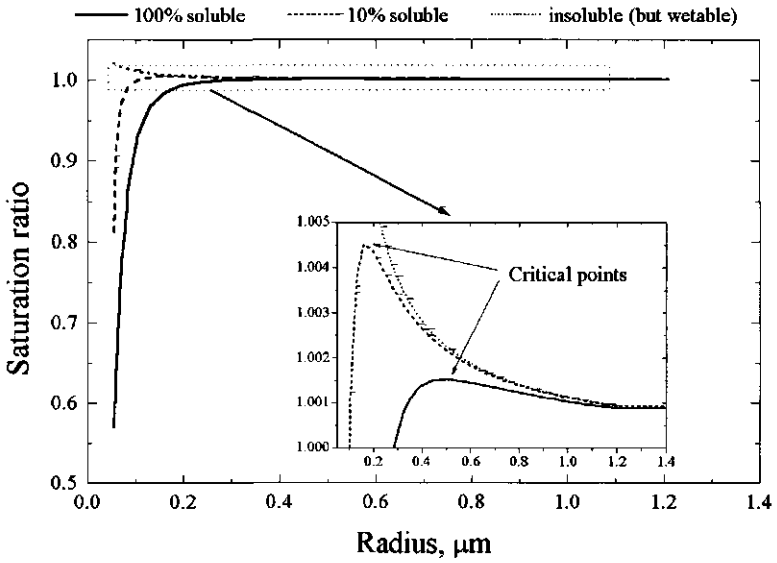

Figure 2.8. *The Köhler curve of an ammonium sulfate particle (dry radius 0.05 μ m) with different mass fractions of soluble material. Also the Köhler curve of an insoluble, but wetable particle is given.*

$$r_{crit} = \sqrt{\frac{3B}{A}} \qquad 2.4$$

$$S_{crit} = 1 + \frac{2}{3}\sqrt{\frac{A^3}{3B}} \qquad 2.5$$

in which:

$$A = \frac{2\,\sigma\,M_w}{\rho_w\,R\,T} \qquad 2.6$$

$$B = \frac{i\,\varepsilon\,\rho_{dry}\,r_{dry}^3\,M_w}{\rho_w\,M_s} \qquad 2.7$$

The second term on the right-hand side of Eq.2.5 represents a value above the saturation point (S = 1) and is usually called the critical supersaturation. The smaller the particle and the smaller its water-soluble content, the higher its critical supersaturation (Fig.2.8b).

The Köhler curve shows that between the relative humidity of deliquescence and relative humidity of 100%, there is only one equilibrium state. If a relative humidity is above 100%, particles may have no or two equilibrium states: one stable (below the critical point) and one unstable (above the critical point). Relative humidity above 100% represents supersaturated conditions, which are encountered in clouds and fogs. If a particle is at a supersaturation that is higher than its critical supersaturation, equilibrium is not possible at all. This is because the vapor pressure at the droplet surface will be always lower than that in the environment. The difference in vapor pressures will cause the vapor to condense onto the droplet and the growth will continue infinitely, as long as there is sufficient vapor to provide for condensation. This process is usually called cloud activation and will be discussed in more detail further in this thesis in a chapter dealing with the indirect aerosol effect.

If the supersaturation in the environment is lower than the critical point of a particle and the particle is in equilibrium below the critical point (*i.e.* its size is smaller than the critical size), the equilibrium is stable. Above the critical point the equilibrium is unstable. For example, suppose the particle has a size larger than its critical size and is in equilibrium with the (supersaturated) environment. Assume that a small fluctuation causes a few molecules of water to be added to the particle. This will cause the saturation ratio at the surface to decrease which, in turn, will cause the water flux towards the particle to continue and the droplet will continue to grow, which is similar to the phenomenon of cloud activation mentioned above. On the other hand, the reverse can happen with the same probability. If a fluctuation causes a few molecules of water to evaporate from the particle, the saturation ratio at the surface will increase which will accelerate the water flux from the particle and the droplet will evaporate until a stable equilibrium is achieved below the critical point.

Equilibrium sizes

The saturation ratio is, in fact, the relative humidity, if expressed in percent units. Consequently, the Köhler equation gives the equilibrium sizes of hygroscopic particles as a function of relative humidity. The increase in size due to the hygroscopic growth for ammonium sulfate particles is demonstrated in Fig.2.9. Ammonium sulfate was chosen because this is one of the dominant compounds in the ambient aerosol. Figure 2.9 shows that the relative humidity has a drastic effect on the size of the particle which is exponentially increasing with increasing relative humidity. The increase in size is especially pronounced in the region close to 100%.

The equilibrium vapor pressure over a droplet of a given composition and size can be readily calculated using equation 2.2, but the inverse problem of calculating the equilibrium size requires solving

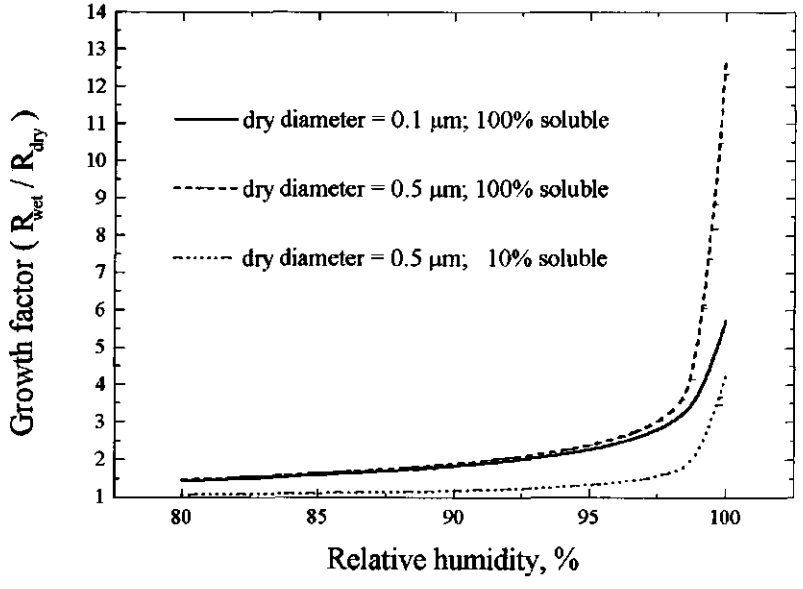

Figure 2.9. *Growth factors of ammonium sulfate particles versus relative humidity.*

equation 2.2 numerically for r. Though the numerical solution with a very good accuracy takes a very short time even on a personal computer, one may use approximation formulas for equilibrium sizes of aerosols which were developed to simplify the calculations. *Fitzgerald* [1975] has derived an approximation formula for calculating equilibrium sizes of aerosol particles composed of inorganic salts like $(NH_4)_2SO_4$, NaCl and NH_4NO_3. The formula is applicable for dry aerosol diameters from 0.05 to 3.0 μm and for a relative humidity between 81% and 99.5%. The formula approximates equilibrium sizes with accuracy within 5%.

The chemical composition of atmospheric aerosols, however, is highly complex, and varies considerably with time and place. For this reason one may doubt the application of the Fitzgerald approximation to ambient aerosols. For atmospheric aerosols *Winkler* [1973] has derived a semi-emperical formula based on a set of (mass) growth curves of 28 impactor samples collected near Mainz, Germany. Because impactors do not allow to distinguish differences in chemical composition of separate particles, it was assumed that all or at least most of the individual particles consist of the same mixture of substances. However, it was shown by other researchers that atmospheric aerosols can represent an external mixture of soluble and insoluble material [*McMurry and Stolzenburg*, 1989; *Svenningsson et al.*, 1994]. More hygroscopic particles will grow to larger sizes than the less hygroscopic particles, which makes the above assumption questionable.

For a comparison, the growth curves of a soluble particle calculated with the Winkler model and of an ammonium sulfate particle calculated with the Fitzgerald model and using Eq.2.2 are given in Fig.2.10. The dry radius is 0.5 μm, and the density of the dry particle was assumed to be 2 g/cm^3 (this assumption was necessary to translate size to mass). Both models demonstrate a similar effect of the relative humidity on the particle size. The differences between equilibrium sizes of ambient particles calculated with the Winkler model and those of ammonium sulfate particles may be attributed to the differences in chemical composition. Given the variability and uncertainties in

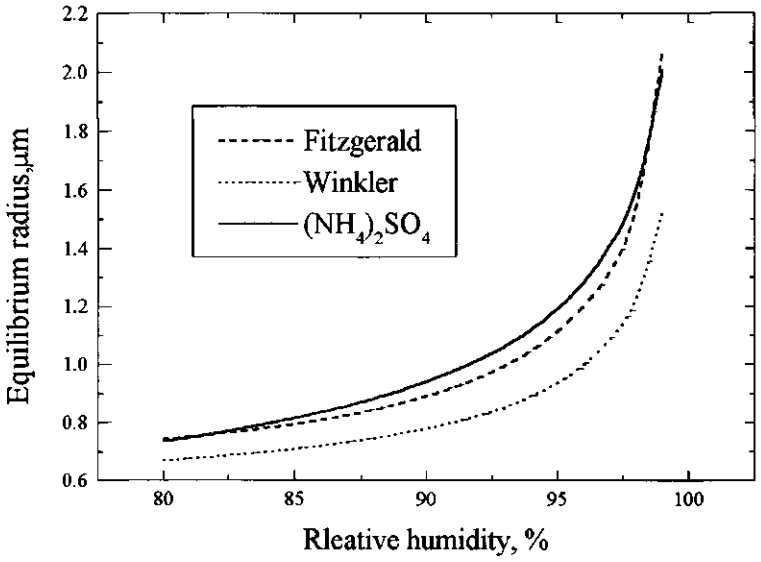

Figure 2.10. *Growth curves of atmospheric particle calculated with the Winkler model and ammonium sulfate particle calculated with the Fitzgerald approximation and using Eq.2.2.*

chemical composition of the ambient aerosol these differences may be neglected and one may estimate the equilibrium sizes of ambient particles using the sizes of, for example, ammonium sulfate aerosol.

One important conclusion can be drawn from Figure 2.10. It demonstrates that, similarly to pure-salt aerosols, ambient aerosol particles considerably change their size with the relative humidity. The strong effect of the relative humidity on sizes of atmospheric particles was experimentally demonstrated using the tandem differential mobility analyzers [*McMurry and Stolzenburg*, 1989; *Svenningsson et al.*, 1994] and the so-called humidity controlled nephelometry [*Rood et al.*, 1989; *Veefkind et al.*, 1996]. As will be discussed further in this thesis, it is this dependence of size on the relative humidity that makes the hygroscopicity of ambient particles very important for environmental issues.

Kinetics of hygroscopic size changes

To evaluate the influence of the hygroscopic growth on the size of ambient particles, one should know how fast particles adjust themselves to changes in the environmental relative humidity. For instance, for the direct aerosol effect it is necessary to know how fast particles adjust their size to changes in the relative humidity in the atmospheric boundary layer, where most of the anthropogenic pollution is situated. The times scales in this case are in the order of a few minutes to a few hours. For the indirect aerosol effect the time scales of cloud formation, in the order of minutes, are relevant. Kinetics of the hygroscopic growth is briefly discussed in this section.

The transport of mass to or from a wet particle is caused by the difference between vapor densities (or pressures) in the environment and on the surface of the droplet. The steady state mass change rate of a droplet, motionless relative to an infinite, uniform medium, is equal to the net vapor flux at the drop surface and is given by the maxwellian equation [*Fuchs*, 1959]:

$$\frac{dm}{dt} = 4\pi r D_v (\rho_\infty - \rho_r) \qquad 2.8$$

in which m is the mass of the drop, t is time, r is droplet's radius, D_v and ρ denote the diffusion coefficient and the density of water vapor. The subscripts r and ∞ denote parameters describing the droplet and the environment, respectively. It should be noted that the diffusion coefficient should be corrected for gas kinetic effects [*Pruppacher and Klett*, 1978], but because this correction is of the order of a few percent it is not considered here for the sake of simplicity. This equations can be expressed in terms of the vapor pressure p and temperature T by applying the universal gas law:

$$\frac{dm}{dt} = 4\pi r \frac{D_v M_w}{R} \left(\frac{p_\infty}{T_\infty} - \frac{p_r}{T_r} \right) \qquad 2.9$$

Neglecting the density change rate (which is especially valid for dilute solutions), the mass change rate can be expressed in terms of the radius change rate:

$$\frac{dr}{dt} = \frac{D_v M_w}{r \rho R} \left(\frac{p_\infty}{T_\infty} - \frac{p_r}{T_r} \right) \qquad 2.10$$

Water vapor transport to or from a droplet necessarily involves the flow of heat as well, owing to release or consumption of latent heat. In a growing droplet, the condensation of water vapor will cause the droplet to warm up relatively to the environment due to release of the latent heat. The increase in temperature will increase the vapor pressure at the surface which, in turn, will slow down the growth. The difference in temperature, on the other hand, will cause a sensible heat flux from the droplet to the environment and the difference in temperatures will decrease. In the steady state the latent heat flux equates the sensible heat flux:

$$L_h \frac{dm}{dt} + 4 \pi k r (T_\infty - T_r) = 0 \qquad 2.11$$

in which L_h is the latent heat and k is the thermal conductivity of moist air. It should be noted again, that the thermal conductivity coefficient should also be corrected for gas kinetic effects [*Pruppacher and Klett*, 1978]. The first term on the left-hand side represents the latent heat flux to the droplet due to condensation of water vapor. The second term represents the sensible heat flux from the droplet. From the above equation it follows that droplet's temperature during the growth (evaporation) is:

$$T_r = T_\infty + \frac{L_h \rho r}{k} \frac{dr}{dt} \qquad 2.12$$

This equation shows that a growing droplet has temperature higher than its environment and an evaporating droplet - lower. Substituting the expression for droplet temperature into Eq.2.10 gives:

$$y = \frac{D_v M_w}{r \rho R} \left(\frac{p_\infty}{T_\infty} - \frac{p_r(y)}{T_r(y)} \right) \qquad 2.13$$

in which y is the change rate of the radius. The problem in solving equation 2.13 analytically is that this equation is implicit for the radius change rate. However, some approximations can be made to linearize equation 2.13 to obtain an analytical solution [*Mason*, 1971; *Pruppacher and Klett*, 1978; *Hänel*, 1987; *Rogers and Yau*, 1989], for example:

$$\frac{dr}{dt} \approx \frac{(p_\infty - p_r)}{r\rho\left(\frac{RT}{D_v M_w} + \frac{L_h p_r}{kT}\left(\frac{L_h M_w}{RT} - 1\right)\right)} \qquad 2.14$$

in which p_r is the water vapor pressure above the surface at the temperature of the environment.

In Appendix 2 it is shown, using the same approximations as used to obtain Eq.2.14, that the radius change rate is slowed down by a constant factor relatively to the radius change rate at no latent heat transfer:

$$\frac{dr}{dt} = y_o \frac{1}{1 + s_r C} \qquad 2.15$$

in which y_o is the growth rate, as given by equation 2.13, with the droplet temperature equal to the temperature of the environment (*i.e.* no correction is done for the latent heat transfer), s_r is the saturation ratio above the particle surface and C is a coefficient that depends on ambient temperature (at 20°C it is equal 2.1). If the saturation ratio above the particle surface is 1, the radius change rate at 20°C is slowed down by a factor of 3 due to the latent heat transfer.

Characteristic times for hygroscopic growth

To evaluate the extent of the hygroscopic growth of aerosol particles in the atmosphere one needs to estimate equilibration rates or times particles need to adjust to changes in the ambient relative humidity. The most common way to calculate characteristic times is to divide the difference between the initial and the final (equilibrium)

sizes by the growth (or evaporation) rate at the beginning of the equilibration process:

$$\tau = \frac{r_{end} - r_0}{y_0} \qquad 2.16$$

in which τ is the characteristic time, r_0 and r_{end} are the initial and the final radii, and y_0 is the growth rate at the beginning of the growth (or evaporation). This simple method is very useful for comparisons with characteristic times of other processes. However, characteristic times obtained in this way depend on the difference in the initial and the final equilibrium states and thus are specific for any size change in question. To make the concept of characteristic times of hygroscopic equilibration more universal, the following approach was proposed [*Schwartz and Freiberg*, 1981]. The characteristic time at any size or any relative humidity is calculated using Eq.2.16 at the limit of $\Delta RH \rightarrow 0$:

$$\tau(f) = \lim_{\Delta f \to 0} \frac{r_{eq}(f+\Delta f) - r_{eq}(f)}{y_0} \qquad 2.17$$

in which f is the relative humidity, r_{eq} is the equilibrium radius and y_0 is the size change rate at the beginning of the equilibration process.

Characteristic equilibration times at 20°C calculated using Eq.2.17 of ammonium sulfate particles with 0.1, 0.5 and 1 μm dry diameters as a function of RH are shown in Fig.2.11. The characteristic times were calculated accounting for the effect of latent heat transfer (see the previous section). The characteristic equilibration times increase with the particle dry size and the relative humidity. For a range of relative humidity common for the atmospheric boundary layer (below 100% RH) submicrometer particles may be considered to be in equilibrium with the environment, because the times required for equilibration are shorter than the characteristic times of changes in relative humidity (minutes to hours).

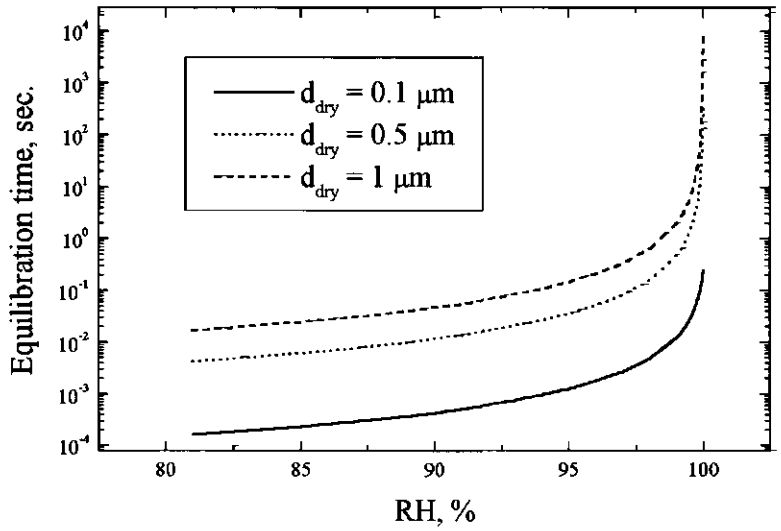

Figure 2.11. *Characteristic equilibration times of ammonium sulfate particles as a function of relative humidity.*

Effect on the light scattering

The effect of the hygroscopic growth on the magnitude of the direct radiative forcing follows from the equation for the areal mean direct forcing, analogous to Eq.2.1 [*Charlson et al.*, 1992]:

$$\Delta F_R = -\tfrac{1}{2} F_T T^2 (1 - A_c)(1 - R_s)^2 \beta \delta_a \qquad 2.18$$

in which F_T is the global mean top-of-atmosphere radiative flux, T is the fraction of incident light that is transmitted by the atmospheric layer above the aerosol layer, A_c is the fractional cloud cover, R_s is the mean surface albedo, β is the upward fraction of scattered light by the aerosol and δ_a is the areal mean optical depth of the aerosol. The negative sign denotes the cooling tendency. This equation shows that the forcing depends linearly on the aerosol optical depth and on the

upscatter fraction. Both parameters are dependent on the relative humidity [*Nemesure et al.*, 1995], hence the forcing is also dependent on the relative humidity, which is briefly discussed below.

The aerosol optical thickness (or depth) δ_a is the particle scattering coefficient, B_{sp}, integrated over the solar spectrum and over the vertical path from 0 to the height of the boundary layer, H, where most of the tropospheric aerosol is found:

$$\delta_a = \int_0^H \int_{\lambda_1}^{\lambda_2} B_{sp}\, d\lambda\, dz \qquad 2.19$$

The scattering coefficient at a given wavelength λ is:

$$B_{sp}(\lambda) = \int_0^\infty \frac{\pi}{4} D^2\, Q_s(p)\, N(D)\, dD \qquad 2.20$$

in which D is the diameter of a particle, Q_s is the scattering efficiency from the Mie theory under assumption of homogeneous spheres, $N(D)$ is the aerosol number per unit size, $p = \pi D/\lambda$ is the dimensionless parameter relating the particle size to the wave length of the light.

Equation 2.18 shows that the areal mean direct forcing is proportional to the aerosol optical thickness, which in turn depends on the particle scattering coefficient. The particle scattering coefficient is quadratically dependent on the size of the particles. Thus, an increase in size with increasing relative humidity results in a strong increase in the aerosol optical thickness. The particle scattering efficiency, Q_s, and the upscatter function β in Eq.2.18 also change with relative humidity [*Nemesure et al.*, 1995]. Their dependence on the relative humidity is rather complex and is given by the Mie theory. The scattering efficiency attains its maximum when the particle size is approximately equal to the wave length of light, while its magnitude depends on the complex refractive index, which in turn depends on the amount of water absorbed by the particle [*Nemesure et al.*, 1995]. The upscatter fraction depends both on the particle size, the refractive index and the solar zenith angle. However, the overall result of the hygroscopic growth on

the magnitude of the direct forcing is dominated by the increase in size [*Nemesure et al.*, 1995; *Pilinis et al.*, 1995]. The forcing increases strongly with increasing relative humidity, especially at relative humidity greater than 80% [*Nemesure et al.*, 1995]. *Pilinis et al.* [1995] have computed direct aerosol forcing by the "global mean" aerosol, adapted from *Andreae* [1995], as a function of relative humidity using a box model. They concluded that relative humidity is the single most influential parameter in determining direct aerosol forcing. An increase of relative humidity from 40% (at which point the aerosol is assumed to be in the dry state) to 80% was computed to lead to an increase in radiative forcing by a factor of 2.1.

The effect of hygroscopic growth on the light scattering by atmospheric aerosols was investigated in a number of experimental studies [*Rood et al.*, 1989; *Veefkind et al.*, 1996]. Modeling of optical properties of atmospheric aerosols from the size distribution of chemical species is very complex, thus a direct measurement with an optical instrument was employed in these studies.

The study of *Veefkind et al.* [1996] was performed in the Netherlands and thus is discussed here at some length. Measurements of light scattering by atmospheric aerosols as a function of relative humidity were performed in a facility similar to that used in the study by *Rood et al.* [1989]. The system basically represents a heater-cooler combination which is used to vary the relative humidity. In order to scan the "lower" part of the hysteresis loop, the aerosol first is heated to initiate its crystallization, then the air is cooled which increases the relative humidity. By changing the temperature of the cooler a scan of lower part of the hysteresis loop is obtained. The system is operated to a maximum relative humidity of 90%. A typical scan over the lower hysteresis branch takes 30 - 45 min. Also the "upper" hysteresis branch is scanned. In contrast to the scan of the "lower" hysteresis branch, the relative humidity is first increased to ensure that the aerosol passes its deliquescence point and thus is in the wet state. Then the air is heated to decrease the relative humidity.

The increase in light scattering caused by the accretion of water at a given relative humidity is commonly expressed as the enhancement factor $f(RH)$, defined as:

$$f(RH) = \frac{B_{sp}(RH)}{B_{spd}} \qquad 2.21$$

where $B_{sp}(RH)$ is the particle scattering coefficient at a relative humidity RH, B_{spd} is the particle scattering coefficient at a reference low relative humidity. This reference humidity was typically less than 30%. Whereas it is assumed that at these humidities the aerosol is dry, it will be shown below that these humidities are often not sufficiently low for drying of typical continental aerosol in The Netherlands.

The performance of the system was checked with a reference aerosol. Aerosol losses in the system are negligible as a comparison of the light-scattering in directly sampled air and air sampled via the humidifier / drier revealed. Only in arctic marine air some loss of coarse sea salt occurred, which is not considered of importance since very large particles do not contribute significantly to light scattering, as was discussed in the previous sections of this thesis. Since the drying is accomplished by heating, this might affect the amount of volatile ammonium nitrate in the system. It was found that volatilization was negligible at temperatures below 40°C. Therefore care was taken not to exceed this temperature in the heater.

Measurements of the effect of humidity on the light-scattering of the ambient aerosol were performed during six weeks in November and December 1993. Two types of air flows were studied: continental air flows with their combination of clear-skies and high anthropogenic aerosol loadings (conditions at which the effect of anthropogenic aerosols is maximal) and relatively clean arctic marine air flows which were used as the reference for the natural aerosol in The Netherlands.

The humidity tests of the light-scattering indicated the presence of two types of continental aerosol. Examples of these two types (Fig.2.12) illustrate the differences. Figure 2.12a gives an example of aerosol in

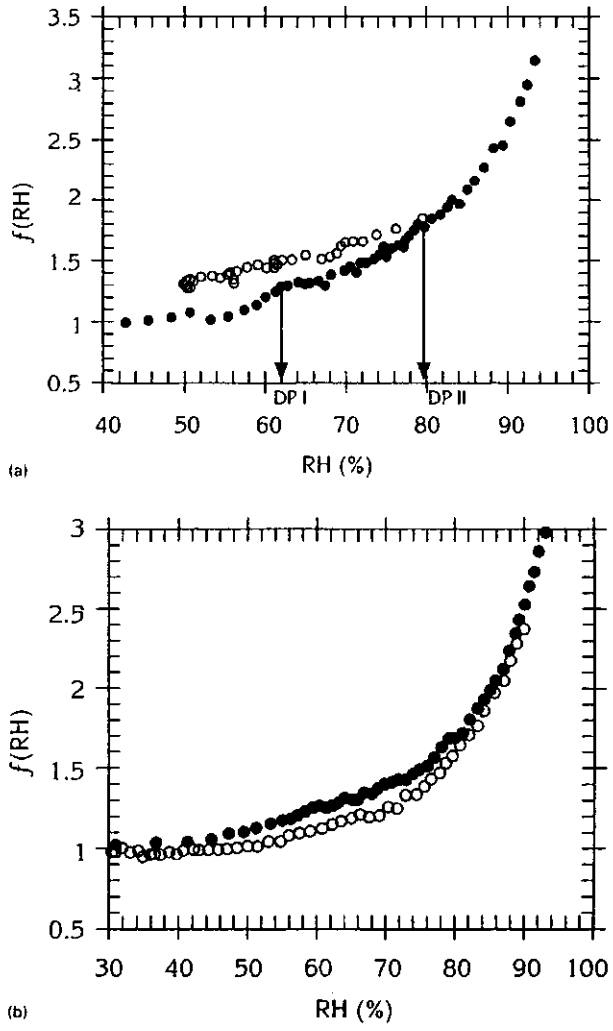

Figure 2.12. *The enhancement factor (Eq.2.21) as a function of relative humidity for two types of ambient aerosol: (a) in which two deliquescence points are observed (DP I and DP II) and (b) in which no deliquescence was found. Filled circles represent the scan of the lower hysteresis branch, the open circles - the scan of the upper hysteresis branch.*

which two deliquescence points were found, a first point at 62% RH and a second at 80% RH. The second deliquescence point is less obvious in the lower branch of the hysteresis curve. This point is better appreciated from the complete "hysteresis" loop (Fig.2.12a): when the humidity is decreased down from 90% RH the upper hysteresis curve deviates from the lower curve at 80% RH.

Fig.2.12b shows an exaple of the other aerosol type in which deliquescence is not observed: $f(RH)$ gradually increases with relative humidity but followes the same line when lowering the humidity, down to humidities of 20%. This indicates that the particles are not dried at the lowest humidity attained in the drying cycle. In this type of aerosol the amount of nitrate was appreciably higher than that of sulfate. It was concluded that the difference in the deliquescence behavior of the two types of continental aerosol is associated with the difference in the ratio of nitrate to sulfate.

In clear arctic marine air, the scattering coefficient (B_{spd} = 0.2 10^{-4} m^{-1}) is small which gave rise to appreciable noise in $f(RH)$. Nevertheless, a deliquescence point was observed at 75% RH, the deliquescence point of sea salt - NaCl, showing that this natural aerosol component governs the dependence on the relative humidity of the aerosol light-scattering in arctic marine air.

Figure 2.12 shows that hygroscopic growth has a strong effect on the light scattering. The light scattering is exponentially increasing with relative humidity, being about 1.7 and 2.5 times stronger relatively to the dry state at 80 and 90% RH, respectively. In the upper hysteresis curve the light scattering is increased by 30 to 40% relatively to the dry state (see Fig.2.12a). Because generally it is not possible to tell whether ambient particles have experienced a rising or falling relative humidity history, the hysteresis envelope brings an uncertainty in calculating the magnitude of direct forcing. For instance, Chuang et al. [1997] in their modeling assessment of the global direct forcing used the average of the optical properties in the upper and the lower hysteresis branches. However, for the reasons outlined below, it

seams more realistic to assume that aerosols in the atmospheric boundary layer are in the upper hysteresis branch.

Annual mean direct aerosol forcing is mostly determined by the summer half of the year (because of a higher solar energy influx) and especially under cloudless skies. Under such conditions high solar irradiance results over land in a rather strong convection, which induces mixing of the atmospheric boundary layer. As a result, the relative humidity is increasing with height, reaching values of up to 100%. Because of the cycling of air parcels in the boundary layer, aerosol particles experience different relative humidities. As long as the lowest relative humidity in the boundary layer is not sufficient to induce crystallization, the aerosol particles, once encountered a relative humidity higher than their deliquescence point, will stay in the wet state ("upper" hysteresis branch). Taking into account that the relative humidity of crystallization of ammonium sulfate is about 39% [*Tang and Munkelwitz*, 1994] and that compounds such as ammonium nitrate and ammonium bisulfate have crystallization relative humidities below 10%, it is clear that aerosols should experience a rather low relative humidity to induce their crystallization. Fig.2.12b demonstrates that lowering the relative humidity down to 30% was not sufficient to induce the crystallization of the ambient aerosol. Thus, one may conclude, that aerosols in the atmospheric boundary layer are most probably present in the wet form.

The exponential increase of the light scattering with increasing relative humidity has the following implication. General circulation models, due to the limited spatial resolution, use an average relative humidity over vast areas to calculate the aerosol optical properties. However, because the light scattering increases exponentially with relative humidity, the average light scattering will be higher than the light scattering at the average relative humidity. Thus, the models most probably underestimate the forcing. The same argument is valid for the effect of vertical relative humidity profile in the atmospheric boundary layer: the light scattering in the upper part of the boundary layer may dominate the scattering in the total boundary layer. A high relative humidity (up to 100%) is achieved within the boundary layer

height, when an adiabatic temperature profile exists within the boundary layer. Even though the temperature lapse rate may not always be adiabatic, one may still expect that the average relative humidity within the boundary layer is well above that at the ground. Unfortunately, there is no consistent data available on the "average" distribution of relative humidity with height. The absence of such data lead to the uncertainty in the "average" relative humidity in the boundary layer to be tens of percent RH. Such an uncertainty combined with the very high sensitivity of the aerosol light scattering to changes in relative humidity (Fig.2.12) may easily lead to uncertainty in the average light scattering within the boundary layer to be in the order of a factor of 2 which is larger than the uncertainty of about a factor of 1.2 adopted in the assessments by *the IPCC* [1995].

The relative humidity dependence of the size of ambient aerosols is crucial for the so-called radiation column "closure" experiments and in the remote sensing of aerosol from satellites by means of back-scattering of solar radiation. The humidity dependence of the aerosol light scattering discussed above was used in the column closure experiments [*Veefkind et al.*, 1996]. First, the light scattering of the (dry) ambient aerosol is measured with the humidity-controlled nephelometry at the ground. Then, the light scattering as a function of height is calculated from the vertical humidity profile and the dependence of the light scattering on relative humidity. Then the total column aerosol optical depth is calculated. The calculated optical depth is compared with the optical depth directly measured with a solar meter. In this way a "closure" between the two methods is achieved, thus decreasing the uncertainties of both of the methods. The local instantaneous direct radiative forcing measured at midday during these experiments was estimated at around -13 W/m^2 [*Veefkind et al.*, 1996].

Influence of the hygroscopic growth on particle deposition velocity.

Hygroscopic size changes of ambient aerosols have strong effect on the dry deposition velocity of aerosol particles, which in turn influences

the aerosol life time. A major discrepancy was observed between dry deposition velocities measured during wind-tunnel experiments and velocities measured by micro-meteorological methods over vegetation. Wind tunnel experiments indicate low deposition velocities, in the order of 0.1 cm/s for 0.1 - 1 μm particles, while, for instance, measurements over Speulder Bos (an 18 m tall Douglas fir forest), in the Netherlands, carried out by several independent methods result in dry deposition velocities of over 1 cm/s [*BIATEX*, 1997]. The difference in deposition velocities is very important for calculations of exceedances of critical loads for acidification and eutrofication in Europe and has lead to frequent scientific debates [*BIATEX*, 1997]. It is possible that hygroscopic growth of particles during the deposition process can explain the difference [*Ruijgrok et al.*, 1994]. An increased humidity over vegetation induces particle growth and, hence, may favor deposition, which strongly depends on the particle size (Fig.2.13).

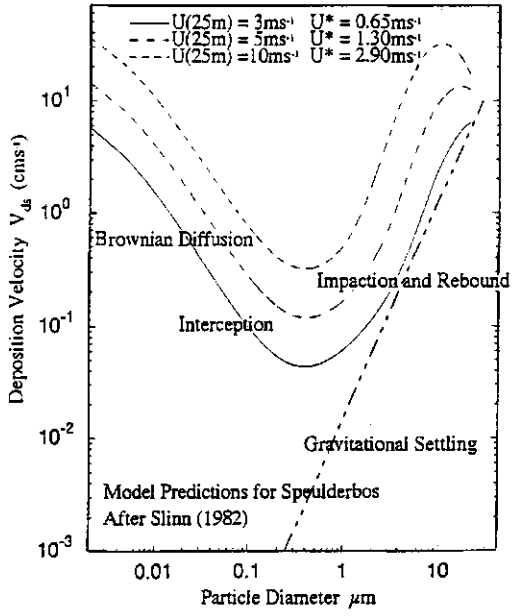

Figure 2.13. *Deposition velocity as a function of particle size predicted by the Slinn [1982] model for Speulder Forest for different wind speeds (adopted from BIATEX [1997]).*

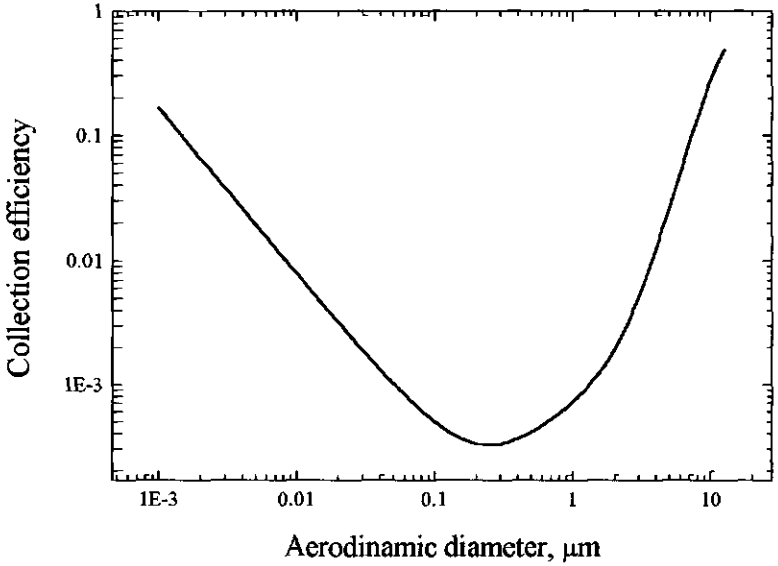

Figure 2.14. *Collection efficiency as a function of particle size predicted by the Slinn [1982] model for friction velocity of 1 m/s and characteristic size of collecting ellements of 1 mm (99%) and 10 μ m (1%).*

The dry deposition velocity of aerosols depends on many parameters, like wind speed, character of vegetation, etc. [*e.g. Slinn*, 1982]. However, it is the size-dependent efficiency of particle deposition onto the (vegetation) surface that controls the shape of the deposition curve (Fig.2.14) and it is the collection efficiency that is effected by the hygroscopic growth. The collection efficiency and thus the deposition velocity of particles smaller than approximately 0.1 μm in aerodynamic diameter is controlled by Brownian diffusion. The collection efficiency in this region scales with approximately $[(d_p + 2\lambda)/d_p^2]^{2/3}$ (d_p being the diameter and λ being the mean free path of air molecules, *e.g. Fuchs* [1964]). For particles larger than about 1 μm in aerodynamic diameter gravitational settling and impaction are the dominant removal processes. Gravitational settling velocity scales with d_p^2. To account for

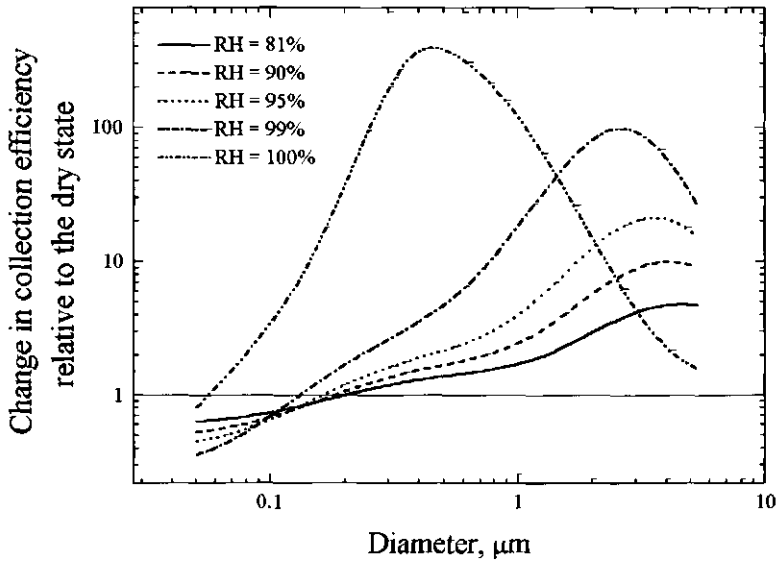

Figure 2.15. *Effect of relative humidity on collection efficiency as a function of particle size for ammonium sulfate particles predicted by the Slinn [1982] model with the same parameters as in Fig.2.14.*

a distribution of wind speed in the canopy *Slinn* [1982] approximated the impaction efficiency by $St^2/(1+St^2)$, in which St is an "average" Stokes number, which is linearly proportional to the average wind speed inside the canopy multiplied by d_p^2. The intermediate region between 0.1 and 1 μm in diameter is controlled by interception, the efficiency of which scales with $d_p/(d_p+A)$, in which A is a characteristic size of collecting objects in the canopy [*Slinn*, 1982]. This region, though containing most of the anthropogenic aerosol mass (see Appendix 1) has the lowest deposition velocity (Fig. 2.14). The overall collection efficiency is then corrected for "rebound" or particle "bounce-off", which is more pronounced for larger particles [*Slinn*, 1982]. It should be noted, that hygroscopic growth reduces the rebound, because after the deliquescence particles are liquid droplets.

The magnitude of the effect that hygroscopic growth has on the deposition efficiency is illustrated in Fig.2.15. At a relative humidity in the canopy of 100% (which is a very probable condition, as dew events in Dutch forests are expected to happen about 200 nights a year) the deposition efficiency for particles with sizes between 0.1 and 1 μm dry diameter (where most of the atmospheric sulfate and nitrate is concentrated, see Appendix 1) is increased by up to hundred times.

The influence of the hygroscopic growth on the deposition velocity should depend on the characteristic growth times of the particles. If a particle grows not fast enough, it will be deposited before reaching the equilibrium size which will decrease the influence of hygroscopic growth on the deposition velocity. The characteristic time that particles spend in the canopy is estimated in the following way. The characteristic time of turbulent transfer is taken as the lowest limit of the deposition time. The characteristic deposition time within a canopy is estimated as the canopy height (approximately 5 m) divided by the friction velocity [*W.Rijgrok*, personal communications]. The friction velocity is approximately equal to the wind speed at the reference height divided by 10. This estimation gives times in the order of 10 sec. The upper limit for the deposition time is the time that particles spend within the canopy (approximately, the canopy height divided by the deposition velocity). Such an estimation gives times in the order of 1000 sec.

The characteristic growth times (Fig.2.11) show that at a relative humidity in the canopy below 100% all particles are in equilibrium with the environment, as in this case the estimated time that particles spend within the canopy is sufficient for the equilibration. At 100% RH particles smaller than about 0.5 μm in diameter have sufficient time for equilibration. Hence, the hygroscopic growth should (strongly) effect the dry deposition velocity of aerosol particles.

An observation of the deposition curve (Fig.2.13) and the dependence of the equilibrium size on relative humidity shows that at a relative humidity of about 100% the deposition velocity of particles with sizes of around 0.5 μm in diameter (approximately the midpoint of

the sulfate and nitrate mass size distributions, see Appendix 1) may be increased by 10 to 100 times relative to the dry state due to the hygroscopic growth. The deposition velocity can be in the order of 1 cm/s, a value corresponding to forest deposition measurements [*BIATEX*, 1997].

CONCLUSIONS

In the Netherlands, and by deduction in the West Europe, the contribution of nitrate to the light scattering and thus to the direct radiative forcing is of the same order as sulfate or even higher. Because there are indications that a similar situation is found also in other parts of the globe, and because nitrate was neglected in climate models, it is clear that the current estimates of the direct radiative forcing by anthropogenic aerosols are too low.

The high light scattering efficiency of nitrate is explained by its size distribution. In continental air flows that dominate the direct effect, nitrate is present in submicrometer particles of about the same size as sulfate particles. This, as well as measurements in some parts of the USA, demonstrates that the assumption, accepted by the IPCC, that nitrate is present only in supermicrometer particles, is not valid.

In continental air flows both sulfate and nitrate are fully neutralized by ammonium. The mass size distributions of these compounds are practically the same and are centered at around 0.5 μm in diameter, which renders both compounds a very effective light scattering per unit mass.

Ammonium sulfate and ammonium nitrate are the species that dominate the direct radiative forcing in the Netherlands. There are indications from both light scattering and impactor measurements, that organic aerosol compounds are also major contributors to the

direct forcing, responsible for up to 30% of the total light scattering by continental aerosol.

Measurements show that light scattering by aerosols in polluted continental air flows is up to 2 orders of magnitude stronger than in clean arctic marine air flows, indicating the magnitude of anthropogenic influence on the radiation balance in the Netherlands.

In order to assess the radiative cooling by anthropogenic aerosols both the size and the chemical composition of the aerosols must be known. However, such measurements of ammonium nitrate are complicated by sampling artifacts due to volatility of this compound. New sampling techniques (thermodenuders and SJAC samplers) have been developed for artifact-free measurements of this compound. These new techniques may be employed for routine measurements even in background locations. Samplers of the SJAC type also allow on-line size- segregated measurements of chemical composition without sampling artifacts with a good time resolution.

Measurements of bulk compounds in aerosols in the Netherlands with the new artifact-free sampling techniques lead to the conclusion that the mass concentration of nitrate in aerosol is about the same as that of sulfate or even slightly higher. Measurements by other researchers, who have applied a sampling instrument similar to the SJAC to measurements of ambient aerosols in Texas, indicate the same situation: concentrations of nitrate in aerosol are higher than the sulfate concentrations at that location in the USA. This suggests that nitrate concentrations reported in literature are most probably underestimated. As only very limited sets of measurements, which are not influenced by the artifacts, are available, it is not possible to draw a general conclusion with certainty. So the conclusion is warranted that artifact-free characterization of bulk elements in aerosol regarding total composition as well as size distribution should have a high priority.

Both ammonium sulfate and ammonium nitrate are hygrocopic compounds, which absorb water vapor. As a result the particle size is

exponentially increasing with the relative humidity which is especially pronounced close to 100% RH. For the range of relative humidity common for the atmospheric boundary layer the times required for submicrometer particles to equilibrate with a humid environment are short and the particles may be considered to be in equilibrium with the environment.

Hygroscopic growth results in a strong increase in light scattering. As a result of this, relative humidity in the atmospheric boundary layer strongly enhances the magnitude of direct aerosol forcing. The forcing increases strongly with increasing relative humidity, especially at relative humidity greater than 80%. An increase of relative humidity from 40% (at which point the aerosol is assumed to be in the dry state) to 80% was estimated to lead to an increase in radiative forcing by about a factor of 2. Because relative humidity in the atmospheric boundary layer rarely becomes sufficiently low (especially in the Netherlands) to initiate crystallization, the aerosols are most probably always in the wet state (the upper hysteresis branch) even at a relative humidity below the deliquescence point. Because climate models usually accept aerosols to be in the dry state, if the relative humidity is below the deliquescence, one may conclude that the models underestimate the forcing.

The hygroscopic growth also effects the dry deposition velocity of aerosols and thus their life times in the atmosphere. Due to the hygroscopic growth the dry deposition rates of aerosol increase by up to a factor of a hundred, if the relative humidity is close to 100%.

The contribution of particulate nitrate to acid deposition and eutrophication is generally estimated to be low. If nitrate concentrations are higher than assumed and as indications exist that the deposition velocity of small particles is also higher than formerly reported [*BIATEX*, 1997], the contribution of particulate nitrate to deposition and eutrophication is probably much higher than generally assumed.

Chapter 3

The indirect effect

INTRODUCTION

Alongside with the direct forcing anthropogenic aerosols also influence the radiation balance of the Earth indirectly by increasing the reflectivity of clouds and increasing their life time. Clouds cover vast areas of the globe and thus play a major role in the global radiation balance by controlling the amount of incoming short-wave solar radiation and outgoing terrestrial infrared radiation. Clouds form by condensation of water on preexisting water-soluble aerosol particles, the so-called cloud condensation nuclei (CCN). The concentration of aerosol particles thus governs the concentration of cloud droplets. Anthropogenic aerosols usually contain large quantities of water-soluble substances, like sulfate, and thus can also act as CCN. It has been originally argued by *Twomey* [1977a,b; 1991] that clouds formed in polluted regions have higher droplet number concentrations which leads to an increase in reflection (albedo) of clouds. In contrast, an increase in droplet number concentration does not lead toa stronger absorption of infrared terrestrial radiation [*Grassl*, 1990]. Anthropogenic aerosols, thus, act (in an indirect way) as a radiative cooling factor in the atmospheric radiation balance.

Marine stratus and stratocumulus clouds are of central importance for the indirect effect for the following reasons. First, this cloud type covers (non-overlapped by other clouds) estimated 30% of the total surface of the globe [*Charlson et al.*, 1992], thus controlling approximately 1/3 of the planetary albedo. Secondly, these clouds have a short-wave reflectivity of around 0.5. As will be shown further in this

chapter, clouds with such a reflectivity are most sensitive to changes in droplet number concentration. Third, these clouds have low droplet number concentrations, which also makes their albedo very sensitive to changes in their droplet number concentration. One of the striking examples of how anthropogenic aerosols (drastically) increase reflectivity of marine clouds was found in satellite images of marine stratocumulus clouds modified by emissions from ships [*Coakley et al.*, 1987; *Albrecht*, 1989; *Radke et al.*, 1989; *King et al.*, 1993]. The so-called "ship tracks", the regions of increased reflectivity where the droplet number concentration was increased by the input of additional CCN from ship exhausts, are clearly visible in satellite images as white lines against a gray background of unpolluted cloud sheet (Fig.1.3).

Apart from their effect on the albedo of clouds increased droplet number concentrations are expected to result in smaller sizes of cloud droplets which inhibits the rain-out of these clouds [*Albrecht*, 1989]. The persistence of clouds could be the reason for the increased cloudiness over the last decades in coastal regions in Europe [*Liepert et al.*, 1994; *Russak*, 1990]. Increased life time of clouds means increased cloud cover. Increased cloud cover leads to more short-wave solar radiation being blocked from reaching the Earth's surface, which consequently enhances the indirect cooling. On the other hand, an increase in life time of clouds would also enhance the infrared absorption by clouds, thus enhancing the greenhouse effect. For this reason, the effect of longer cloud life times, which is the net result of these opposing effects, is very uncertain and requires a more accurate treatment of cloud processes in climate models [*Schwartz and Slingo*, 1996]. Further on in this thesis only the effect of anthropogenic aerosols on droplet number concentrations and thus on the cloud albedo will be discussed.

Though the compound effect of the increased life time of clouds is very unclear, the central principle of the indirect aerosol effect remains the fact that anthropogenic aerosol particles increase the number concentration of cloud droplets in polluted conditions relatively to the unperturbed environment, thus exerting a cooling influence on the climate. However, one of the major questions in the assessment of the

magnitude of indirect effect is how effective anthropogenic aerosol particles are as extra cloud nuclei, or in other words: to what extent are anthropogenic particles able to serve as CCN. The main part of the work covered in this thesis was devoted to an experimental assessment of cloud forming properties of anthropogenic aerosols in the Netherlands. In this chapter the approach to this study is formulated. First, the basic mechanisms underlying the indirect effect are discussed. Also, the basics of droplet formation on aerosol particles are considered in order to assess which parameters are critical for a particle to serve as a CCN. A review of the experimental studies of anthropogenic influence on cloud droplet number concentrations is made. On the basis of this the approach to the experimental study, which is described in the following chapters, is formulated. The cloud forming properties of ambient aerosols in the Netherlands were investigated in a cloud chamber which, as will be shown in the following chapters, has several features that make it unique for such a study. These features include reproducible stable supersaturations common for marine clouds of interest, large size and flow (about 20 m^3/min) which make it possible to employ several aerosol instruments simultaneously, including cascade impactors and conventional cloud-droplet monitors.

DROPLET NUMBER AND CLOUD ALBEDO

The sensitivity of cloud albedo to increase in droplet number concentration is obtained from an expression describing the albedo of a cloud. According to the two-stream approximation [*Twomey*, 1991] the cloud albedo is:

$$R = \frac{0.15\,\delta}{2 + 0.15\,\delta} \qquad 3.1$$

in which R is the cloud-top albedo and δ is the cloud optical depth. The cloud optical depth can be found from Eq.2.19. Because sizes of cloud

droplets are substantially greater than the wave length of visible light, the scattering efficiency, Q_s, may be approximated to be constant and equal 2. From Eq.2.20 on integration one obtains:

$$\delta = 2\pi H \bar{r}^2 N \qquad 3.2$$

in which H is the cloud thickness (or height of the cloud layer), N is the total cloud droplet concentration and

$$\bar{r}^2 = \frac{1}{N} \int r^2 n(r)\, dr \qquad 3.3$$

is the mean square radius of the droplet distribution, $n(r)$ is the number size distribution of cloud droplets. If it is assumed that the concentration of cloud water, the so-called liquid water content (LWC), does not depend on the total droplet number concentration, *i.e.* the droplet number does not effect micro-meteorology of the cloud, the mean square radius can be approximated as:

$$\bar{r}^2 = \left(\frac{3L}{4\pi N}\right)^{2/3} \qquad 3.4$$

in which L is the liquid water content. Equation 3.2 then becomes:

$$\delta = 2\pi H \left(\frac{3L}{4\pi}\right)^{2/3} N^{1/3} \qquad 3.5$$

Using equations 3.1 and 3.5 an expression is derived for the sensitivity of cloud-top albedo, R, to change in the droplet number concentration, N, by differentiating Eq.3.1 with respect to N:

$$\frac{dR}{dN} = \frac{R(1-R)}{3N} \qquad 3.6$$

This quantity was introduced by *Twomey* [1991] and is called cloud susceptibility (sensitivity to a change in droplet number). From Eq.3.6 it follows that the susceptibility exhibits a maximum value of 0.25 at cloud-top albedo, R, of 0.5. It is also clear that the susceptibility strongly decreases with increasing droplet number concentration.

Sensitivity studies show that the clouds, which are most affected by anthropogenic aerosols, are marine stratus and stratocumulus close to polluted continents [*Wigley*, 1989; *Twomey*, 1991; *Charlson et al.*, 1992; *Platnick and Twomey*, 1994; *Taylor and McHaffie*, 1994]. There are two reasons for this. Marine clouds are optically thin and have low droplet number concentrations, because the background concentrations of marine (natural) aerosol are low [*Hoppel et al.*, 1990; *Andreae et al.*, 1995]. Consequently, even a small number of anthropogenic aerosol particles thus has the greatest (relative) influence. Also it was argued that a saturation occurs with respect to the numbers of cloud droplets in air with high loading of aerosol [*Jensen and Charlson*, 1984; *Leaitch et al.*, 1986; *Gillani et al.*, 1995]. Marine stratus and stratocumulus clouds cover approximately 30% of the oceanic surface [*Charlson et al.*, 1987], which has a very low surface albedo (5% - 10%). This in combination with the high sensitivity of their reflectance to anthropogenic pollution makes marine stratiform clouds the most important cloud type for the indirect aerosol climate forcing.

Equation 3.6 can be rewritten in terms of a fractional change in droplet number concentration:

$$\Delta R = \frac{1}{3} R\,(1-R)\,\Delta \ln N \qquad 3.7$$

For the range of cloud-top albedo, characteristic for marine stratus clouds ($0.28 < R < 0.72$), the fractional change in cloud-top albedo can be approximated, accurately to within 10%, as [*Schwartz and Slingo*, 1996]:

$$\Delta R \approx 0.075\,\Delta \ln N \qquad 3.8$$

Equation 3.8 shows that the cloud albedo is very sensitive to (fractional) changes in cloud droplet number concentration. An increase in droplet number concentrations due to anthropogenic aerosols would, thus, result in an increase of the global albedo, exerting a negative climate forcing. For example, a 30% increase in droplet number concentration due to anthropogenic aerosol, estimated for Northern Hemisphere, corresponds to a 2.25% increase in cloud albedo

[*Schwartz*, 1988; *Charlson et al.*, 1992]. This brightening of clouds translates into a hemispheric-mean forcing of -1.1 W/m^2, which is comparable to the forcing by greenhouse gases [*Shine et al.*, 1990]. This example shows that indirect forcing is very sensitive to changes in droplet number concentration of marine stratiform clouds. However, data on the relationship between the droplet number and the number of aerosol particles is very scares [*Schwartz and Slingo*, 1996].

CLOUD ACTIVATION, CLOUD DROPLETS AND CLOUD CONDENSATION NUCLEI (CCN)

Clouds form when an air parcel is cooled (usually by the adiabatic lifting) below its dew point temperature, *i.e.* when the air becomes supersaturated. In the previous chapter it was mentioned that in supersaturated conditions particles that have their critical supersaturation (see Eq.2.5 or below) lower than the supersaturation of the environment are able to grow by condensation of water vapor to very large sizes. As was discussed in the previous chapter, the critical supersaturation is found by differentiating the Köhler curve (Eq.2.2) and putting the differential equal to zero [*Twomey*, 1977a]:

$$S_{crit} = \frac{2}{3}\sqrt{\frac{A^3}{3B}} \qquad 3.9$$

in which:

$$A = \frac{2\,\sigma\,M_w}{\rho_w\,R\,T} \qquad 3.10$$

$$B = \frac{i\,\varepsilon\,\rho_{dry}\,r_{dry}^3\,M_w}{\rho_w\,M_s} \qquad 3.11$$

in which S_{crit} is the critical supersaturation, T is temperature, σ is the surface tension, M_w and M_s are, respectively, the molecular weights of

water and water-soluble salt, comprising the particle. ρ_w and ρ_{dry} are, respectively, the density of water and of dry particle. R is the gas constant, i is the van't Hoff factor (Eq.2.3) and ε is the mass fraction of water-soluble salt in the particle.

Particles whith a critical supersaturation lower than the supersaturation in the surrounding air, will grow infinitely, because the vapor pressure at their surface will be always lower than that in the environment. In contrast, particles, which critical supersaturations is higher than that of the environment, cease growing after reaching an equilibrium size below their critical size (Eq.2.4). This process is usually called cloud activation: particles which have passed their critical size are called activated. It should be noted, however, that the concept of cloud activation, which is directly related to critical supersaturation, should only be considered as a useful criterion characterizing the cloud nucleating ability of an aerosol particle. Cloud formation is a dynamic process and supersaturation in a developing cloud is not constant, depending both on the updraught velocity and the amount of growing particles present in the air parcel, which will be discussed in the following sections.

Relation between cloud nucleation and size / chemical composition

The minimum size of a soluble particle that can be activated at a given supersaturation, S, can be found from equation 3.9 [*Twomey*, 1977a]:

$$r_{min} = S^{-2/3} \left(\frac{32\,\sigma^3\,M_w^2\,M_s}{27\,\rho_w^2\,R^3\,T^3\,i\,\varepsilon\,\rho_{dry}} \right)^{1/3} \qquad 3.12$$

For a pure ammonium sulfate particle the minimum size, if expressed in centimeters and if the supersaturation expressed in percent units, is:

$$r_{min} = 1.45 \cdot 10^{-6}\,S^{-2/3} \qquad 3.13$$

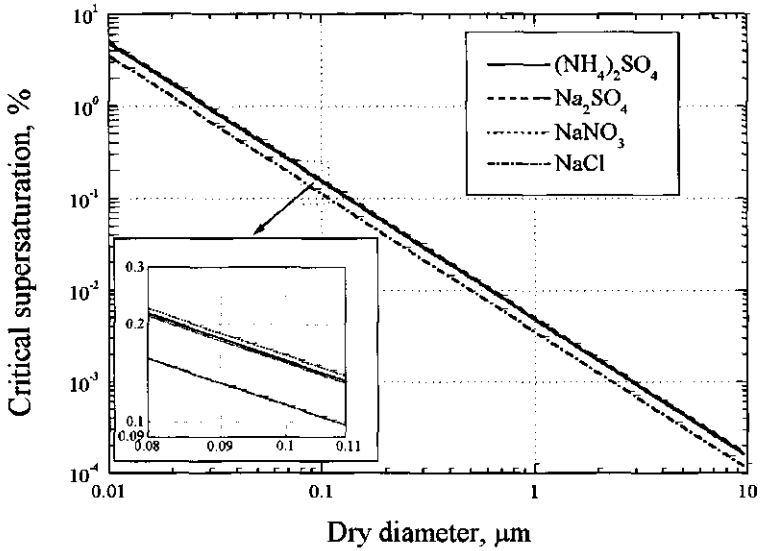

Figure 3.1. *Critical supersaturation of a pure-salt aerosol particle vs. its dry size for four atmospherically relevant salts.*

Figure 3.1 shows the dependence of critical supersaturation on the dry size of a particle for four atmospherically relevant salts. The figure shows a strong dependence of critical supersaturation on the dry size and a rather weak dependence on the chemical composition of water-soluble components in the particle. It can be also inferred that the higher the supersaturation, the smaller the particles that can be activated. For a given (constant) supersaturation only particles above the corresponding threshold size (Eq.3.12) can be activated. On the other hand, the critical supersaturation of a particle depends on its soluble content, being higher for particles with higher insoluble content (Fig.3.2). Large soluble particles are the easiest to activate, while small and insoluble particles require a higher supersaturation.

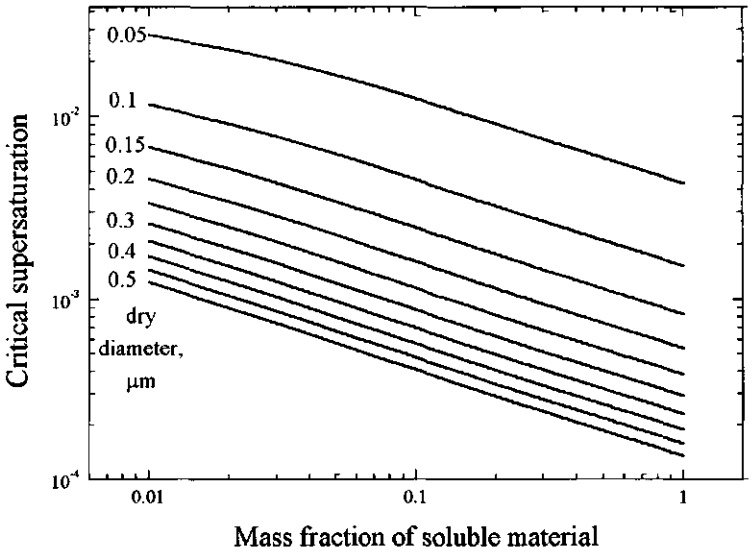

Figure 3.2. *Critical supersaturation of a pure-salt ammonium sulfate particle as a function of the mass fraction of soluble material.*

Influence of water soluble gases on cloud activation

Recently it was shown that water-soluble gases, like nitric acid, can substantially influence the critical supersaturation of an aerosol particle [*Kulmala et al.*, 1993]. The basic idea is that the dissolved gas increases (virtually) the aerosol mass, thus decreasing the molar fraction of water in the droplet and consequently decreasing the vapor pressure above the droplet surface. To demonstrate this, Eq.2.2, describing the equilibrium saturation ratio for a salt particle, can be rewritten, substituting number of moles per droplet for masses of salt and water, as:

$$S_{salt} = 1 + \frac{A}{r} - \frac{\nu_{salt}}{\nu_{water}} \qquad 3.14$$

in which ν denotes the number of moles of a substance (water, salt ions or gas molecules/ions) per droplet. When some gas is dissolved in the droplet the above equation becomes:

$$S_{salt+gas} = 1 + \frac{A}{r} - \frac{\nu_{salt} + \nu_{gas}}{\nu_{water}} \approx S_{salt} - \frac{\nu_{gas}}{\nu_{water}} = S_{salt} - K\, p_{gas} \qquad 3.15$$

in which p_{gas} is the vapor pressure of the gas in equilibrium with the droplet, K is the equilibrium constant for the equilibrium "gas - dissolved gas" (effective Henry's law constant). The critical point can be found by differentiating Eq.3.15 for number of moles of water and putting it equal to zero:

$$\frac{\partial S_{salt+gas}}{\partial \nu_{water}} = \frac{\partial S_{salt}}{\partial \nu_{water}} - K \frac{\partial p_{gas}}{\partial \nu_{water}} = 0 \qquad 3.16$$

If the partial pressure of the gas is maintained constant, the differential of the system "salt-water-gas" will be exactly the same as the differential of the system "salt-water". In this case the number of moles of water (or mass of water) per droplet at the critical point will be the same as in the case when no soluble gas is present. Consequently, the decrease in the critical supersaturation due to the dissolved gas is:

$$\Delta S_{crit} = -K\, p_{gas} \qquad 3.17$$

It is clear that the higher the partial pressure of the water-soluble gas and the higher its solubility, the stronger will be the reduction of the critical supersaturation. However, at ambient concentrations only very soluble gases can significantly reduce the critical supersaturation. For example, to reduce the critical supersaturation by 0.01% a gas, being present at 1 ppbv, should have an effective Henry's law constant of $5.6 \cdot 10^6$ M/atm. On the other hand, such a high solubility would cause most of the gas to dissolve in droplets reducing its partial pressure and thus reducing its effect on the critical supersaturation. In this case one should find the exact solution of Eq.3.16, which will depend both on the size distribution of aerosol particles and the total number concentration.

Cloud condensation nuclei (CCN) and potential cloud nuclei (PCN)

Particles that can be activated at a (constant) supersaturation which can be encountered in clouds are called cloud condensation nuclei (CCN). It should be noted that, when using the term CCN, one should always refer to the supersaturation at which the CCN were measured. Neglecting the effect of water soluble gases on cloud activation, one can estimate the sizes of particles that may serve as CCN in stratiform clouds. In marine atmosphere ammonium sulfate is the dominant compound in the smallest and most numerous particles [*Twomey*, 1977a]. Marine stratus and stratocumulus clouds have supersaturations ranging from 0.1% to 0.3% [*Albrecht et al.*, 1988; *Hudson*, 1983]. According to equation 3.12 particles larger than 0.065 - 0.135 μm in diameter can (but not necessarily do, as discussed below) serve as nuclei for cloud droplet formation in marine stratiform clouds.

Though due to the so-called saturation effect (see the following section) the number of CCN at a given supersaturation may be not equal to the number of cloud droplets, the CCN number concentration is a very convenient means of characterizing the cloud nucleating ability of a given aerosol. The CCN number concentration is usually determined with cloud chambers [*Twomey*, 1977a; *Hagen et al.*, 1990; *Hudson*, 1989]. However, care should be taken that the supersaturation used in the chamber is comparable to that in the clouds of interest. If the supersaturation used to count CCN is higher than in the cloud, small and insoluble particles, that would not be active in the cloud, are also counted. The number of CCN thus may be strongly overestimated.

Another, simpler, method can be employed to estimate number concentration of CCN. At a given supersaturation only particles that are larger than the corresponding activation threshold size (Eq.3.12) can be active as CCN. Thus, one may measure the number concentration of particles larger than a certain size to obtain an estimate of the CCN concentration. Again, the threshold size should be chosen according to the (maximum) supersaturation expected in the cloud. To avoid confusion with actual CCN, particles that are larger

than the activation threshold will be further on referred to as potential cloud nuclei (PCN), meaning that these particles have a potential to act as CCN, as opposed to particles that are smaller than the activation threshold. In other words PCN are those particles which, according to their size, would act as cloud nuclei at a given supersaturation (see Eq.3.12), but it is the amount of insoluble material in them and their number concentration that determine whether they actually act as such. As will be shown in the following chapters of this thesis the number concentration of PCN is not equal to that of CCN, which is due to the saturation effect (see the following section) and a high content of insoluble material in some of the particles.

Saturation effect

There are two factors that may prevent a particle larger than the activation threshold size (a particle that is a PCN) to become activated: a high content of insoluble material (see Fig.3.2) and a high number concentration of the particles. Supersaturation in a developing cloud is not constant in time. Increase in supersaturation due to the underlying physical process, like adiabatic cooling due to the lifting of the air parcel, is counteracted by the water vapor consumption by the growing cloud droplets. When the number of growing particles is high, the depletion rate of water vapor is substantial, which hampers the growth of some of the particles. For this reason the droplet number does not proportionally increase with the number of CCN obtained at a constant supersaturation. This effect is also believed to be the limiting factor for cloud droplet number concentration [*Jensen and Charlson*, 1984; *Leaitch et al.*, 1986; *Gillani et al.*, 1995] and is usually called the saturation effect (the droplet number "saturates" with increasing number of cloud nuclei).

Another possible reason for the nonlinear dependence of droplet concentration on the CCN number concentration is considered here. It was shown in the previous chapter (the section discussing kinetics of the hygroscopic growth) that the rate of change of the radius is inversely proportional to the size of the droplet (Eq.2.10, 2.14 and 2.15),

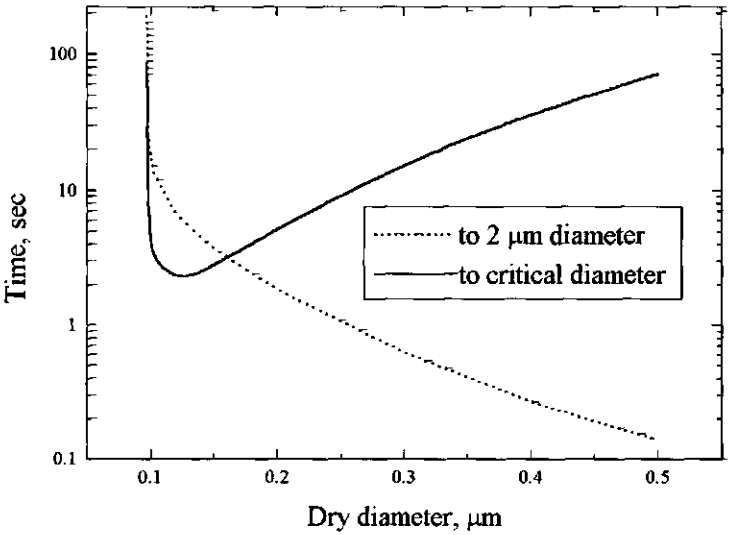

Figure 3.3. *Time required for a particle to grow to 2 μ m in diameter and time required to reach its critical point at a constant supersaturation of 0.16%.*

i.e. larger droplets change their size slower than smaller droplets. Figure 3.3 shows the time a particle needs to reach its critical size at a constant supersaturation of 0.16% as a function of its dry size. It can be seen that the growth time progressively increases with the particle dry size and the smaller particles activate faster (within the first few seconds of the growth) than the larger ones. However, larger droplets, which change thier size relatively slow, consume water vapor faster than smaller droplets (Eq. 2.9). Growing droplets formed on larger particles, though not being yet activated are still larger than droplets formed on (already activated) smaller particles, because they started growth from a larger size. If the source of supersaturation will stop (if for instance the updraft ceases), these growing large particles will continuously "distill" water from (even activated) droplets formed on smaller particles. The activated droplets would consume all the water

vapor above its saturation value and would have a very large size. The smaller particles, though some of them were activated at an earlier time, would have sizes below the critical point corresponding to the equilibrium at 100% RH. This means that, if the source of the supersaturation would not resume, the only activated particles after a sufficiently long time would be the largest particles of the initial aerosol spectrum. Such a situation is hardly possible due to the limited life time of clouds and thus was never observed. However, it is still possible that "distillation" of vapor from smaller onto larger droplets and the resultant deactivation of the smallest droplets may be responsible, at least partly, for the saturation effect.

Cloud droplets

In cloud physics, traditionally, only particles that were activated, *i.e.* passed the critical point, are considered as cloud droplets [*Jensen and Charlson*, 1984]. One should note, however, that there is no reliable experimental method that can distinguish between activated and non-activated particles. Experimentally only number or mass size distribution of particles (or droplets) can be measured. Because the critical size depends on the dry size and the soluble material content of the particle, it is impossible to tell from the measured wet size whether the particle is activated. For example, the critical diameter of an ammonium sulfate particle of 0.1 μm diameter is approximately 1 μm, while the critical diameter of an 0.5 μm particle is 11 μm. The latter particle even at 100% RH has the equilibrium size which is more than 6 times larger than the critical size of an 0.1 μm particle. Acoording to its optical and other physical properties such a large, though not activated, wet particle may be considered a cloud droplet.

Another complication is that in the cloud formation one should consider kinetics of the droplet growth. In the previous section it was shown that smaller particles activate faster than larger ones (Fig.3.3). However, due to water depletion by growing (though not yet activated) larger particles, these activated small droplets may evaporate during later stages of the cloud formation. Consequently, a particle being

activated at one moment will not be necessarily activated at a later time.

Given the above considerations, it is clear that the traditional concept of a cloud droplet as a particle that has passed its critical point does not have a practical meaning. From a practical point of view it is preferable to classify particles into droplets and "interstitial aerosol" according to their size, because this parameter can be directly measured and because the size controls most of the microphysical properties of a droplet. This classification will, of cause, always be an arbitrary one, but can be adjusted for any particular problem. For example, for studies of clouds with supersaturations in the order of 0.1%, like in marine stratus clouds, one can take a threshold of 1 μm in diameter. Given that the first size-channels of cloud monitors like the Forward Scattering Spectrometer Probe (FSSP, PMS Inc.) have a poor accuracy, it is preferable to shift the threshold somewhat higher, for example to 2 μm. The time needed for droplets to reach this size is rather short, a few seconds (Fig.3.3), and, consequently, kinetics can be neglected. Also the light scattering efficiency is fairly constant above this size [*Twomey*, 1977a]. The present classification according to the size follows that of *Leaitch et al.* [1986], who proposed to use the size of 2 μm as a criterion for cloud droplets.

STUDIES OF THE INFLUENCE OF ANTHROPOGENIC AEROSOLS ON CLOUD DROPLET NUMBER CONCENTRATION

In the assessments of the indirect forcing, only the effect of the (extra) man-made sulfate has been considered [*Wigley*, 1989; *Charlson et al.*, 1992; *Boucher and Lohmann*, 1995]. A linear relation was assumed between the mass concentration of anthropogenic sulfate and the number concentration of cloud droplets. *Leaitch et al.* [1986] indeed found in approximately adiabatic cloud parcels a linear relation

between the mass-concentration of sulfate and submicron particle number concentration (particles larger than 0.17 μm in diameter) and a linear relation between cloud droplet number and submicron particle number (less than approximately 750 cm^{-3}). This suggested a linear relation between sulfate mass (concentration) and droplet number. However, at aerosol number concentrations higher than 750 cm^{-3} the droplet number did not increase linearly with the particle number. More recent measurements in more general cloud parcels [*Leaitch et al.*, 1992], using the amount of sulfate in the cloud water as a reference, indicated a strongly nonlinear relation between sulfate concentration and droplet number concentration. It should be further appreciated that the above study and most of the other studies in the past [*Daum et al.*, 1987; *Hegg et al.*, 1984; *ten Brink et al.*, 1987] were done in the framework of wet deposition studies and thus were focused on assessing the amount of aerosol-sulfate incorporated into clouds rather than on the number of anthropogenic aerosols serving as cloud nuclei.

Outside of Europe several studies were performed in recent years in which activation of the ambient aerosol was studied in terms of number concentrations [*Leaitch et al.*, 1986; *Gillani et al.*, 1995; *Anderson et al.*, 1994; *Gras*, 1995; *Andreae et al.*; 1995, *Hoppel et al.*, 1994]. *Novakov and Penner* [1993] focused more on assessing the composition of the cloud nuclei and its influence on cloud formation. It should be appreciated, however, that the effect of anthropogenic aerosol on cloud microstructure is a regional phenomenon because of the limited residence time of aerosol particles in the atmosphere. Because of the difference in aerosol characteristics from place to place, results obtained outside of Europe cannot easily be extrapolated to the European aerosol.

In Europe measurements of the number of particles acting as cloud nuclei in marine air have been recently performed in an airborne cloud study off the coast of England [*Martin et al.*, 1994]. The number of aerosol particles before cloud formation was compared with the number of cloud droplets formed in the same air. It was found that in maritime air masses the droplet number concentration was very close to the aerosol number concentration. In air masses, which had passed over

land and which had higher aerosol concentrations, the droplet number concentration was approximately two times less than the aerosol number concentration. The authors suggested that the incomplete activation is due to the presence of hydrophobic material and stressed the importance of chemical characterization of the aerosol. It should be noted, however, that a particle sizer was used which measured the number of particles larger than 0.1 μm in diameter. The estimated supersaturations in the study were in the order of 0.3%. At this supersaturation particles as small as 0.065 μm act as cloud nuclei. Consequently, the validity of a comparison between measured particle concentration and droplet number concentration is limited. Also in most of the studies mentioned below the aerosol particles were measured with similar aerosol sizers with a similar insufficient lower size limit.

In another recent airborne study near the British Isles [*Raga and Jonas*, 1995] a comparison was made of the aerosol number concentration and the number of CCN. Also these authors used a particle sizer with a lower threshold at 0.1 μm. The number of CCN, at 0.8% supersaturation, was measured with a cloud chamber. At this supersaturation particles down to 0.035 μm in diameter serve as cloud nuclei. Another complication mentioned in the study is the uncertainty in the aerosol number concentration measurement, estimated to be at least 50%. This is an example of the experimental uncertainty in assessing the magnitude of the indirect aerosol effect.

In Europe, apart from the mentioned aircraft studies over the UK, the cloud properties of orographic ("mountain") clouds were studied. Results from the "Kleiner Feldberg Cloud Experiment" [*Hallberg et al.*, 1994a,b; *Svenningsson et al.*, 1994] are of a more local interest because the experiment was performed at a continental location. Another complication is that in orographic clouds entrainment and mixing processes interfere with the cloud-activation process [*Choularton et al.*, 1986] which complicate a comparison of aerosol number versus cloud droplet number.

REQUIREMENTS FOR A CLOUD CHAMBER STUDY

In the experimental study, described further in this thesis, the cloud forming properties of marine aerosols in the Netherlands were measured in a large cloud chamber. Though it is always difficult to translate results obtained with a chamber on ground level to the real clouds, the use of a cloud chamber has several advantages over in-situ cloud measurements. First, because it is relatively inexpensive, a cloud chamber may be used much more frequently. There is also much more confidence in the performance of instruments at the ground than in the air. Many aerosol monitors are too delicate for aircraft use. For instance, optical instruments and differential mobility analyzers may be disturbed by rapid accelerations and decelerations and by vibrations of the aircraft. Cloud chambers also allow a better understanding of the basic micro-physical processes of cloud formation by studying cloud activation of laboratory generated aerosols. For these reasons cloud chambers are usually applied for studies of nucleation properties of aerosols. For the same reasons it was decided to use a cloud chamber in this study. However, this chamber has several advantages over the conventional cloud chambers, as will be shown in the following chapter describing the characterization of the chamber.

The following requirements were set for the operation of the cloud chamber:

1. Low supersaturations. Marine stratiform clouds are of the main interest for studies of the indirect effect. Supersaturations in such clouds are low, 0.1 - 0.3% [*Albrecht et al.*, 1988; *Martin et al.*, 1994]. Thus, special care was taken to establish a supersaturation in the chamber that is within this range, namely, around 0.15%.

2. Stability and reproducibility. Stability is required in order to obtain a reliable measurements with an aerosol instrument during the required measuring time. For example, if one is to measure chemical composition of the aerosol with cascade impactors and relate it to the observed CCN number, the chamber should be stable for at least

several hours to allow for the impactor to collect sufficient material for the analysis. Reproducibility is needed for a reliable generalization of results obtained on different days. It will be shown in the following chapter that the chamber satisfies these criteria.

3. Large size / flow. Number, size and solubility are the principle factors for particles to serve as cloud condensation nuclei [*Pruppacher and Klett*, 1978; *Twomey*, 1977a]. These parameters are critical for a study of cloud forming properties of ambient aerosols. The small size and flows (of the order of *l*/min) of the conventional cloud chambers do not allow measurements of these parameters. Specifically, chemical caracterization requires sampling flows of at least several liters per minute. One of the advantages of the chamber used in this study is its large size and throughput flow rate (21 m^3/min) which solves this problem. The chamber allows to compare, simultaneously, the aerosol before cloud formation, inside the cloud and after cloud processing using several aerosol monitors at once including instruments which are conventionally used in cloud studies like FSSP (PMS Inc.). This also reduces instrumental uncertainties so common for measurements of CCN and clouds [*NASA*, 1980].

The cloud chamber used in this study is ideally located for a study of marine aerosols, because it is situated in a rural area close to the coast of the North Sea (200 meters from the shore line). Because there are no significant anthropogenic aerosol sources in the near vicinity, such a location allows to study marine aerosols which are not affected by local / continental sources. The present study was centered on cloud forming properties of marine aerosols because marine (stratiform) clouds dominate the indirect effect. For this reason the measurements were mostly confined to air masses coming from the sea (SW - N wind directions) (Fig.3.4). Continental air masses were considered to be of lesser interest because they are rarely associated with stratiform clouds. However, it is possible that continental aerosol blown off from the continents may participate in formation of marine clouds and thus contribute to the indirect effect. For this reason some measurements were performed with continental or mixed marine-continental air masses.

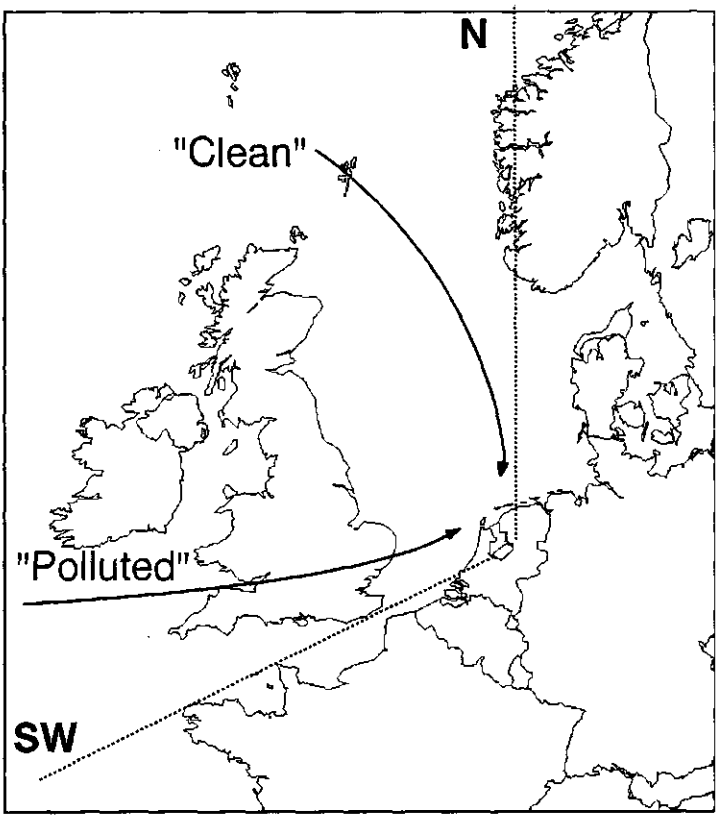

Figure 3.4. *Classification of air mass types according to wind direction.*

The activation properties of the "clean" marine aerosol, in arctic N - NW air flows, were compared with those of the marine aerosol polluted with anthropogenic emissions (Fig.3.4). An increase in cloud nuclei (due to anthropogenic aerosol) is expected in air coming from the direction of the UK (SW - W). The difference in the number of activated particles in these two air flows is a first measure of the influence of anthropogenic aerosol on cloud formation and is used for a simple estimation of the local indirect forcing further in this thesis.

Chapter 4
Cloud chamber

INTRODUCTION

In the experimental study, described further in this thesis, the cloud forming properties of marine aerosols in the Netherlands were measured in a large cloud chamber. The following requirements were set for the operation of this chamber (see the previous chapter): 1) the chamber should operate at a low supersaturation around 0.1%, as in marine stratiform clouds [*Albrecht et al.*, 1988; *Martin et al.*, 1994]; 2) its operation should be stable for several hours and reproducible; 3) the chamber should have a large size and throughput flow to allow application of several aerosol monitors. This chapter describes characterization of the cloud chamber according to these criteria. It will be shown that the chamber fulfills the above requirements. This makes it unique in comparison to the conventional cloud chambers, which is explained below.

For low supersaturation ranges relevant to marine stratiform clouds isothermal haze and continuous flow thermal diffusion cloud chambers are usually used [*Alofs et al.*, 1981; *Hagen et al.*, 1990]. A combination of an isothermal and a diffusion cloud chambers was reported as a CCN spectrometer by *Hudson* [1989]. The operation of conventional thermal gradient cloud chambers at low supersaturations (lower than 0.2%) is extremely difficult because of the difficulties associated with maintaining a very small temperature difference between the plates of the chamber. In addition, temperature changes due to compression or decompression of the air flow in different parts of the system can not be neglected at low supersaturations [*Gerber*, 1991].

Isothermal cloud chambers, the most often used for measurements of CCN concentrations at low supersaturations, extrapolate the critical supersaturation of particles from their equilibrium size at 100% RH [*Twomey*, 1977a]. However, uncertainties in chemical composition of ambient aerosols and presence of organic materials may result in large errors [*Corradini and Tonna*, 1979]. The chamber used in this study does not have such problems because it has a different operation principle than the conventional gradient cloud chambers, as will be discussed in this chapter.

One of the drawbacks of the conventional cloud chambers is a small size and the associated low sampling flow rate (usually less than a few liters per minute). The small size and flows of these chambers, except for a system with a flow of 30 *l*/min reported by *Williams et al.* [1994], do not allow (simultaneous) measurements of such critical parameters as number concentration, size and chemical composition of the aerosol. One of the advantages of the chamber used in this study is its large size and throughput flow rate (20 m^3/min) which solves this problem. The unique large size of the chamber and the associated high throughput flow allowed unperturbed use of conventional cloud instrumentation, like the Forward Scattering Spectrometer Probe (FSSP-100, PMS Inc.) for sizing and counting of droplets. Also high-flow Berner cascade impactors for chemical analysis of aerosol were used, even inside the chamber. The use of instruments with different measuring principles reduces experimental uncertainties so common for measurements of CCN and clouds [*NASA*, 1980].

The high throughput flow of the cloud chamber which is described here brings a new feature to its operation the droplet growth occurs under turbulent conditions. *Benner et al.* [1989] reported a concurrent flow cloud chamber which also operated under turbulent conditions. Unfortunately, the authors could not determine the supersaturation in their chamber, which makes it difficult to make a comparison with the chamber used in this study.

A laboratory generated ammonium sulfate aerosol was used to determine supersaturations in the chamber. Ammonium sulfate was

chosen because this compound dominates the number of PCN in marine air flows, which follows from the impactor measurements, discussed in Chapter 2. The water depletion effect at high number concentrations was characterized during experiments with ammonium sulfate aerosol by varying the total number concentration and keeping the size distribution constant. The cloud forming efficiency of laboratory generated ammonium sulfate aerosol is used to characterize cloud forming efficiency of ambient aerosols, which will be discussed in the following chapter.

DESCRIPTION OF THE CLOUD CHAMBER

It was mentioned already that the chamber employed in this study is completely different from the conventional cloud chambers. In fact, originally it was not designed as a cloud chamber, but as a chamber for equilibrated (at 100% RH) fog studies [*Mallant et al.*, 1988]. However, it was noted that at a certain setting the chamber produces low (in the order of 0.1%), though very stable, supersaturation. Characterization of the chamber, operating under supersaturation, was done in this study and is described in this chapter.

The chamber operates in the following way. The sample air stream is saturated with water vapor at a temperature that is a few degrees higher than the central vessel of the chamber. The warm saturated air stream is then introduced into the central vessel. The high flow rate results in a turbulent flow through the vessel, which leads to a constant stirring of the air inside the vessel. Contacting the colder walls of the vessel, the air cools, which according to the Clausius - Clapeyron equation (which states that water vapor pressure is exponentially increasing with temperature) becomes supersaturated [*e.g. Pruppacher and Klett*, 1978]. According to the Clausius - Clapeyron equation it follows that the stronger the cooling, the higher the supersaturation. Consequently, the larger the temperature difference between the walls

and the incoming air stream, the higher is the resulting supersatuation. This principle is used to control the supersaturation, which is described below.

The general view and a scheme of the cloud chamber is shown in Figure 4.1. Outdoor air is led into the chamber by a blower at a rate of 21 m^3/min. Before entering the chamber the air passes through a humidifier. The humidifier is a 3 meter high 1.15x1.15 meter tower, part of which (2 m^3) is filled with about 90000 ceramic Raschig rings of 2.5 cm diameter. Water is poured over the column at a rate of 150 *l*/min from the top, against the flow of the incoming air stream. The water is heated by a controllable 50 kW electric heater. It is important that the output of the humidifier does not depend on the outside weather conditions for the following reasons. The colder the outside air relative to the room air (20°C) and the lower its relative humidity, the more difficult it is to saturate the air to a temperature several degrees higher than room temperature. If the humidifier would fail to saturate the air stream at the preset temperature, it would result in a different supersaturation (if any) in the chamber and thus the supersaturation would be difficult to reproduce. For this reason the humidifier was designed such that it is about 2 times "oversized" [*Mallant et al.*, 1988]. The humidifier proved to be able to maintain the necessary temperature difference even during days with low ambient temperatures and low relative humidity (11°C and 65%).

After the humidifier the saturated air stream enters a cylindrical vessel (2.5 m i.d., 4.3 m high) of approximately 21 m^3 volume. The vessel is made of welded 1 cm thick aluminum sheets. Contacting the colder walls of the vessel, the incoming air becomes supersaturated. Supersaturation is set by maintaining the water in the humidifier several degrees warmer than the room air. A higher supersaturation is achieved at a higher temperature difference. The room air temperature is measured at 4 points situated at half-height of the chamber, 10 cm from the vessel walls (the length of a thermocouple element used for the temperature measurements).

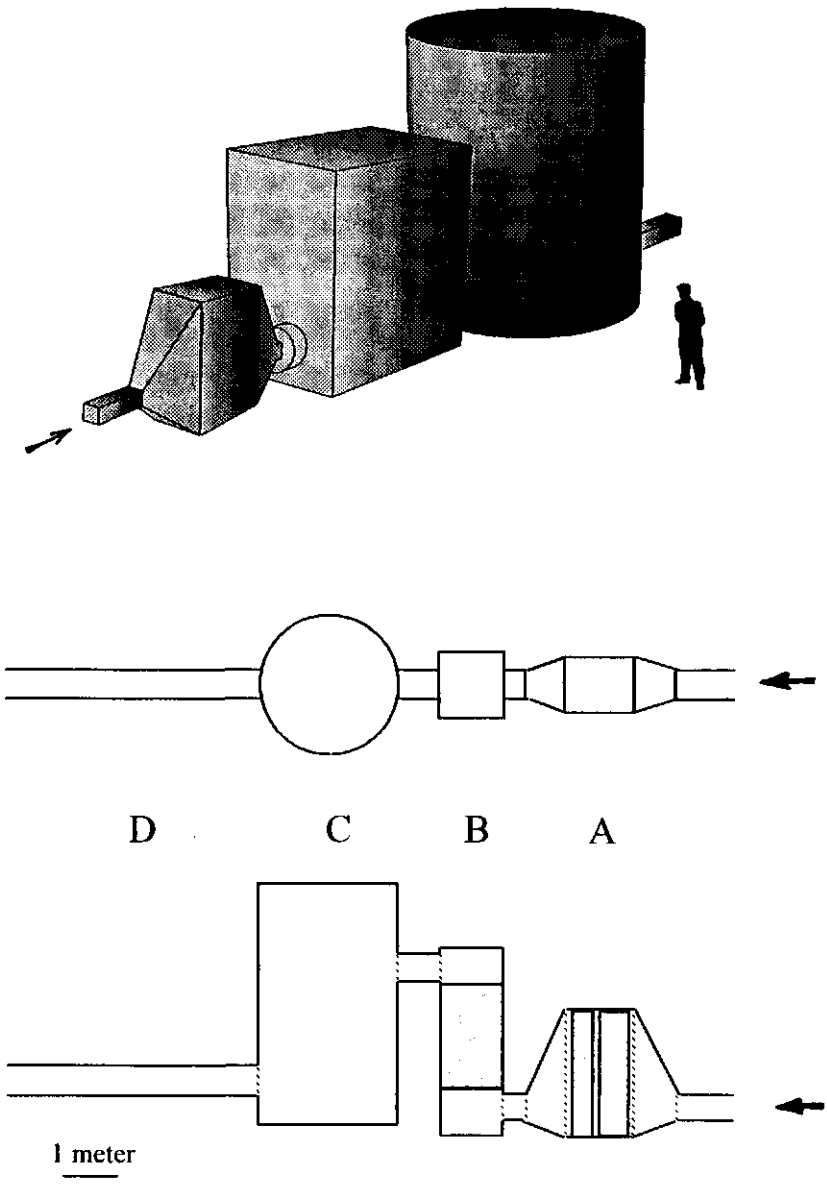

Figure 4.1. *General view, view from the top and vertical cross-section of the ECN cloud chamber. A: filter housing; B: humidifier; C: chamber; D: tunnel.*

One may suggest that the best way to control the supersaturation is by directly controlling the temperature difference between the walls and the incoming air stream. This would mean that the wall temperature and the temperature of the saturated air stream should be directly controlled. However, this is not done for the following reasons. To achieve a low supersaturation one would need to control and maintain a temperature difference of about 1°C. Such a precision controll is highly problematic due to the large scales of the chamber: approximately 2.7 ton aluminum vessel and about 0.5 ton water reservoir of the humidifier. It was found that a more stable performance of the chamber was achieved when controlling the temperature difference between the water in the reservoir and the air temperature around the vessel, which is usually set at about 8°C to achieve an 0.15% supersaturation, as will be shown later in this chapter.

The heat balance of the chamber is established in the following way. The heater in the humidifier is the major source of energy in the chamber. It heats the water reservoir of the humidifier which in turn warms up the incoming air stream. The warm air stream exchanges its thermal energy with the walls of the chamber: walls warm up and the air cools down. The walls, in turn, exchange heat with the air surrounding the vessel. This results in a negative temperature gradient from the walls to the bulk of the air in the room (14x10x8 m) in which the chamber is situated. The room air in turn exchanges heat with the "universe" via an air conditioner and windows of the room. To enhance the heat exchange between the walls and the room two large fans are placed at the ceiling of the room to stir the air. This is also done to avoid temperature gradients in the room. If it would not be done, warm air would accumulate with time in the upper part of the room, which would lead to a smaller temperature difference in the top of the vessel than in its bottom part, hence changing the conditions in the chamber with time, which should be avoided.

Due to the exchange of heat between the air stream, walls and the room air the following situation is established (Fig.4.2a): $T_{room} < T_{air\ measured} < T_{walls} < T_{air\ stream}$. Consequently, the measured air

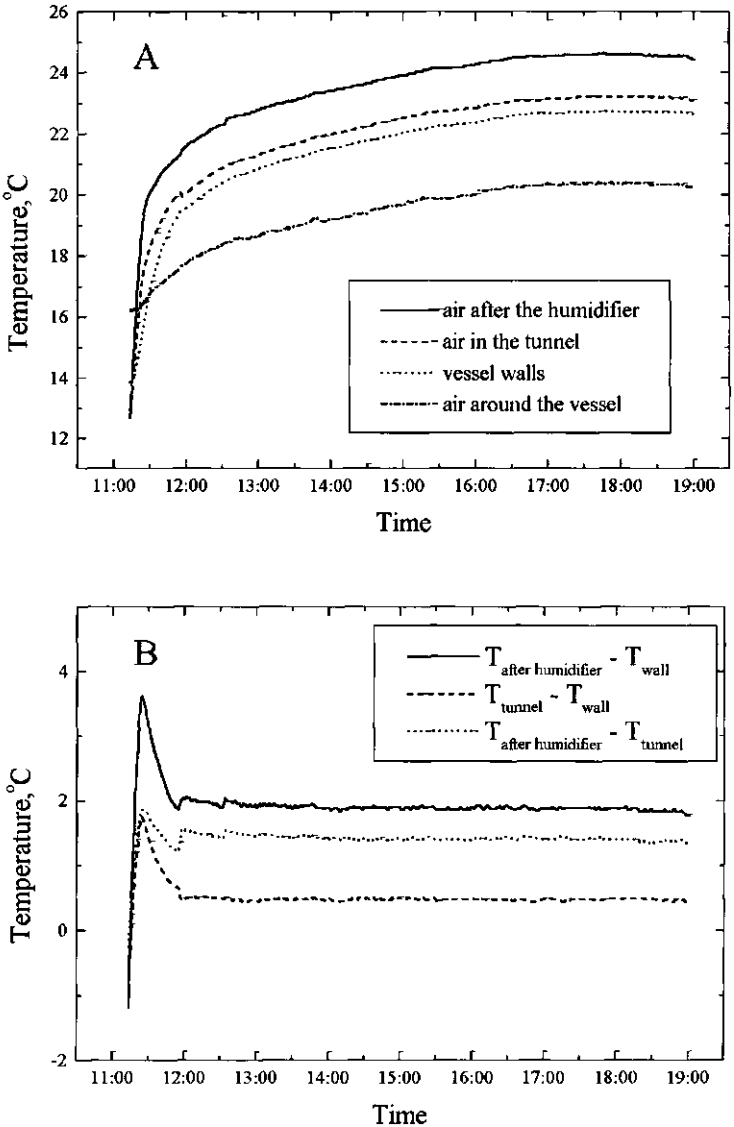

Figure 4.2. *A: Time evolution of air and wall temperatures in the chamber. B: Time evolution of differences in temperature between the air entering the vessel (as measured after the humidifier), leaving the vessel (as measured in the tunnel) and the walls of the vessel.*

temperature difference is larger than the actual difference between the walls and the air stream, and thus is easier to control. Remarkably, it is the large heat capacity of the chamber, that makes the operation of the chamber so stable. The temperature difference between the air stream and the walls (or the temperature by which the air stream is cooled inside the vessel), which causes the supersaturation, remains stable for hours (Fig.4.2b). The stable temperature difference results in a stable LWC and thus in a stable supersaturation, as will be shown in the following sections.

The air leaves the vessel through a 5 meter long 50x50 cm tunnel. Droplets formed in the chamber by condensation of the supersaturated water on aerosol particles are measured in this tunnel. Because the air is somewhat accelerated in the tunnel due to its smaller cross-section relative to that of the central vessel, one may expect that the air stream may cool due to this acceleration and thus produce an extra supersaturation. The acceleration can be readily converted into the temperature decrease: the gain in kinetic energy should be equal to the loss in thermal energy. The air stream in the tunnel is accelerated by about 1.5 m/s relatively to the flow in the vessel. Such an acceleration would result in cooling of the order of only 0.001°C, which is certainly negligible.

AEROSOL LOSSES / ARTIFACTS

The losses of particles in the chamber were assessed by measuring the aerosol spectrum before and after the chamber with a DMPS (TSI Inc.). The measurements indicated only a small loss (10% or less) of particles with diameters smaller than approximately 0.1 μm (Fig.4.3). These losses most probably occur in the humidifier which has a very developed surface (because it is filled with Raschig rings). Since these particles do not activate at supersaturations of around 0.15% which was used in the experiments, the losses of such small particles do not

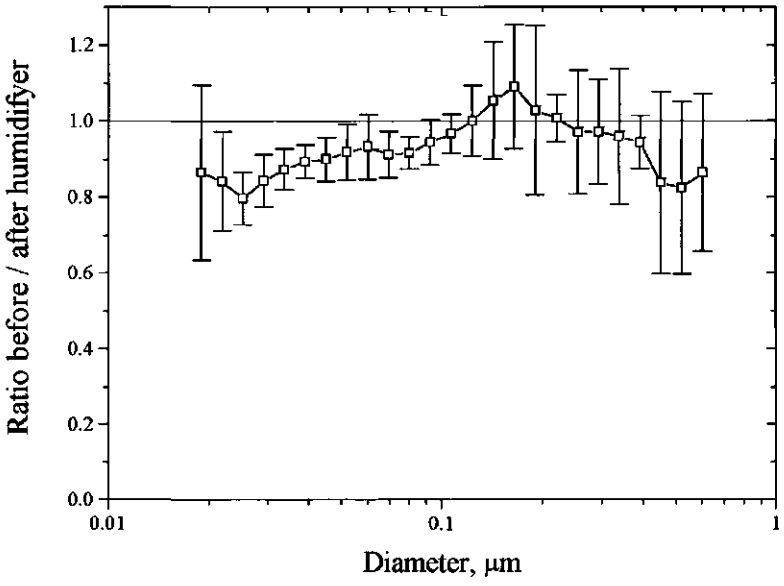

Figure 4.3. *Losses in the cloud chamber of ammonium sulfate particles as a function of size.*

pose any problem for interpretation of the results of activation experiments. The loss of large droplets was also tested. Comparison of the impactor spectra before and after passage through the (dry) chamber indicated no loss of particles with diameters less than 2 μm, but substantial loss of larger particles [*Kruisz*, 1992], again presumably in the humidifier due to impaction onto the Raschig rings. However, the number of particles larger than 2 μm is negligible, both in the tests with the reference aerosol and those with ambient aerosol, as compared to the number of smaller particles growing into cloud droplets.

A possibility exists that droplets, grown on particles during activation, are lost in the chamber (most probably due to sedimentation). If such a loss occurs, the number of droplets and thus the number of activated particles would be underestimated. For this reason, the extent of such losses was also checked. Since the liquid

water content (LWC) is mostly determined by larger droplets and because these large droplets would be in the first place affected by the losses, a loss of the LWC was measured. Experiments by *Mallant et al.* [1988] have shown that the loss of droplets with mass median diameter of 11-15 μm is smaller than 12%. Calibration of the counting efficiency of an FSSP (PMS Inc.), which was done in the present study (see the section describing aerosol instruments which were used in this study) can be also used as an indirect measure of the droplet losses in the chamber. During these experiments the number of droplets measured with the FSSP was compared to the number of activated particles as measured with a DMPS (TSI Inc.), which is described further in this chapter. If the droplet loss would be substantial, the droplet number would be consistently lower than the number of activated particles. It was found that the differences in the number of droplets as measured with the FSSP and as derived from the DMPS measurements are random and are within 10%. Thus, it may be concluded that the losses of droplets inside the central vessel are negligible.

During measurements in aerosol free-air it was found that the humidifier produces a very broad, irregular spectrum of droplets with the total number concentration of 50 ±10 cm^{-3}. These droplets originate from bursting water bubbles appearing as the water, running from the column, splashes into the reservoir in the bottom part of the humidifier. The droplet number measured during all of the experiments reported in this study was corrected for the presence of the background droplets.

AEROSOL GENERATION

Ammonium sulfate aerosol was used to check the performance of the chamber and to calibrate the chamber for the interpretation of results of ambient aerosol activation experiments. Ammonium sulfate aerosol was chosen (see Chapter 2) because it is the dominant

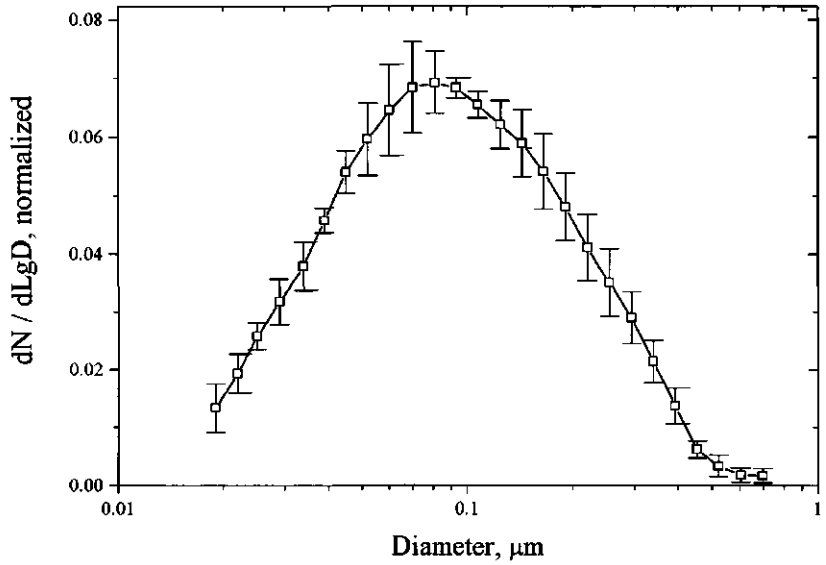

Figure 4.4. *Number size distribution of the reference ammonium sulfate aerosol.*

compound determining the number of PCN in marine air flows in the Netherlands. During experiments with ammonium sulfate aerosol the air before entering the humidifier passed through high flow absolute filters to remove the ambient aerosol. The reference aerosol was introduced after the humidifier. The aerosol was generated by spraying ammonium or sodium sulfate solution with a Wiesbadener Doppel-Inhalator or TSI 6-jet atomizer. These nebulizers were chosen due to the stability of their output. The criterion for stability was that the total number concentration was stable within 10% during about 5 hours. The nebulizer output, before entering the chamber was mixed with a tenfold stronger flow of dry (RH < 10%) aerosol-free pressurized air stream in order to dry the droplets of salt solution produced by the nebulizer. The size distribution of the reference aerosol (Fig.4.4) was set to be centered (in the dry state) at around 0.1 μm in diameter and maintained constant from experiment to experiment. Activation tests

were done varying the total aerosol number to check its influence on the number of resulting cloud droplets.

AEROSOL / DROPLET MONITORING AND SAMPLING

The size and number concentration of the incoming aerosol was measured before the chamber with a Differential Mobility Particle Sizer (DMPS, TSI Inc.). The DMPS was set to measure particles from 0.019 to 0.6 μm in diameter. The aerosol and the sheath air flows of the DMPS were dried before entering the DMPS with a silica gel diffusion dryer to bring the aerosol to a reference state at a low relative humidity. Aerosol size and number concentration were also measured behind the chamber with another DMPS system. To correct for the residence time inside the chamber the second DMPS system was sampling with a delay of 1 minute relative to the first DMPS. Before entering the second DMPS (sampling from the tunnel behind the chamber) the tunnel the air stream passed an impactor with an 0.8 μm cutoff to remove the droplets, then was heated slightly and dried with a silica gel diffusion dryer to bring the aerosol to the dry reference state. In this way the spectrum of inactivated particles is obtained. Comparing the spectra and absolute numbers of the aerosol before and after the chamber the number and size of the activated particles are obtained.

It is important to bring the aerosol to the dry reference state to allow direct comparison of the aerosol size and number concentration before and after the chamber. The aerosol must be dried below the crystallization point otherwise the aerosol after the chamber will be larger than its dry size due to the hysteresis effect below the deliquescence point. The dry size also allows estimation of the supersaturation from an "activation threshold". The activation threshold can be defined as the largest dry size of a particle that has not been activated (see Eq.3.12). The activation threshold is a measure

of "effective" supersaturation in the chamber. The activation threshold is found from the dry aerosol spectra before and after the chamber.

The sizing accuracy of the DMPS systems was calibrated with monodisperse polystyrene latex (PSL) aerosol. The counting efficiency of the DMPS systems was checked against a CPC (TSI model 3020 or 3022 were used), which was used as a reference, and against each other. Such calibrations were done before each of the experiment (both with ammonium sulfate and ambient aerosols) reported in this study. The counting efficiency of the DMPS systems was 10 to 20% lower than that of the CPC. The concentration measurements obtained with DMPS systems were consequently corrected with the corresponding factor. Counting efficiency of a DMPS, calibrated in this way, was occasionally compared with that of a LAS-X (PMS Inc.). The results of the two instruments were comparable within 10%. Since the instruments employ different measuring principles (the DMPS uses electrostatic classification, while the LAS-X uses optical sizing), the close results suggest that the found concentration is the best representative of the actual number concentration. Much attention was devoted to the calibration of the counting efficiency of aerosol instruments because aerosol and droplet number concentration are the central parameters for quantification of the indirect effect. Calibration of number counting is always extremely problematic because no absolute standard exists for such a calibration as opposed to monodisperse PSL aerosol for sizing calibration. Advantage of this study lies in the possibility to compare results from aerosol monitors with different measuring principles. Such inter-comparison was possible due to the very large size of the chamber. The large size also allows to use several instruments in parallel, which also reduces the counting uncertainty. For instance, as will be shown below, DMPS measurements of aerosol before and after the chamber may be used as a check or a back-up for measurements of droplet number concentration which in this study was measured with an FSSP (PMS Inc.).

The liquid water content (LWC) of the droplets formed on the aerosol was used to estimate the supersaturation in the chamber (see the corresponding section in this chapter) as well as for monitoring its

stability. The LWC was measured in the tunnel with a PVM-100 probe (Gerber Scientific, Inc.). The PVM-100 probe was calibrated against filter measurements of the liquid water content [*Arends et al.*, 1992]. Since the cloud chamber is to be used for activation studies on actual ambient aerosol, the stability of the LWC in the system was checked with ambient aerosol to have direct evidence that the performance of the chamber is not affected by variations in the spectral and chemical composition of aerosol.

The droplet spectra and the number of droplets were measured with an FSSP-100 (PMS Inc.). This instrument measures size and concentration of water droplets with sizes between 1 and 95 μm in diameter. Cloud droplets were considered to be those particles that are larger than 2 μm, as was discussed in the previous chapter, similarly to an empirical criterion of *Leaitch et al.* [1986], who proposed to use this size as a criterion for classification on droplets and interstitial aerosol. The size calibration of the FSSP was performed with glass beads. The sensing volume of the FSSP was measured with a wire controlled by a micro-positioner [*Dye and Baumgardner*, 1984]. The droplet concentration was corrected for probe dead time and coincidence error [*Baumgardner et al.*, 1985].

Apart from the calibration of the FSSP according to the above standard method a very careful test was made in which the number of cloud droplets was compared with the number of activated ammonium sulfate particles as deduced from DMPS measurements. This was done in the following way. First, the dry spectrum of ammonium sulfate aerosol was measured before it was subjected to a supersaturation in the chamber. After the chamber the droplets ("activated" particles) are removed with an impactor with a cutoff diameter of about 0.9 μm. This size is approximately the equilibrium size at 100% RH of largest particles that can not be activated at 0.15% supersaturation (as will be shown further in this chapter such a supersaturation was actually achieved). Thus, this cutoff diameter is a good separator between the sizes of wet interstitial particles and droplets. After the droplets are removed with the impactor, the interstitial aerosol is dried with a diffusion dryer and its size distribution is measured with the DMPS.

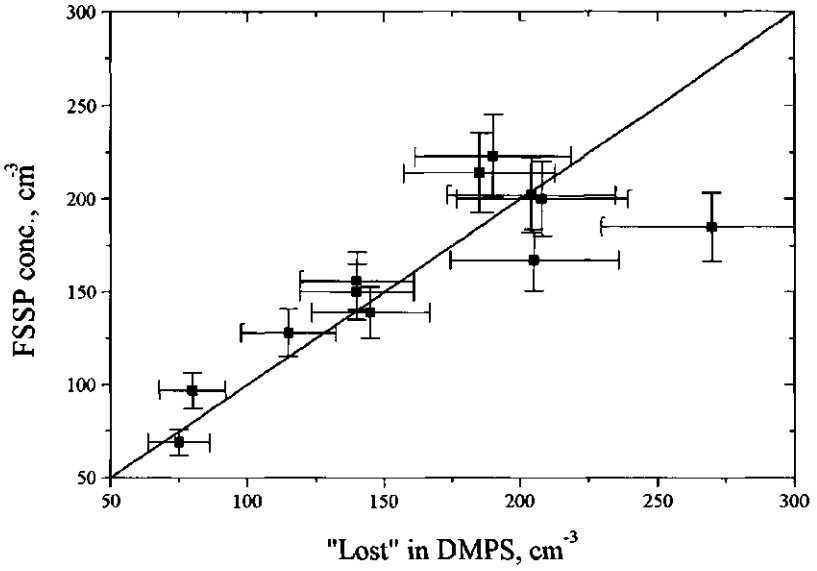

Figure 4.5. *Comparison of droplet concentration as measured with FSSP and concentration of activated aerosol particles as derived from DMPS measurements.*

The difference in particle number concentration before and after the chamber should correspond to the number of cloud droplets formed. Low aerosol number concentrations were used in order to avoid complications arising from the saturation effect at high number concentrations (see further in this chapter). Indeed the number of particles activated was within 10% of the number of cloud droplets formed (Fig.4.5). Actually this is a combined check on the performance of the cloud droplet counter (FSSP) and the particle counter(s) used. It is possibly the first calibration of this kind.

As was mentioned previously, the humidifier produces about 50 ± 10 cm^{-3} droplets. All droplet concentrations measured in the chamber were corrected for this "background". At droplet number concentrations lower than 100 cm^{-3} the noise in the "background" droplet concentration

is becoming substantial in comparison to total number concentration, exceeding the estimated accuracy of counting (10%, see above). To cope with this problem, the actual droplet number concentration was calculated as the average of the concentration measured with the FSSP and the amount of activated particles which is deduced from the DMPS measurements. DMPS measurements are not affected by the background, because the background droplets are larger than the upper sizing limit of the DMPS (0.86 μm) and thus are not counted by the DMPS.

During experiments with ambient aerosol cascade impactors were used for collecting the aerosol as a function of size for weighing and chemical analysis [*Berner*, 1989], see Appendix 1. Aerosol samples were collected on aluminum foils. After collection the samples were weighed with a precision balance (1 μg accuracy), then dissolved in 7 ml of doubly demineralized water and analyzed for soluble inorganic species with IC and flow injection analysis.

The size and the insoluble material content of a particle govern its activation [*Pruppacher and Klett*, 1978; *Twomey*, 1977a]. Particles with a higher content of insoluble material need to be substantially larger to be activated (Fig.3.2). The amount of insoluble material in ambient aerosols was deduced from the impactor measurements by subtracting the mass of soluble material from the total aerosol mass. It should be noted that measuring the composition of the smallest, most numerous potential cloud nuclei is very difficult: even though they represent the majority of the number they contain very little mass. Sampling for several hours provides an aerosol deposit in the smallest impactor stage with a mass in the order of a few micrograms which is comparable to the weighing error. On some occasions it was necessary to extrapolate the composition measured at larger diameters to lower sizes, analogous to the extrapolations of *Novakov and Penner* [1993].

RESIDENCE TIME DISTRIBUTION OF AIR INSIDE THE CHAMBER

Due to the very high flow rate and its large dimensions the cloud chamber operates under turbulent conditions. A turbulent flow may result in "dead pockets" regions of stagnant flow. If such pockets are present, aerosol particles in such pockets would be under substantially different conditions than in the main flow. For this reason the mean residence time and time distribution of the air inside the chamber were measured to characterize the flow in the chamber. These parameters were found by measuring the time response to a step input of aerosol of constant concentration. The response of the chamber to the step input is shown in Fig.4.6. The residence time distribution was derived from a smoothed response curve [*Levenspiel*, 1972] and is shown in Fig.4.7. The mean residence time in the chamber was found to be 61 sec. The

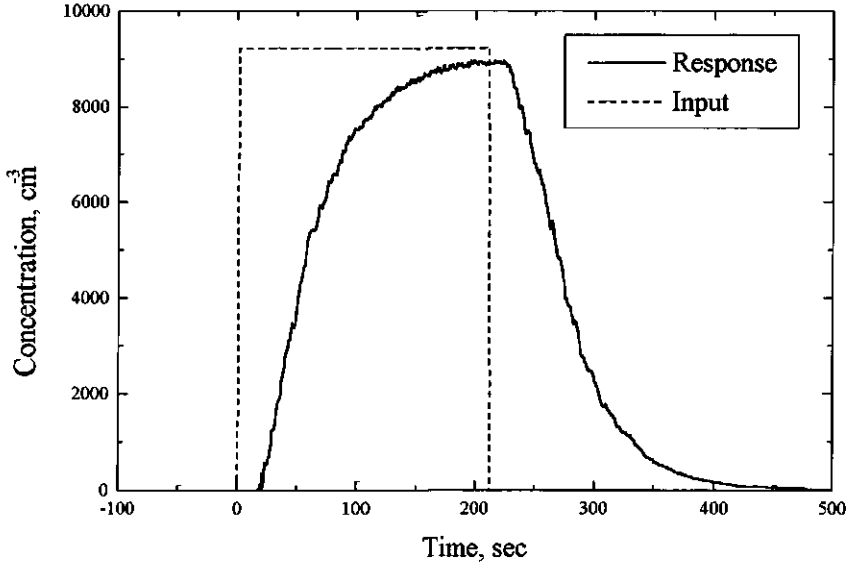

Figure 4.6. *Time response of the aerosol concentration in the chamber to a step-change in the aerosol input.*

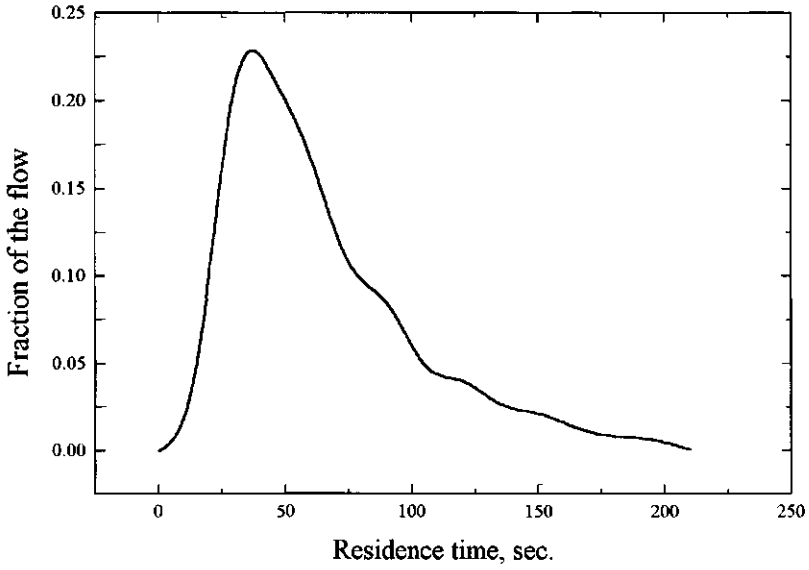

Figure 4.7. *Residence time distribution of the air inside the chamber (fraction of the flow leaving the chamber per unit time).*

flow rate through the chamber is thus approximately 20 m^3/min. From the residence time distribution it follows that the air in the chamber is well mixed and there are no internal re-circulation, dead pockets or shunting. Despite the spread in time that different air parcels spend in the chamber, the droplet spectra in the chamber are rather narrow, which will be demonstrated further in this chapter. This is considered as an additional proof that the air stream in the chamber is well mixed and that the supersaturation in the chamber is quite uniform.

The time that air spends in the chamber is sufficient for particles to reach 2 μm diameter (Fig.3.3). This size, as was discussed in the previous chapter, is used in this study as the criterion for classification on droplets ("activated" particles) and interstitial aerosol (non-activated particles). Even considering the spread in the residence time, most of

the "activated" particles would have sufficient time to reach the 2 μm size.

STABILIZATION OF THE CHAMBER

Due to the large geometry and the associated high heat capacity of the chamber, the system requires 1.5 - 2 hours for stabilization until the heat exchange between the vessel and the room achieves its steady-state. Figure 4.8 shows an "initiation" peak during the first 1.5 hours after the system was switched on. The initiation peak is due to an initially higher temperature difference between the chamber and the incoming air stream (Fig.4.9). As the walls warm up and the

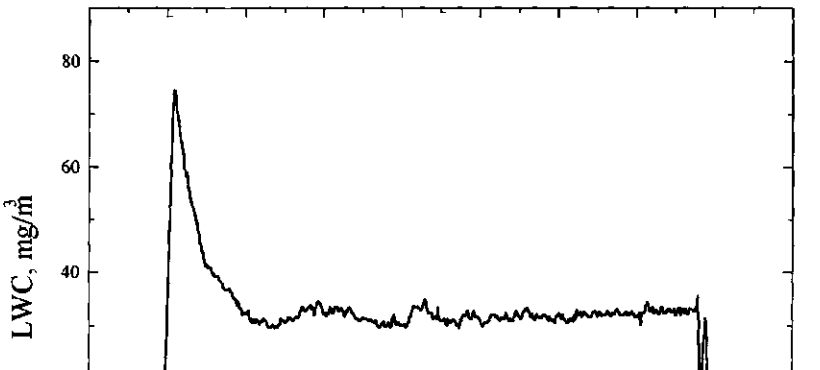

Figure 4.8. *Example of LWC measurement (the system was switched on at 12:50).*

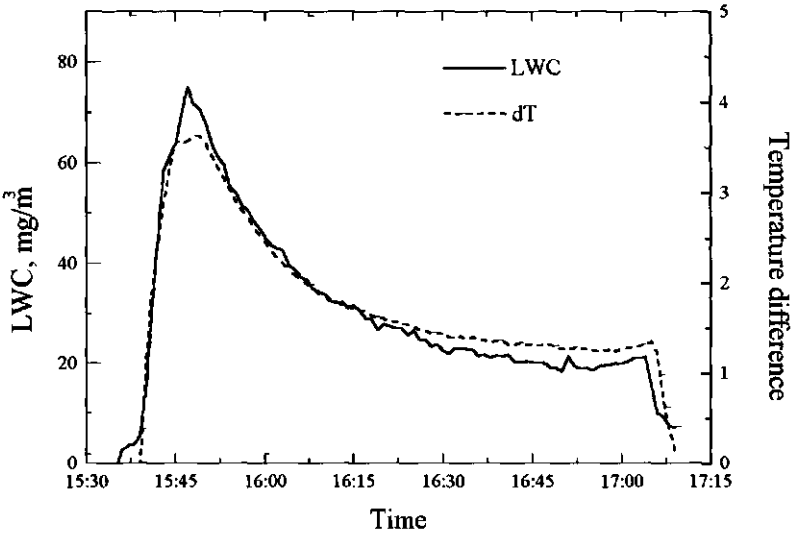

Figure 4.9. *LWC and temperature difference between the incoming air stream and the walls of the chamber.*

steady-state heat exchange between the air, the walls and the room is established. For this reason that actual tests were performed only after 2 hours to allow for the system (and supersaturation) to stabilize.

STABILITY OF THE CHAMBER

As was discussed in the previous sections, one of the most important characteristics of a cloud chamber is its stability. Since cascade impactors were used to relate chemical composition to the cloud activation properties of ambient aerosols, the chamber should be

stable for at least several hours to allow for impactor to collect aerosol mass sufficient for analysis.

As a criterion for the stability of the chamber the liquid water content (LWC) was chosen. The LWC may be considered as a measure of the supersaturation in the chamber (see the corresponding section in this chapter discussing measurements of the supersaturation). The stability of the LWC, hence, may be regarded as the stability of supersaturation in the chamber. The stability of the LWC was tested during activation experiments with ambient aerosol to check the influence of the variability of ambient aerosol on the performance of the chamber. The chamber has consistently proven to be able to maintain a stable LWC for several hours (Fig.4.8). This is the best evidence for a stable performance of the chamber. The standard deviation in the LWC values during a 5 hour run was on average 7%.

The stable performance at low supersaturations (about 0.15%, see the next sections) makes the chamber unique in its kind. The operation of conventional thermal gradient cloud chambers at low supersaturation is extremely difficult because of the difficulties associated with maintaining a very small temperature difference between the plates of a gradient cloud chamber. In addition, temperature changes due to compression or decompression of the air flow in different parts of the system can not be neglected at low supersaturations [*Gerber*, 1991]. Isothermal cloud chambers, the most often used for measurements of CCN concentrations at low supersaturations, extrapolate the critical supersaturation of particles from their equilibrium size at 100% RH. However, uncertainties in chemical composition of ambient aerosols and presence of organic materials may result in counting errors of up to 80% [*Corradini and Tonna*, 1979].

SUPERSATURATION IN THE CHAMBER

As was discussed in the previous chapter, it is important to establish a supersaturation in the chamber such that it is relevant to the cloud type of our interest - marine stratiform clouds. One of the aims of experiments with the reference aerosol was to search for conditions at which the supersaturation in the chamber is of the order of 0.1%. This value was chosen because supersaturation in marine stratiform clouds is estimated to be between 0.1 and 0.3% [*Albrecht et al.*, 1988; *Martin et al.*, 1994]. Conventional thermal-gradient cloud chambers reliably operate at 0.2 - 0.3%, for lower supersaturations isothermal cloud chambers are used, which deduce the critical supersaturation from a size at 100% RH. However, this requires several assumptions [*Laktionov*, 1972]. For this reason there are no direct results available of measurements at supersaturations below 0.2% and thus it was decided to achieve a supersaturation at around 0.1%.

A direct measurement of the supersaturation in the chamber with a dew-point probe is not reliable because of the measuring uncertainty of such probes at low supersaturations [*Gerber*, 1991]. For this reason experiments with the reference aerosol were used to estimate the supersaturation in the chamber. The supersaturation was estimated at low total aerosol number concentrations (100 - 200 cm^{-3}), because of the complications arising at higher aerosol numbers due to competition for water vapor between individual particles and between the particles and the walls of the chamber, which is discussed further in this chapter.

The degree of supersaturation in the chamber was estimated from the activation threshold, which was defined in the previous sections (see Eq.3.13). The dry spectrum of non-activated particles was measured with a DMPS. First, the droplets ("activated" particles) are removed with an impactor with a cutoff diameter of about 0.9 μm. This size is approximately the equilibrium size at 100% RH of largest particles that can not be activated at 0.15% supersaturation (as will be shown below such a supersaturation was actually achieved). Thus, this

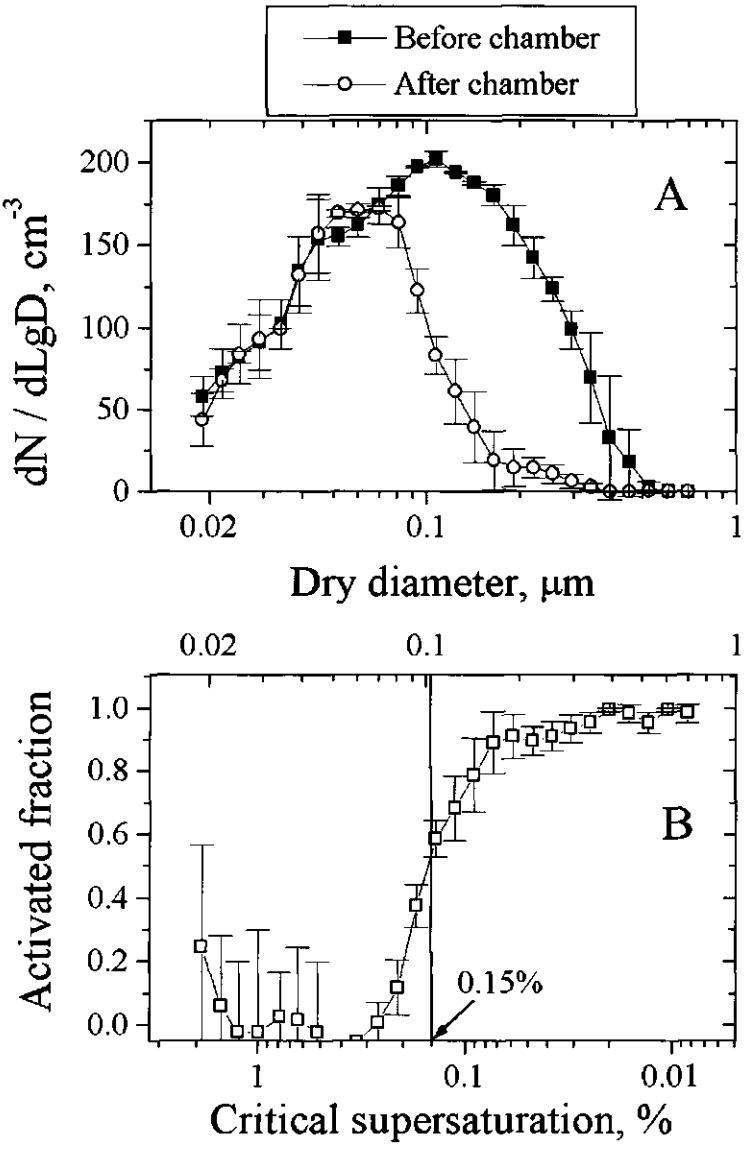

Figure 4.10. *A: Comparison of dry spectra of reference ammonium sulfate aerosol before and after the chamber. B: Fraction of activated particles as a function of size.*

cutoff diameter is a good separator between the sizes of wet interstitial (non-activated) particles and droplets. After the droplets are removed with the impactor, the interstitial aerosol is dried with a diffusion dryer and its size distribution is measured with the DMPS. The activation threshold is then found from the difference in the dry aerosol spectra before and after the chamber (Fig.4.10a). The larger particles have disappeared after the chamber because they have grown into droplets (became activated) while the smallest particles have not. A graph showing the fraction of activated particles as a function of size is given in Fig.4.10b.

The graphs show an activation "cutoff". Because the chamber operates under turbulent conditions, there is inevitably a spread in supersaturation inside the chamber, which leads to the activation cutoff that is not perfectly uniform, but is S-shaped. The size at half-height of the activation "cutoff" is used to estimate the supersaturation. Due to turbulence, it is possible that air parcels experience different supersaturations in their way through the chamber. Thus, the estimated supersaturation should be understood as an "effective" supersaturation, meaning that such a supersaturation would have the same effect on the aerosol spectrum (in terms cloud activation) as the average result of all supersaturations experienced by all air parcels in the chamber. Calibration tests with ammonium sulfate aerosol at the temperature difference set at 8°C gave an activation threshold at around 0.1 μm (Fig.4.10b), which corresponds to a critical supersaturation of 0.15 % (Eq.3.13).

Error in determination of the supersaturation from the activation threshold arises mainly from the size resolution of the DMPS. The DMPS channels are spaced such that r_{i+1}/r_i = 1.15. As the activation threshold is at around 0.1 μm in diameter, the uncertainty in size leads to the uncertainty in supersaturation of (less than) 0.01%.

Another way to estimate the supersaturation is via the amount of condensed water (LWC). The condensed water was initially available for condensation in the vapor form and consequently is a measure of the amount of vapor above its saturation value. Knowing the LWC and

temperature in the tunnel the water vapor content can be deduced from which, in turn, the supersaturation in the system is deduced:

$$S_{eff} = \frac{LWC}{p_{sat}} \frac{RT}{M_w} 100\% \qquad 4.1$$

in which S_{eff} is the effective supersaturation, R is the gas constant, M_w is the molecular weight of water psat is the saturation vapor pressure, T is temperature, LWC is the liquid water content and is equal to m/V with m being the mass of condensable water and V being the volume.

The supersaturation estimated in this way was found to be 0.11 ±0.01 %. This value is in fair agreement with the supersaturation found from the activation threshold, see above. A complication is the fact that droplets can only exist in equilibrium with supersaturated vapor. The equilibrium supersaturation for droplets of 5 - 10 μm size is in the order of 0.001%, which is an insignificant amount as compared to the calculated supersaturations. A second complication in using the latter method to assess the initial supersaturation is the fact that condensation may not have been completed during the residence time in the chamber. However, a variation in the number of aerosol particles indicated only little dependence of condensed water on aerosol number: when the number concentration is increased from 280 to 35500 cm^{-3} (*i.e.* by approximately a factor of 127) the LWC increases by a factor of 2.3. If the condensation would not be completed within the residence time, the LWC would increase by exactly the same factor as the aerosol concentration is increased. This is evidence that the residence time in the chamber is sufficient for condensation of the available water. The observed increase in LWC with the aerosol number concentrations is most probably explained by competition for water vapor between the particles and the walls of the chamber. Higher aerosol concentrations provide larger sink for water vapor and thus more water condenses on the particles before it condenses on the walls.

Since the supersaturation in the chamber arises from cooling of the warm air stream by the colder walls, one can expect, according to the Clausius - Clapeyron equation) a higher supersaturation at higher (absolute) ambient (and consequently room) temperatures. Indeed,

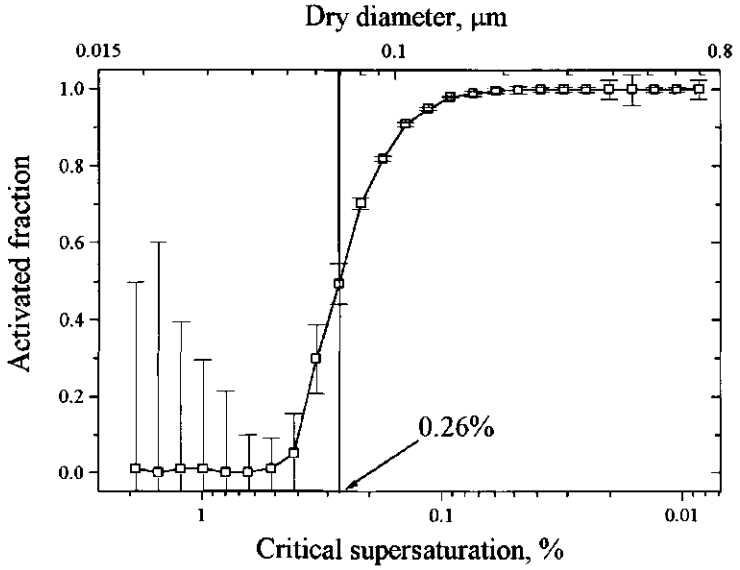

Figure 4.11. *Fraction of activated particles as a function of particle size at high room temperatures (30 - 35°C) and temperature difference set at 8°C.*

during calibration tests at outside air temperature 30°C the activation threshold for ammonium sulfate was at around 0.07 μm diameter (Fig.4.11), which corresponds to 0.26 % supersaturation. To compensate the increase in supersaturation due to a higher room temperature the temperature difference between the humidifier and the room was reduced. At the difference of 4°C the threshold diameter was (again) at 0.1 μm, corresponding to critical supersaturation of 0.15 %. For the temperature difference setting of 4°C during these high temperature experiments the supersaturation according to the LWC was 0.12 ±0.02%. For the temperature difference of 8°C it was 0.27 ±0.02%. Both values are in rather good agreement with the supersaturations corresponding to the activation thresholds. This example shows a possibility to control the supersaturation in the chamber by varying the temperature difference setting. Unfortunately, due to the very high

heat capacity of the chamber it is not possible to make "fast" supersaturation scans. Every time the temperature setting is changed the system requires 1-2 hours to stabilize again.

The effect of temperature on the supersaturation in the chamber did not pose large problems during experiments with ambient aerosols. As was discussed in the previous chapter, the measurements with ambient aerosols were confined to marine air flows. Such air flows are rarely associated with high (above 20°C) temperatures and air conditioners in the room, where the chamber is placed, have sufficient power to maintain the room temperature around 20°C, at which the temperature difference setting of 8°C was used. For a check, the supersaturation during the ambient measurements was always monitored using the LWC method (Eq.4.1). The measurements at which the supersaturation according the LWC exceeded the limits of 0.12 ±0.02% (the range at which the more accurate threshold method gave 0.15%) were discarded.

It should be noted here that the tests are performed at higher temperatures than the temperatures in actual clouds. However, according to *Pruppacher and Klett* [1978] cloud activation of aerosol is almost independent of temperature. The main aim of this study is an assessment of the influence of anthropogenic aerosol on low marine clouds which are warm wet clouds with temperatures at cloud base which are at most ten degrees below surface temperature, which is small compared to differences in the physicochemical cloud activation characteristics of the relevant salts [*Pruppacher and Klett*, 1978].

INFLUENCE OF THE TOTAL NUMBER CONCENTRATION

Activation experiments were done as a function of aerosol number maintaining the size distribution constant, in order to check for the

water depletion effect discussed in the previous chapter. The amount of activated particles vs. total aerosol number concentration (particles larger 0.019 μm in diameter) is given in Fig.4.12. The droplet number does not increase proportionally to the number of particles, which indicates the saturation effect due to water depletion by growing droplets (see the section on the saturation effect in the previous chapter). The relation between the droplet number concentration and the concentration of particles that are larger than the threshold size of 0.1 μm is given by:

$$N_{droplet} = 11.2(\pm 1.2)\, N_{aerosol}^{0.53(\pm 0.01)} \qquad 4.2$$

Due to the water depletion the droplet spectrum progressively shifts to smaller sizes with increasing aerosol (and droplet) number concentration (Fig.4.13 and 4.14). The activation cutoff, in turn, shifts to larger sizes (Fig.4.15). This happens because particles that have sizes just above the activation threshold size have the highest critical

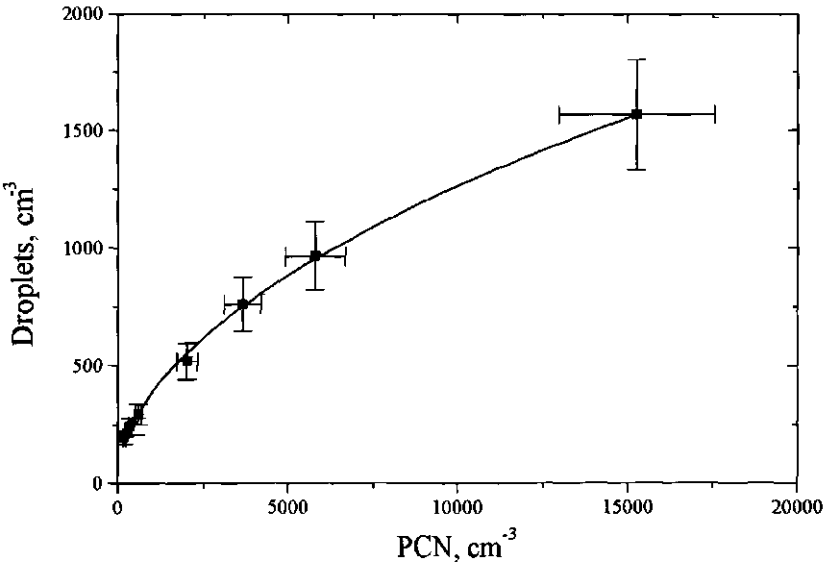

Figure 4.12. *Droplet number concentration versus PCN number concentration.*

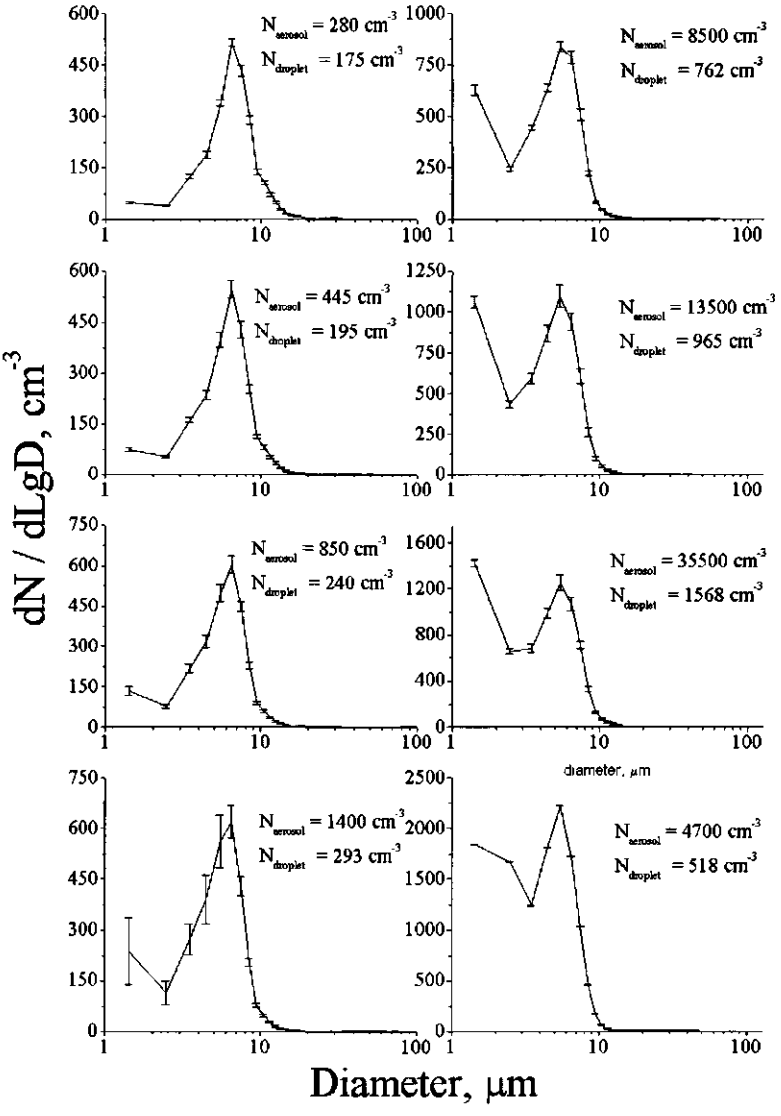

Figure 4.13. *Droplet spectra at different total aerosol number concentrations.*

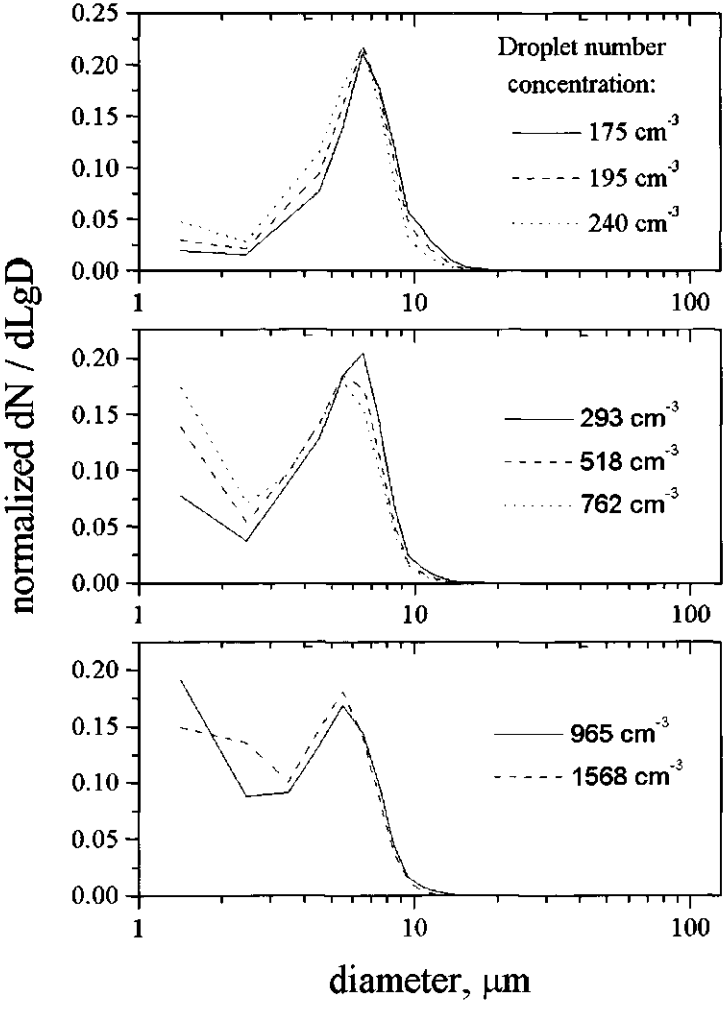

Figure 4.14. *Same as Fig.4.13, but the spectra were normalized to the total droplet number concentration (the areas under the graphs are equal to each other). Note how the spectrum shifts to smaller sizes with increasing droplet number concentration.*

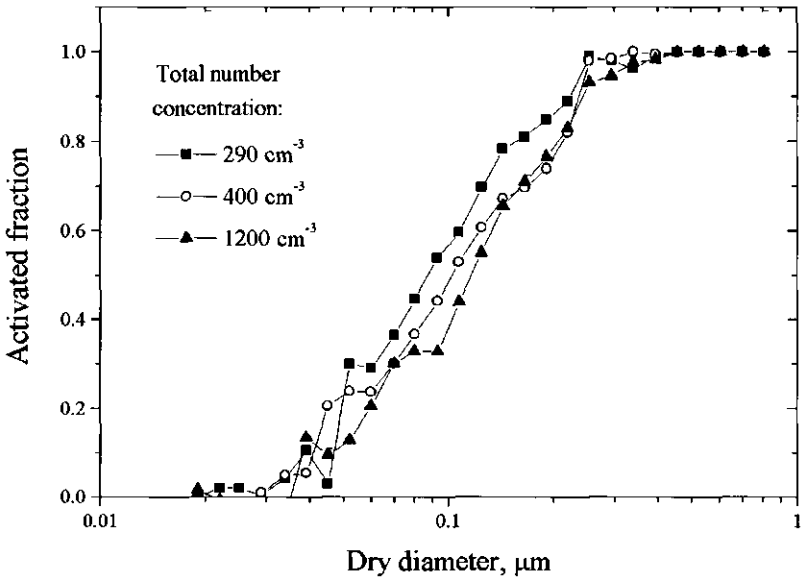

Figure 4.15. *Activation cutoff (as in Fig.4.10B) at different aerosol number concentration. Note that the cutoff shifts to larger sizes with increasing number concentration.*

superaturation among particles that are larger than the threshold and, thus, are the first to "suffer" from the water depletion. However, the shift of the cutoff to the larger sizes is not possible to observe after a certain aerosol number concentration (a few thousand per cm^3) is reached. This is because at high number concentrations more and more non-activated particles have wet sizes larger than the cutoff diameter of the impactor (0.86 μm), which can also be observed in the droplet spectra (Fig.4.13).

It is thus concluded that the maximum supersaturation in the chamber depends on the total number concentration of aerosol particles. For simplicity, interpretation of results obtained during activation experiments with ambient aerosols (see the following chapter) will be done on the basis of the "effective" supersaturation

which is measured at low aerosol number concentrations (200 - 300 cm^{-3}). The cloud forming efficiency (or cloud activation efficiency) of ambient aerosol is evaluated as the number of droplets formed per number of particles that are larger than the activation threshold (the so-called potential cloud nuclei, PCN, see the previous chapter) as determined with the reference ammonium sulfate aerosol. To compensate for the water depletion effect the observed activation efficiency is then compared with the activation efficiency of the reference aerosol as measured at the same number concentration of potential cloud nuclei.

Chapter 5

Activation of ambient aerosol

INTRODUCTION

This chapter presents the results of cloud activation experiments with ambient aerosols at a coastal site in the Netherlands which were done in order to obtain a first order estimate of the local indirect forcing. This study was performed in a high-throughput cloud chamber, which was described in the previous chapter. The cloud chamber was used because it allows to study the basics of the anthropogenic influence on clouds more accurately, as was discussed in Chapter 3.

Clouds form when a rising air parcel cools below its due point temperature, *i.e.* becomes supersaturated. The supersaturation causes water vapor to condense on aerosol particles. The condensation proceeds preferably onto particles, that are larger than a certain threshold size (Eq.3.12) and that have a high content of water-soluble material. These particles eventually form cloud droplets. The initial stage of cloud formation takes a few tens of seconds (Fig.3.3) at which stage the droplet number concentration is determined. During the following stage of the cloud development the formed droplets continue their growth which leads to the liquid water content to increase with height. The droplet number in stratiform clouds, however, remains fairly constant with height [*Albrecht et al.*, 1995; *Daum et al.*, 1987; *Martin et al.*, 1994; *Leaitch et al.*, 1996]. Because the residence time of air inside the chamber is about 1 min., results obtained in the chamber represent the first stage of cloud formation, *i.e.* processes occurring at the cloud-base, where the residence time of the air in the actual cloud is similar to the residence time of the air in the chamber. Because the

number concentration of droplets is the central parameter for assessing the indirect effect (see Chapter 3) and because the droplet number concentration is determined at the cloud base, the droplet number concentration observed in the chamber at a given supersaturation is expected to be a representative measure for the droplet concentration in clouds which supersaturation was as that used in the cloud chamber. The (maximum) supersaturation in marine stratus and stratocumulus clouds is estimated to be between 0.1 - 0.3% [*Albrecht et al.*, 1989; *Martin et al.*, 1994]. For this reason the supersaturation used in the experiments was set within this limits, being at around 0.15%.

The main attention in this study was given to marine aerosols (SW - N wind directions) (Fig.3.4), because marine stratiform clouds are the most influences by anthropogenic aerosols. The site where the measurements were carried out is ideally located for a study of marine aerosol, since it is situated directly on the border of the North Sea (200 meters from the shore line) and, hence, has practically no problems associated with local sources. Continental air masses were considered to be of comparatively smaller interest because they are rarely associated with stratiform clouds, which dominate the indirect effect. However, it is possible that continental aerosol blown off from the continents participates in formation of marine clouds and thus contributes to the indirect effect. For this reason some measurements were performed with continental or mixed marine-continental air masses.

Activation tests reported here were performed in the spring - autumn periods of 1992 and 1994. Table 5.1 gives a list of days on which the measurements were performed, together with an indication of weather conditions on those days. The instruments used and major air type (marine / continental) are also indicated. For 72-hour back-trajectories the reader is referred to Appendix 1. The weather maps for the days on which activation experiments were done are given in Appendix 3. As was discussed previously, the attention was given to the influence of chemical composition on the cloud forming properties of the aerosol. For this reason the activation experiments were done as much as possible in combination with impactor measurements. Impactor

Table 5.1. Brief description of weather conditions during activation tests.

Date	Weather general	Air mass type	Instruments used			Local wind direction		
			DMPS entrance	DMPS tunnel	Impactor	Average	Start (deg.)	End (deg.)
26-06-92	sunny/hazy	continental	no	no	yes	NNE	60	60
29-06-92	sunny/hazy	continental	no	no	yes	SSE	160	350
30-06-92	very hazy	continental	no	no	yes	ESE	160	80
1-07-92	humid/cloudy	cont./marine	no	no	yes	SW	220	230
2-07-92	sunny/clear	marine/cont.	no	no	yes	NE	40	40
3-07-92	sunny/clear	cont./marine	no	no	yes	E	90	70
6-07-92	sunny/clear	marinne/cont.	no	no	yes	NE	40	40
5-07-93	sunny spells	marine	yes	no	yes	N	360	350
6-07-93	sunny spells	marine	yes	no	yes	NW	285	300
8-07-93	sunny spells	marine	yes	no	yes	SW	240	230
12-04-94	sunny/clear	cont / marine	yes	yes	yes	N	25	360
13-04-94	sunny/clear	marine	yes	yes	yes	N	360	355
14-04-94	cloudy	marine	yes	yes	yes	N	350	360
15-04-94	overcast	cont / marine	yes	yes	yes	ENE	50	70
10-06-94	sunny spells	marine	yes	yes	no	W	250	275
05-10-94	sunny spells	marine	yes	yes	no	N	350	200

Note: FSSP and PVM were used on all of the days

measurements were performed by the personnel of University of Vienna (Dr. A.Berner and C.Kruisz). These measurements were the limiting factor for the number of days discussed in this study

DATA EVALUATION

The droplet forming efficiency (or cloud activation efficiency) of ambient aerosol is evaluated as the number of droplets formed per number of particles that are larger than the activation threshold (the potential cloud nuclei, PCN) as determined with the reference ammonium sulfate aerosol (see the previous section). Ammonium sulfate was chosen because it is expected to be the dominant compound in the submicrometer marine aerosol in the Netherlands (for individual mass size distributions see Appendix 1) and is dominating the number of PCN in marine air masses. To account for the water depletion effect at high number concentrations the observed activation efficiency is compared with the activation efficiency of the reference laboratory generated ammonium sulfate aerosol as measured at the same number concentration of potential cloud nuclei.

The supersaturation during the experiments was monitored via the LWC and temperature in the tunnel of the chamber (Eq.4.1). The measurements at which the supersaturation according to the LWC exceeded the limits of 0.15 ±0.02% were discarded.

The number of PCN in ambient air was calculated using the activation efficiency of ammonium sulfate aerosol (Fig.4.10) as follows. The activation efficiency of ammonium sulfate aerosol as a function of size is calculated as the ratio of the dry spectrum before activation to the dry spectrum of non-activated particles:

$$E(r_i) = 1 - \frac{N_{non\text{-}act}(r_i)}{N(r_i)} \qquad 5.1$$

in which r_i is the midpoint size of a (i-th) DMPS channel, E is the activation efficiency, $N(r_i)$ and $N_{non\text{-}act}(r_i)$ are, respectively, the total number and the number of non-activated ammonium sulfate particles per the i-th DMPS channel. The PCN concentration (C_{PCN}) is then determined as:

$$C_{PCN} = \sum_{r_i} E(r_i)\, N_{amb}(r_i) \qquad 5.2$$

in which $N_{amb}(r_i)$ is the number of particles per the i-th DMPS channel in the ambient aerosol.

The accuracy of the activation efficiency curve (activation threshold) is one DMPS channel (see Chapter 4). Hence, the uncertainty in the number concentration of PCN, is approximately the number of particles in the DMPS channel at 0.1 μm to the total number of PCN. On all of the reported days this uncertainty was 10% or less. The uncertainty in the overall counting by the DMPS is estimated at 10% (Chapter 4). The overall uncertainty in the PCN number concentration is thus estimated at 15%.

The uncertainty in the droplet number concentration is about 10% (Chapter 4). During most of the measurements a second DMPS was installed in the tunnel of the chamber. Droplets were separated from non-activated aerosol particles with an impactor with the 50% cut-off diameter of 0.86 μm. The non-activated particles were then dried with a diffusion dryer and their spectrum was measured with the DMPS. In this way the spectrum of non-activated particles is obtained. The difference in the original spectrum as measured with the first DMPS before the chamber and the spectrum of non-activated particles is the number of "activated" particles. It was used as a back-up measurement for the FSSP measurements of droplet concentration. As was discussed in Chapter 4, the humidifier produces about 50 ±10 cm^{-3} droplets. All droplet concentrations measured in the chamber were corrected for this "background". At droplet number concentrations lower than 100 cm^{-3} the noise in the "background" droplet concentration is becoming substantial in comparison to the total droplet number concentration, exceeding the estimated accuracy of counting (10%, see above). To cope

with this problem, the actual droplet number concentration was calculated as the average of the concentration measured with the FSSP and the amount of activated particles which is deduced from the DMPS measurements. DMPS measurements are not affected by the background, because the background droplets are larger than the upper limit of the DMPS (0.86 μm) and thus are not counted by the DMPS.

AEROSOL SIZE SPECTRA

Number size distributions of ambient aerosols during activation experiments reported here are given in Fig 5.1. The aerosol spectra show rather large variability even on a 15 minute basis. The region below 0.1 μm in diameter is especially variable, while the spectra of larger particles are more constant. The size distributions have mostly a bimodal number distribution with one mode centered between 0.03 - 0.06 μm and the other mode at around 0.15 μm. At high aerosol number concentrations (concentration of particles larger 0.019 μm higher than about 5000 cm^{-3}) the two modes usually are not clearly separated and the spectrum tends, with increasing total number concentrations, to become uni-modal, centered between 0.05 and 0.1 μm.

The bimodal size spectrum of ambient aerosol may have the following implication: the saturation effect (see Chapter 3) may be less pronounced than in the uni-modal ammonium sulfate aerosol used for chamber characterization (see Chapter 4). Because the "gap" between the modes in the ambient aerosol is close to the size of the activation threshold (approximately 0.1 μm), a relatively small part of potential cloud nuclei has sizes close to the threshold. This is different in the uni-modal reference aerosol in which a larger part of PCN had sizes close to the size of activation threshold (Fig.4.4). Particles with sizes close to the activation threshold are most "affected" by the competition for water vapor. The vapor above their surface is higher than that above larger particles, as was discussed in Chapter 3. Smaller particles

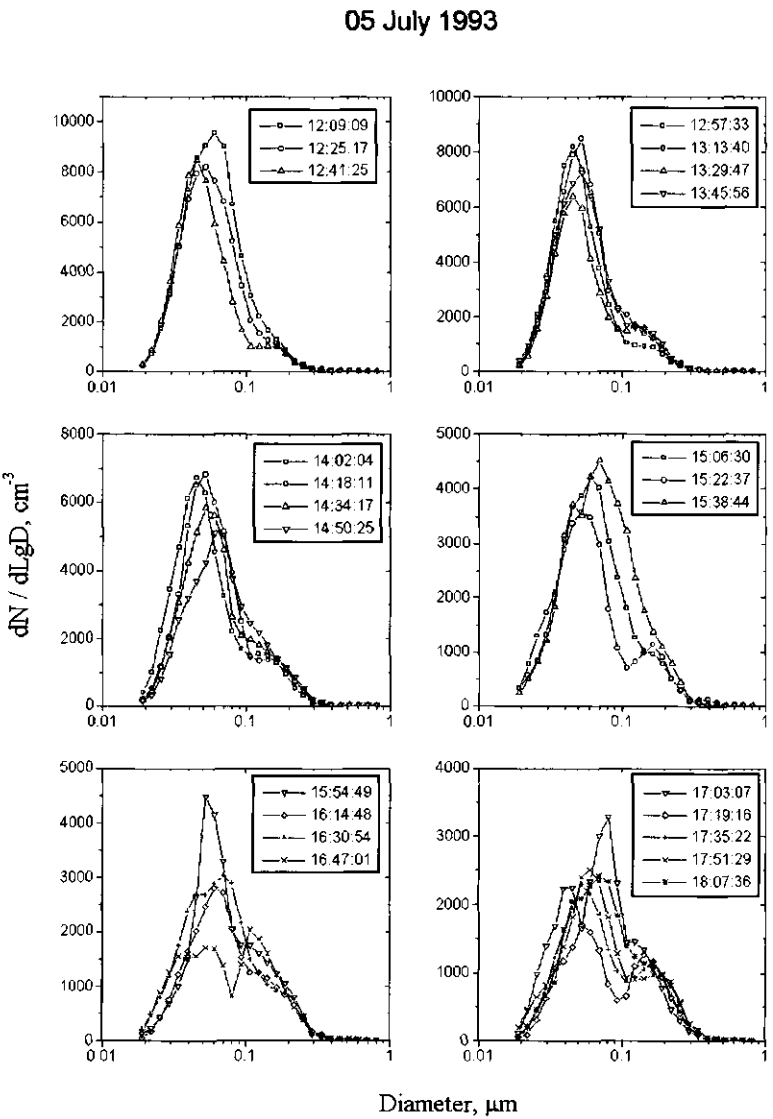

Figure 5.1. *Aerosol number size distributions during the cloud activation experiments (continued on the next pages).*

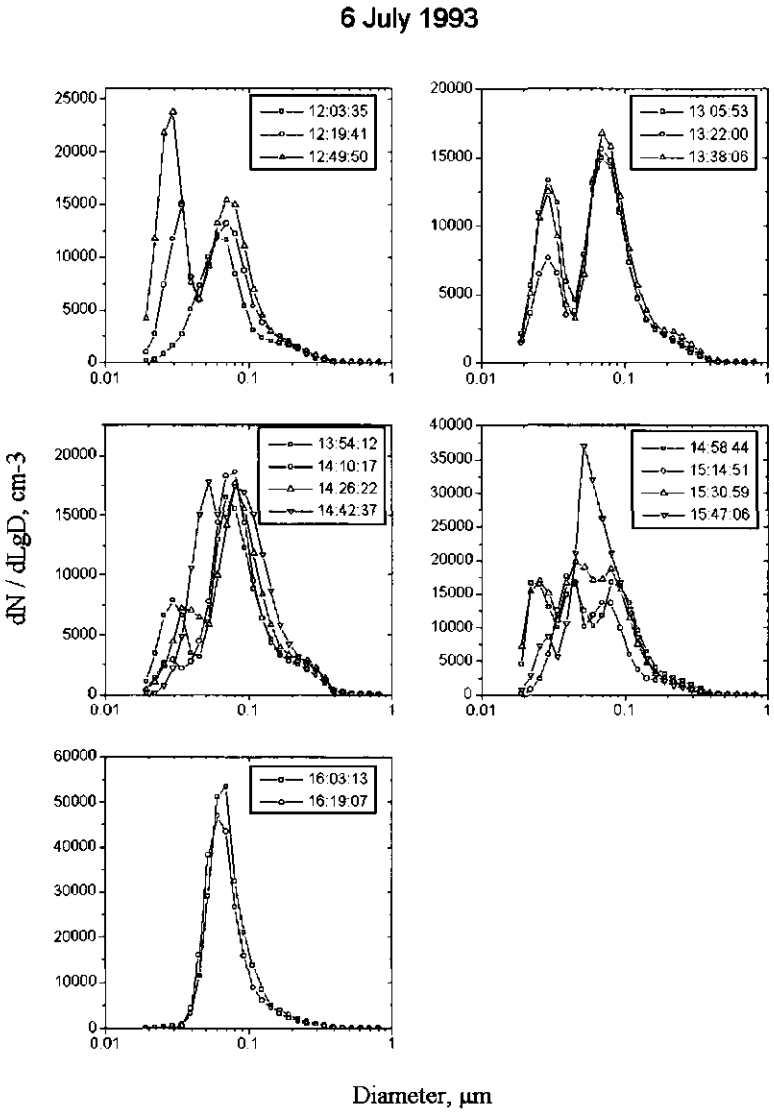

Figure 5.1. *Aerosol number size distributions during the cloud activation experiments (continued).*

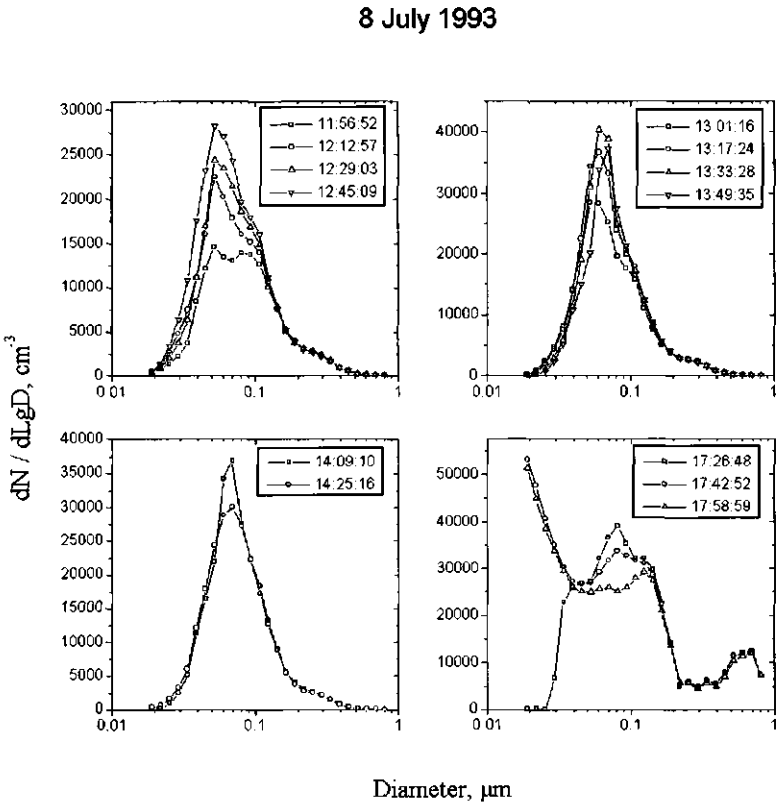

Figure 5.1. *Aerosol number size distributions during the cloud activation experiments (continued).*

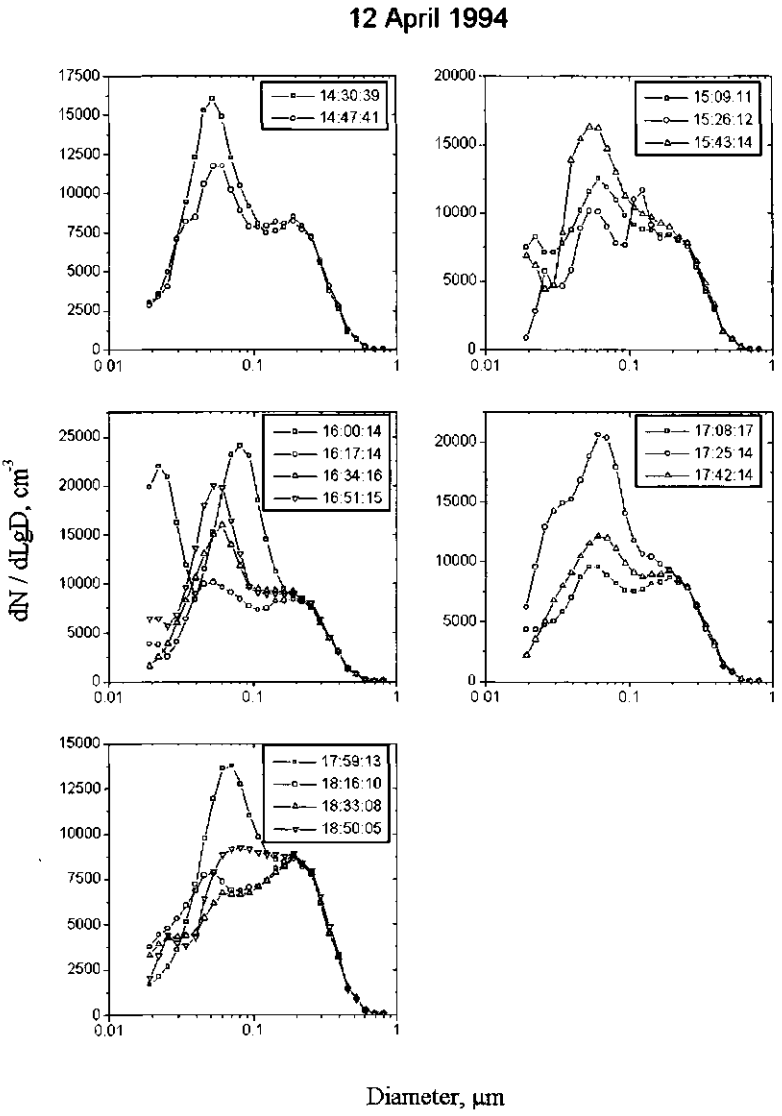

Figure 5.1. *Aerosol number size distributions during the cloud activation experiments (continued).*

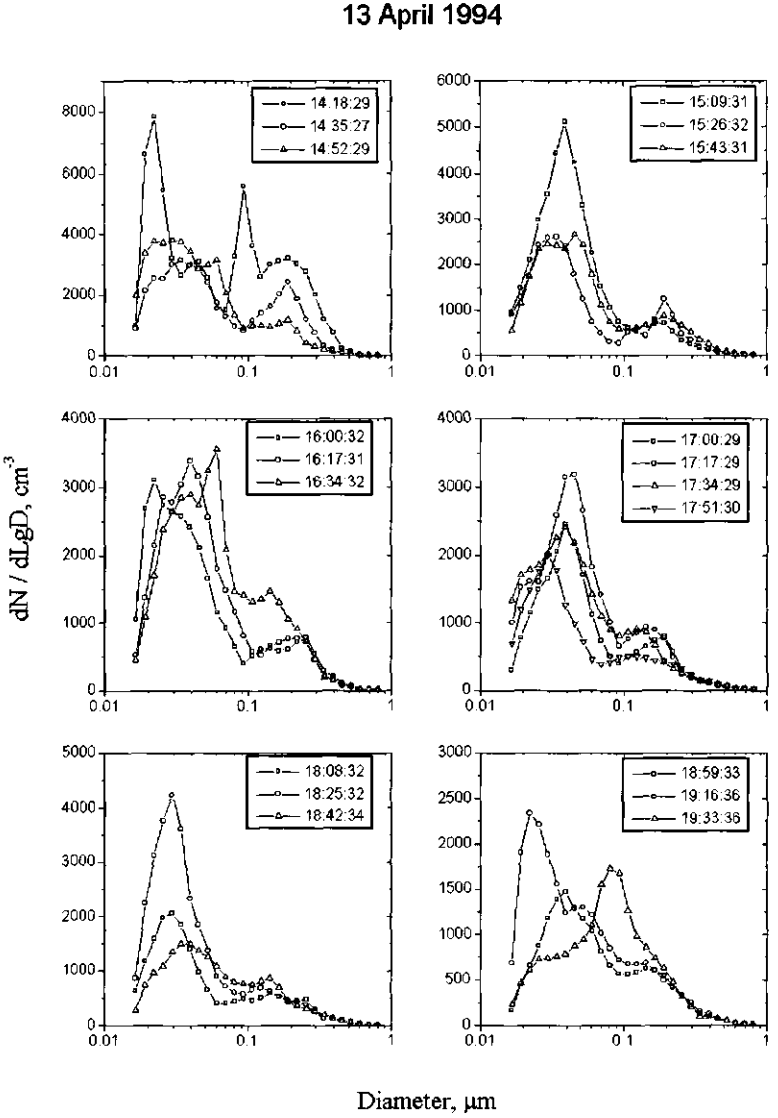

Figure 5.1. *Aerosol number size distributions during the cloud activation experiments (continued).*

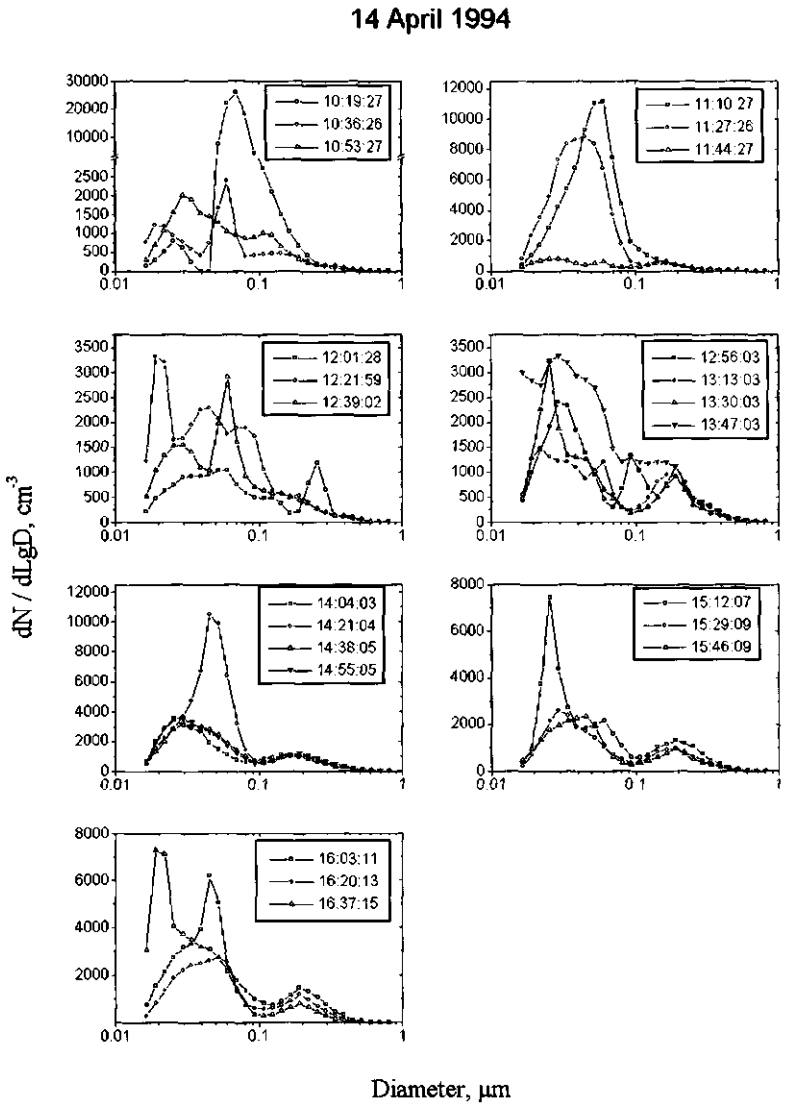

Figure 5.1. *Aerosol number size distributions during the cloud activation experiments (continued).*

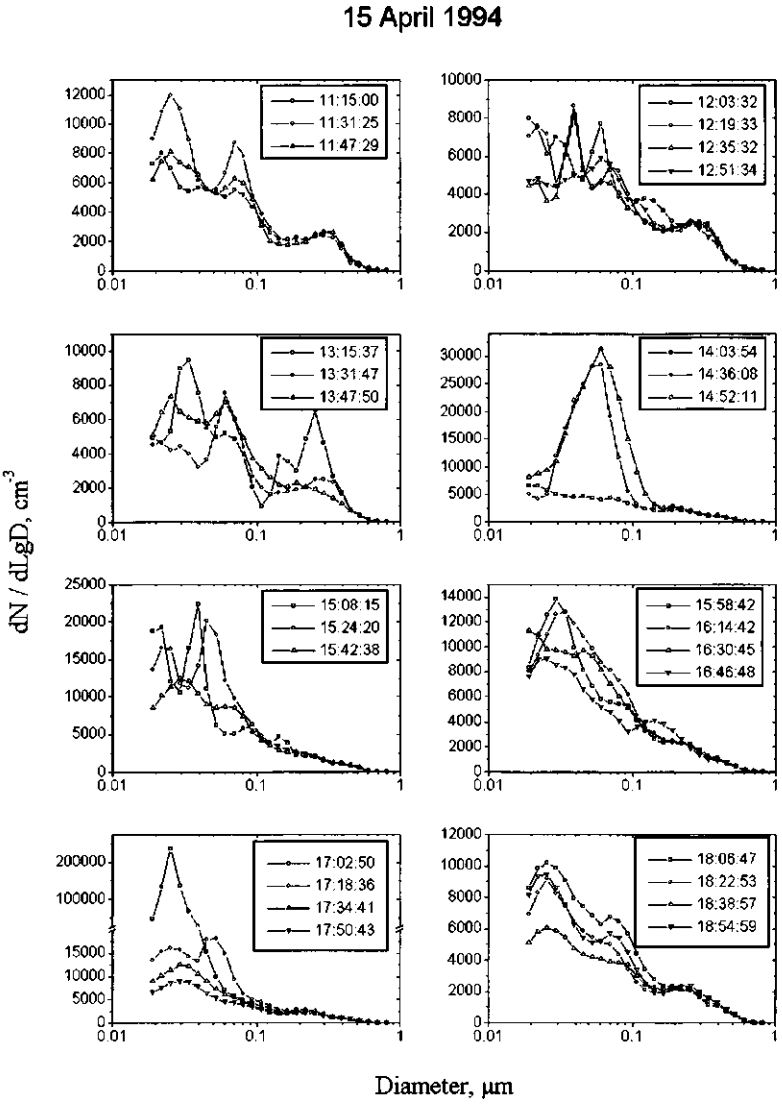

Figure 5.1. *Aerosol number size distributions during the cloud activation experiments (continued).*

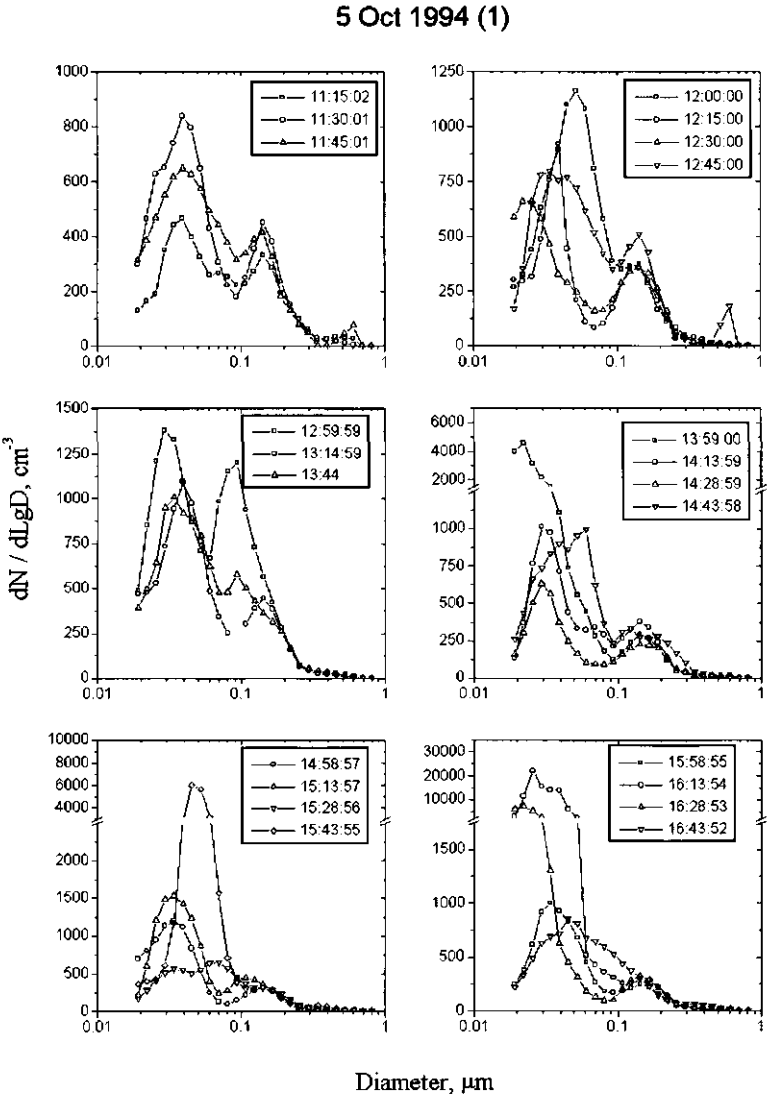

Figure 5.1. *Aerosol number size distributions during the cloud activation experiments (continued).*

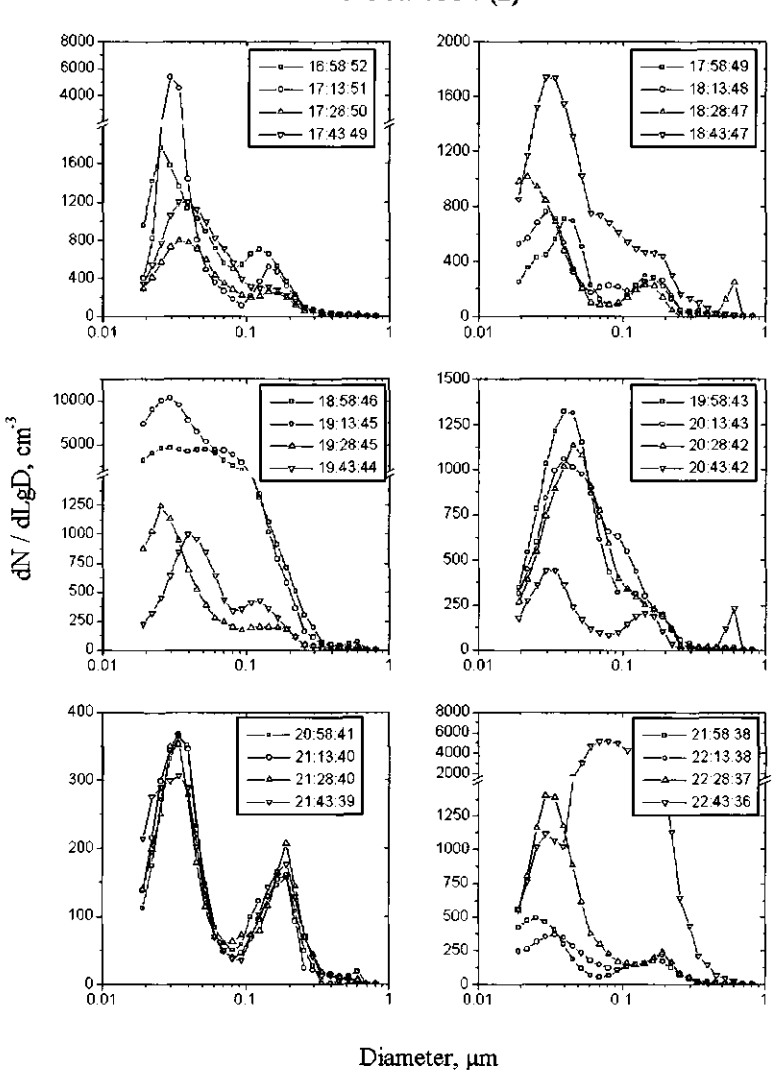

Figure 5.1. *Aerosol number size distributions during the cloud activation experiments (continued).*

also change their size faster than larger particles. These factors make small particles more sensitive to changes in supersaturation. As the supersaturation is lowered due to the depletion of water vapor by the growing droplets, the smallest PCN, that would form droplets if the supersaturation were constant, do not activate. Because there are relatively more particles close to the activation threshold in the model aerosol, the saturation effect is expected to be less pronounced in the bi-modal ambient aerosol than in the uni-modal reference aerosol.

CHEMICAL COMPOSITION

The impactor measurements show (see Appendix 1) that the water-soluble inorganic fraction of the marine aerosol in the proper size range is dominated by sulfate, which is a justification for the use of the artificial sulfate salt in the characterization / reference tests described in the previous chapter. The spectra show that relatively large particles (above approximately 0.5 μm in diameter) are in part composed of sodium sulfate. The activation (cloud forming) properties of this compound are similar to those of ammonium sulfate (see Fig 3.1).

In continental air flows nitrate has a similar mass size distribution to the distribution of sulfate, which was discussed in Chapter 2. This suggests that the nitrate aerosol has a contribution, similar to that of sulfate, to the number of aerosol particles. Because of its high solubility the nitrate aerosol thus strongly contributed to the number concentration of CCN. The absence of nitrate in the lower size range (0.1 - 0.3 μm) of the mass distribution in polluted marine air flows may be caused by evaporative losses from the impactor stages with lowest cut-off diameters (see Chapter 2). This, however, needs further verification. A relative contribution of sulfate and nitrate to the number concentration of particles larger than 0.1 μm in diameter (approximately the number of PCN at 0.15% supersaturation) was estimated from the mass distributions of these compounds. Lognormal

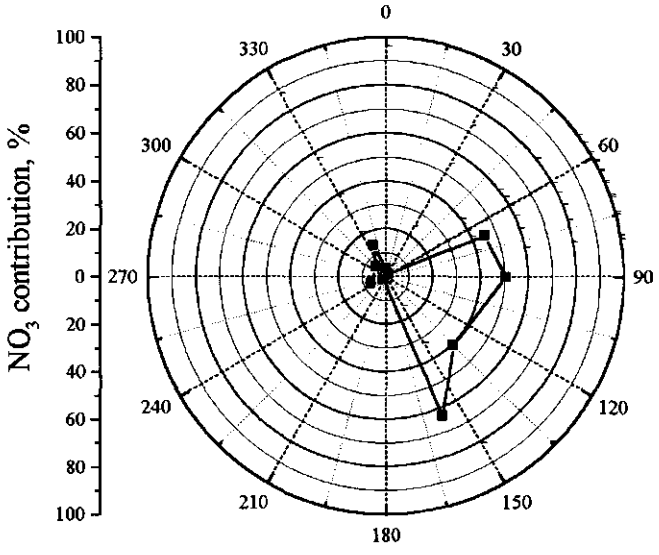

Figure 5.2. *Relative contribution of (ammonium) nitrate to the number concentration of particles larger than 0.1 μ m in diameter as a function of wind direction. The number concentration was derived from the aerosol mass distribution (see Appendix 1), assuming that particles are composed only of ammonium sulfate and ammonium nitrate.*

distributions were fitted to the impactor data (for the parameters of the obtained lognormal distributions see Appendix 1). The fitted mass distributions were then converted to lognormal number size distributions from which the number concentration of particles larger than 0.1 μm in diameter was obtained. Such an analysis shows that in continental air flows (ammonium) nitrate has a contribution to the aerosol number concentration consistently similar in magnitude to that of sulfate aerosol (Fig.5.2). This suggests that nitrate aerosol is another

Table 5.2. *Content of insoluble material in submicrometer aerosol particles. Total submicrometer mass concentration is also given.*

Date	Concentration, μg/m^3	Insoluble content, %
26-06-92	21.4 ± 0.2	63 ± 2
29-06-92	13.7 ± 0.5	16 ± 1
1-07-92	8.5 ± 0.3	22 ± 1
2-07-92	0.9 ± 0.3	0 ± 6
3-07-92	11.0 ± 0.3	77 ± 2
6-07-92	2.7 ± 0.1	52 ± 2
5-07-93	0.8 ± 0.2	43 ± 12
6-07-93	15 ± 0.3	59 ± 2
8-07-93	5.2 ± 0.4	58 ± 5
12-04-94	13.4 ± 0.4	25 ± 1
13-04-94	3.4 ± 0.3	18 ± 2
14-04-94	1.8 ± 0.3	29 ± 4
15-04-94	5.9 ± 0.2	41 ± 2

major anthropogenic compound influencing the number of CCN in polluted air masses. Extrapolating chemical composition from continental air masses to marine air, however, may be not valid.

In Chapter 3 it was shown that insoluble material affects cloud activation properties of aerosol particles. Cloud droplets form preferably on particles which have a higher soluble content. It was demonstrated in cloud-model simulations by *Kulmala et al.* [1996] that the distribution of insoluble material among individual particles affects the overall cloud activation efficiency of the aerosol. The impactor measurements show that on average about 40% of submicrometer aerosol mass is insoluble (Table 5.2). However, impactor measurement

Table 5.3. *Comparison of black carbon content (BCC) and concentration of insoluble material insubmicrometer particles (units μ g/m^3).*

Date	Insoluble	BCC
12-4-94	3.4	4.7
13-4-94	0.6	0.6
14-4-94	0.5	0.4

provide only the average content of insoluble material per size class, but do not give information on how it is distributed among individual particles. It will be shown further in this chapter that there is an indirect evidence that most of the insoluble material is concentrated only in some of the particles, *i.e.* the insoluble material is externally mixed with the water-soluble compounds.

On three days (13 - 15 April 94) measurements of black carbon content (BCC) were carried out parallel to the activation experiments. The BCC found on these days is given in Table 5.3 along with the content of insoluble material derived from the impactor measurements by subtracting the total weight of soluble compounds from the total weight found on the impactor stages. Both the BCC and the insoluble content are very close to each other and the differences may be attributed to the weighing and analysis errors. Comparison of the mass distributions of black carbon and insoluble material also shows that the spectra are reasonably close to each other (Fig.5.3). These facts suggest that the insoluble material is soot. The small number of BCC measurements and the very low mass concentrations close to the detection limits, however, do not allow to draw a definite conclusion.

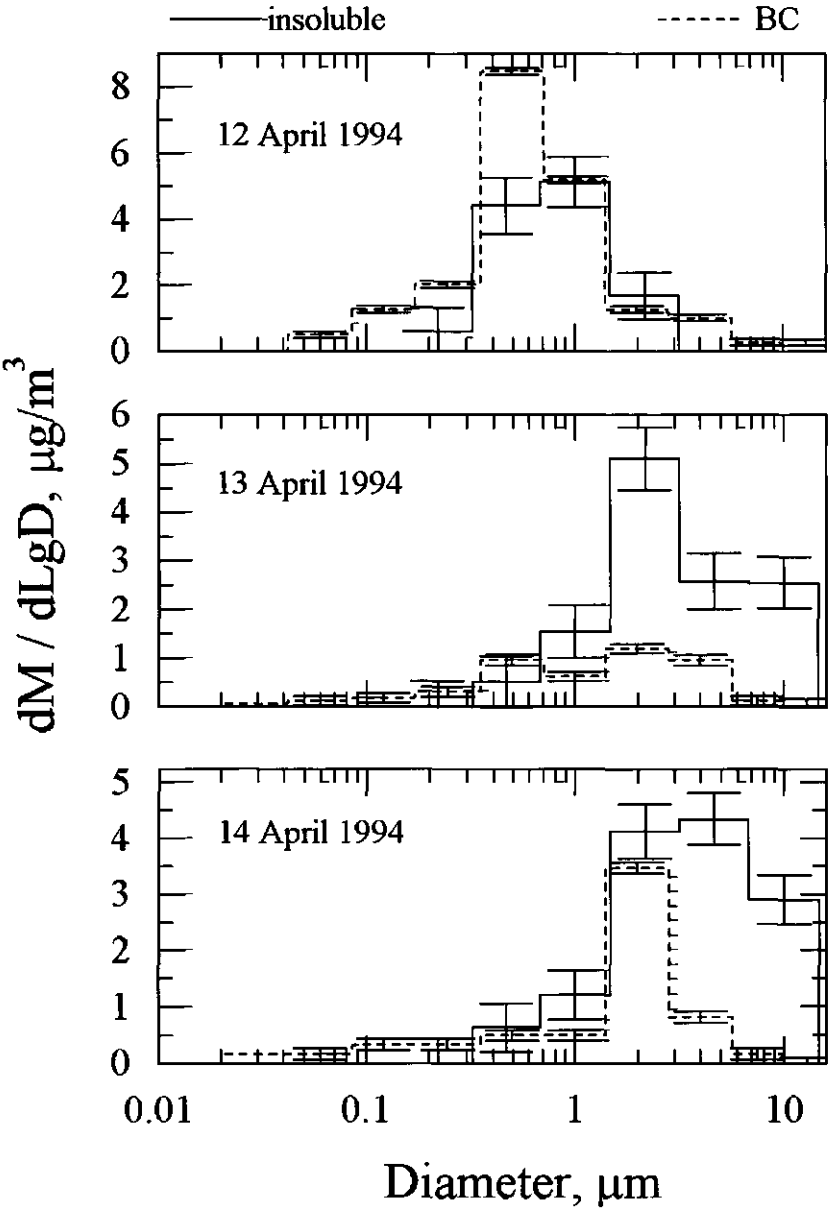

Figure 5.3. *Comparison of mass distributions of black carbon and insoluble material.*

DROPLET NUMBER VERSUS AEROSOL NUMBER

The time evolution of total aerosol number, PCN number and droplet number concentrations for the days on which the DMPS measurements were performed is shown in Fig.5.4. The individual data are given in Table 5.4. The droplet number concentration versus the total aerosol number concentration is given in Fig.5.5. The aerosol spectra (Fig.5.1) show that the total number concentration (particles larger than 0.019 μm in diameter) is dominated by particles smaller than 0.1 μm in diameter. The activation threshold during the experiments is at 0.1 μm in diameter corresponding to the used supersaturation of 0.15%. This demonstrates that the total aerosol number concentration largely overestimates the number concentration of PCN and thus the number concentration of droplets.

For an assessment of the number concentration of CCN in the ambient aerosol the number concentration of potential cloud nuclei (particles larger than the threshold) was used. The comparison between the droplet number and the number of potential cloud nuclei is given in Fig.5.6. At PCN concentrations lower than approximately 100 cm^{-3} the droplet number concentration does not significantly differ from the one-to-one line within the experimental uncertainty which means that all potential cloud nuclei are activated. At higher number concentrations the droplet number concentration progressively deviates from the one-to-one line. The sub-lenear dependence of droplet number concentration on the number concentration of PCN may be caused by two factors: high aerosol number concentration (the so-called saturation effect) and a high content of insoluble material, which was discussed in Chapter 3. The experiments with ammonium sulfate aerosol (Chapter 4) have shown the saturation effect of a similar magnitude (see Eq.4.2). For a comparison the fit-curve to the results of the experiments with ammonium sulfate aerosol is shown in Fig.5.6. Activation at different PCN number concentration is discussed in more detail below.

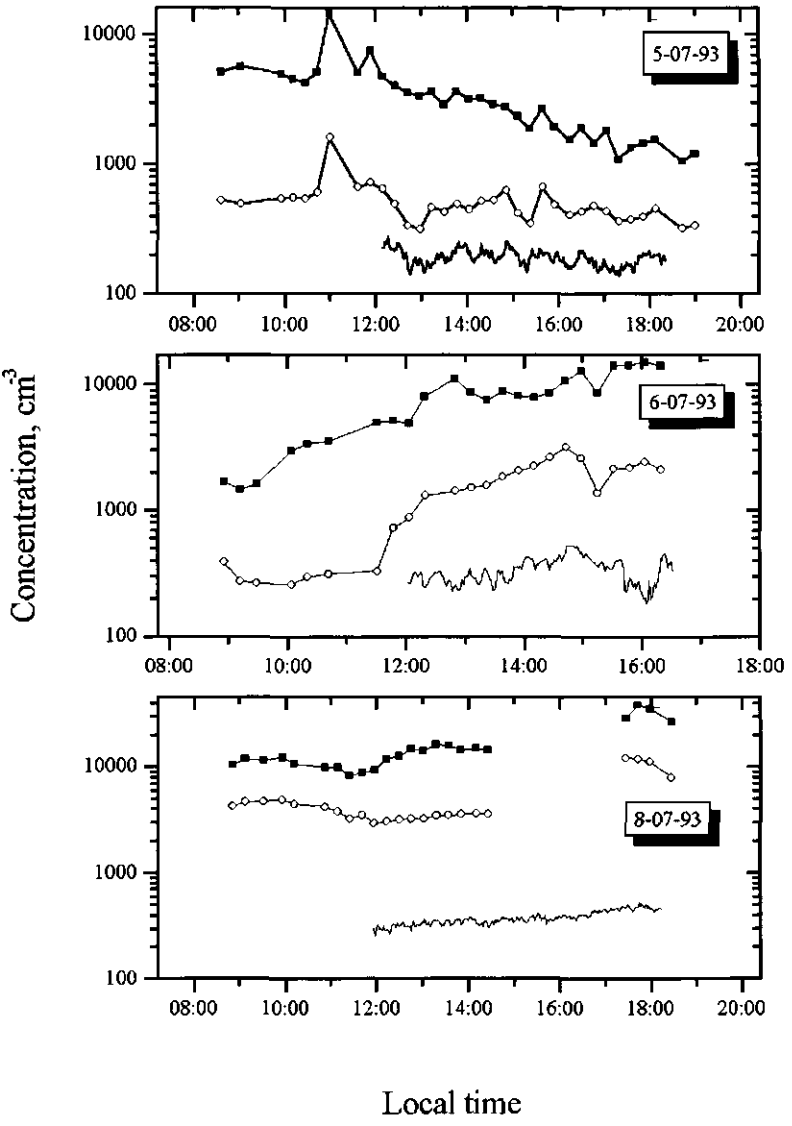

Figure 5.4. *The time evolution of total aerosol number, PCN number and droplet number concentrations for the days on which the DMPS measurements were performed during the activation experiments*

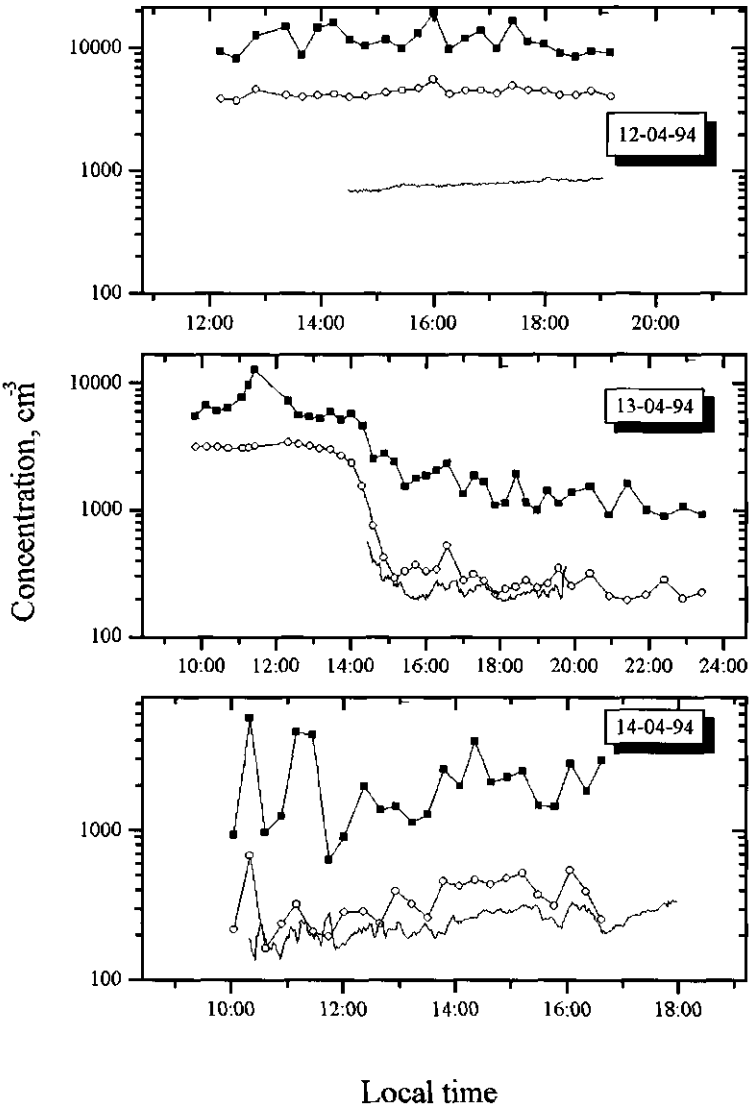

Figure 5.4. *The time evolution of total aerosol number, PCN number and droplet number concentrations for the days on which the DMPS measurements were performed during the activation experiments (continued).*

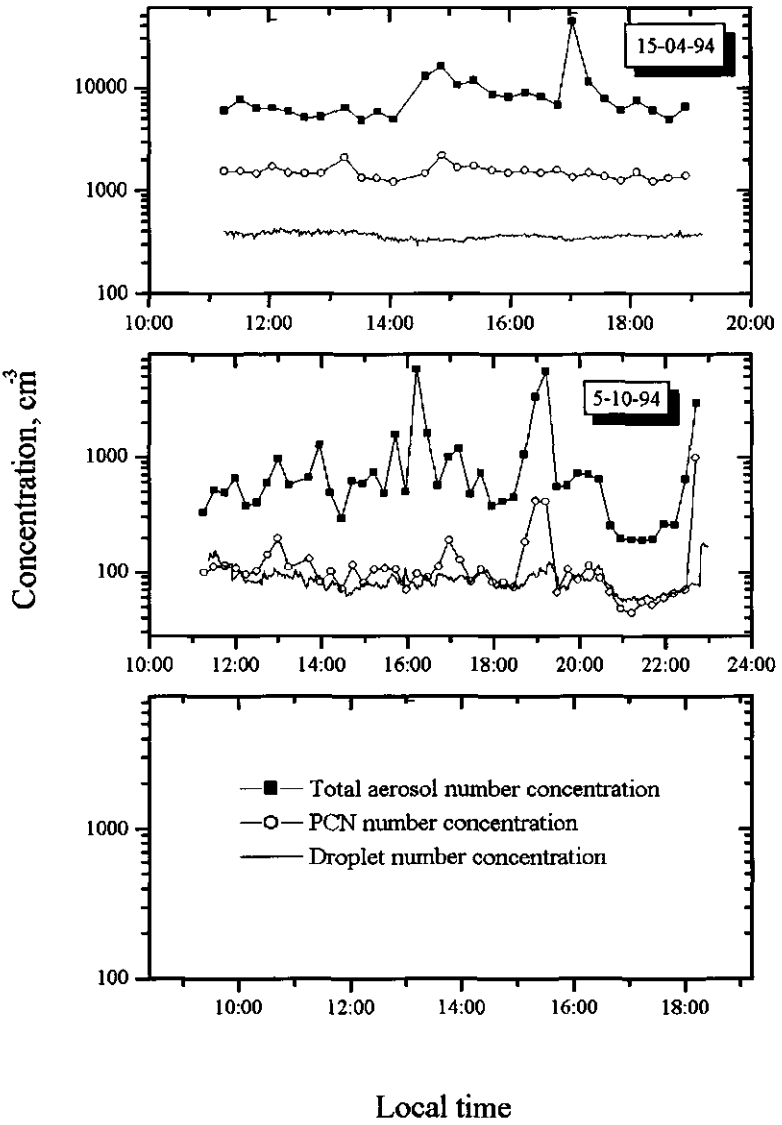

Figure 5.4. *The time evolution of total aerosol number, PCN number and droplet number concentrations for the days on which the DMPS measurements were performed during the activation experiments (continued).*

Table 5.2a. *Total aerosol number, PCN number and droplet number concentrations (in cm^{-3}).*

Time	Total	PCN	Ndrop
5-07-93			
12:09	4751	649	236
12:25	4065	490	217
12:41	3561	338	172
12:57	3337	315	166
13:13	3648	467	184
13:29	2858	429	194
13:45	3613	498	234
14:02	3160	448	191
14:18	3248	516	210
14:34	2896	530	187
14:50	2760	629	226
15:06	2340	416	173
15:22	1884	345	202
15:38	2688	664	198
15:54	1936	488	189
16:14	1555	407	175
16:30	1896	432	195
16:47	1467	481	164
17:03	1807	434	153
17:19	1085	363	160
17:35	1340	375	174
17:51	1462	394	202
18:07	1539	456	190
6-07-93			
12:03	4941	876	299
12:19	8007	1311	285
12:49	11013	1424	263
13:05	8680	1508	294
13:22	7525	1583	287
13:38	8775	1847	303
13:54	8088	2073	393
14:10	7870	2244	375
14:26	8488	2632	400
14:42	10698	3195	514
14:58	12728	2618	420
15:14	8527	1373	363
15:30	13987	2121	353
15:47	14079	2180	252
16:03	14988	2439	234
16:19	13998	2110	389

Time	Total	PCN	Ndrop
8-07-93			
11:56	9331	2956	292
12:12	11787	3035	298
12:29	12529	3175	317
12:45	14740	3249	319
13:01	14126	3225	332
13:17	16174	3468	335
13:33	15918	3480	340
13:49	14588	3549	355
14:09	15048	3660	331
14:25	14589	3538	332
17:26	28908	12091	463
17:42	38932	11932	483
17:58	35711	11057	451
12-04-94			
14:30	11686	4024	689
14:47	10318	4054	691
15:09	11759	4350	748
15:26	9924	4535	772
15:43	13293	4738	769
16:00	19377	5581	763
16:17	9770	4192	768
16:34	11870	4509	784
16:51	13920	4529	787
17:08	9836	4273	797
17:25	16653	4986	812
17:42	11267	4581	822
17:59	10764	4520	862
18:16	9179	4170	847
18:33	8441	4170	847
18:50	9385	4515	860

Table 5.2b. *Total aerosol number, PCN number and droplet number concentrations (in cm^{-3}).*

Time	Total	PCN	Ndrop
13-04-94			
14:18	4584	1548	504
14:35	2555	757	357
14:52	2781	417	285
15:09	2421	290	251
15:26	1543	331	208
15:43	1791	368	207
16:00	1866	329	234
16:17	2052	342	256
16:34	2355	524	263
17:00	1337	276	222
17:17	1864	312	250
17:34	1661	277	239
17:51	1087	217	203
18:08	1138	239	201
18:25	1911	248	220
18:42	1157	281	229
18:59	1001	244	215
19:16	1427	263	233
19:33	1124	344	241
14-04-94			
10:19	5637	679	190
10:36	967	163	164
10:53	1248	238	194
11:10	4546	320	218
11:27	4348	209	212
11:44	632	195	198
12:01	907	284	201
12:21	1975	289	220
12:39	1365	239	219
12:56	1448	393	212
13:13	1129	324	220
13:30	1274	261	208
13:47	2572	457	238
14:04	1969	424	256
14:21	3928	468	281
14:38	2101	438	288
14:55	2277	481	295
15:12	2489	520	312
15:29	1478	372	267
15:46	1442	315	253
16:03	2782	542	314
16:20	1814	392	267
16:37	2926	254	219

Time	Total	PCN	Ndrop
15-04-94			
11:15	5978	1547	389
11:31	7673	1544	371
11:47	6235	1459	391
12:03	6323	1711	406
12:19	5924	1494	397
12:35	5117	1471	390
12:51	5222	1474	394
13:15	6410	2112	398
13:31	4795	1323	382
13:47	5830	1311	345
14:03	4932	1210	334
14:36	12823	1471	332
14:52	16135	2194	331
15:08	10490	1681	332
15:24	11720	1721	344
15:42	8704	1587	367
15:58	8156	1494	368
16:14	8923	1566	370
16:30	8196	1488	355
16:46	6758	1596	340
17:02	44706	1343	343
17:18	11591	1478	349
17:34	7824	1375	359
17:50	6063	1242	371
18:06	7511	1506	365
18:22	6013	1223	365
18:38	4952	1321	372
18:54	6477	1393	375
10-06-94			
17:42	2436	555	327
17:58	2135	482	316

Table 5.2c. *Total aerosol number, PCN number and droplet number concentrations (in cm^{-3}).*

Time	Total	PCN	Ndrop	Time	Total	PCN	Ndrop
5-10-94				*5-10-94*			
11:15	329	99	81	17:12	1195	127	101
11:30	517	111	132	17:27	475	83	89
11:45	492	114	127	17:42	719	106	92
12:00	646	107	106	17:57	373	82	80
12:15	376	95	91	18:12	413	82	90
12:30	402	102	95	18:27	448	74	88
12:45	591	141	110	18:42	1053	184	95
12:59	957	197	171	18:57	3328	414	153
13:14	576	110	98	19:12	5504	410	238
13:43	658	130	111	19:27	556	67	78
13:58	1272	81	76	19:42	561	105	100
14:13	485	101	89	19:57	715	86	92
14:27	289	71	80	20:12	695	114	96
14:42	619	115	83	20:27	639	88	89
14:57	586	80	89	20:42	254	67	64
15:12	738	106	101	20:57	195	48	55
15:27	480	108	97	21:12	193	44	54
15:42	1565	105	86	21:27	192	54	61
15:57	498	70	86	21:42	196	52	64
16:12	5712	97	97	21:57	263	60	76
16:27	1601	89	97	22:12	257	66	73
16:42	568	112	94	22:27	639	70	76
16:57	994	188	122	22:42	2953	990	138

At PCN concentrations lower than approximately 100 cm^{-3} the droplet number concentration does not significantly differ from the one-to-one line within the experimental uncertainty (see the previous section) which means that all potential cloud nuclei are activated. Figure 5.7 shows an example of the aerosol spectra before and after the activation (an average of 5 DMPS samples taken between 20:45 and 22:00 on 5 October 1994). There is a small fraction of particles larger than the threshold which are not activated and a small fraction of particles with sizes smaller than the threshold which are activated. This is attributed to a spread in supersaturations in the chamber. This is similar to the activation pattern of the reference ammonium sulfate aerosol (Fig.4.10a). Knowing the activation efficiency of the reference sulfate aerosol as a function of size (Fig. 4.10b), a spectrum of non-activated aerosol expected after the chamber was calculated as:

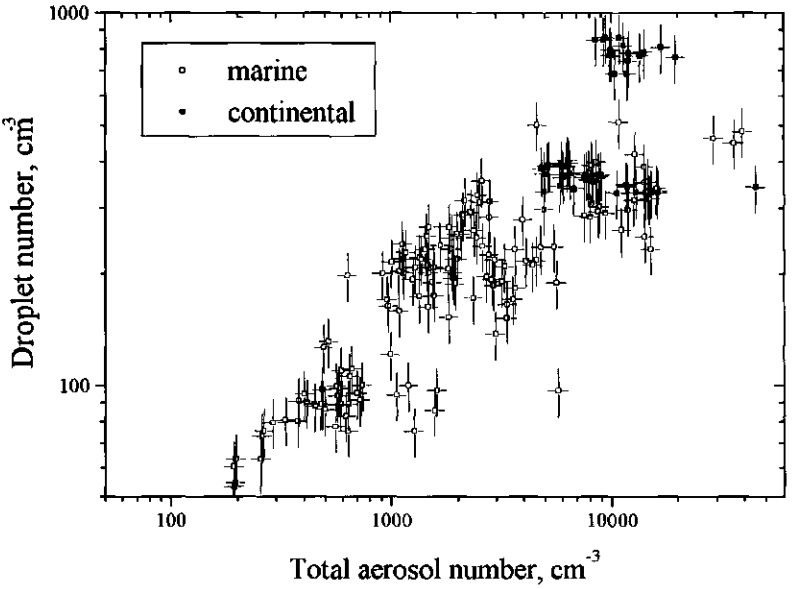

Figure 5.5. *Droplet number concentration versus total aerosol number concentration*

$$N_{expected}(r_i) = (1 - E(r_i))\,N_{amb}(r_i) \qquad 5.3$$

in which r_i is the midpoint size of a (i-th) DMPS channel, $E(r_i)$ is the activation efficiency as determined with the reference aerosol, $N_{amb}(r_i)$ and $N_{non\text{-}act}(r_i)$ are, respectively, the aerosol number concentration in the i-th DMPS channel of ambient aerosol before activation (as measured at the entrance to the chamber) and that of dry non-activated particles expected in the tunnel, if the aerosol would behave as the laboratory generated ammonium sulfate aerosol. This exercise shows that all potential cloud nuclei are indeed activated (Fig.5.7). Consequently, all aerosol particles above the threshold size are effective cloud nuclei.

In marine air at high PCN number concentrations (higher than approximately 1000 cm^{-3}) only a small fraction (on average 16%) of PCN

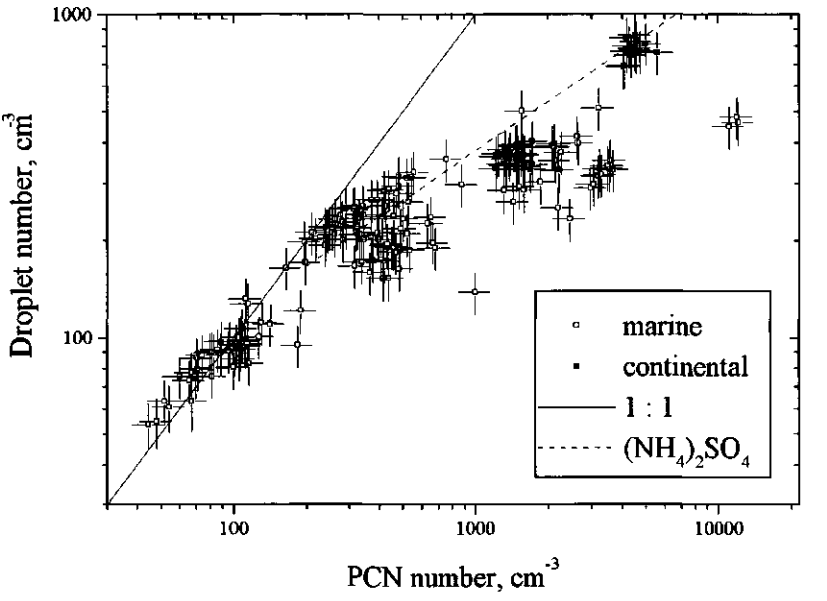

Figure 5.6. *Droplet number concentration versus number concentration of potential cloud nuclei.*

was activated. The poor cloud forming efficiency can be explained for the better part by the so-called "saturation" effect (see Chapter 3). This effect is caused by the competition between the nuclei for the available water vapor. The number of droplets formed per number of PCN at these number concentrations is on average smaller than in the reference aerosol (Fig.5.6) which suggests that the saturation effect was enhanced by the presence of insoluble material in (some of) the particles.

A few measurements with continental aerosol show that the activation efficiency of continental particles is similar to that of polluted marine aerosol with PCN number concentrations higher than about 1000 cm^{-3}. However, on some occasions the activation efficiency of continental aerosol was higher than that of marine aerosol and equal to

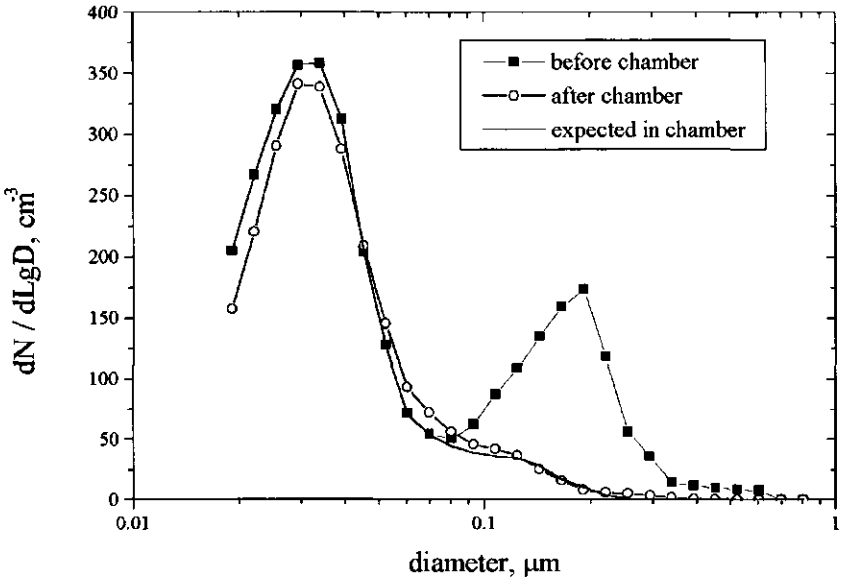

Figure 5.7. *Aerosol spectra before and after the cloud chamber in clean marine air.*

the activation efficiency of the reference sulfate aerosol. This shows that continental particles can be very hygroscopic.

At PCN number concentration between approximately 100 and 1000 cm^{-3}, the cloud forming efficiency of marine aerosols varies between 30 and 100%. On some occasions, when the number concentration of PCN was below 300 cm^{-3}, the droplet number concentration was equal to that of PCN within the experimental uncertainty. Figure 5.6 shows that at PCN concentrations between approximately 300 and 500 cm^{-3} activation efficiency of the ambient aerosol was, on most occasions, the same as that of the reference aerosol or even lower. However, due to the difference in spectral shapes between the ambient and the reference aerosols one would expect the saturation effect to be less pronounced in the ambient aerosol, as was discussed in "Aerosol spectra" section. This suggests that some of the

particles were practically insoluble. This preposition is discussed in the following section.

EFFECT OF INSOLUBLE MATERIAL

In the previous section it was demonstrated that the activation efficiency of the ambient aerosol at PCN number concentrations higher than approximately 300 cm^{-3} is often lower than expected according to the experiments with the reference ammonium sulfate aerosol. The most probable reason for it is that some of the (anthropogenic) potential cloud nuclei are completely insoluble or consist to a great extent of insoluble material. This explanation is supported by the content of insoluble material in the aerosol (Fig.5.8, Table 5.2). On days with low aerosol concentrations it was not possible to assess the insoluble material content on the impactor stage with 0.15 μm cut-off diameter and for this reason only bars indicating the error in the measurements are given. Extrapolation from the larger sizes suggests that up to 40% of the aerosol mass is insoluble in the PCN size range. Further evidence that a substantial part of the PCN mass is insoluble comes from the composition data gathered with the impactor on days with higher mass concentrations.

The importance of how the insoluble material is distributed between the particles was demonstrated in cloud-model simulations by *Kulmala et al.* [1996]. It was shown that particles with a higher soluble content are preferably activated. An uneven distribution of insoluble material between particles in ambient aerosol was observed in several studies. *Okada et al.* [1990] in a study of the nucleation properties of ambient aerosol in Japan found that up to 30% of the particles in the size range 0.1 - 0.33 μm were not activated even at 1% supersaturation. Those particles were similar in structural features to carbon particles or made up of a central soluble core covered with a layer of insoluble (organic) material. *Svenningsson et al.* [1994] in a study of continental

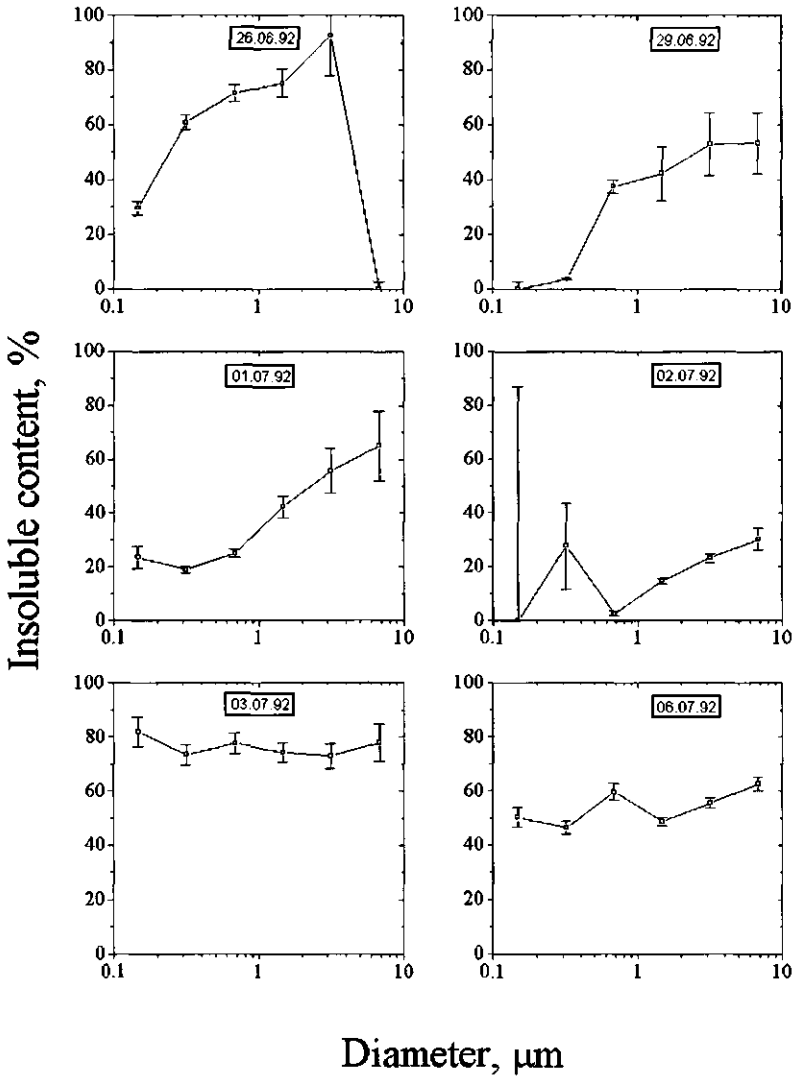

Figure 5.8a. *Insoluble material content as a function of size as derived from impactor measurements.*

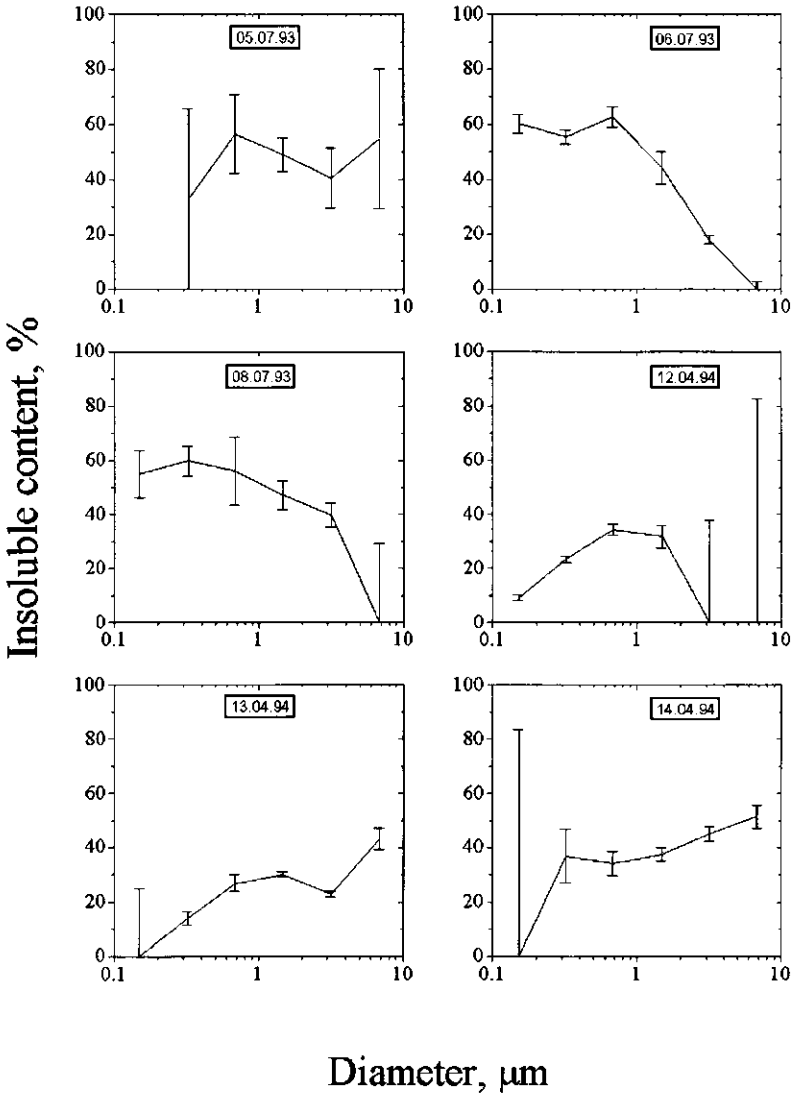

Figure 5.8b. *Insoluble material content as a function of size as derived from impactor measurements.*

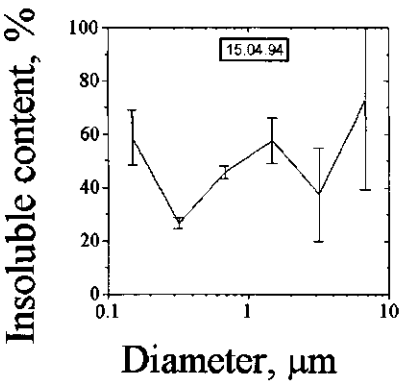

Figure 5.8c.

Insoluble material content as a function of size as derived from impactor measurements.

clouds in Germany found that approximately half of the aerosol particles contained less than 5% of soluble material. Measurements on Mount Kleiner Feldberg in Germany by *Eichel et al.* [1996] indicated that about 25% of particles larger than 0.4 μm in diameter (the lower size limit of the experimental method used in the study) have only about 9% of water-soluble material.

The impactor data do not provide information on how the insoluble material is distributed among the individual particles (internal or external mixing of soluble and insoluble material). However, from the aerosol spectra measured before and after the chamber the number and size of potential cloud nuclei that were not activated can be deduced. Using the activation efficiency of the reference sulfate aerosol as a function of size (Fig. 4.10b), the spectrum of non-activated PCN is calculated as:

$$N_{non\text{-}act}(r_i) = N_{tunnel}(r_i) - (1 - E(r_i))\,N_{amb}(r_i) \qquad 5.4$$

in which r_i is the midpoint size of a (i-th) DMPS channel, $E(r_i)$ is the activation efficiency as determined with the reference aerosol, $N_{amb}(ri)$, $N_{tunnel}(r_i)$ and $N_{non\text{-}act}(r_i)$ are, respectively, the aerosol number concentration in the i-th DMPS channel of ambient aerosol before

activation (as measured at the entrance to the chamber), of dry non-activated ambient particles (as measured in the tunnel after the droplet are removed with an impactor) and of non-activated PCN.

However, such an exercise is possible only at relatively low PCN number concentrations, at about 300 cm^{-3} or lower. At higher PCN number concentrations the saturation effect causes the activation threshold to shift to larger sizes. This shift was not possible to quantify accurately, which was discussed in Chapter 4, in the section describing the saturation effect during experiments with ammonium sulfate aerosol. For this reason the procedure described by Eq.5.4 becomes less accurate.

The spectrum of non-activated particles was assessed for two days, 13 and 14 April 1994, on which the PCN number concentration was around 300 cm^{-3} allowing to apply the procedure described by Eq.5.4. Figure 5.9 shows that on both days there is a "mode" of non-activated particles that is centered at approximately 0.2 - 0.25 μm. Because this mode includes particles with diameters larger than 0.4 μm in diameter it can be concluded that this mode consists most probably of purely insoluble particles. The number and size of the insoluble mode allow estimation of the volume fraction of insoluble material in the potential cloud nuclei size range. These estimates show that the non-activated particles comprise 25 - 30% of the total volume in its size range. Assuming that the density of all particles is the same the estimated mass fraction of not activated particles can be compared with the mass fraction of insoluble material found from the impactor measurements. The impactor measurements give 20 - 40% insoluble content. Because the two values are comparable it is concluded that all or most of the insoluble material is in the hydrophobic (containing no soluble material) particles that were not activated. Thus it is concluded that, for the better part, the "insoluble" material is not mixed with the soluble material (*i.e.* is externally mixed).

The further support for the hypothesis, that the insoluble material is externally mixed with the soluble material, comes from the similarity of the spectra of the non-activated particles and of the insoluble

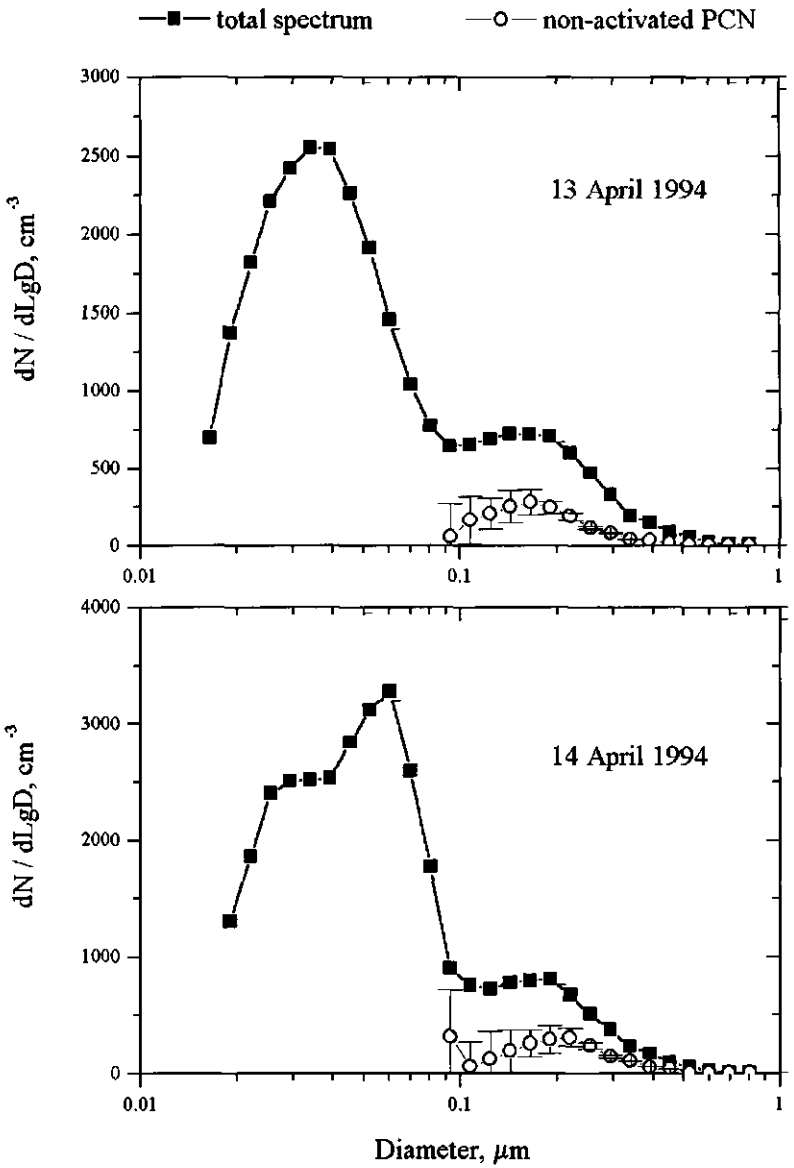

Figure 5.9. *Number distribution of non-activated particles as derived from DMPS measurements before and after the chamber.*

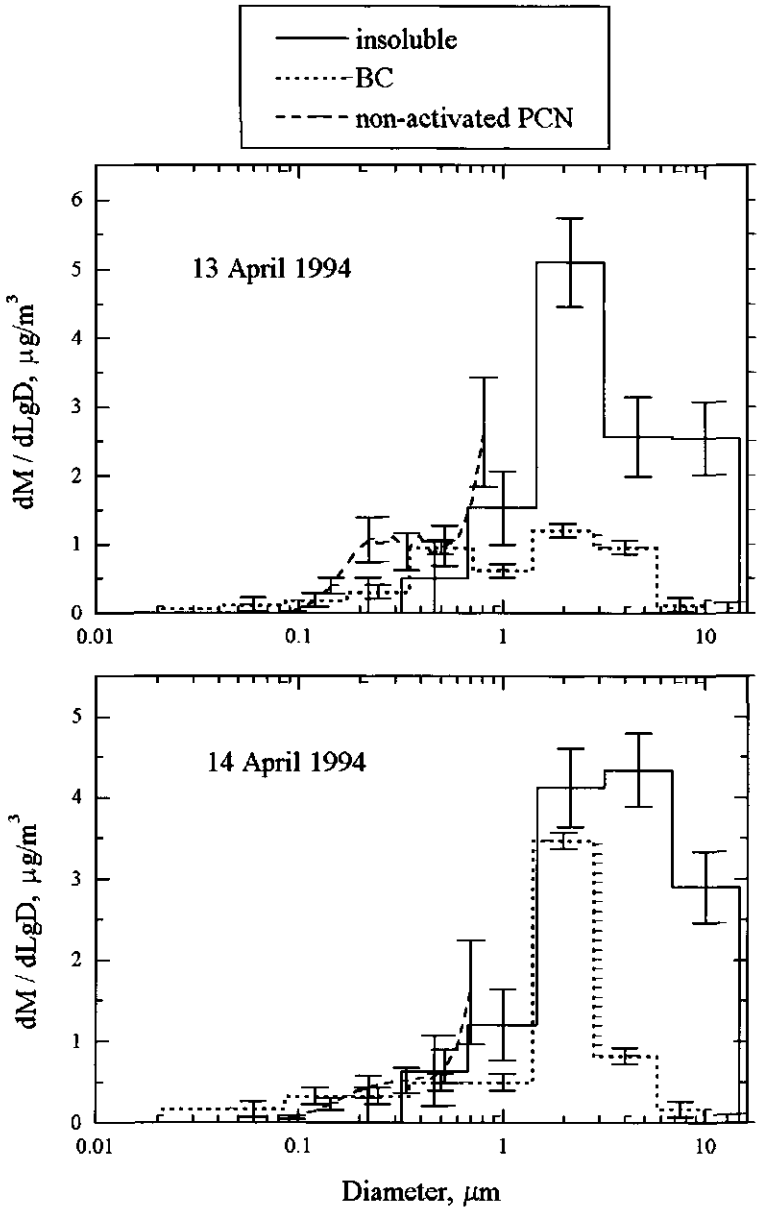

Figure 5.10. *Comparison of size distributions of non-activated particles, insoluble material content and of black carbon.*

material (Fig.5.10). The similarity of the size distributions of the insoluble material and of the black carbon (BC), which was measured on these days, suggests, in turn, that the non-activated particles were composed of soot. One of the sources of soot in the atmosphere is combustion of fuel in diesel engines. In a study by *Weingartner et al.* [1997] it was shown that particles, for a large part composed of soot, produced by combustion of diesel fuel do not activate at supersaturations lower than approximately 0.2%. *Chylek et al.* [1996] also obserevd a low cloud forming ability of soot: only about 9% of black carbon was incorporated into cloud water in stratiform clouds. The results of the present study may also be considered as an indirect evidence of the poor cloud activation efficiency of soot particles at low supersaturations. This, however, needs to be verified by further measurements.

DROPLET NUMBER VERSUS AEROSOL MASS

In the modeling of the indirect aerosol forcing the anthropogenic influence on the droplet number concentration is usually parameterized by relating the sulfate aerosol mass concentration to the droplet number concentration using empirically derived relationships [*Jones et al.*, 1994; *Boucher and Lohmann*, 1995]. *Boucher and Lohmann* [1995] have summarized several sets that related sulfate aerosol mass concentration to the number concentration of CCN [*Berresheim et al.*, 1993; *Quinn et al.*, 1993; *Hegg et al.*, 1993], a study that related sulfate concentration to the number of particles in the accumulation mode [*van Dingenen et al.*, 1995] and a study by *Leaitch et al.* [1992] relating cloud water sulfate concentration and droplet number concentration assuming that 60% of the sulfate aerosol mass was incorporated into the cloud.

The above approach has two problems: 1) a relation is assumed between the aerosol mass concentration and the number concentration

of particles in the cloud-active size range (PCN) and 2) also between the number concentration of PCN and the concentration of cloud droplets. It was demonstrated in the previous sections that the droplet number concentration depends non-linearly on the number of PCN and that the amount of insoluble material has a strong influence on the cloud forming properties of aerosol particles. The existence of a reliable relationship between (sulfate) aerosol mass and the number concentration of PCN is also questionable because of the variability of the ambient aerosol spectra.

Given the problems of relating aerosol mass to the droplet number concentration, nonetheless, an attempt is made here to relate droplet number concentration observed in this study to the simultaneously measured aerosol sulfate concentration, both total and in the submicrometer size range (Fig.5.11a,b). Similarly to the mentioned above studies the data set was fitted with the following relationship:

$$\lg(N_{dr}) = a + b \lg(M_{SO4}) \qquad 5.5$$

The best fit parameters, a and b, are given in Table 5.5 along with those from *Boucher and Lohmann* [1995] and a study by *Novakov et al.* [1994] in which the aerosol sulfate concentration was directly compared to the measured droplet number concentration at a mountain site in

Table 5.5. *The best fit parameters for sulfate / droplet number relationship (Eq.5.5).*

Data set	a	b
This study, total	2.55 ±0.41	0.18 ±0.12
This study, submicrometer	2.53 ±0.39	0.29 ±0.12
Boucher and Lohmann [1995]	2.21	0.41
Novakov et al. [1994]	2.32	0.09

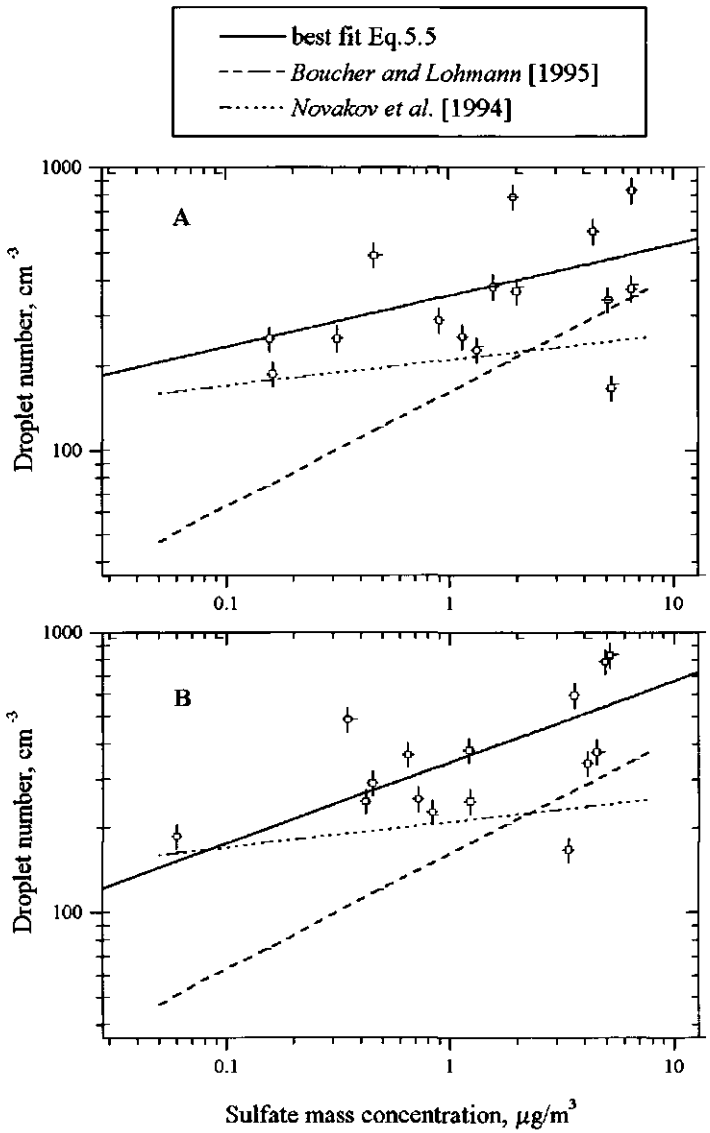

Figure 5.11. *Droplet number concentration versus sulfate mass concentration. A: total sulfate concentration. B: sulfate concentration in submicrometer particles. For comparison best fit curves from data sets of Boucher and Lohmann [1995] and Novakov et al. [1994] are given.*

Puerto Rico (this study was not included into the data set of *Boucher and Lohmann*). It should be also noted that the study by *Novakov et al.* and the studies summarized by *Boucher and Lohmann* (except for the study by *van Dingenen et al.*) were performed outside of Europe and may be not representative for this region.

COMPARISON WITH AIRCRAFT STUDIES

A comparison of the chamber results with actual measurements from aircraft is by nature focused on those studies performed in marine air in the Atlantic and in particular over the UK by *Martin et al.* [1994]. The best conditions for a comparison of the chamber tests and actual cloud measurements would be those at cloud-base, where the residence time of the air in the actual cloud is similar to the residence time of the air in the chamber. However, at cloud-base *Martin et al.* [1994] notice a substantial variation in the cloud droplet number concentration. Therefore the results of this study are compared with droplet numbers at a location somewhat higher up in the cloud.

The number of aerosol particles before cloud formation was compared with the number of cloud droplets formed in the same air. *Jones et al.* [1994] analyzed these data and obtained the following relationship between the droplet number concentration and the concentration of aerosol particles larger than 0.1 μm in diameter:

$$N_{dr} = 375\ (1 - e^{-Naer/400}) \qquad 5.6$$

This relationship was tested on the data set obtained in the present study on days with marine air flows. A very good agreement was found (Fig.5.12), suggesting a similar agreement between the results of this study and those from the aircraft cloud measurements by *Martin et al.* [1994].

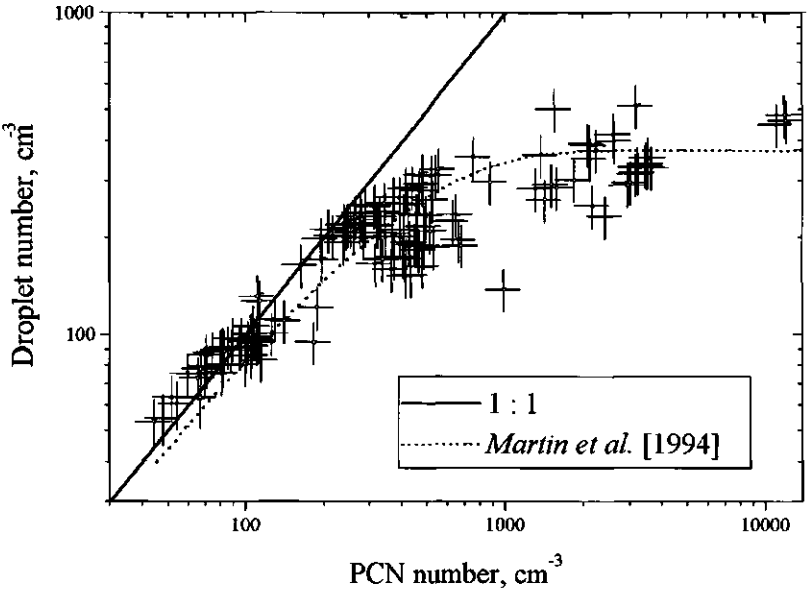

Figure 5.12. *Comparison of the present measurements in marine air with the best fit curve by Jones et al. [1994] to the data set of Martin et al. [1994] obtained during aircraft measurements in marine stratiform clouds near and over the British Isles.*

The maximum droplet number concentration observed by *Martin et al.* [1994] in polluted marine air masses did not exceed 500 cm^{-3}, which is consistent with the results found in this study on days of mostly marine origin. In air masses with low aerosol number *Martin et al.* [1994] found that the droplet number was equal to the aerosol number which was also found in the present measurements in the clean air.

As *Martin et al.* [1994] measured only aerosol particles larger than 0.1 μm, the cloud droplet number was occasionally higher than the aerosol number. The experiments with ammonium sulfate aerosol (Chapter 4) show that at supersaturations higher than 0.15% the number of aerosol particles larger than 0.1 μm underestimates the

number of cloud nuclei. One can expect that at a higher supersaturation which can be encountered in clouds even smaller particles can be activated.

The good agreement between the study by *Martin et al.* [1994] and the present study suggests that the results obtained in the chamber may be assumed representative for the real clouds in the West-European region. However, it should be noted that even though the results of this study are similar to those of the actual cloud measurements, the processes of cloud formation in the chamber may differ from those occurring in real clouds. Since simulation of the processes inside the chamber is very difficult, a comparison with measurements in the actual clouds above the measurement site is required. Such a comparison is foreseen in the near future.

CONCLUSIONS

Activation tests with marine aerosol show that the droplet number concentration did not exceed 500 cm^{-3} on any of the days, even though the total aerosol number concentration in the polluted air masses was as high as 17600 cm^{-3}.

At potential cloud nuclei number concentrations lower than approximately 100 cm^{-3} the droplet number concentration was equal to that of potential cloud nuclei within the experimental uncertainty. At higher number concentrations the cloud forming efficiency progressively decreases with increasing concentration of potential cloud nuclei due to the so-called saturation effect and due to the presence of insoluble material.

It was found that in "clean" marine air, with the PCN number concentrations below 100 cm^{-3}, all particles larger than the activation

threshold size were activated. This shows that all of the particles are hygroscopic and are effective cloud nuclei.

In polluted marine air the cloud forming efficiency of particles progressively decreases with increasing number concentration due to limitations in the amount of available water (saturation effect) and the presence of insoluble material.

Aerosol spectra of non-activated PCN observed on two days, when the saturation effect was not significant, suggest that the non-activated particles are practically insoluble and are most probably composed of soot. Due to a very limited number of measurements it is not possible to draw a definite conclusion on the nature of the insoluble material, which needs further verification.

The amount of insoluble material is a key factor in the activation of aerosol particles. It needs further characterization with respect to composition and sources. It should be considered, though, that chemical analysis of the particles in the cloud nuclei size range is very difficult because they represent very little mass.

The chemical composition of ambient aerosols in marine air flows shows that the water-soluble inorganic fraction in the PCN size range is dominated by sulfate. However, on few days it was found that nitrate had a similar or even stronger contribution to the number of CCN. Similar contribution of nitrate to the aerosol number concentration is consistently found in continental air flows. It is possible that the nitrate content in marine aerosols is underestimated especially at low aerosol sizes due to evaporative losses from the impactor stages. This, however, needs further verification.

The number of aerosol particles activated in the chamber tests was in good agreement with the number of activated particles in actual marine stratus over and near the UK. The good agreement indicates that the results obtained at our site are representative for the West-European region.

A few measurements with continental aerosol show that the activation efficiency of continental particles is similar to that of heavily polluted marine aerosol. However, on some occasions the activation efficiency of continental aerosol was higher than that of marine aerosol and equal to the activation efficiency of the reference sulfate aerosol. This shows that continental particles can be very hygroscopic.

Chapter 6.

Estimate of the local aerosol radiative forcing

INTRODUCTION

In this chapter a simple "order-of-magnitude" estimation of the local aerosol radiative forcing is done on the basis of the experimental data discussed in the previous chapters. The term radiative forcing is used to quantify a potential climate change mechanism. Radiative forcing is defined as the perturbation to the energy balance of the Earth (in W/m^2) following, for example, a change in concentration of carbon dioxide or aerosol particles. A positive radiative forcing tends to warm the surface, while negative - to cool. As was discussed in Chapter 1, anthropogenic radiative forcing can be divided into two major types: the greenhouse forcing due to increased concentrations of the greenhouse gases and the aerosol forcing. The greenhouse forcing is positive and thus has a warming influence on climate, while the aerosol forcing acts in the opposite way.

The radiative forcing by the anthropogenic greenhouse gases since pre-industrial times is estimated to be 2.45 W/m^2 with the uncertainty to be about 15% [*IPCC*, 1996]. The greenhouse gases are uniformly distributed over the globe and so is the greenhouse forcing. The aerosol climate forcing consists of the direct and the indirect forcing, which complement each other. Due to the short life times of aerosol particles the aerosol forcing is spatially non-uniform. The *IPCC* [1996] gives for the direct forcing by sulfate only aerosols an estimate of -0.4 W/m^2 with a factor of 2 uncertainty. In a number of studies the magnitude of the

indirect aerosol forcing was estimated to be between -0.5 and -1.5 W/m^2 (see Chapter 1). However, referring to the uncertainty in quantifying the indirect effect and despite the fact that all of the cited in the IPCC report studies give a mean indirect forcing substantially below zero, the IPCC does not accept any midrange estimate and gives only a range between 0 and -1.5 W/m^2. The accepted by the IPCC values for the aerosol radiative forcing, however, most probably represent a low-end estimate because of the omission of other important anthropogenic aerosol compounds like ammonium nitrate, which was shown in this thesis to be a major aerosol constituent in the size range relevant to the climate forcing.

The main experimental part of this thesis was devoted to an assessment of the cloud forming properties of the local ambient aerosol, which were discussed in the previous chapter. For this reason, the central attention here is given to estimation of the local indirect forcing. However, because the indirect effect is complemented by the direct forcing, (*i.e.* the direct forcing occurs when clouds are not present), a simple estimation of the local direct forcing is also done here. The direct forcing is estimated using the data of the aerosol light scattering in the Netherlands from the study of *ten Brink et al.* [1996a] and *Veefkind et al.* [1996] which were discussed in Chapter 3. The estimated combined local aerosol forcing is then compared to the forcing by the greenhouse gases.

LOCAL INDIRECT FORCING

The local annual mean indirect forcing is estimated here by comparing the average droplet number concentration observed during activation experiments (see Chapter 5) with the droplet number concentration observed in "clean" air. The indirect forcing is estimated using an expression given by *Schwartz and Slingo* [1996] for the

change in cloud-top albedo of marine stratiform clouds caused by a change in droplet number concentration:

$$\Delta R \approx 0.075 \ln\left(\frac{N_{poluted}}{N_{clean}}\right) \qquad 6.1$$

in which R is the cloud top albedo and N is the droplet number concentration. The local forcing is obtained by multiplying the annually averaged reflection of marine stratiform clouds, estimated to be around 50 W/m^2 [*Schwartz and Slingo*, 1996], by the increase in albedo.

Clean marine aerosol is expected in air flows coming from the sea which did not pass over land (air trajectories from the NW-N sector). The measurements showed, however, that though correlating with the wind direction the aerosol number concentration can vary rather strongly from day to day even with the same wind direction, presumably because of different air mass histories. Therefore it was decided to use the total aerosol number concentration for characterization of air masses. The criterion for "clean" air was chosen in the following way. The lowest total (larger than 0.019 μm in diameter) aerosol number concentration encountered at the site was around 100 cm^{-3}. Consequently, it was decided that "clean" marine air masses have total aerosol concentrations in the order of 100 cm^{-3}. Further support for this criterion is obtained from a study by *van de Vate et al.* [1982, 1984] which was performed at the same location as the present study. In that study the low total number concentrations (below 200 cm^{-3}) were associated with low radon concentrations indicating that the air was practically unaffected by anthropogenic emissions over land.

The above criterion for the classification of air masses is similar to that used in *Anderson et al.* [1994], who classified an air mass as clean when the total aerosol number concentration was below 500 cm^{-3}. *Hoppel et al.* [1990] reported mean total aerosol number concentrations (from about 0.02 μm in diameter) in the remote Atlantic of around 200 cm^{-3} with the lowest observed concentration being 100 cm^{-3}. *Andreae et al.* [1995] in a study in South Atlantic (which might be not indicative

for North Atlantic background aerosol) observed concentrations as low as 50 cm^{-3} with the mean concentrations during "clean" conditions being around 220 cm^{-3}. Since references to lower aerosol concentrations were not found in the literature, the lowest observed value at our site can be considered as being representative for marine background aerosol and the criterion for the "clean" aerosol to be justified.

Equation 6.1 shows that the increase in cloud top albedo is very sensitive to choosing the reference ("clean") droplet number concentration. Unfortunately, there is, practically, no data on droplet number concentrations in "clean" marine clouds in Northern hemisphere, perhaps, because there is no place left that is not affected by anthropogenic influence. A few measurements in remote Atlantic [*Hoppel et al.*, 1990; *Andreae et al.*; 1995] indicate that the droplet number concentration in "clean" clouds should be a few tens of droplets per cm^3. The lowest droplet number concentration observed in this study was approximately 50 cm^{-3}. This value is within the expected range of concentrations for remote marine clouds and will be used further as the reference "clean" droplet number concentration. However, it is still uncertain, perhaps, to a factor of 2 whether this value can be attributed to an unperturbed droplet number concentration. The uncertainty of a factor of 2 in choosing the reference droplet number concentration translates (using Eq.6.1) into uncertainty in forcing of about 2.5 W/m^2.

The average droplet number concentration observed during the activation of the local ambient aerosol (Chapter 6) is approximately 280 cm^{-3}, which corresponds to an increase by a factor of 5.7 relative to 50 cm^{-3}. Such an increase in droplet number concentration translates into increase in albedo of 13%. According to this the local annual mean indirect forcing is estimated to be -6.5 ±2.5 W/m^2. However, the limited number of days on which the activation experiments were performed is, perhaps, not sufficient to generalize the observed average droplet number. However, it was shown in the previous chapter that the droplet number concentration versus the PCN concentration on all days with marine air follows the relationship observed in the study by *Martin et al.* [1994]. This relationship (Eq.5.6) shows that the droplet

number concentration "saturates" at high PCN number concentrations, with its asymptotic value being 380 cm^{-3}. This value can be used as the measure of the maximum droplet number concentration in marine stratiform clouds. This "maximum" droplet number concentration is used here to estimate the upper limit for the indirect radiative forcing. The concentration of 375 cm^{-3} is 7.5 times higher than the chosen "clean" droplet number concentration of 50 cm^{-3}. Such an increase in droplet number concentration corresponds to a forcing of -7.6 W/m^2, which is within the limits of the forcing estimated from the average droplet number concentration.

LOCAL DIRECT FORCING

The local annual mean direct aerosol forcing is estimated here using the approach of *Charlson et al.* [1992], adopted for the local case. For an optically thin aerosol layer (aerosol optical depth, $\delta_a << 1$), the annual mean direct forcing ΔF_{direct} is :

$$\Delta F_{direct} = -\tfrac{1}{2} F T^2 (1 - A_c)(1 - R_s)^2 \beta \Delta\delta_a \qquad 6.2$$

in which F is the top-of-the-atmosphere radiative flux, T is the fraction of incident light that is transmitted by the atmospheric layer above the aerosol layer, A_c is the annual mean fractional cloud cover, R_s is the mean surface albedo, β is the annual mean upward fraction of scattered light by the aerosol and $\Delta\delta_a$ is the annual mean change in the aerosol optical depth due to anthropogenic aerosols. The factors T^2 and $(1-R_s)^2$ take into account transmittance of incident and scattered radiation. The term $(1-A_c)$ is introduced because the direct forcing occurs mainly when clouds are not present.

It is assumed, following *Charlson et al.* [1992], that the anthropogenic aerosol is concentrated in the boundary layer. The aerosol optical depth, then, is the particle scattering coefficient, B_{sp}

(Eq.2.20), integrated over the solar spectrum and over the optical path from 0 to H, the height of the boundary layer (see Eq.2.19). Further, it is assumed that the boundary layer is well mixed allowing to extrapolate the aerosol scattering coefficient as measured at the ground to the whole boundary layer. This assumption is done on the following basis. The annual mean forcing is expected to be mostly determined by the forcing during the summer half of the year. During summer the solar zenith angle is smaller then in winter, which provides for a much higher insolation (the average local top-of-the-atmosphere insolation is more than 7 times higher in June than that in December). In addition, the direct forcing is strongest on clear sky days (see Eq.6.2). Hence, sunny summer days are expected to have the largest weight in determining the annual mean forcing. On such days the boundary layer becomes readily mixed owing to convectivity arising from a rapid heating of the Earth's surface. Thus, on the days that contribute most to the annual forcing the boundary layer is mixed, which justifies the assumption.

Results of the measurements of the (dry) aerosol light scattering by *ten Brink et al.* [1996a] and the study of *Veefkind et al.* [1996] on the effect of relative humidity on the aerosol light scattering (both of these studies were discussed in detail in Chapter 2) are used here to estimate the local direct forcing. To separate the effect of relative humidity, Eq.2.19 is rewritten in the following form:

$$\delta_a = \int_0^H \int_{\lambda_1}^{\lambda_2} B_{sp}(RH_0)\, f(RH)\, d\lambda\, dz \qquad 6.3$$

in which $f(RH)$ is the increase in light scattering caused by the accretion of water at a given relative humidity, RH, as measured with an integrating nephelometer, relative to the light scattering at a reference low (typically 30% RH) relative humidity RH_0 (see Eq.2.21).

In the study by *ten Brink et al.* [1996a] the dry aerosol light scattering was measured with the nephelometer at a wavelength of 0.525 μm. In order to estimate the forcing over the whole solar spectrum, the light scattering at 0.525 μm must be extrapolated to

other wavelengths. This is done, following *Veefkind et al.* [1996], by assuming a dependence on wavelength of the light-scattering as given by the Ångström formula:

$$\delta(\lambda) = b\,\lambda^{-a} \qquad 6.4$$

in which λ is the wavelength in μm, b is the turbidity coefficient and a is the wavelength exponent. The ratio of the light scattering at a wavelength λ to that at λ_0 is:

$$\frac{\delta(\lambda)}{\delta(\lambda_0)} = \left(\frac{\lambda_0}{\lambda}\right)^a \qquad 6.5$$

Measurements of aerosol size distributions and optical properties in the Netherlands indicate that a is between 1.3 and 1.7 [*van der Meulen*, 1986]. Further support for this range of values for a came from the study by *Veefkind et al.* [1996]. Using Eq.6.5 with the indicated values for a, a mean aerosol light scattering over solar spectrum was extrapolated from the measurements at 0.525 μm in the following way. Aerosol light scattering integrated over the solar spectrum may be approximated by scattering at an "effective" wavelength of about 0.7 μm [*Kiehl and Briegleb*, 1993]. Extrapolation from 0.525 to 0.7 μm according to Eq.6.5 requires a correction factor of between 0.61 and 0.69 (dependent on the value of a), with the average being 0.65.

The dependence of $f(RH)$ in Eq.6.3 (which in the study by *Veefkind et al.* was measured at 0.475 μm) on wavelength of light is rather difficult to assess, however, a simple analysis of its dependence is given here. The light scattering coefficient depends quadratically on the particle size and on the extinction coefficient (Eq.2.20). The extinction coefficient has a complicated wavelength dependence given by the Mie theory and is dependent on the ratio between the particle size and the wavelength of light. The extinction coefficient has its maximum value (approximately 4) when the particle diameter is equal to the wavelength divided by π. At larger sizes the extinction coefficient decreases to its asymptotic value of 2. A shift in size would result in particles being at their maximum of the Mie curve at one wavelength to

shift to the maximum of the Mie curve at another wavelength. The change of the extinction coefficient over the solar spectrum averaged for the whole size distribution thus is not expected to be large. Most of the light scattering enhancement is due to the increase in particle size. Consequently, it is assumed here that $f(RH)$ does not depend on wavelength. Equation 6.3 then becomes:

$$\delta = 0.65\, B'_{sp}(RH_0) \int_0^H f(RH)\, dz \qquad 6.6$$

in which $B'_{sp}(RH_0)$ is the light scattering coefficient of dry aerosol at 0.475 μm.

The annual average value for the enhancement factor (the integral in Eq.6.6) is not available, as there is no statistics on the relative humidity distribution of the RH with height. The minimum average relative humidity in the summer half of the year in the Netherlands is 60 - 70% [*KNMI*, 1972]. Since in the boundary layer the relative humidity rarely decreases below its value at the ground and because the aerosol contains large amounts of hygroscopic nitrate which does not crystallize even at a very low relative humidity (10%), the aerosol in the boundary layer is in a wet state (upper hysteresis branch). The measurements by *Veefkind et al.* [1996] and *ten Brink et al.* [1996a] indicate that the enhancement factor at these relative humidities is between 1.4 and 1.7, which should be considered as minimum estimates. In Chapter 2 it was demonstrated that the increase in relative humidity with height may lead to an enhancement factor over the boundary layer to be up to 2 times higher than the enhancement factor at the ground. For this reason, the average enhancement factor over the boundary layer is estimated here to be 2 ±0.5.

The annually averaged value for the aerosol light scattering coefficient measured at Petten, the Netherlands, is 0.7 10^{-4} m^{-1}, which is at least one order of magnitude higher than the scattering coefficient in clean arctic air [*ten Brink et al.*, 1996]. Thus, the value of 0.7 10^{-4} m^{-1} is considered to be mostly due to the anthropogenic perturbation.

There is no statistics on the boundary layer height in the Netherlands. The boundary layer during summer half of the year is estimated here to be 1.2 ±0.3 km. The annual mean optical depth is then estimated to be 0.11 ±0.04 with the uncertainty arising mostly due to the absence of data on the boundary layer height and the distribution of relative humidity within it.

To estimate the local annual mean direct forcing the following values are used (see Eq.6.2). The top-of-the-atmosphere flux F = 1370 W/m^2, the transmittance of the atmosphere T = 0.76 [*Charlson et al.*, 1992]. The average surface albedo in the Netherlands is 0.2 [*Velds*, 1992]. The annual mean cloud cover in the Netherlands (taken as that in the summer half of the year) is 0.65 [*KNMI*, 1972]. The upscatter fraction, β = 0.3 [*Charlson et al.*, 1992].

Using the above values and substituting them into Eq.6.2, the local annual mean direct forcing is estimated to be -3 ±1.1 W/m^2. The uncertainty is to a large extent due to the uncertainty in the relative humidity distribution with height and in the height of the boundary layer.

CONCLUSIONS / IMPLICATIONS

On the basis of the measurements performed at Petten, the Netherlands, the local annual-mean indirect radiative forcing is estimated to be -6.5 ±2.5 W/m^2. The uncertainty in the indirect forcing arises mostly due to the uncertainty in choosing the reference "clean" droplet number concentration.

The local annual-mean direct forcing is estimated to be -3 ±1.1 W/m^2. The main source of uncertainty in the direct forcing arises from the absence of data on the height of the atmospheric boundary layer

and from the absence of data on the relative humidity distribution within the boundary layer.

The total annual mean local radiative forcing by anthropogenic aerosols is thus estimated to be about -9.5 ±3 W/m^2, which is about 4 times higher than the (positive) forcing by all anthropogenic greenhouse gases. The net local radiative forcing, *i.e.* the combined forcing by the anthropogenic greenhouse gases and aerosols, is estimated to be -7 ±3 W/m^2.

It should be noted that the above estimates are based on the measurements at Petten, which is a cleaner location than most of the Netherlands. For example, sulfate concentrations at Petten are on 1.5 to 2 times lower than on average in the Netherlands [*Arends et al.*, 1996]. It shows that anthropogenic aerosols largely dominate the radiative forcing in the Netherlands and, by deduction, in Western Europe. Recognition of this means that anthropogenic aerosols play a major role in the global radiative balance of the Earth and further characterization of aerosol properties is extremely important for understanding of man's influence on climate.

Approximately one third of the local direct radiative forcing (*i.e.* about -1 W/m^2) and a part (perhaps substantial) of the local indirect forcing is due to ammonium nitrate aerosol. This compound, though demonstrated to be present in substantial quantities in other parts of the world, is completely neglected in assessments by the *IPCC* [1995]. The demonstrated large contribution of ammonium nitrate to the radiative forcing makes such an omission unjustified and requires a better assessment of the contribution of this compound to the global aerosol radiative forcing.

Anthropogenic aerosols, due to their very strong radiative forcing, may at present substantially mask the warming by the constantly accumulating anthropogenic greenhouse gases. Global warming may accelerate sharply in the future, especially if emissions of aerosols and their precursors are reduced in order to fight acid deposition, eutrification, adverse health effects, etc. Recognition of this means that

a further major research for an accurate assessment of factors controlling the magnitude of the aerosol radiative forcing is required for confident policy making towards the control of air pollution.

References

Albrecht B.A., Randal D.A. and Nicholls S. (1988). Observations of marine stratocumulus clouds during FIRE. *Bull.Am.Meteor.Soc. V69*, 618-626.

Albrecht B.A. (1989). Aerosols, cloud microphysics, and fractional cloudiness. *Science V262*, 226-229.

Albrecht B.A., Bretherton C.S., Johnson D., Scubert W.H. and Frisch A.S. (1995) The Atlantic Stratocumulus Transition Experiment - ASTEX. *Bull. Amer. Meteorol. Soc. V76*, 889-904.

Alofs, D.J. and Liu, T.-H. (1981) Atmospheric measurements of CCN in the supersaturation range 0.013-0.681%. *J. Atmos. Sci. V38*, 2772-2778.

Anderson T.L., Covert D.S. and Charlson R. (1994). Cloud droplet number studies with a counterflow virtual impactor. *J.Geophys.Res. V99*, 8249-8256.

Andreae M.O. (1995) Climatic effects of changing atmospheric aerosol levels. *In: World Survey of Climatology*, V16, *Future Climates of the World (ed.* Henderson-Sellers), Elsevier, New York.

Andreae M.O., Elbert W. and de Mora S.J. (1995) Biogenic sulfur emissions and aerosols over the tropical South Atlantic. 3. Atmospheric dimethylsulfide, aerosols and cloud condensation nuclei. *J.Geophys.Res. V100*, 11335-11356.

Appel B.R., Tokiwa Y. and Haik M. (1981) Sampling of nitrates in the atmosphere. *Atmos. Environ. V15*, 283-289.

Arends B.G., Kos G.P.A., Wobrock W., Schell D., Noone K.J., Fuzzi S. and Pahl S. (1992) Comparison of techniques for measurements of fog liquid water content. *Tellus 44B*, 604-611.

Arends B., Baard J. and ten Brink H.M. (1996) Trends in summer sulfate in Europe, *submitted to Atmos.Environ.*

Baumgardner, D., Strapp, J.W. and Dye, J.E. (1985) Evaluation of the forward scattering spectrometer probe. Part II: corrections for coincidence and dead time errors. *J. Atmos. Oceanic Technol. V2*, 626-632.

Benner, W.H., Hansen, A.D.A. and Novakov, T. (1989) A concurrent-flow cloud chamber study of incorporation of black carbon into droplets. *Aerosol Sci. Technol. V10*, 84-92.

Berner A., Lurzer C.H., Pohl L., Preining O. and Wagner P. (1979) The size distribution of the urban aerosol in Vienna. *Sci. Total Environ. V13*, 245-261.

Berner, A. (1989) Haze and its relation to the atmospheric accumulation aerosol. *Sci. Total Environ. V86*, 251-261.

Berresheim H., Eisele F.L., Tanner D.J., McInnes L.M., Ramsey-Bell D.C. and Covert D.S. (1993) Atmospheric sulfur chemistry and cloud condensation nuclei (CCN) concentrations over the Northeastern Pacific coast. *J.Geophys.Res. V98*, 12701-12711.

BIATEX Final Report (1997) *Biosphere-Atmosphere Exchange of Pollutants and Trace Substances* (ed. Slanina J.) Springer Verlag, Berlin, Heidelberg, New York.

Blanchet J.-P. (1995) Mechanisms of direct and indirect climate forcing by aerosols in the Arctic region. *In: Aerosol Forcing of Climate: Report of the Dahlem Workshop on Aerosol Forcing of Climate, Berlin 1994, April 24-29* (ed. R.J.Charlson and J.Heintzenberg), Wiley & Sons, Chichester, pp.109-121.

Boucher O. and Anderson T.L. (1995) GCM assessment of the sensitivity of direct climate forcing by anthropogenic sulfate aerosols to aerosol size and chemistry. *J.Geophys.Res. V100*, 26061-26092.

Boucher O. and Lohmann U. (1995) The sulfate - CCN - cloud albedo effect. A sensitivity study with two general circulation models. *Tellus V47B*, 281-300.

Charlson R.J., Lovelock J.E., Andreae M.O. and Warren S.G. (1987) Oceanic phytoplankton, atmospheric sulphur, cloud albedo and climate. *Nature V326*, 655-661.

Charlson R.J., Langner J., Rodhe H., Leovy C.B. and Warren S.G. (1991) Perturbation of the northern hemisphere radiative balance by backscattering from anthropogenic sulfate aerosols. *Tellus 43A-B*, 152-163.

Charlson R.J., Schwartz S.E., Hales J.M., Cess R.D., Coakley J.A.Jr., Hansen J.E. and Hofmann D.J. (1992) Climate forcing by anthropogenic aerosols. *Science V255*, 423-430.

Charlson R.J. and J.Heintzenberg (1995) Aerosols as a cause of uncertainty in climate forecasts. *In: Aerosol Forcing of Climate: Report of the Dahlem Workshop on Aerosol Forcing of Climate, Berlin 1994, April 24-29* (ed. R.J.Charlson and J.Heintzenberg), Wiley & Sons, Chichester, pp.1-10.

Choularton T.W., Consterdine I.E., Gardiner B.A., Gay M.J., Hill M.K., Latham J. and Stromberg I.M. (1986) Field studies of the optical and microphysical characteristics of clouds enveloping Great Dun Fell. *Quart.J.R.Met.Soc. V112*, 131-148.

Chuang C.C., Penner J.E., Taylor K.E. and Walton J.J. (1994) Climate effects of anthropogenic sulfate: simulation from a coupled chemistry, climate model. *Preprints of the the Conference on Atmospheric Chemistry, Nashville, Tennessee, January 1994*, Am.Meteorol.Soc., Boston USA, pp.170-174.

Chuang C.C., Penner J.E., Taylor K.E., Grossman A.S. and Walton J.J. (1997) An assessment of the radiative effects of anthropogenic sulfate. *J.Geophys.Res. V102*, 3761-3778.

Chylek P., Banic C.M., Johnson B., Damiano P.A., Isaac G.A., Leaitch W.R., Liu P.S.K., Boudala F.S., Winter B. and Ngo D. (1996) Black carbon: Atmospheric concentrations and cloud water content measurements over southern Nova Scotia. *J.Geophys.Res. V101*, 29105-29110.

Coakley J.A., Cess R.D. and Yurevich F.B. (1983) The effect of tropospheric aerosols on the Earth's radiation budget: A parameterization for climate models. *J.Atmos.Sci. V40*, 116-138.

Coakley J.A. Bernstein R.L. and Durkee P.A. (1987) Effect of ship-track effluents on cloud reflectivity. *Science V237*, 1020-1022.

Corradini C. and Tonna G. (1979) Condensation nuclei supersaturation spectrum: Analysis of the relationship between the saturation droplet radius and the critical supersaturation in the Laktionov isothermal chamber. *J. Aerosol Sci. V10*, 465-469.

Daum P.H., Kelly T.J., Strapp J.W., Leaitch W.R., Joe P., Schemenauer R.S., Isaac G.A., Anlauf K.G. and Wiebe H.A. (1987) Chemistry and physics of a winter stratus cloud layer: A case study. *J.Geophys.Res. V92*, 8426-8436.

Diederen, H.S.M.A., Guicherit R. and Hollander J.C.T. (1985) Visibility reduction by air pollution in The Netherlands. *Atmos. Environ. V19*, 377-383.

Dye, J.E. and Baumgardner, D. (1984) Evaluation of the forward scattering spectrometer probe. Part I: electrical and optical studies. *J. Atmos. Oceanic Technol. V1*, 229-344.

Eichel C., Krämer M., Schütz L. and Wurzler S. (1996) The water-soluble fraction of atmospheric aerosol particles and its influence on cloud microphysics. *J.Geophys.Res. V101*, 29499-29510.

EMEP (1996) EMEP / MSC-W Status Report 1/96. Transboundary air pollution in Europe. Part 1: Estimated sdispersion of acidifying agents and of near surface ozone. ISSN 03332-9879.

Fitzgerald J.W. (1975) Approximation formulas for the equilibrium size of an aerosol particle as a function of its dry radius and composition and the ambient relative humidity. *J.Appl.Meteorol. V14*, 1044-1049.

Forrest J., Spandau D., Tanner R. L. and Newman L. (1982) Determination of atmospheric nitrate and nitric acid deploying a diffusion denuder with a filter pack. *Atmos. Environ. V16*, 1473-1485.

Fuchs N.A. (1964) *The mechanics of aerosols*. Pergamon, New York.

Fuchs N.A. (1959) *Evaporation and Droplet Growth in Gaseous Media*. Pergamon Press, London.

Gerber H. (1991) Supersaturation and droplet spectral evolution in fog. *J.Atmos.Sci. V48*, 2569-2588.

Gillani N.V., Schwartz S.E., Leaitch W.R., Strapp J.W. and Isaac G.A. (1995) Field observations in continental stratiform clouds: Partitioning of cloud particles between droplets and unactivated interstitial aerosols. *J. Geophys. Res. V100*, 18687-18706.

Gras J.L. (1995) CN, CCN and particle size in Southern Ocean air at Cape Grim. *Atmos. Res. V35*, 233-251.

Grassl H. (1990) Aerosols and climate. *In: Proceed. Symposium World Climate and Aerosols, Bunnik May 1990*, (eds. J.F. van de Vate and H.B. Tirion), ver. LUCHT, Delft, the Netherlands, p.5.

Hagen, D.E., Trueblood, M.B. and Alofs, D.J. (1990) A study of the hydration properties of selected laser dye aerosols including continuous-flow parallel plate and alternating-gradient thermal diffusion cloud chamber measurements in the high supersaturation regime. *Aerosol Sci. Technol. V12*, 547-560.

Hallberg A., Noone K.J., Ogren J.A., Svenningson I.B., Flossman A., Wiedensohler A., Hanson H.-C., Heintzenberg J., Anderson T.L., Arends B.G. and Maser R. (1994a) Phase partitioning of aerosol particles in clouds at Kleiner Feldberg. *J.Atmos.Chem. V19*, 107-127.

Hallberg A., Ogren J.A., Noone K.J., Okada K., Heintzenberg J. and Svenningson I.B. (1994b) The influence of aerosol particle composition on cloud droplet formation. *J.Atmos.Chem. V19*, 153-171.

Harrison R.M. and Pio C.A. (1983) Size differentiated composition of inorganic atmospheric aerosols of both marine and polluted continental origine. *Atmos. Environ. V17*, 1733-1738.

Hänel G. (1987) The role of aerosol properties during the condensation stage of cloud: a reinvestigation of numerics and microphysics. *Beitr.Phys.Atmosph. V3*, 321-339.

Hegg D.A., Hobbs P.V. and Radke L.F. (1984) *Atmos.Environ. V18*, 1939-1946.

Hegg D.A., Ferek R.J. and Hobbs P.V. (1993) Lightscattering and cloud condensation nucleus activity of sulfate aerosol measured over the Northeast Atlantic Ocean. *J.Geophys.Res. V98*, 14887-14894.

Hoppel W.A., Fitzgerald J.W., Frick G.M., Larson R.E. and Mack E.J. (1990) Aerosol size distributions and optical properties found in the marine boundary layer over the Atlantic Ocean. *J.Geophys.Res. V95*, 3659-3686.

Hoppel W.A., Frick G.M., Fitzgerald J.W. and Larson R.E. (1994) Marine boundary layer measurements of new particle formation and the effects nonprecipitating clouds have on aerosol size distribution. *J.Geophys.Res. V99*, 14443-14459.

Hudson J.G. (1983) Effects of CCN concentration on stratus clouds. J.Atmos.Sci. V40, 480-486.

Hudson, J.G. (1989) An instanteneous CCN spectrometer. *J. Atmos. Oceanic Technol. V6*, 1055-1065.

Intergovernmental Panel on Climate Change (IPCC) (1995) *Climate Change 1994. Radiative Forcing of Climate Change and an Evaluation of the IPCC IS92 Emission Scenarios.* (Ed. J.T. Houghton, L.G. Meira Filho, J. Bruce, Hoesung Lee, B.A. Callander, E.Haites N. Harris and K. Maskell) University Press, Cambridge.

Intergovernmental Panel for Climate Change (IPCC) (1996) *Climate Change 1995. The Science of Climate Change.* (Ed. J.T. Houghton, L.G. Meira Filho, B.A. Callander, N. Harris, A. Kattenberg and K. Maskell) University Press, Cambridge.

Janssen L.H.J.M., Visser H., Römer F.G. (1989) Analysis of large scale sulphate, nitrate, chloride and ammonium concentrations in the Netherlands using an aerosol measuring network. *Atmos. Environ. V23*, 2783-2796.

Jensen J.B. and Charlson R.J. (1984) On the efficiency of nucleation scavenging. *Tellus V36B*, 367-375.

Jones A., Roberts D.L. and Slingo A. (1994) A climate model study of indirect radiative forcing by anthropogenic sulfate aerosols. *Nature V370*, 450-453.

Keeling, C.D., Bacastow R.B., and Whorf T.P. (1982). Measurements of the concentration of carbon dioxide at Mauna Loa Observatory, Hawaii. *In: Carbon Dioxide Review: 1982.* (ed. W.C. Clark) Oxford University Press, New York.

Keuken M.P., Schoonebeek C.A.M., van Wensveen-Louter A., Slanina J. (1988) Simultaneous sampling of NH_3, HNO_3, HCl, SO_2 and H_2O_2 in ambient air by wet annular denuder system. *Atmos. Environ. V22*, 2541-2548.

Khemani L.T., Momin G.A., Naik M.S., P.S.P. Rao R.Kumar and Bh.V.R. Murty (1985) Trace elements and sea salt aerosols over the sea areas around the Indian sub-continent. *Atmos. Environ. V19*, 277-284.

Khlystov A., Wyers G.P. and Slanina J. (1995) The Steam-Jet Aerosol Collector. *Atmos.Environ. V29*, 2229-2234.

Kiehl J.T. and Briegleb B.P. (1993) The relative role of sulfate aerosols and greenhouse gases in climate forcing. *Science V260*, 311-314.

Kiehl J.T. and Rodhe H. (1995) Modeling geographical and seasonal forcing due to aerosols. *In: Aerosol Forcing of Climate: Report of the Dahlem Workshop on Aerosol Forcing of Climate, Berlin 1994, April 24-29* (ed. R.J.Charlson and J.Heintzenberg), Wiley & Sons, Chichester, pp.281-296.

King M.D., Radke L.F. and Hobbs P.V. (1993) Optical properties of marine stratocumulus clouds modified by ships. *J.Geophys.Res. V98*, 2729-2739.

King M.D., Si-Chee Tsay and Platnick S. (1995) *In situ* observations of the indirect effect of aerosols on clouds. *In: Aerosol Forcing of Climate: Report of the Dahlem Workshop on Aerosol Forcing of Climate, Berlin 1994, April 24-29* (ed. R.J.Charlson and J.Heintzenberg), Wiley & Sons, Chichester, pp.227-248.

Klockow D., Niessner R., Malejczyk M., Kiendl H., vom Berg. B, Keuken M.P. Waijers-Ypelaan A. and Slanina J. (1989) Determination of nitric acid and ammonium nitrate by means of a computer-controlled thermodenuder system. *Atmos. Environ. V23*, 1131-1138.

KNMI, Royal Dutch Meteorological Institute (1972) *Klimaatatlas van Nederland* (Climate atlas of the Netherlands). Staatsuitgeverij, 's-Gravenhage (In Dutch).

Kruisz C. (1992) Sammlung hygroskopischer Aerosole mit Kaskadenimpaktoren im Windkanal bei ECN/Petten. *Abschlußbericht Projekt Simulation '91. Kommission für Reinhaltung der Luft der Österreichischen Akademie der Wissenschaften*. Institute für Experimentalphysik der Universität Wien, Vienna. (in German).

Kulmala M., Laaksonen A., Korhonen P., Vesala T. and Ahonen T. (1993) The effect of atmospheric nitric acid vapor on cloud condensation nucleus activation. *J.Geoph.Research V98*, 22949 - 22958.

Kulmala M., Korhonen P., Vesala T., Hansson H.-C., Noone K. and Svenningsson B. (1996) The effect of hygroscopicity on cloud droplet formation. *Tellus V48B*, 347-360.

Laktionov A.C. (1972) A constant temperature method of determining the concentration of cloud condensation nuclei. *Izv. Atmos. Ocean. Phys. V8*, 672-677.

Leaitch R., Strapp J.W. and Isaac G.A. (1986) Cloud droplet nucleation and cloud scavenging of aerosol sulfate in polluted atmospheres. *Tellus V38B*, 328-344.

Leaitch R., Isaac G.A., Strapp J.W., Banic C.M. and Wiebe H.A. (1992) The relation between cloud droplet number concentration and anthropogenic pollution: observations and climatic implications. *J.Geophys.Res. V97*, 2463-2474.

Leaitch W.R., Banic C.M., Isaac G.A., Couture M.D., Liu P.S.K., Gultepe I., Li S.-M., Kleinman L., Daum P.H. and MacPherson J.I. (1996) Physical and chemical observations in marine stratus during the 1993 North Atlantic Regional Experiment: Factors controlling droplet number concentrations. *J.Geophys.Res. V101*, 29123-29135.

Levenspiel, O. (1972) *Chemical Reaction Engineering*. John Wiley & Sons, New York..

Liepert B., Fabian P. And Grassl H. (1994) Solar radiation in Germany - observed trends and an assessment of their causes. Part I: Regional Approach. *Beitr. Phys. Atmosph. V67*, 15-29.

Mallant R.K.A.M. (1988) A fog chamber and wind tunnel facility for calibration of cloud water collectors. *ECN Report 88-58*, Petten, the Netherlands. Also presented at the NATO advanced research workshop "Acid deposition processes at high elevation sites", Edinburgh, 8-12 September 1986.

Martin G.M., Johnson D.W. and Spice A. (1994) The measurement and parameterization of effective radius of droplets in warm stratiform clouds. *J.Atmos.Sci. V51*, 1823-1842.

Mason B.J. (1971) *The Physics of Clouds*. Claredon Press.

McDonald J.E. (1953) Erroneous cloud physics use of Rault's Law. *J.Meteor. V10*, 416-433.

McMurry P.H. and Stolzenburg M.R. (1989) On the sensitivity of particle size to relative humidity for Los Angeles aerosols. *Atmos.Environ. V23*, 497-507.

Milford J.B. and Davidson C.I. (1987) The sizes of particulate sulfate and nitrate in the atmospher - a review. *JAPCA V37*, 125-134.

NASA Conference Publication 2212 (1980), "The 3rd International CCN Workshop", Oct. 6-17, 1980.

Nemesure S., Wagener R. and Schwartz S.E. (1995) Direct short-wave forcing of climate by the anthropogenic sulfate aerosol: Sensitivity to particle size, composition, and relative humidity. *J.Geophys.Res., V100,* 26105-26116.

Niessner R., Klockow D.(1980) A thermoanalytical approach to speciation of atmospheric strong acids. *Int.J.Environ.Anal Chem. V8*, 163-175.

Novakov T. and Penner J.E. (1993) Large contribution of organic aerosols to cloud-condensation-nuclei concentrations. *Nature V365*, 823-826.

Novakov T., Rivera-Carpio C., Penner J.E. and Rogers C.F. (1994) The effect of anthropogenic sulfate aerosols on marine cloud droplet concentrations. *Tellus V46B*, 132-141.

Okada K., Tanaka T. and Naruse H. (1990) Nucleation scavenging of submicrometer aerosol particles. *Tellus V42B*, 463-480.

Oms M.T., Jongejan P.A.C., Veltkamp A.C., Wyers G.P. and Slanina J. (1996) Continuous monitoring of atmospheric HCl, HNO_3, HNO_2 and SO_2 by wet-annular denuder sampling with on-line chromatographic analysis. *Intern. J. Anal. Chem. V62*, 207-218.

Penner J.E., Charlson R.J., Hales J.M., Laulainen N.S., Leifer R., Novakov T., Ogren J., Radke L.F., Schwartz S.E. and Travis L. (1994) Quantifying and minimizing uncertainty of climate forcing by anthropogenic aerosols. *Bull. Am. Meteorol. Soc. V75*, 375-400.

Penner J.E. (1995) Carbonaceous aerosols influencing atmospheric radiation: black and organic carbon. *In: Aerosol Forcing of Climate: Report of the Dahlem Workshop on Aerosol Forcing of Climate, Berlin 1994, April 24-29* (ed. R.J.Charlson and J.Heintzenberg), Wiley & Sons, Chichester, pp.1-10.

Pilinis C., Seinfeld J.H. and Grosjean D. (1989) Water content of atmospheric aerosols. *Atmos. Environ. V23*, 1601-1606.

Pilinis C., Pandis S.N. and Seinfeld J.H. (1995) Sensitivity of direct climate forcing by anthropogenic aerosols to aerosol size and composition. *J.Geophys.Res. V100*, 18739-18754.

Platnick S. and Twomey S. (1994) Determining the susceptibility of cloud albedo to changes in droplet concentration with the advanced very high resolution radiometer. *J. Appl.Met. V33*, 334-347.

Pruppacher H.R. and Klett J.K. (1978) *Microphysics of Clouds and Precipitation*. Reidel, Dordrecht.

Quinn P.K., Covert D.S., Bates T.S., Kapustin V.N., Ramsey-Bell D.C. and McInnes L.M. (1993) Dimethylsulfide/cloud condensation nuclei/climate system: relevant size-resolved measurements of the chemical and physical properties of the atmospheric aerosol particles. *J.Geophys.Res. V98*, 10411-10427.

Radke L.F., Coakley J.A. Jr. and King M.D. (1989) Direct and remote sensing observations of the effects of ships on clouds. *Science V246*, 1146-1149.

Raga G.B. and Jonas P.R. (1995) Vertical distribution of aerosol particles and CCN in clear air around the British Isles. *Atmos Environ. V29*, 673-684.

Ramanathan V., Cicerone R.J., Singh H.B. and Kiehl J.T. (1985) Trace gas trends and their potential role in climatic change. *J.Geophys.Res. V90*, 5547-5566.

Rodhe H. (1978) Budgets and turn-over times of atmospheric sulfur compounds. *Atmos.Environ. V12*, 671-678.

Rogers R.P. and Yau M.K. (1989) *A Short Course in Cloud Physics*. Pergamon Press, New York.

Rood M.J., Shaw M.A., Larson T.V. and Covert D.C. (1989) Ubiquitous nature of ambient metastable aerosol. *Nature V337*, 537-539.

Ruijgrok W., Tieben H. and Eisinga P. (1994) Dry deposition of acidifying and alkaline particles to Douglas Fir - A comparison of measurements and model results. *KEMA Report Dutch Priority Program on Acidification.* 20159-KES/MLU 94-3216 No 83397.KC.17-94P02.

Russak V. (1990) Trends of solar radiation, cloudiness and atmospheric transparency during recent decades in Estonia. *Tellus V42B*, 206-210.

Savoie D.L. and Prospero J.M. (1982) Particle size distribution of nitrate and sulfate in the marine atmosphere. *Geophys.Res.Lett. V9*, 1207-1210.

Schwartz S. E. and Freiberg J. E (1981) Mass-transport limitation to the rate of reaction of gases in liquid droplets: Application to oxidation of SO_2 in aqueous solutions. *Atmos. Environ. V15*, 1129-1144.

Schwartz S.E. (1988) Are global cloud albedo and climate controlled by marine phytoplankton? *Nature V336*, 441-445.

Schwartz S.E. (1995) Implications of uncertainties in IPCC estimates of radiative forcing. Presented at: *DOE OHER Atmospheric Chemistry Program Annual Meeting*, Tyson Corner VA, USA.

Schwartz S.E. and Andreae M.O. (1996) Uncertainty in Climate Change Caused by Aerosols. *Science V272*, 1121-1122.

Schwartz S.E. and Slingo A. (1996) Enhanced short-wave cloud radiative forcing due to anthropogenic aerosols. *In: Clouds, Chemistry and Climate. NATO ASI Series, V.I 35* (ed. P.J.Crutzen and V.Ramanathan). Springer-Verlag, Berlin, pp.191-236.

Shine K.P., Derwent R.G., Wuebbles D.J. and Morcrette J.-J. (1990) Radiative forcing of climate. *In: Climate Change: The IPCC Scientific Assessment* (ed. J.T.Houghton, G.JJenkins and J.J.Ephraums), pp.41-68.Cambridge Univ Press, Cambridge.

Simon P.K. and Dasgupta P. (1995) Continuous Automated Measurement of Gaseous Nitric and Nitrous Acids and Particulate Nitrite and Nitrate. *Environ. Sci. Technol. V29*, 1534-1541.

Slanina J., Schoonebeek C., Klockow D. and Niessner R. (1985) Determination of sulfuric acid and ammonium sulfates by means of a computer-controlled thermodenuder system. *Analyt. Chem. V57*, 1955-1960.

Slanina J., de Wild P.J. and Wyers G.P. (1992) The application of denuder systems to the analysis of atmospheric components. *In: Gaseous Pollutants: Characterization and Cycling* (ed. Nriagu J.O.), John Wiley & Sons, Inc, New York, pp. 129-154.

Slanina J., G.P. Wyers, W.M. Kieskamp and H.M. ten Brink (1994) Analytical chemistry in the troposphere. *In: Physico Chemical Behaviour of Atmospheric Pollutants, proceedings of the 6th European Symposium* (Eds. Angeletti and Restelli) EUR 15609, 639-651.

Slanina, J. and G.P. Wyers (1994) Monitoring of atmospheric components by automatic denuder systems. *Fresenius J. Anal. Chem. V350*, 467-473.

Slinn W.G.N. (1982) Predictions for particle deposition to vegetative canopies. *Atmos. Environ. V16*, 1785-1794.

Stelson A.W. and Seinfeld J.H. (1982) Relative humidity and temperature dependence of the ammonium nitrate dissociation constant. *Atmos.Environ. V16*, 983-992.

Svenningsson B., Hanson H.-C., Wiedensohler A., Noone K., Ogren J., Hallberg A. and Colvile R. (1994) Hygroscopic growth of aerosol particles and its influence on nucleation scavenging in cloud: Experimental results from Kleiner Feldberg. *J.Atmos.Chem. V19*, 129-151.

Tang I.N. (1976) Phase transformation and growth of aerosol particles composed of mixed salts. *J.Aerosol Sci. V7*, 361-371.

Tang I.N. (1980) Deliquescence properties and particle size change of hygroscopic aerosols. *In: Generation of aerosols* (Ed. K.Willeke) Ann Arbor Sci. Publishers, Ann Arbor, MI, pp.153-167.

Tang I.N. and Munkelwitz H.R. (1994) Water activities, densities, and refractive indices of aqueous sulfates and sodium nitrate droplets of atmospheric importance. *J. Geophys. Res. V99*, 18801-18808.

Taylor J.P. and McHaffie A. (1994) Measurements of cloud susceptibility. *J.Atmos.Sci. V51*, 1298-1306.

Taylor K.E. and Penner J.E. (1994) Response of the climate system to atmospheric aerosols and greenhouse gases. *Nature V369*, 734-737.

ten Brink, H.M., Mallant, R.K.A.M. and de Vate, J.F. (1981) SO_2 conversion in a marine atmosphere. Part 2. In *Physico-Chemical Behaviour of Atmospheric Pollutants* (eds. B. Versino and H. Ott), Reidel, Dordrecht, p. 319.

ten Brink H.M., Schwartz S.E. and Daum P.H. (1987) Efficient scavenging of aerosol sulfate by liquid-water clouds. *Atmos.Environ. V21*, 2035-2052.

ten Brink H.M., Veefkind J.P., Waijers-IJpelaan A. and van der Hage J.C. (1996a) Aerosol light-scattering in the Netherlands. *Atmos.Environ. V30*, 4251-4261.

ten Brink H.M., Kruisz C., Kos G.P.A. and Berner A. (1996b) Composition/size of the light-scattering aerosol in the Netherlands. *Atmos.Environ., in print.*

ten Brink H.M., Khlystov A., Kruisz C. and Berner A. (1996c) Aerosol size and composition in the Netherlands. *In: Proceedings of Eurotrac Symposium '96,* (eds. P.M.Borrel, P.Borrel, T.Cvitas, K.Kelly and W.Seiler) Computational Mechanics Publications, Southampton.

Trijonis J.C., Malen W.C., Pitchford M. and White W.H. (1990) Visibility: Existing and Historical Conditions - Causes and Effects. *In: NAPAP Report 24.* National Acid Precipitation Assessment Program, 722 Jacson Place, NW, Washington, D.C. 20503.

Twomey S. (1977a) *Atmospheric aerosols*. Elsevier, New York.

Twomey S. (1977b) The influence of pollution on the short-wave albedo of clouds. *J.Atmos.Sci. V34*, 1149-1152.

Twomey S. (1991) Aerosol, clouds and radiation. *Atmos.Environ. V25A*, 2435-2442.

van de Vate J.F., ten Brink H.M. and Mallant R.K.A.M. (1982) *Eindverslag van het deelproject btreffende de verrijking van zeezout-aerosol met spoorbestanddelen in zeewater*. ECN-82-167, ECN, Petten, the Netherlands (in Dutch).

van de Vate J.F., Mallant R.K.A.M., Kos G.P.A., ten Brink H.M., Plomp A. and Vermetten A. (1984) Marine aerosols at the Dutch North Sea coast: Size distributions and fractionantion of trace elements. *Paper presented at the 11th International Conference on Atmospheric Aerosols, Condensation and Ice Nuclei, Budapest, Hangary, 3-7 September 1984*. ECN-84-050, ECN, Petten, the Netherlands.

van der Meulen A. (1986) The Dutch aerosol study: physical aspects. *In: Aerosols* (eds: S. D. Lee et al.) Lewis Publ., Chelsea MI, USA, 283-300.

van Dingenen R., Raes F. and Jensen N.R. (1995) Evidence for anthropogenic impact on number concentration and sulfate content of cloud-processed aerosol particles over the North Atlantic. *J.Geophys.Res. V100*, 21057-21067.

Veefkind J.P., van der Hage J.C.H. and ten Brink H.M. (1996) Nephelometer derived and directly measured aerosol optical depth of the atmospheric boundary layer. *Atmos. Research V41*, 217-228.

Velds C.A. (1992) *Zonnestraling in Nederland* (Solar radiation in the Netherlands). KNMI publication, ISBN 90-5210-140-X (in Dutch with English summary).

Waggoner A.P., Weiss R.E., Ahlquist N.C., Covert D.S., Will S. and Charlson R.J. (1981) Optical characteristics of atmospheric aerosols. *Atmos. Environ. V15*, 1891-1909.

Wall S.M., John W. and Ondo J.L. (1987) Measurements of aerosol size distributions for nitrate and major ionic species. *Atmos.Environ. V22*, 1649-1656.

Wang H.-C. and John W. (1988) Characteristics of the Berner Impactor for sampling inorganic ions. *Aerosol Sci. Technol. V8*, 157-172.

Weingartner E., Burtscher H. and Baltensperger U. (1997) Hygroscopic properties of carbon and diesel soot particles. *Atmos.Environ. V31*, 2311-2327.

Wexler A.S. and Seinfeld J.H. (1991) Second generation inorganic aerosol model. *Atmos. Environ. V25A*, 2731-2748.

White W. (1990) The contribution of fine particle scattering to total extinction. *In: Visibility: Existing and Historical Conditions - Causes and Effects. Acidic Deposition State of Science and Technology Report 24, National Acid Precipitation Assessment Program*, Washington, DC, pp.85-102.

Wigley T.M.L. (1989) Possible climate change due to SO_2 derived cloud condensation nuclei. *Nature V339*, 365.

Williams, A.L., Alofs, D.J., Hagen, D.E., Caughey, M.E. and Schmitt, J.L. (1994) Measurements of the chemical composition of cloud condensation nuclei. *Atmos.Chem. V1*, 27-32.

Winkler P. (1973) The growth of atmospheric aerosol particles as a function of the relative humidity. II. An improved concept of mixed nuclei. *Aerosol Sci. V4*, 373-387.

Wolff G.T. (1984) On the nature of nitrate in coarse continental aerosols. *Atmos.Environ. V18*, 977-981.

Wyers G.P., Otjes R.P. and Slanina J. (1993) A continuous-flow denuder system for the measurement of ambient concentrations and surface-exchange fluxes of ammonia. *Atmos. Environ. V27*, 2085-2090.

Young K.C. and Warren A.J. (1992) Reexamination of the derivation of the equilibrium supersaturation curve for soluble particles. *J.Atmos.Sci. V49*, 1138-1143.

Appendix 1

Impactor data

Mass and composition of ambient aerosols were measured with 6- or 8- stage Berner cascade impactors [*Berner et al.*, 1979; *Berner*, 1989]. The measurements were carried out near Petten, the Netherlands. The site is situated a rural agricultural area, approximately 200 m from the Dutch northwest coast of the North Sea. The aerodynamic cutoff diameters of the 6-stage impactor range from 0.15 to 6.8 μm, increasing by a factor of 2.15. The cutoff diameters of the 8-stage impactor range from 0.06 to 8 μm, increasing by a factor of 2. The performance of the Berner impactors has been extensively tested by *Wang and John* [1988]. The collection surfaces of the impactors were thin aluminum foils which allowed mass determination with a micro-balance as well as subsequent chemical analysis. The accuracy of the weighing is 4 μg per stage. Chemical analysis was performed with IC and AAS/AES for the ionic constituents, after leaching of the samples in double-demineralized water. The limit of detection was around 0.02 mg per kilogram of solution. The accuracy of the analysis is about 5%.

For indication of the origine of the air mass during the measurements, 96-hour back-trajectories are given which were provided by the Norwegian Meteorological Institute (DNMI). The back-trajectories are calculated for 925 mbar level at the Cabauw arrival point, which is situated about 150 km to the southeast of Petten. Unfortunately, there are no trajectory data available for measurements performed in 1992. However, for these days weather maps are available, which are given in Appendix 3.

Table A1.1 gives the parameters of lognormal distributions fitted to the measured sulfate and nitrate size distributions.

Table A2.1. Parameters of lognormal fits into impactor data.

		NO3 mode 1				NO3 mode 2				SO4 mode 1				SO4 mode 2			
Date	WD	M	MMD	σ	χ^2	M	MMD	σ	χ^2	M	MMD	σ	χ^2	M	MMD	σ	χ^2
29-06-92	SE	2.76	0.69	1.76	1E-01					8.97	0.49	1.79	2E-02				
30-06-92	SE	3.11	0.73	1.81	2E-01					6.08	0.51	1.96	4E-02				
1-07-92	SW	1.09	2.69	2.52	4E-02					7.20	0.67	1.91	1E-02				
2-07-92	NE	0.70	2.26	1.76						0.74	0.20	1.72	6E-03	0.71	2.59	2.36	
3-07-92	E	2.58	1.24	3.10						1.96	0.41	3.10	2E-03				
6-07-92	NE	0.73	2.85	1.83	0.06					1.69	0.34	3.67	6E-02				
9-06-93	NE	3.18	0.64	1.29	9E-03	2.08	3.53	2.05	9E-03	14.50	0.52	1.65	2E-02	2.78	4.84	1.51	2E-02
10-06-93	E	18.55	0.69	1.33	1E-01					25.20	0.61	1.49	5E-02				
26-06-93	NE	0.15	0.92	1.37	3E-01					9.00	0.63	1.87	1E-03				
5-07-93	N	0.28	1.98	2.50	0.11					0.16	1.28	2.89	2E-02				
6-07-93	NW	0.20	0.28	1.21	0.00	3.81	13.29	2.82		5.06	0.47	1.82	4E-02				
7-07-93	NW	0.21	0.41	6.00	0.02	1.01	1.31	1.65		0.43	0.39	1.76	6E-03	0.44	2.37	1.74	
8-07-93	SW	0.15	0.29	1.19	0.02	1.55	3.78	2.20		1.25	0.40	1.50	5E-11	0.37	3.52	2.85	
20-07-93	N	0.47	2.87	2.11	1E-01					1.05	0.33	2.07	2E-02	0.64	5.01	2.83	
17-08-93	E	1.13	0.42	1.43	1E-01	1.53	2.76	1.62		0.92	0.43	1.38	4E-02	0.36	2.96	2.81	
18-08-93	variable	4.76	0.70	1.95	3E-01					1.53	0.66	1.81	1E-01				
3-09-93	NNW	0.28	1.49	3.32	3E-02					0.23	0.51	2.68	4E-02	0.25	5.40	1.95	
7-09-93	E	8.51	0.49	1.55	1E-01					2.41	0.43	1.60	1E-01				
19-09-93	E	17.55	0.65	1.49	9E-02					8.58	0.64	1.51	3E-02				
20-09-93	SE	13.19	0.62	1.51	2E-04					5.79	0.62	1.50	3E-03				
19-10-93	E	7.27	0.44	1.38	3E-09					2.70	0.44	1.36	4E-09				
20-10-93	SE	10.56	0.88	1.79	9E-02					6.35	0.85	1.71	2E-02				
23-11-93	SSE	7.69	0.59	1.82	3E-02					7.83	0.67	1.69	6E-03				
12-04-94	N	0.40	0.42	1.48	1E-10	1.55	2.23	2.28	1E-10	6.28	0.51	1.77	3E-02				
13-04-94	N	0.03	0.39	1.72	1E-10	0.29	3.43	1.76	1E-10	2.43	0.81	3.11	2E-02				
14-04-94	N	0.01	0.30	1.18	3E-04	0.14	2.52	2.04	3E-04	0.22	0.35	1.58	7E-10	0.76	1.65	2.70	7E-10
15-04-94	ENE	0.89	0.61	1.92	4E-02					1.94	0.73	1.83	3E-02				
27-05-94	NNW	0.02	0.08	2.35	3E-02	0.23	2.84	1.72	3E-02	0.09	0.25	1.83	3E-02	0.25	3.51	2.23	3E-02
30-05-94	NW	0.37	0.01	4.71	2E-02	0.42	2.53	1.77	2E-02	0.34	0.20	1.51	1E-02	0.22	3.58	2.23	1E-02
13-06-94	NNW	0.04	0.17	3.37	2E-02	0.05	4.78	1.48	2E-02	0.61	0.20	1.69	7E-03				
15-06-94	WSW	0.17	0.13	3.29	6E-02	1.49	2.86	1.63	6E-02	0.70	0.22	1.51	1E-02	1.24	8.34	6.00	1E-03
12-07-94	E	3.15	4.03	1.49	5E-02					12.48	0.35	1.90	1E-01				

WD - wind direction; M - total mass; MMD - mass median diameter.

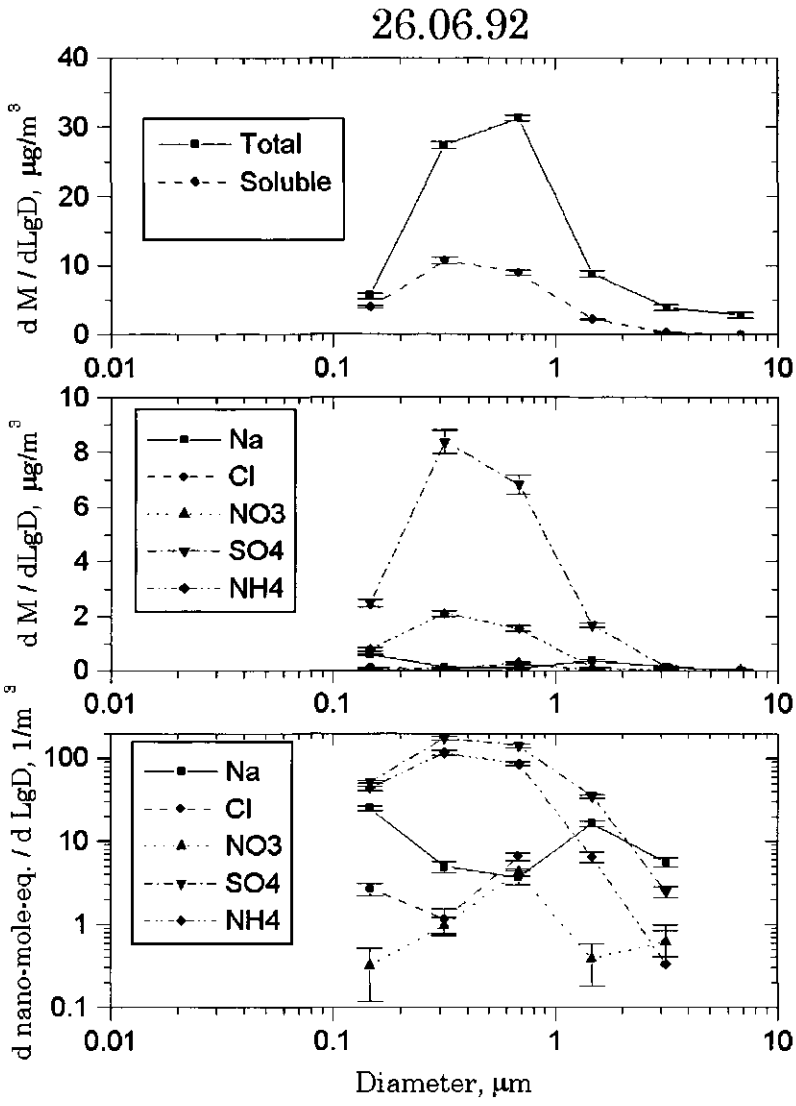
26.06.92
d M / dLgD, µg/m3
Total
Soluble
d M / dLgD, µg/m3
Na
Cl
NO3
SO4
NH4
d nano-mole-eq. / d LgD, 1/m3
Na
Cl
NO3
SO4
NH4
Diameter, µm

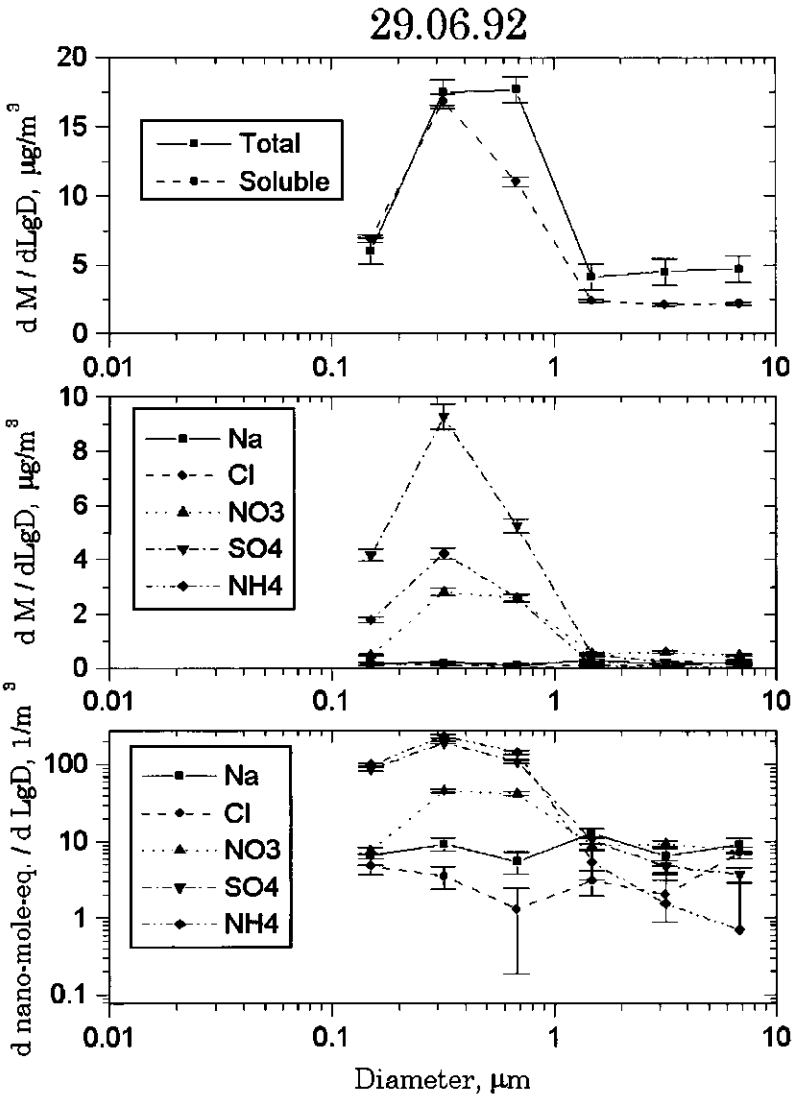
29.06.92
d M / dLgD, µg/m3
Total
Soluble
Na
Cl
NO3
SO4
NH4
d nano-mole-eq. / d LgD, 1/m3
Diameter, µm

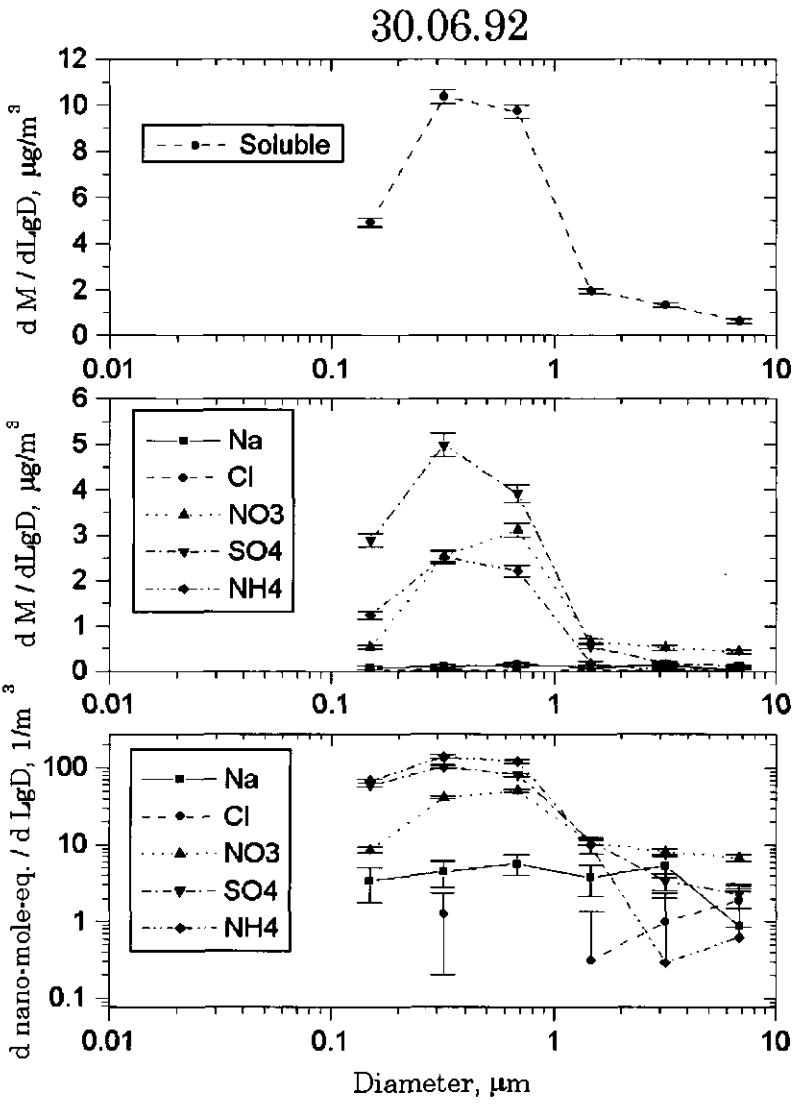
30.06.92
Soluble
d M / dLgD, µg/m³
Na
Cl
NO3
SO4
NH4
d nano-mole-eq. / d LgD, 1/m³
Diameter, µm

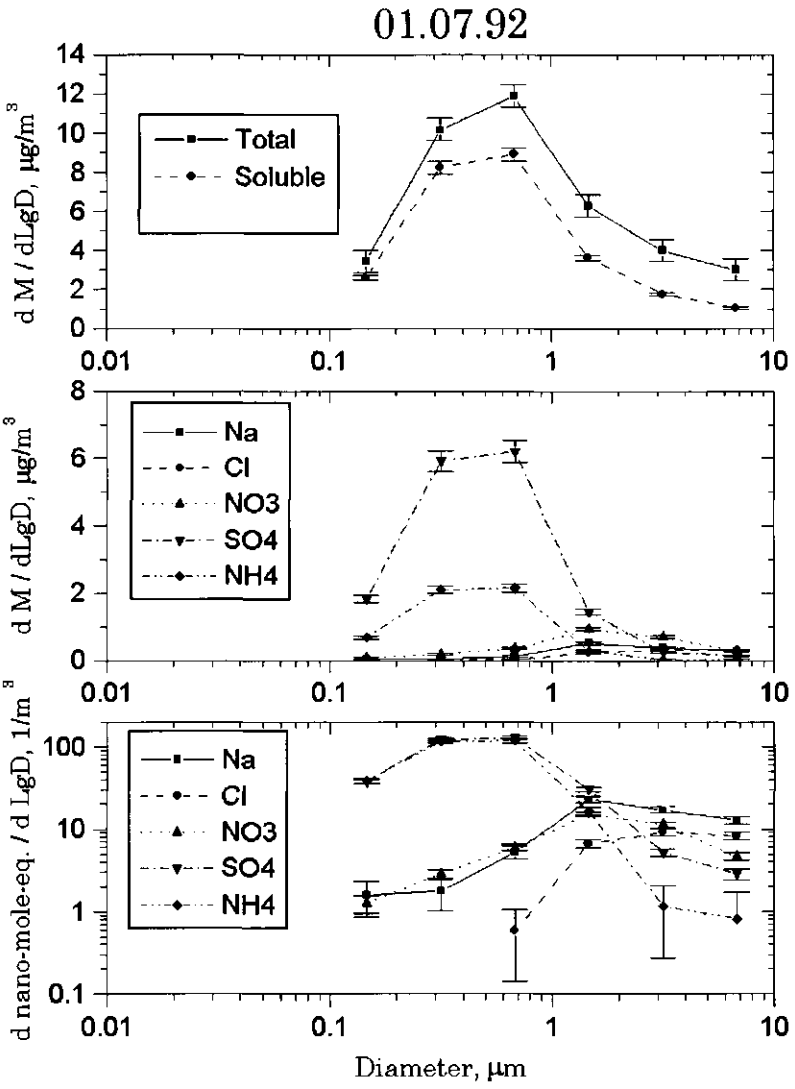
01.07.92
d M / dLgD, µg/m3
Total
Soluble
d M / dLgD, µg/m3
Na
Cl
NO3
SO4
NH4
d nano-mole-eq. / d LgD, 1/m3
Na
Cl
NO3
SO4
NH4
Diameter, µm

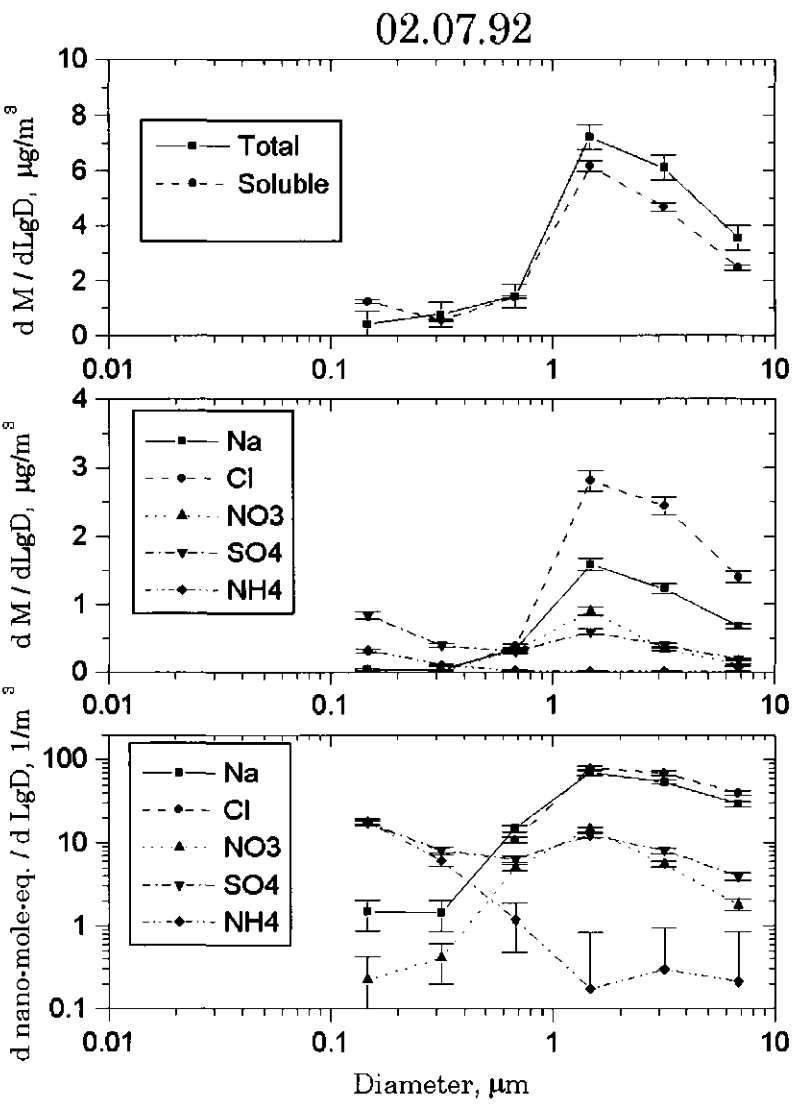
02.07.92
d M / dLgD, µg/m3
Total
Soluble
Na
Cl
NO3
SO4
NH4
d nano-mole-eq. / d LgD, 1/m3
Diameter, µm

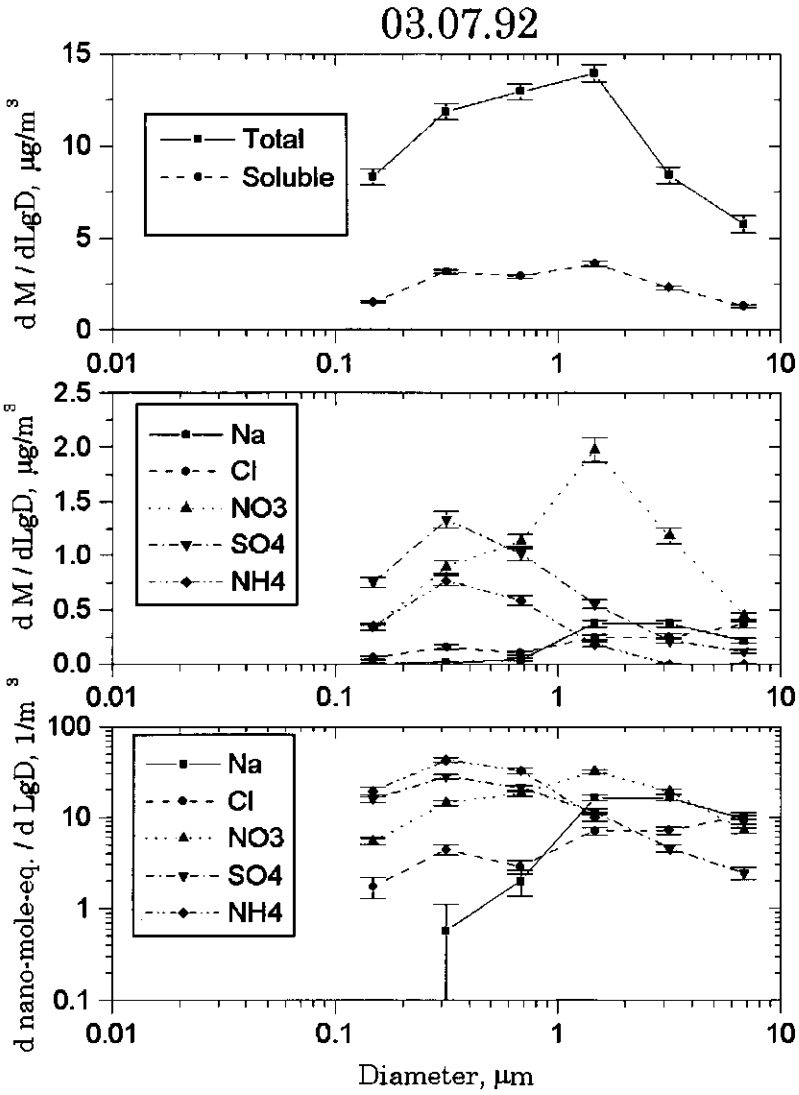
03.07.92
d M / dLgD, µg/m3
Total
Soluble
d M / dLgD, µg/m3
Na
Cl
NO3
SO4
NH4
d nano-mole-eq. / d LgD, 1/m3
Na
Cl
NO3
SO4
NH4
Diameter, µm

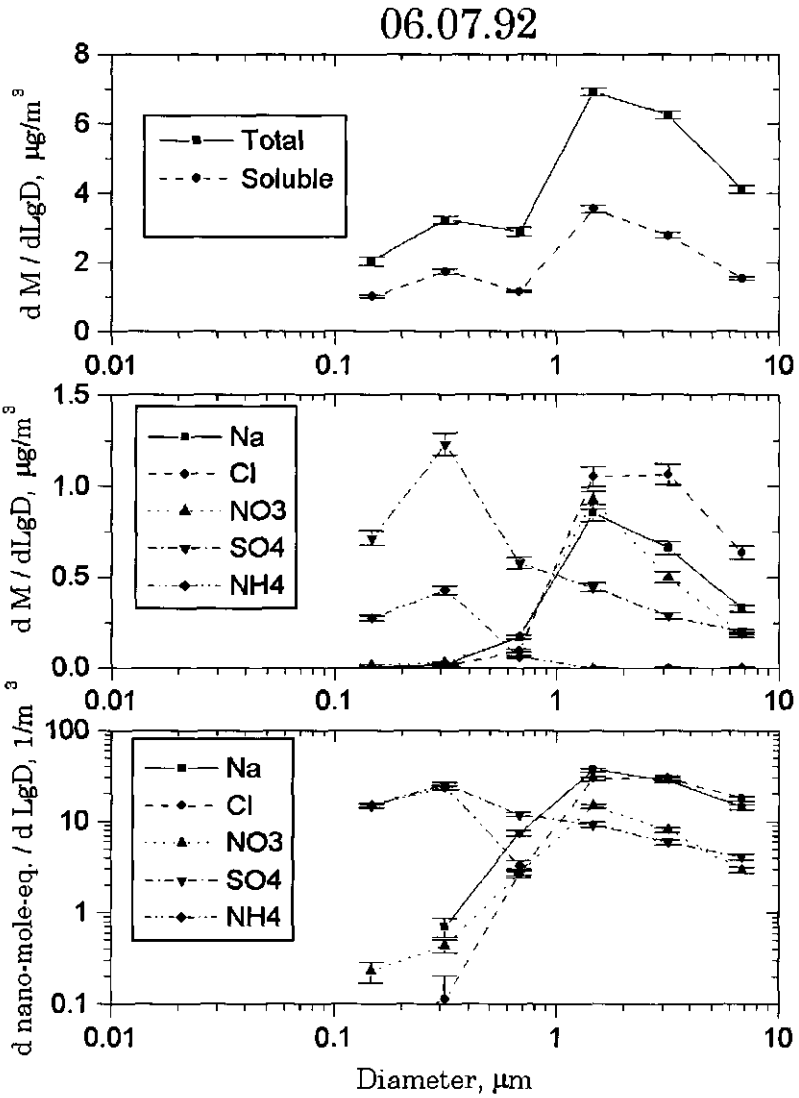
06.07.92
d M / dLgD, µg/m³
Total
Soluble
d M / dLgD, µg/m³
Na
Cl
NO3
SO4
NH4
d nano-mole-eq. / d LgD, 1/m³
Na
Cl
NO3
SO4
NH4
Diameter, µm

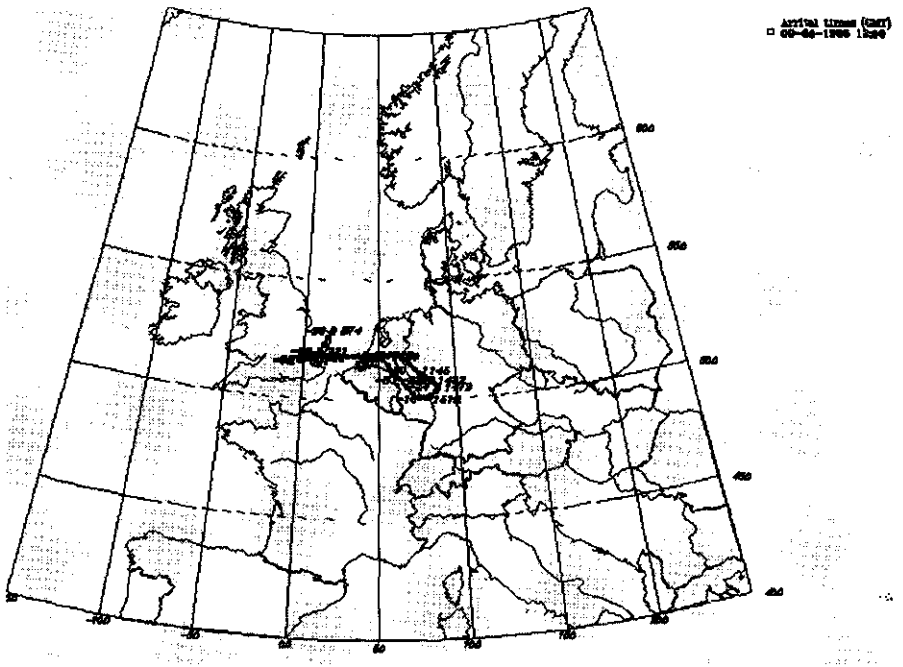

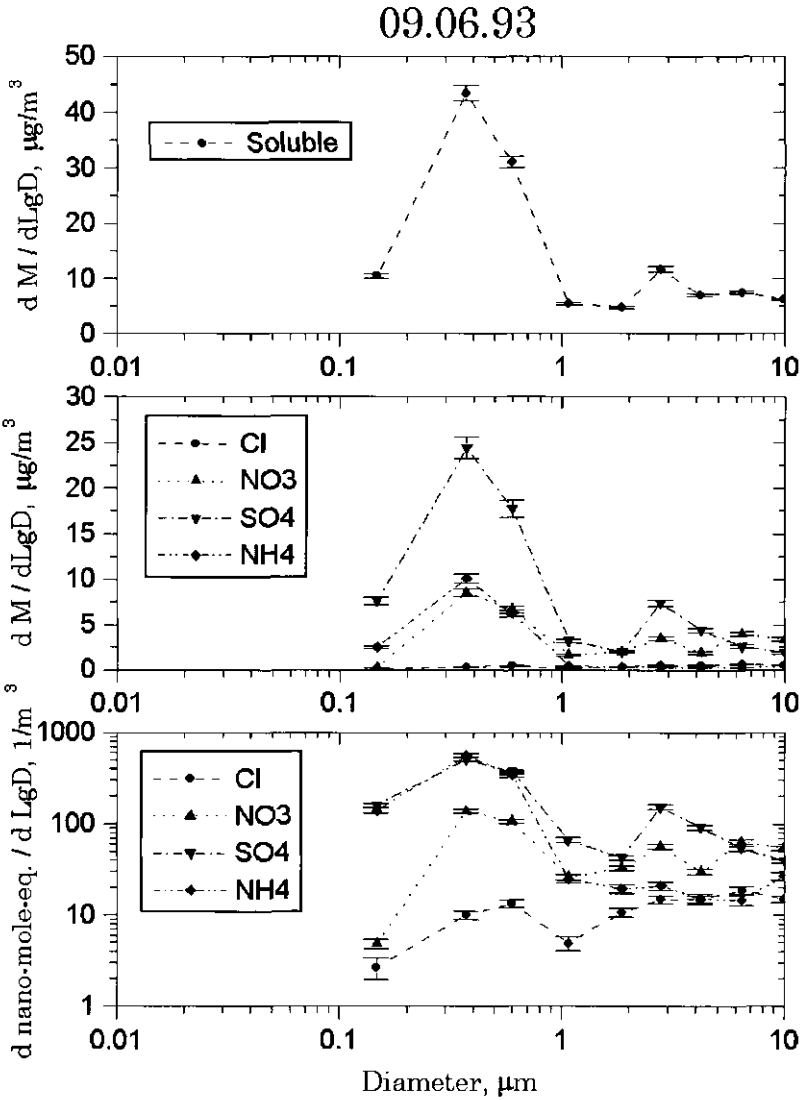
09.06.93
d M / dLgD, µg/m3
Soluble
Cl
NO3
SO4
NH4
d nano-mole-eq. / d LgD, 1/m3
Diameter, µm

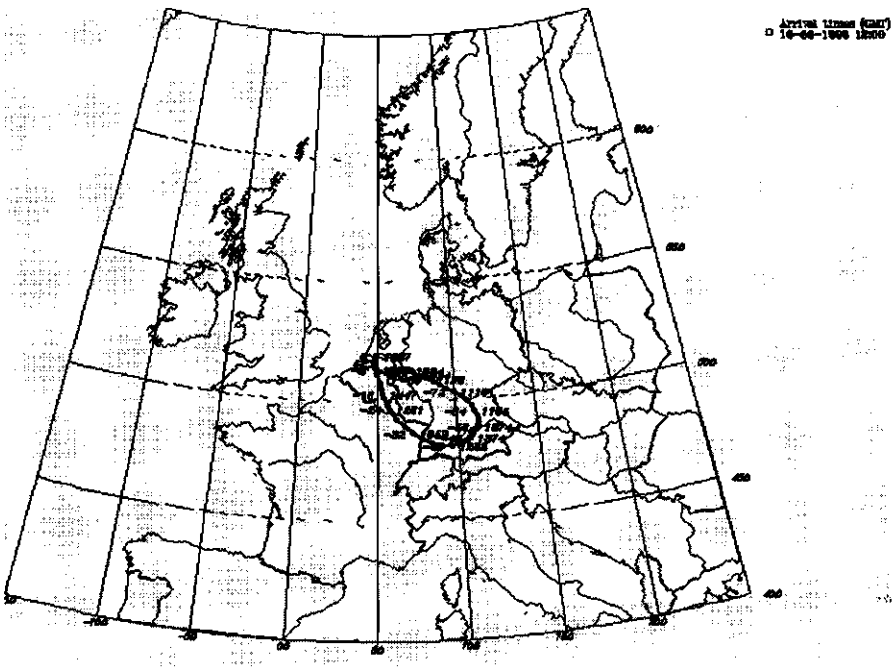
Arrival times (GMT)
16-06-1998 1800

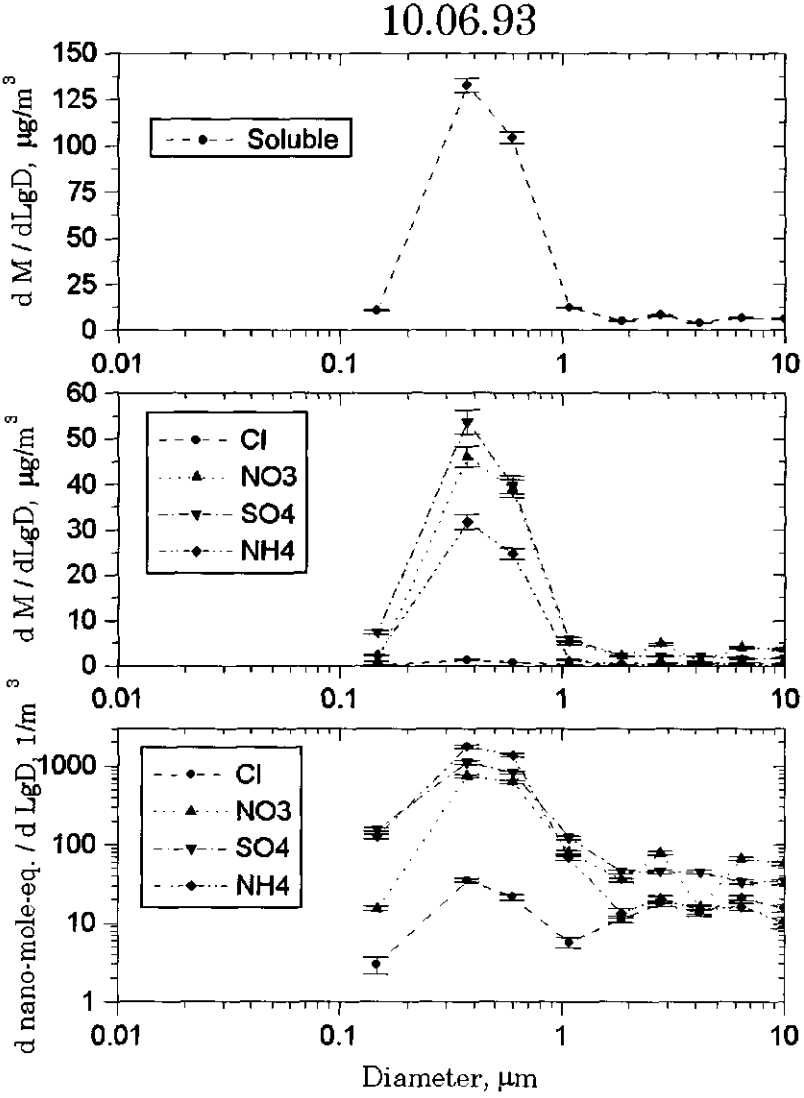
10.06.93
d M / dLgD, µg/m3
Soluble
Cl
NO3
SO4
NH4
d nano-mole-eq. / d LgD, 1/m3
Diameter, µm

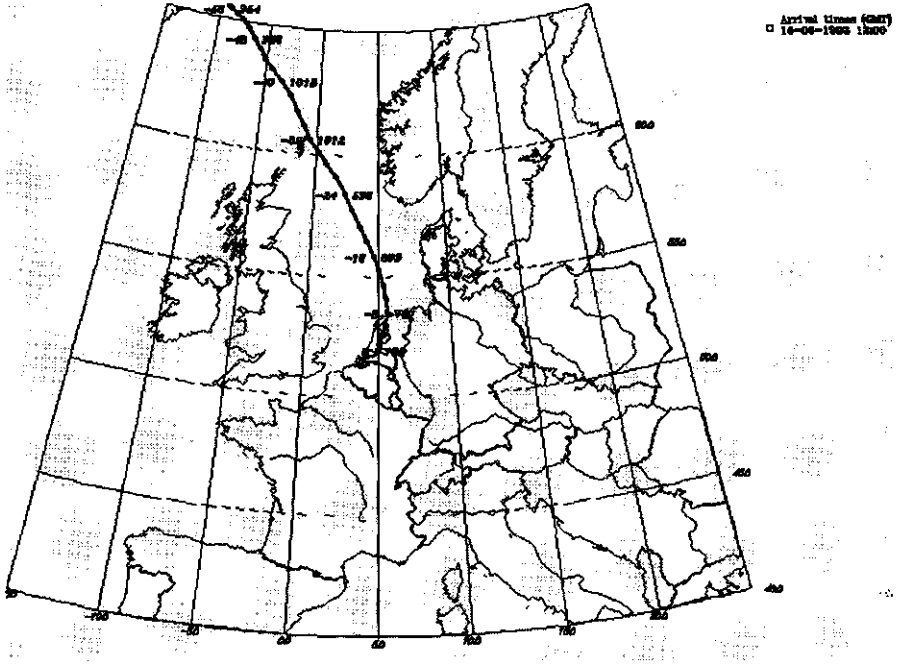

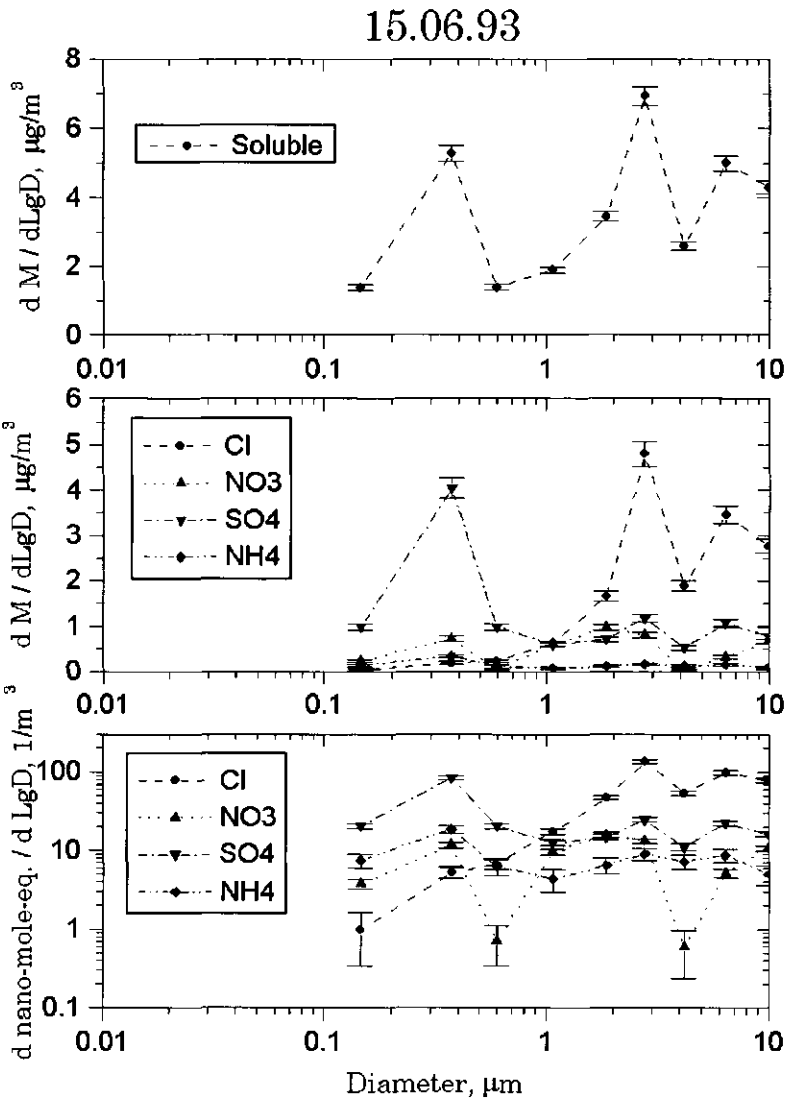
15.06.93
Soluble
d M / dLgD, µg/m³
Cl
NO3
SO4
NH4
d M / dLgD, µg/m³
Cl
NO3
SO4
NH4
d nano-mole-eq. / d LgD, 1/m³
Diameter, µm

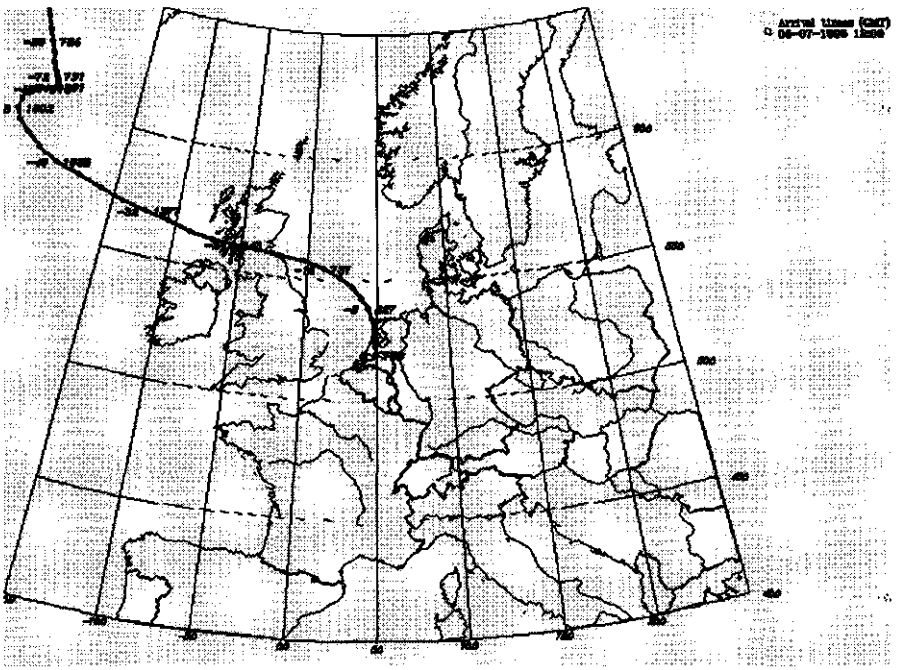

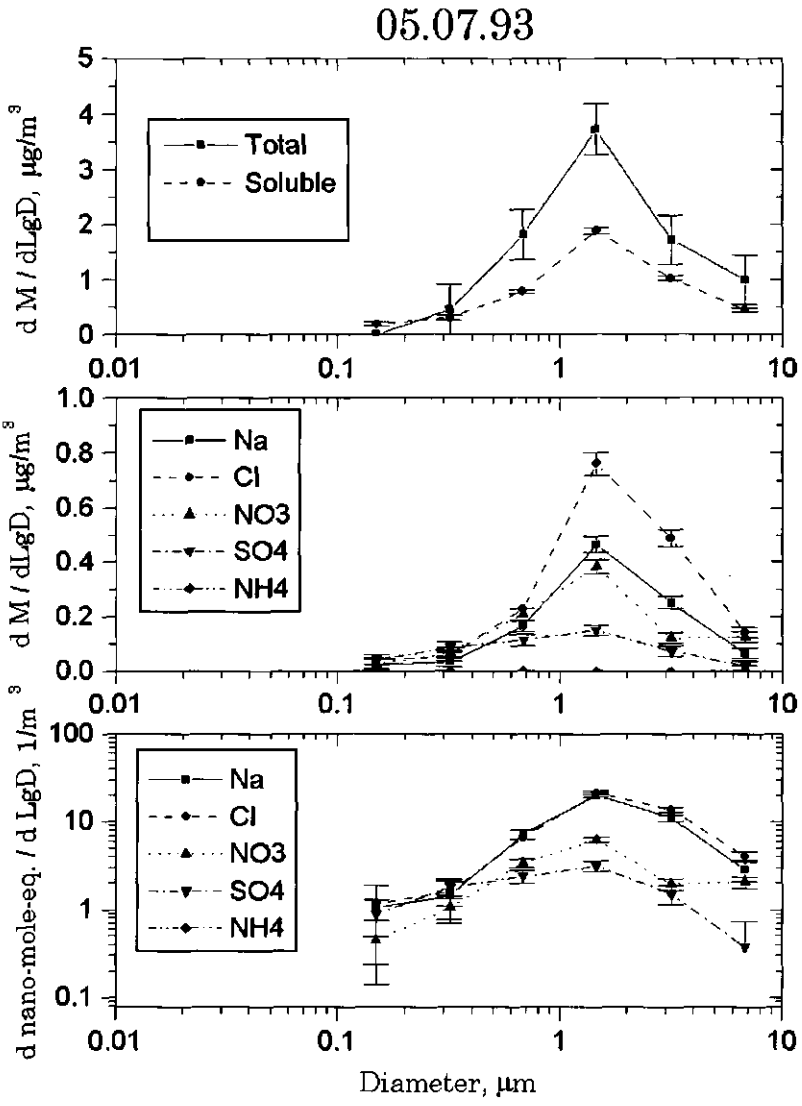
05.07.93
d M / dLgD, µg/m³
Total
Soluble
d M / dLgD, µg/m³
Na
Cl
NO3
SO4
NH4
d nano-mole-eq. / d LgD, 1/m³
Na
Cl
NO3
SO4
NH4
Diameter, µm

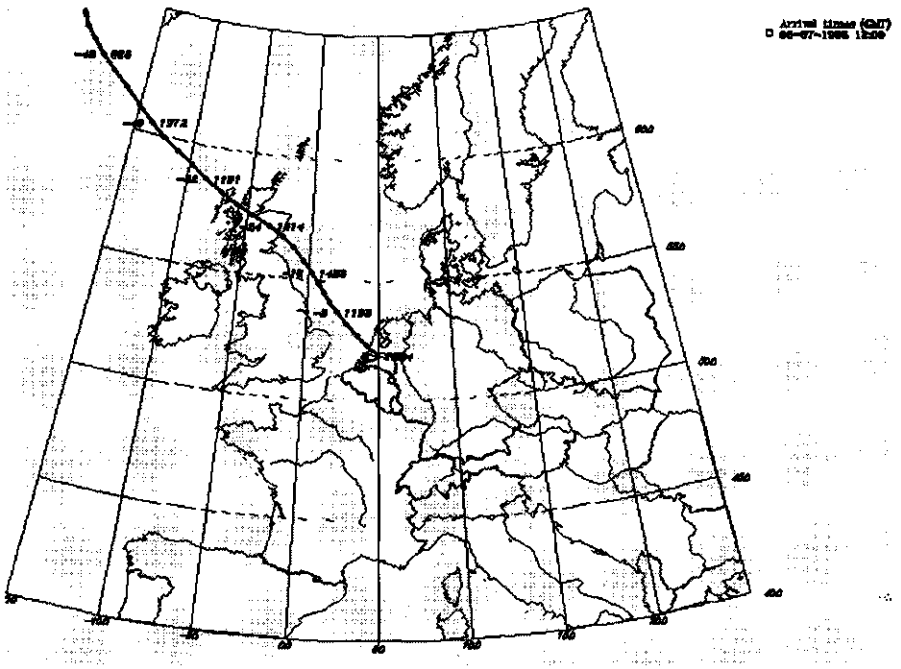

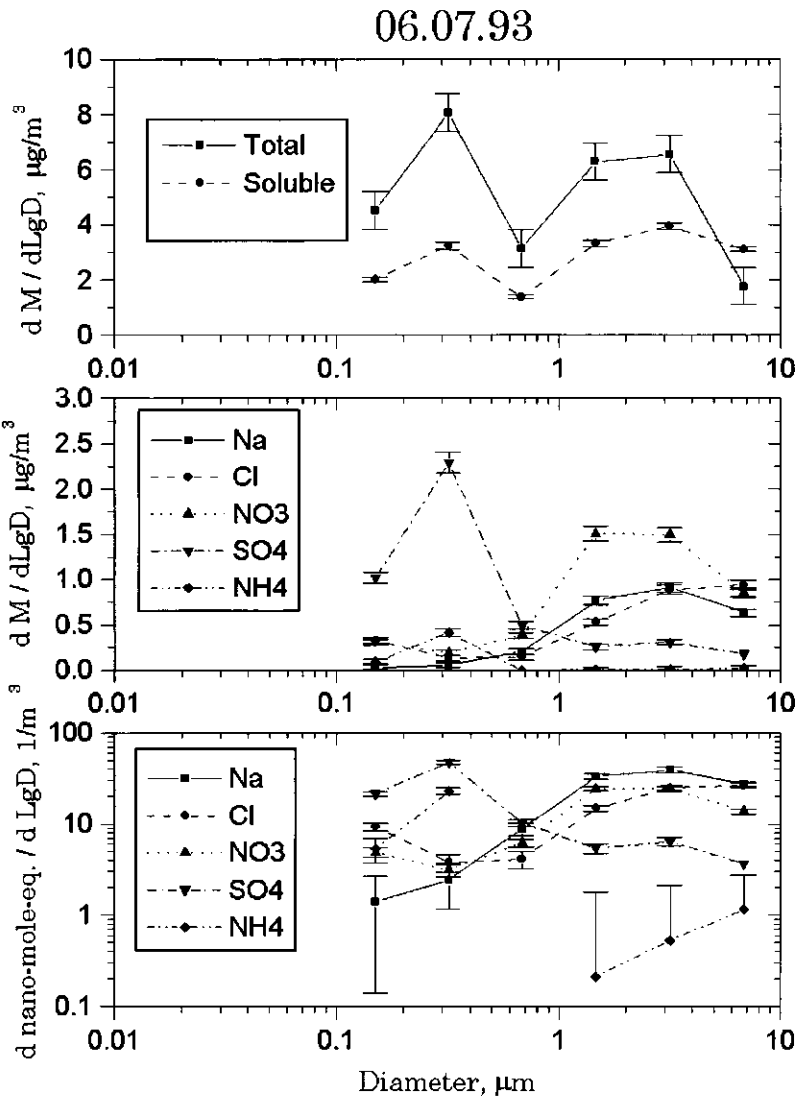
06.07.93
Total
Soluble
d M / dLgD, µg/m3
Na
Cl
NO3
SO4
NH4
d nano-mole-eq. / d LgD, 1/m3
Diameter, µm

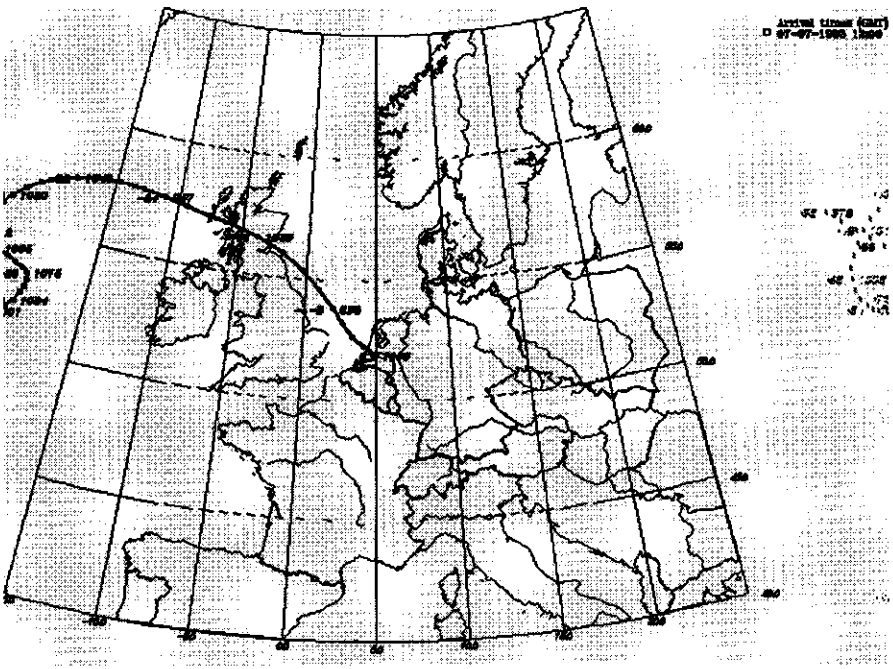

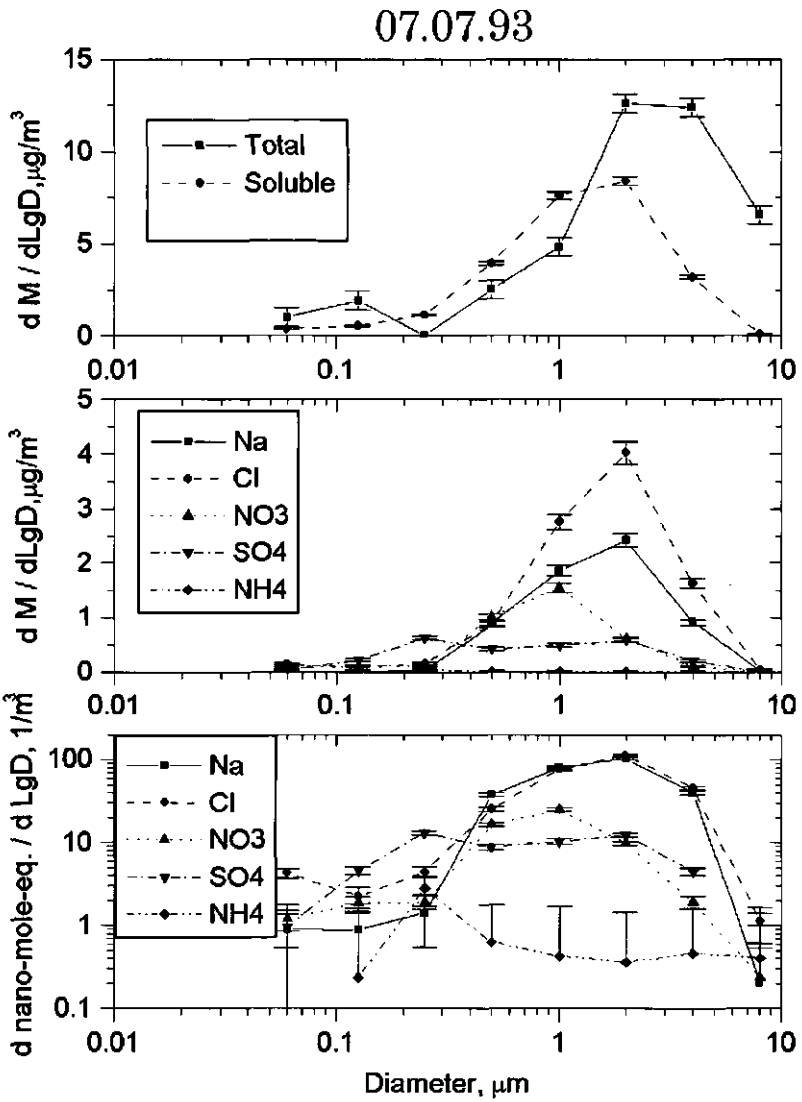
07.07.93
d M / dLgD,µg/m3
Total
Soluble
d M / dLgD,µg/m3
Na
Cl
NO3
SO4
NH4
d nano-mole-eq. / d LgD, 1/m3
Na
Cl
NO3
SO4
NH4
Diameter, µm

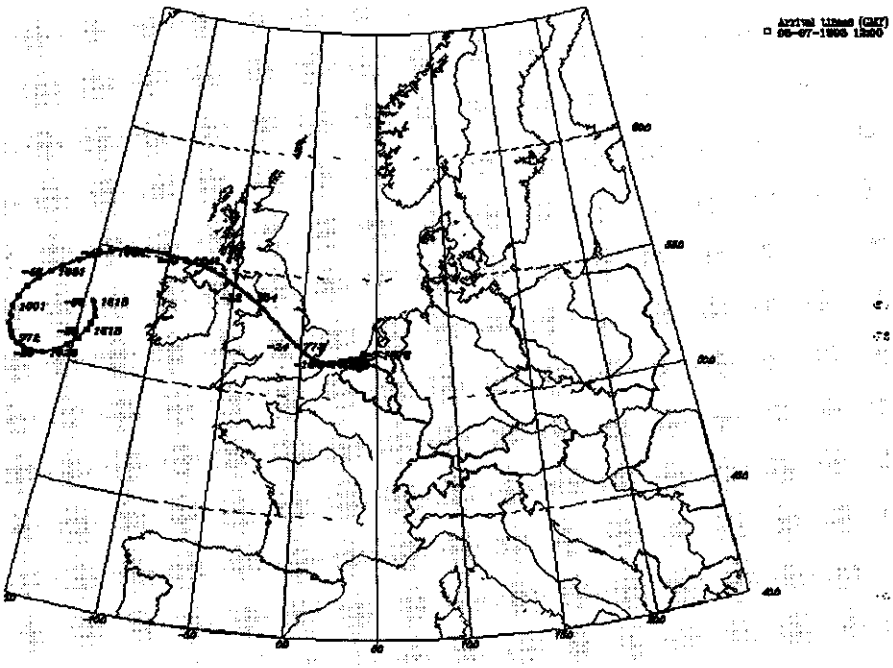

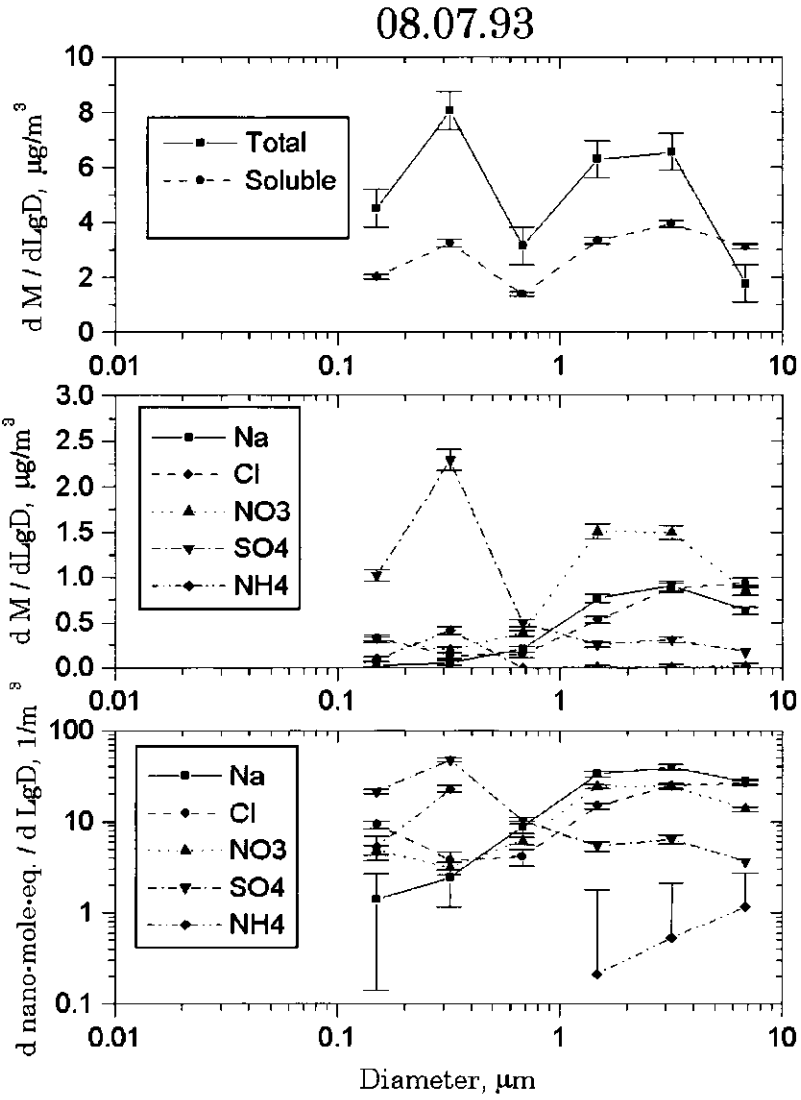
08.07.93
d M / dLgD, µg/m³
Total
Soluble
d M / dLgD, µg/m³
Na
Cl
NO3
SO4
NH4
d nano-mole-eq. / d LgD, 1/m³
Na
Cl
NO3
SO4
NH4
Diameter, µm

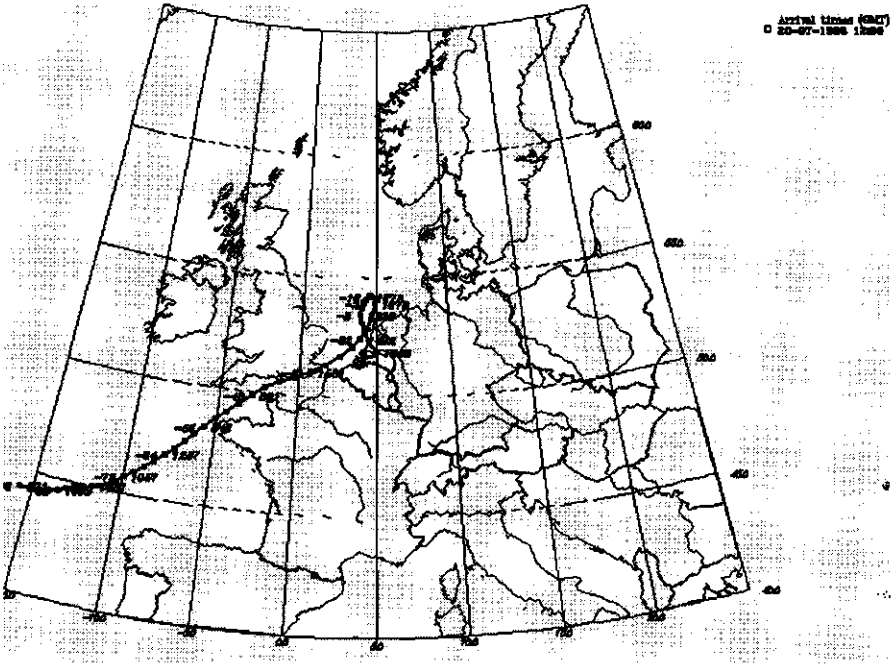

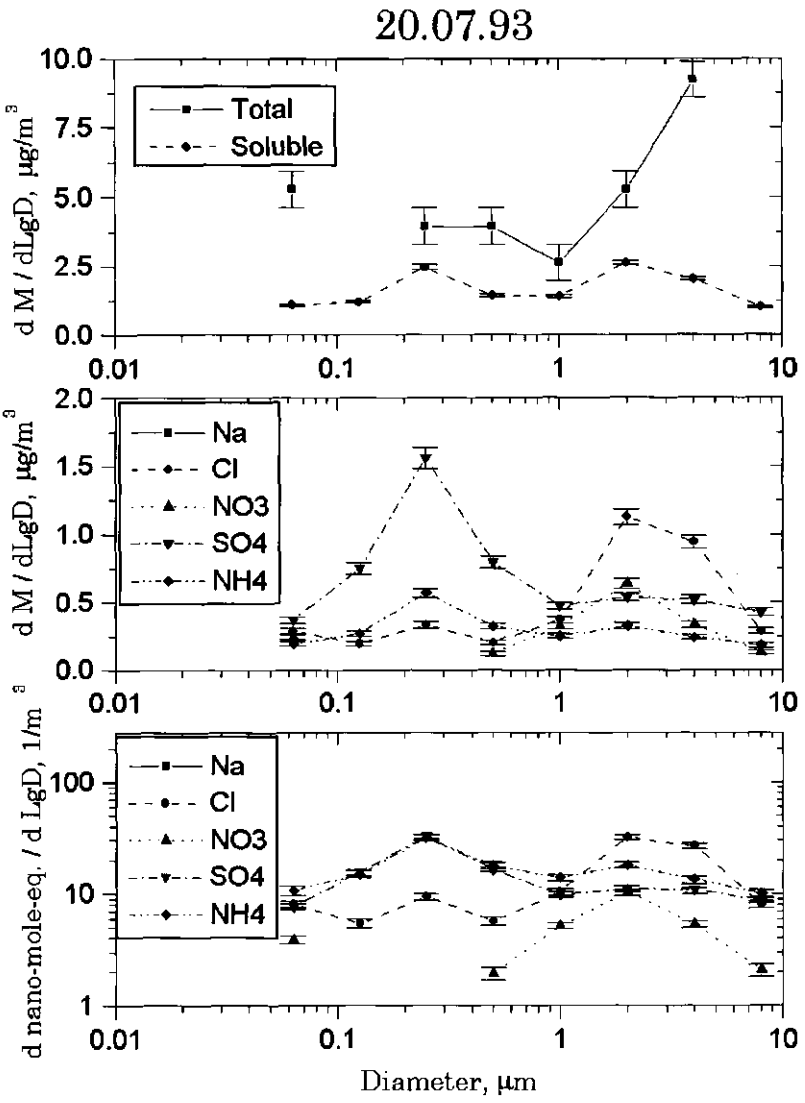
20.07.93
Total
Soluble
d M / dLgD, µg/m3
Na
Cl
NO3
SO4
NH4
d nano-mole-eq. / d LgD, 1/m3
Diameter, µm

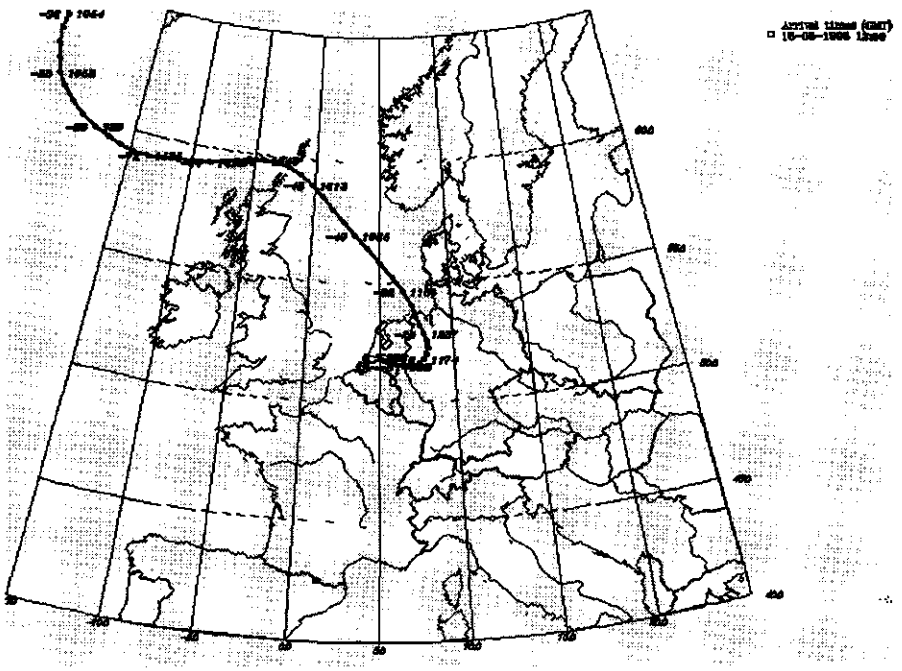

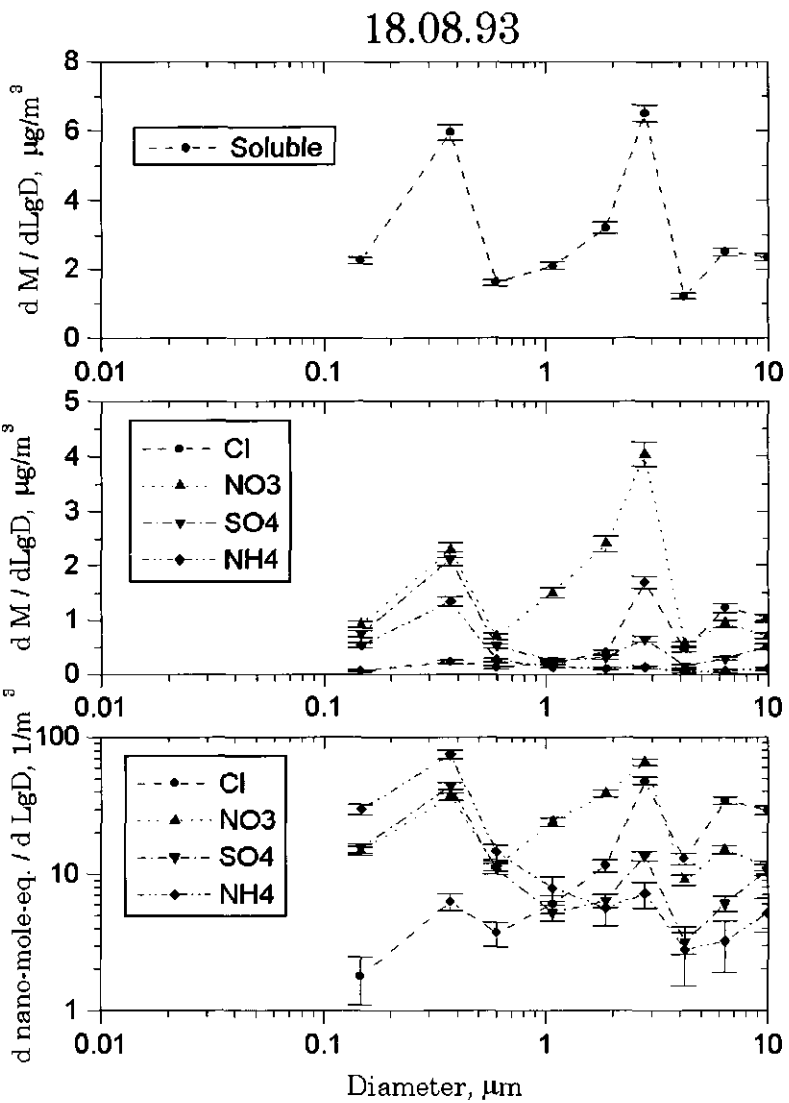
18.08.93
d M / dLgD, µg/m3
Soluble
Cl
NO3
SO4
NH4
d nano-mole-eq. / d LgD, 1/m3
Diameter, µm

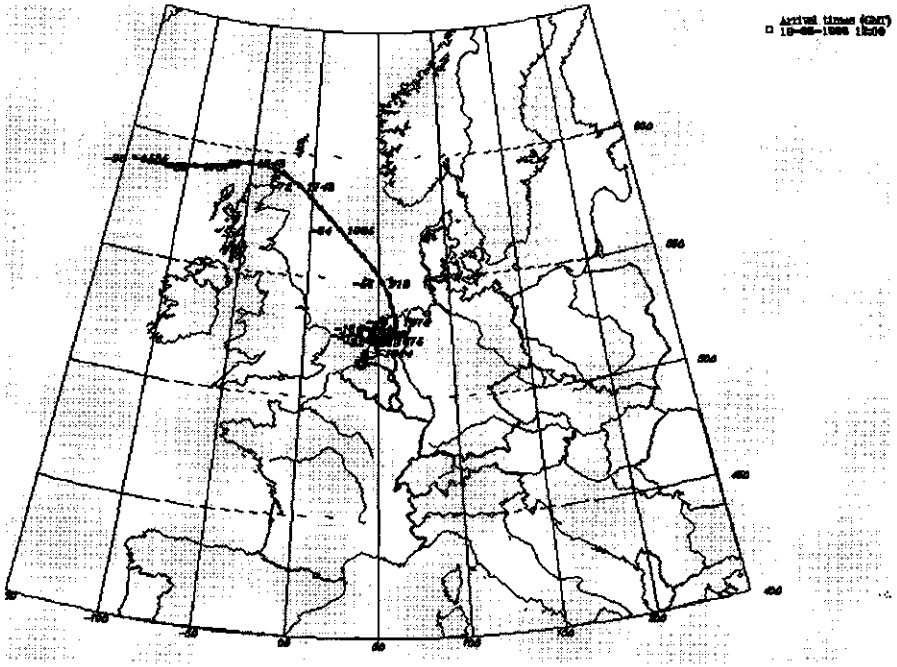

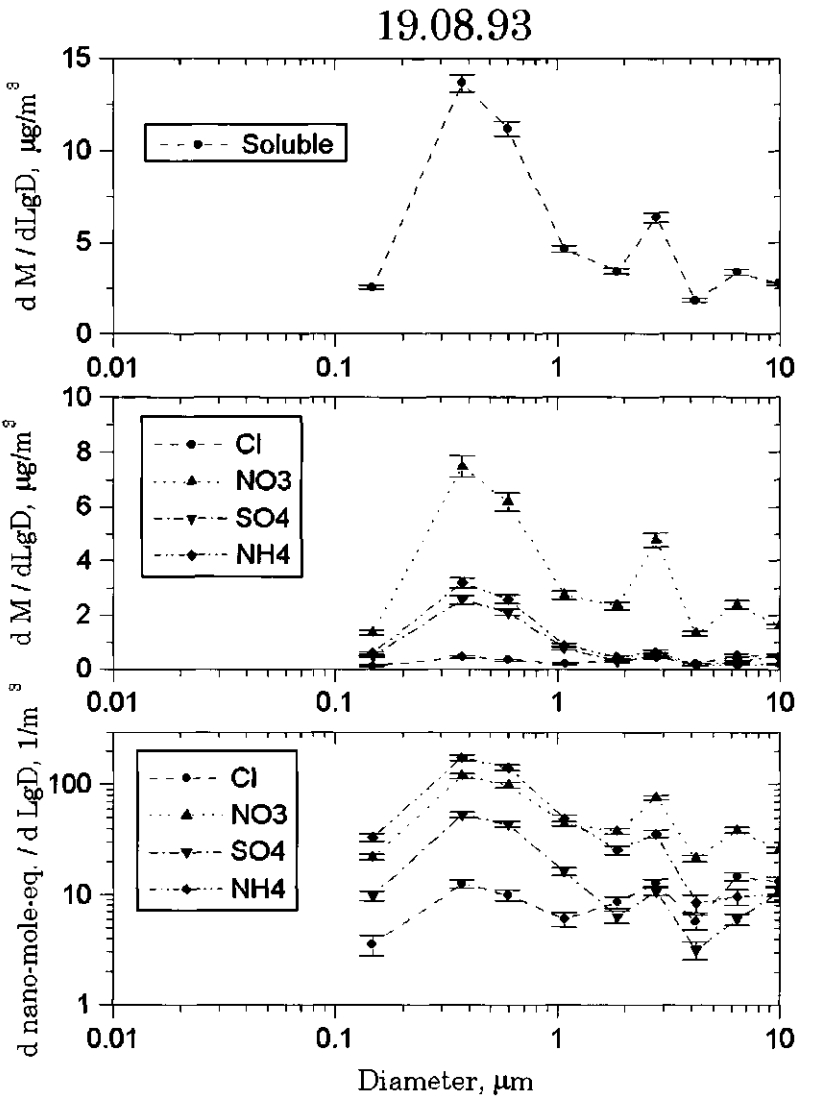
19.08.93
Soluble
Cl
NO3
SO4
NH4
d M / dLgD, µg/m3
d nano-mole-eq. / d LgD, 1/m3
Diameter, µm

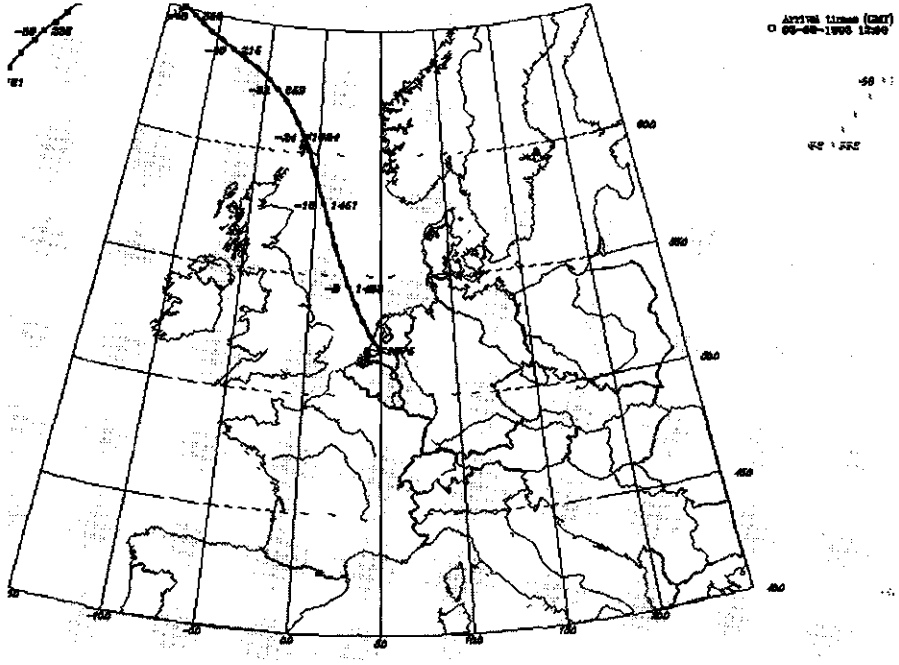

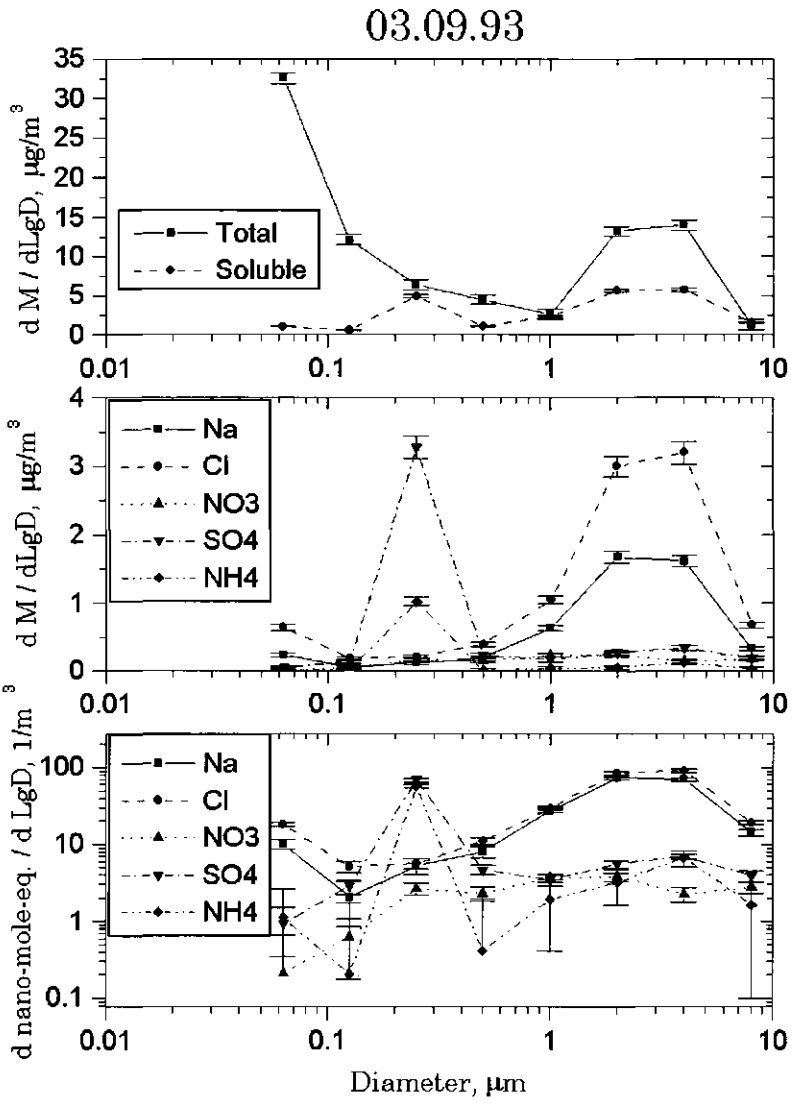
03.09.93
d M / dLgD, µg/m3
Total
Soluble
d M / dLgD, µg/m3
Na
Cl
NO3
SO4
NH4
d nano-mole-eq. / d LgD, 1/m3
Na
Cl
NO3
SO4
NH4
Diameter, µm

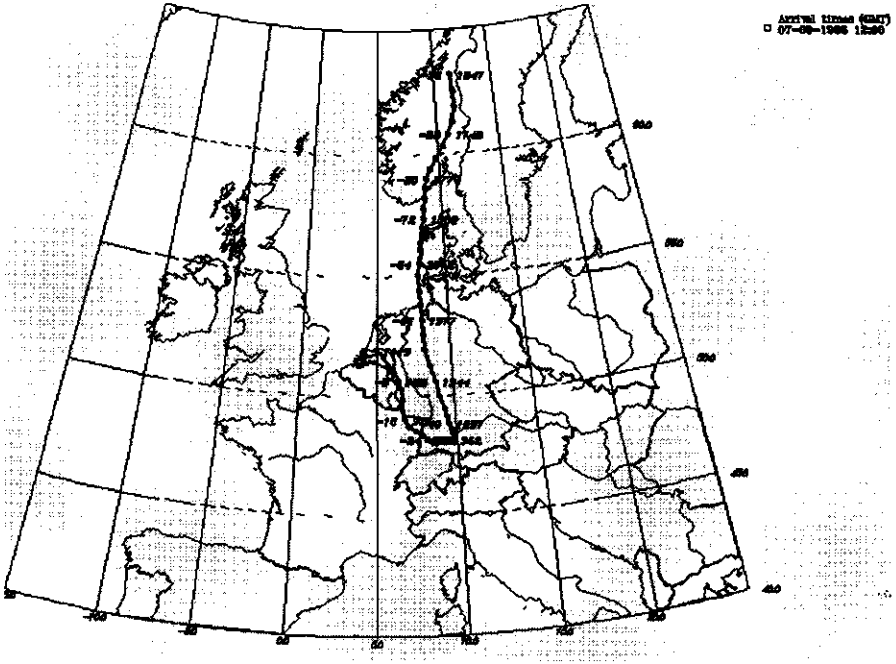

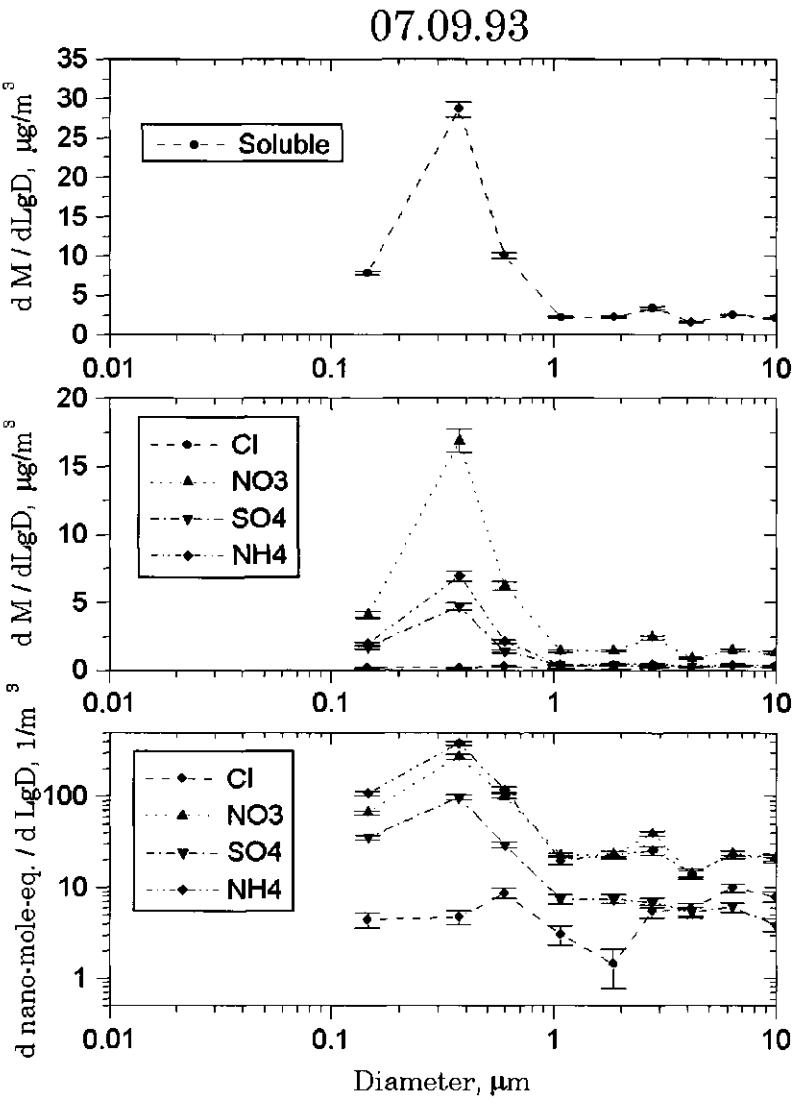
07.09.93
Soluble
Cl
NO3
SO4
NH4
d M / dLgD, µg/m3
d nano-mole-eq. / d LgD, 1/m3
Diameter, µm

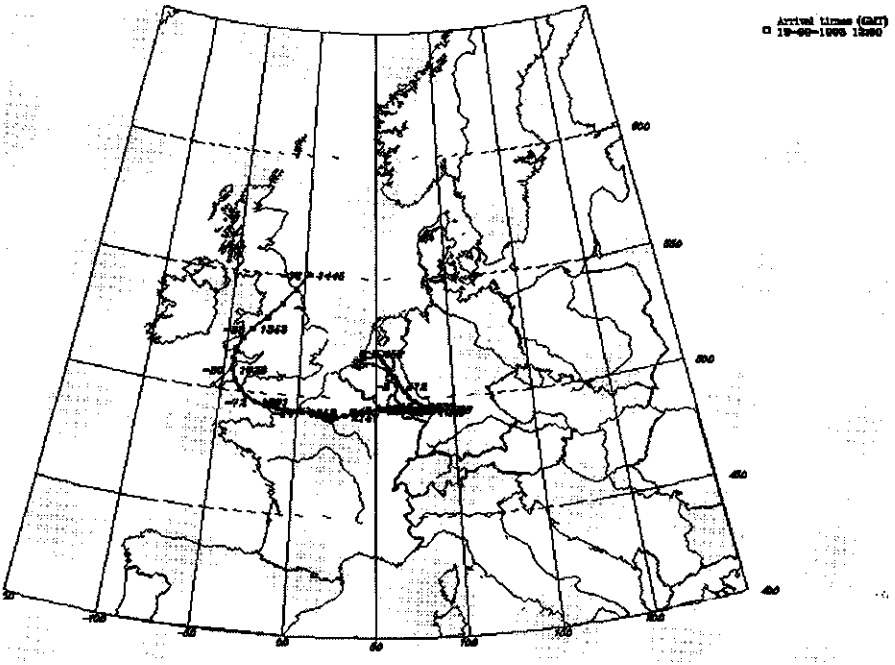

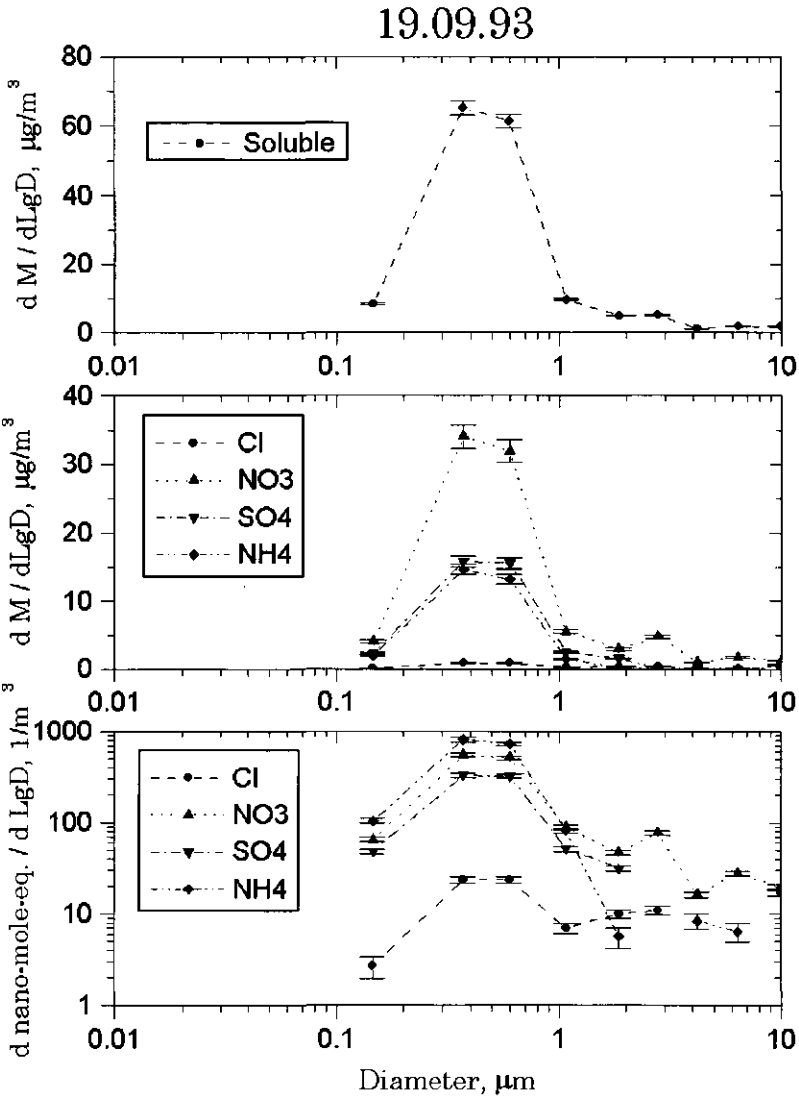
19.09.93
d M / dLgD, µg/m3
Soluble
Cl
NO3
SO4
NH4
d nano-mole-eq. / d LgD, 1/m3
Diameter, µm

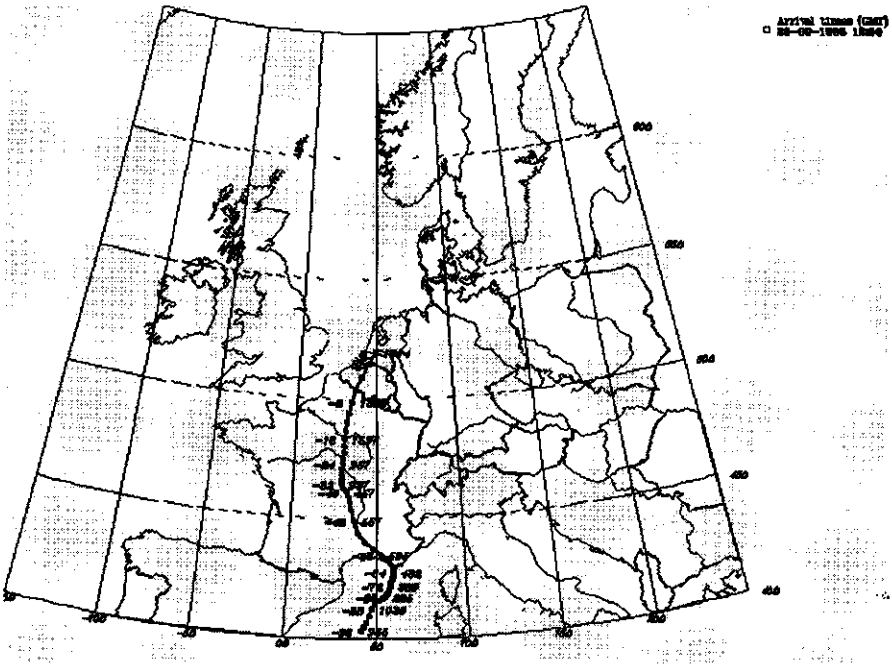

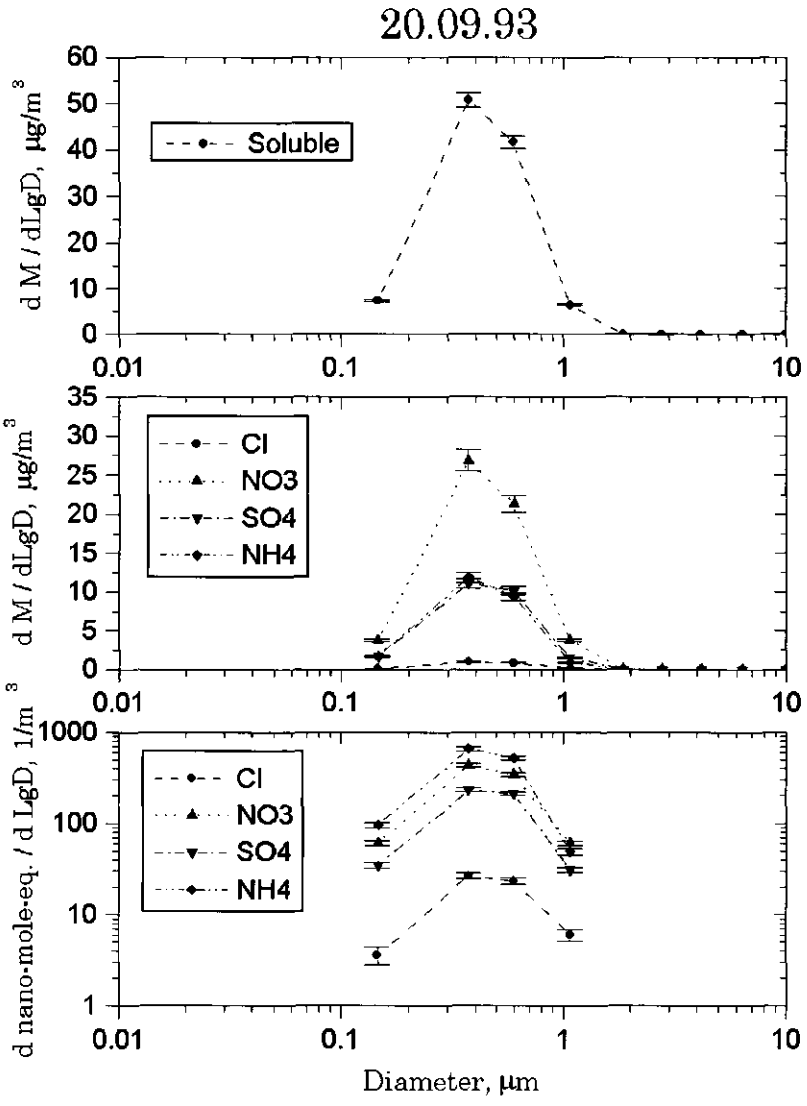
20.09.93
d M / dLgD, µg/m3
Soluble
Cl
NO3
SO4
NH4
d nano-mole-eq. / d LgD, 1/m3
Diameter, µm

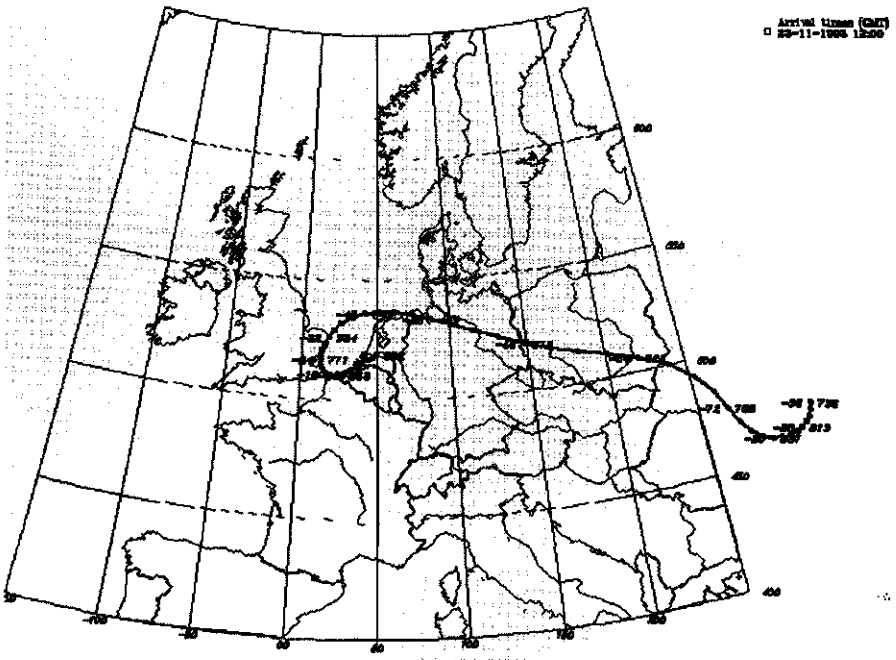

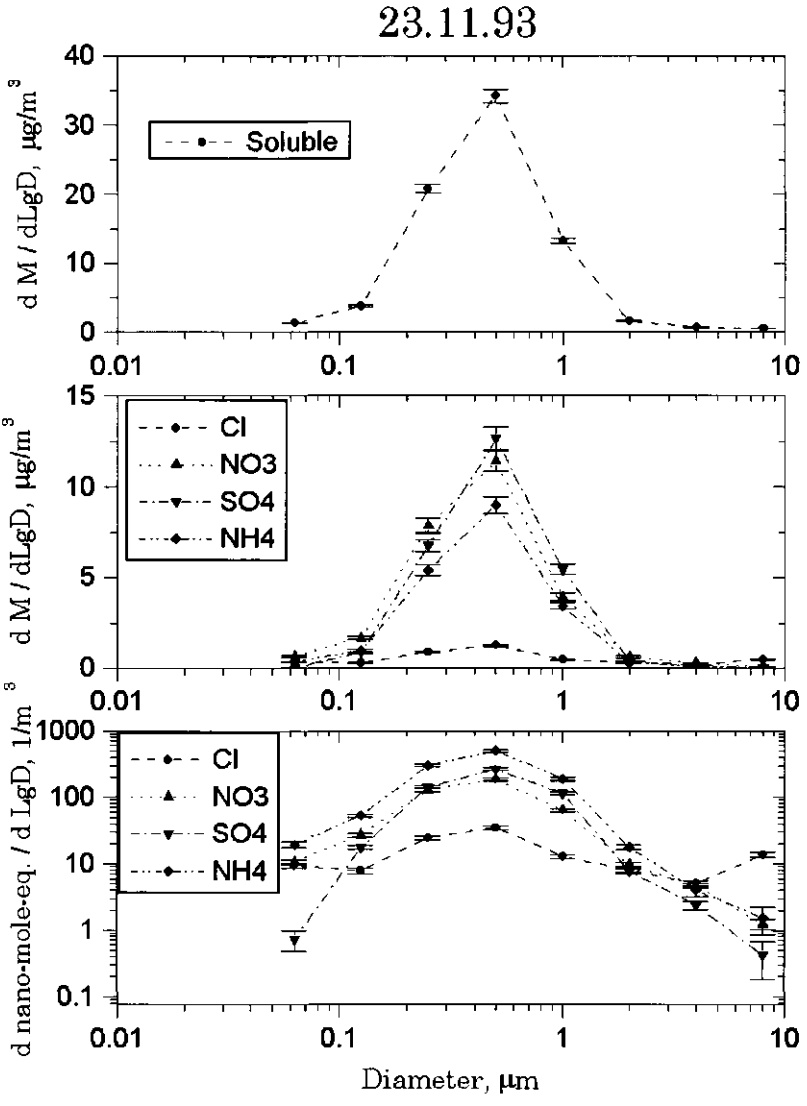
23.11.93
d M / dLgD, µg/m3
Soluble
Cl
NO3
SO4
NH4
d nano-mole-eq. / d LgD, 1/m3
Diameter, µm

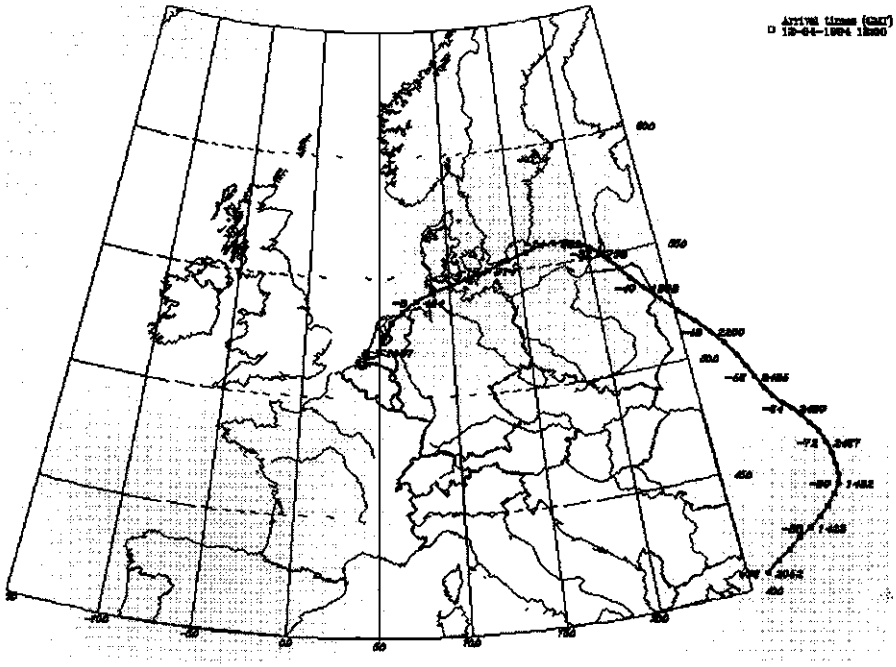

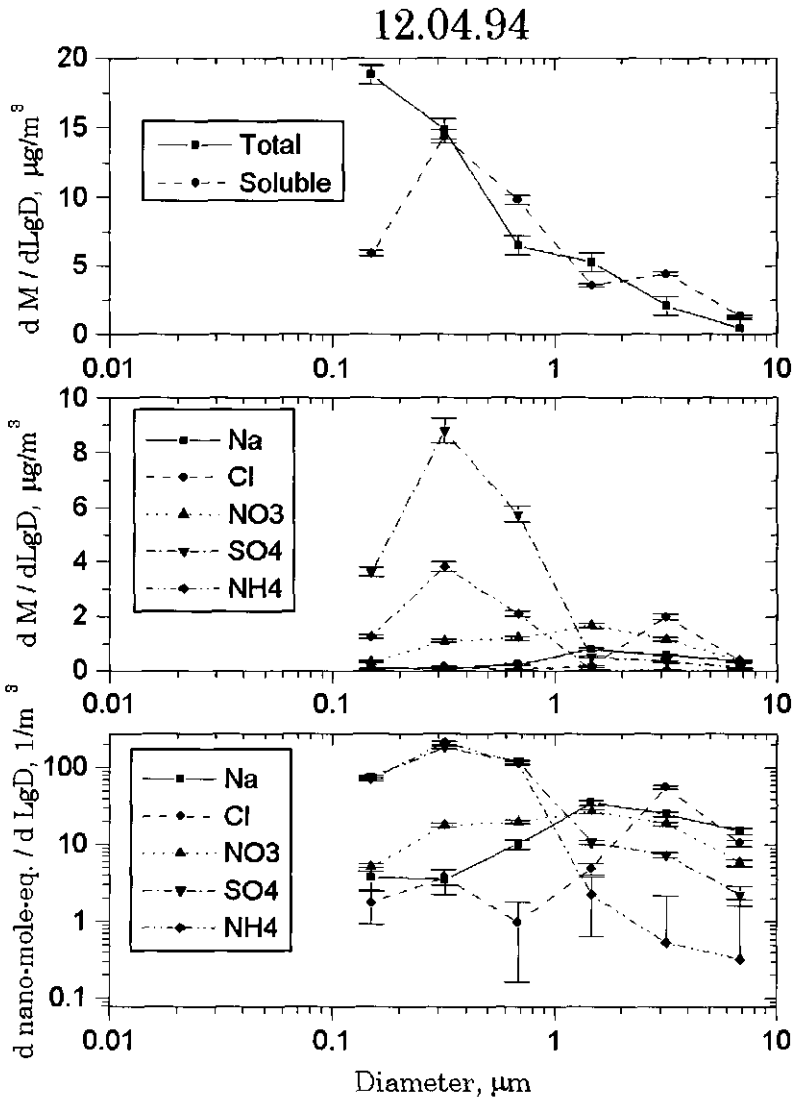
12.04.94
d M / dLgD, µg/m3
Total
Soluble
Na
Cl
NO3
SO4
NH4
d nano-mole-eq. / d LgD, 1/m3
Diameter, µm

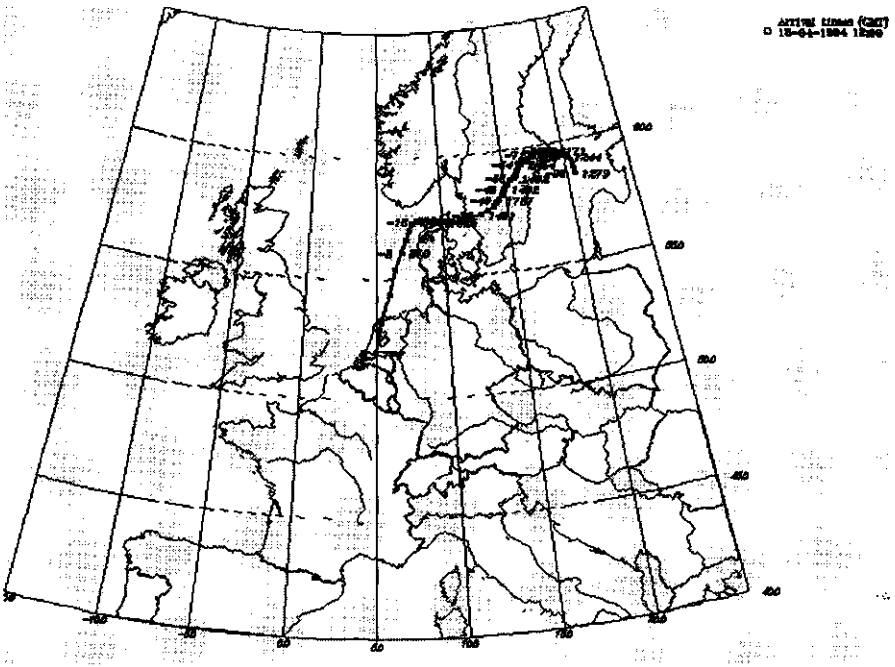

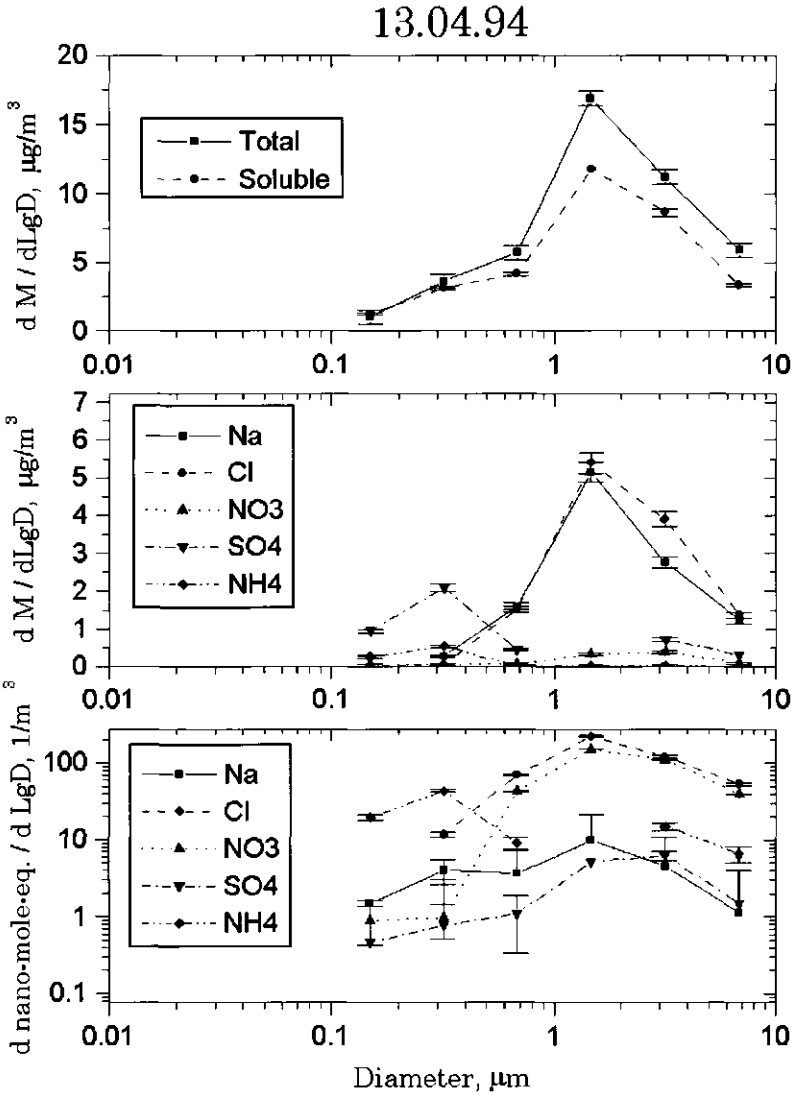
13.04.94
d M / dLgD, µg/m3
Total
Soluble
Na
Cl
NO3
SO4
NH4
d nano-mole-eq. / d LgD, 1/m3
Diameter, µm

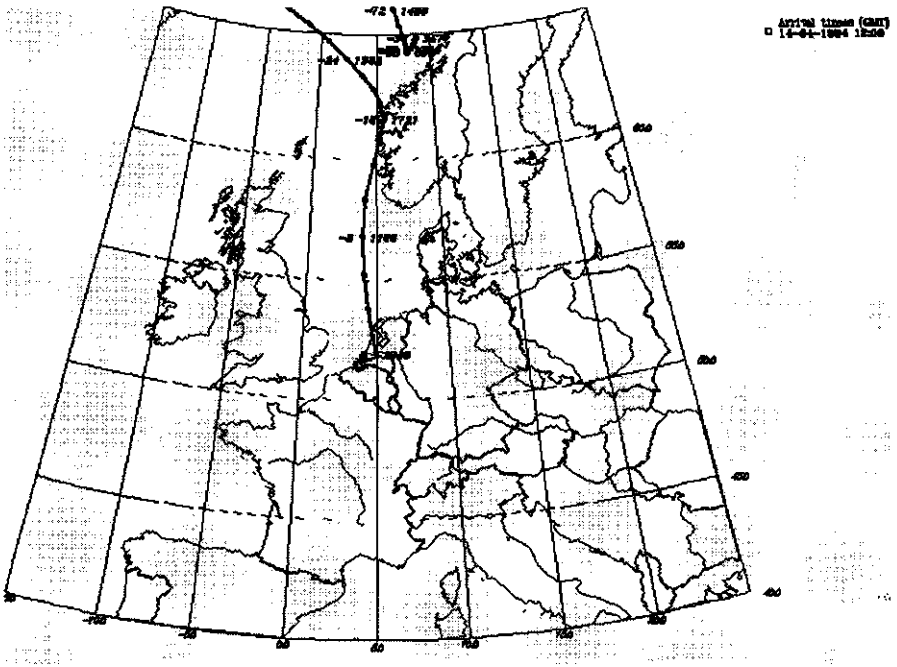

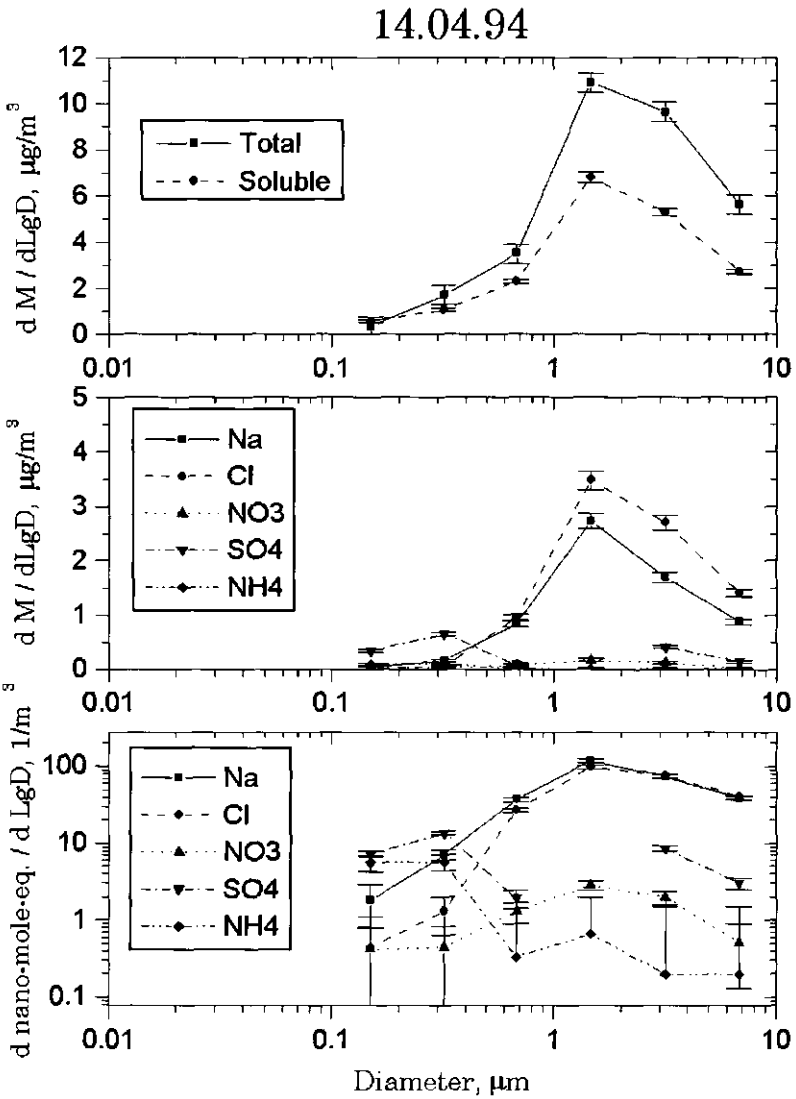
14.04.94
d M / dLgD, µg/m3
Total
Soluble
d M / dLgD, µg/m3
Na
Cl
NO3
SO4
NH4
d nano-mole-eq. / d LgD, 1/m3
Na
Cl
NO3
SO4
NH4
Diameter, µm

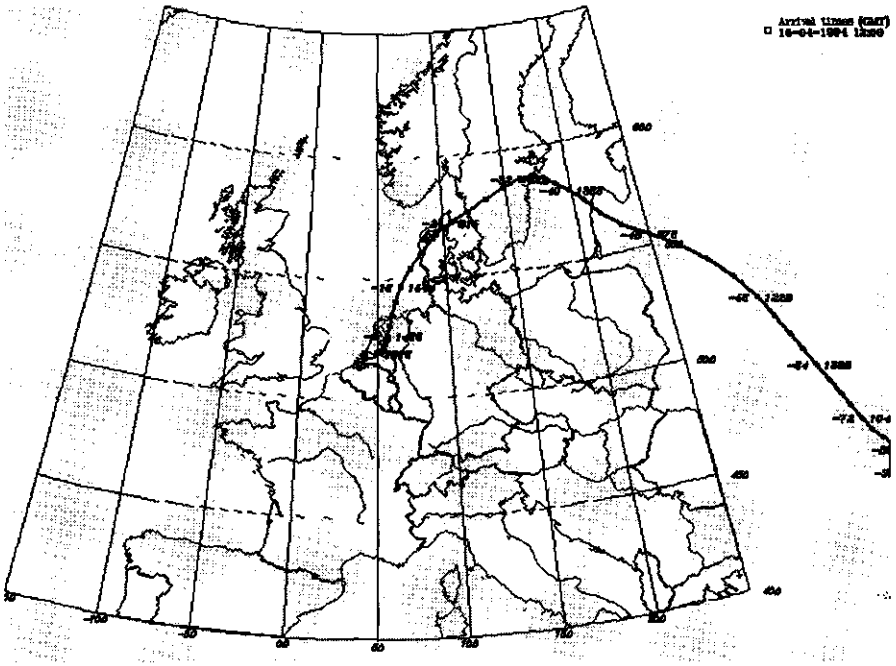

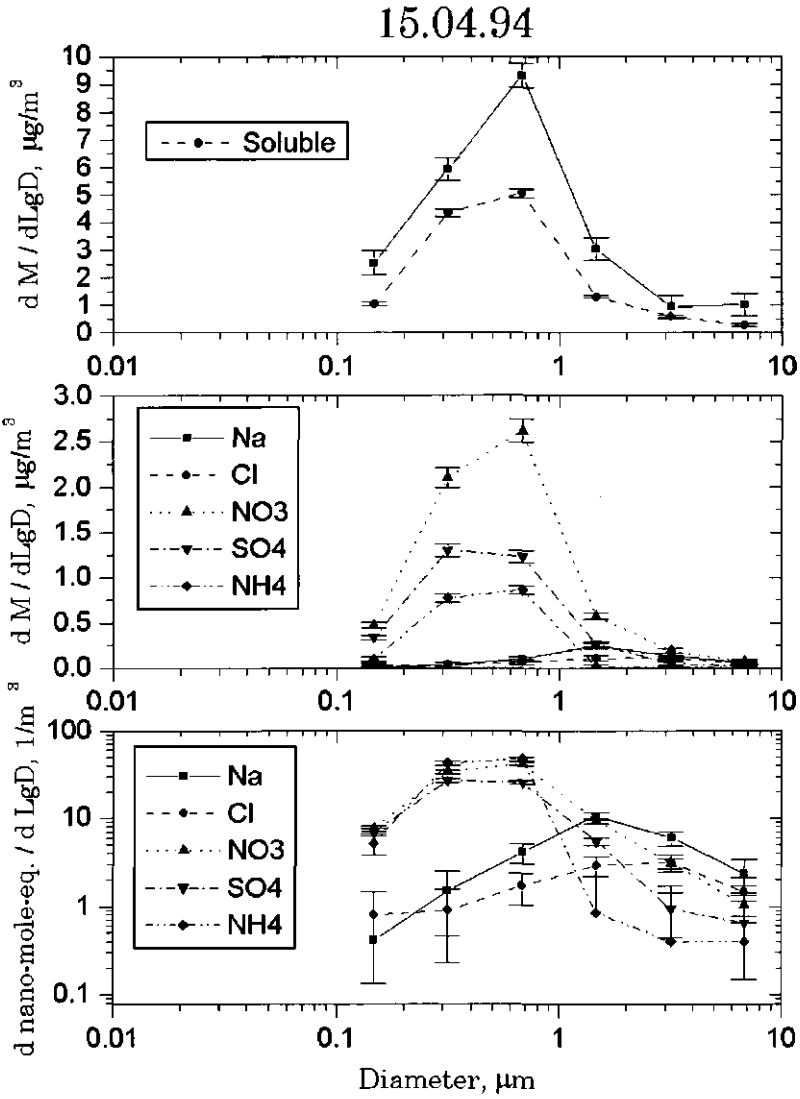
15.04.94
d M / dLgD, µg/m3
Soluble
d M / dLgD, µg/m3
Na
Cl
NO3
SO4
NH4
d nano-mole-eq. / d LgD, 1/m3
Na
Cl
NO3
SO4
NH4
Diameter, µm

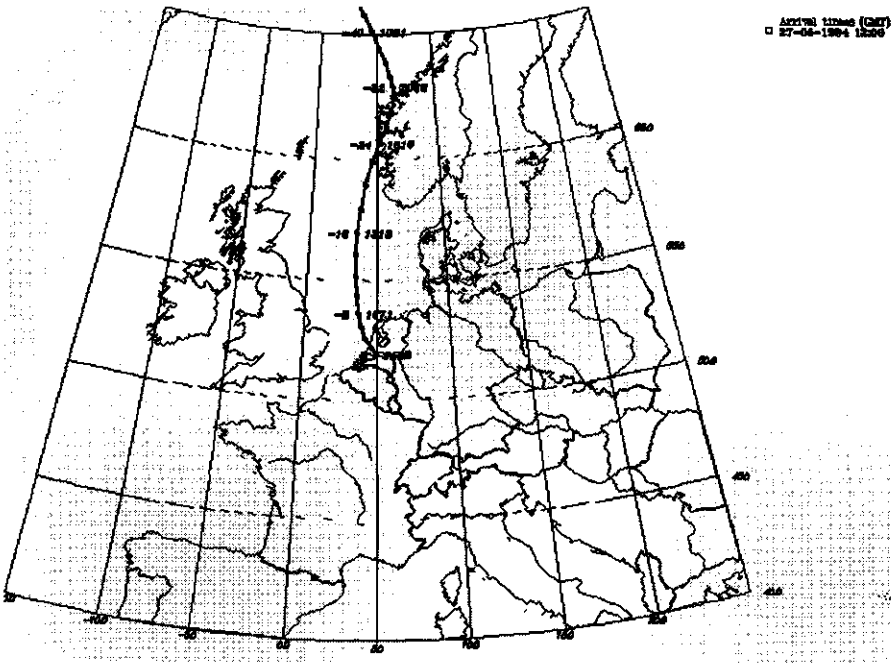

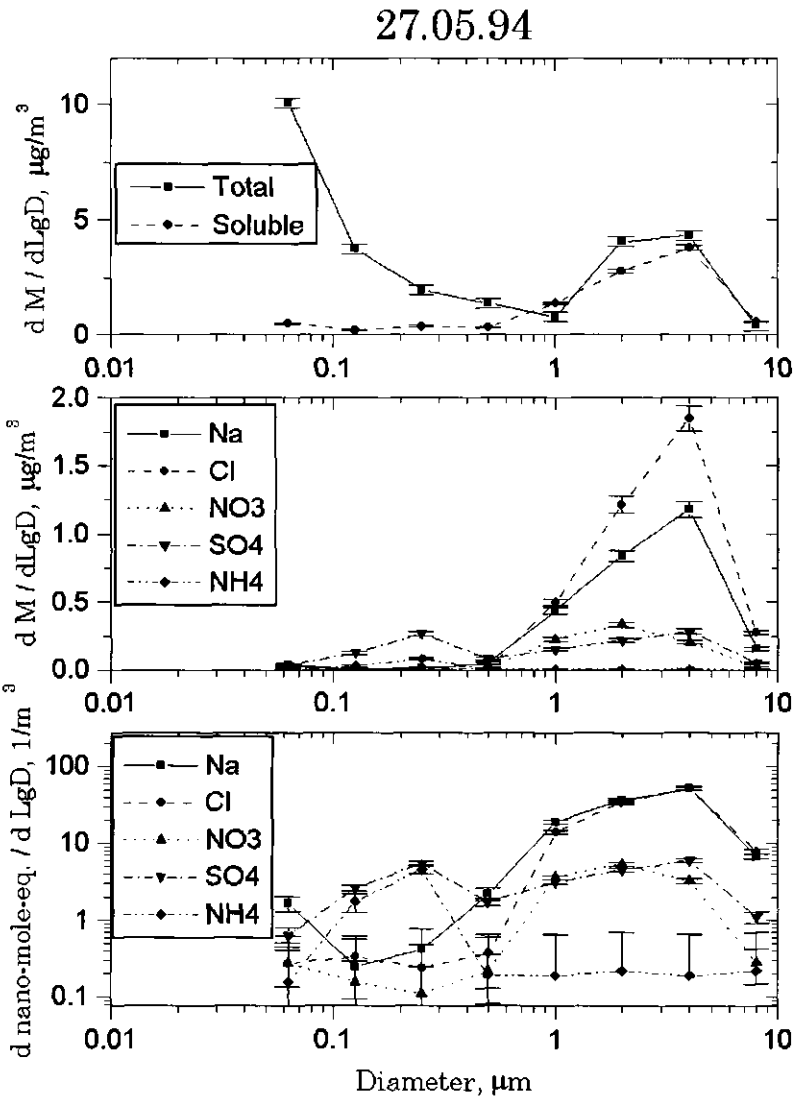
27.05.94
d M / dLgD, µg/m³
Total
Soluble
d M / dLgD, µg/m³
Na
Cl
NO3
SO4
NH4
d nano-mole-eq. / d LgD, 1/m³
Na
Cl
NO3
SO4
NH4
Diameter, µm

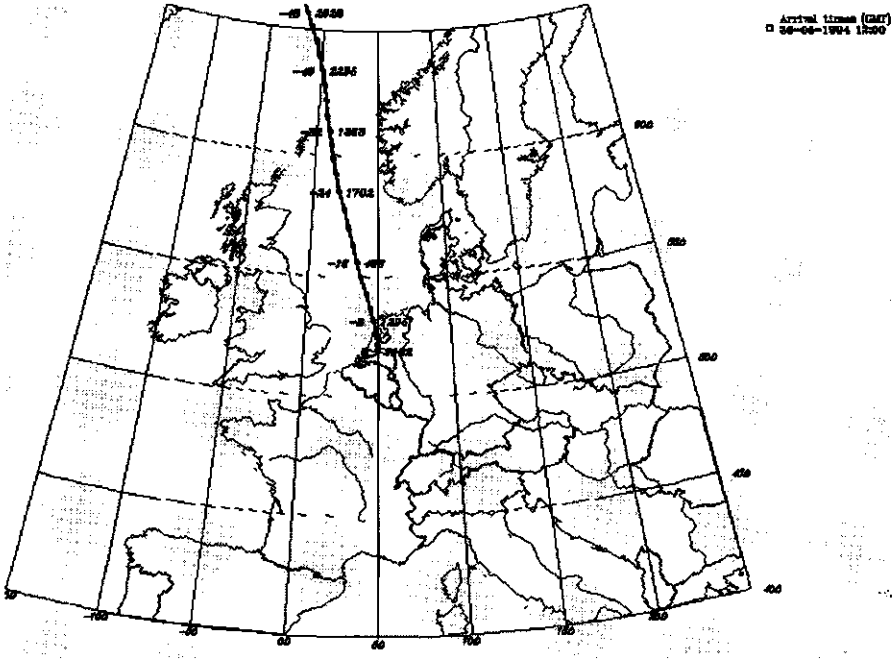
Arrival times (GMT)
26-06-1994 12:00

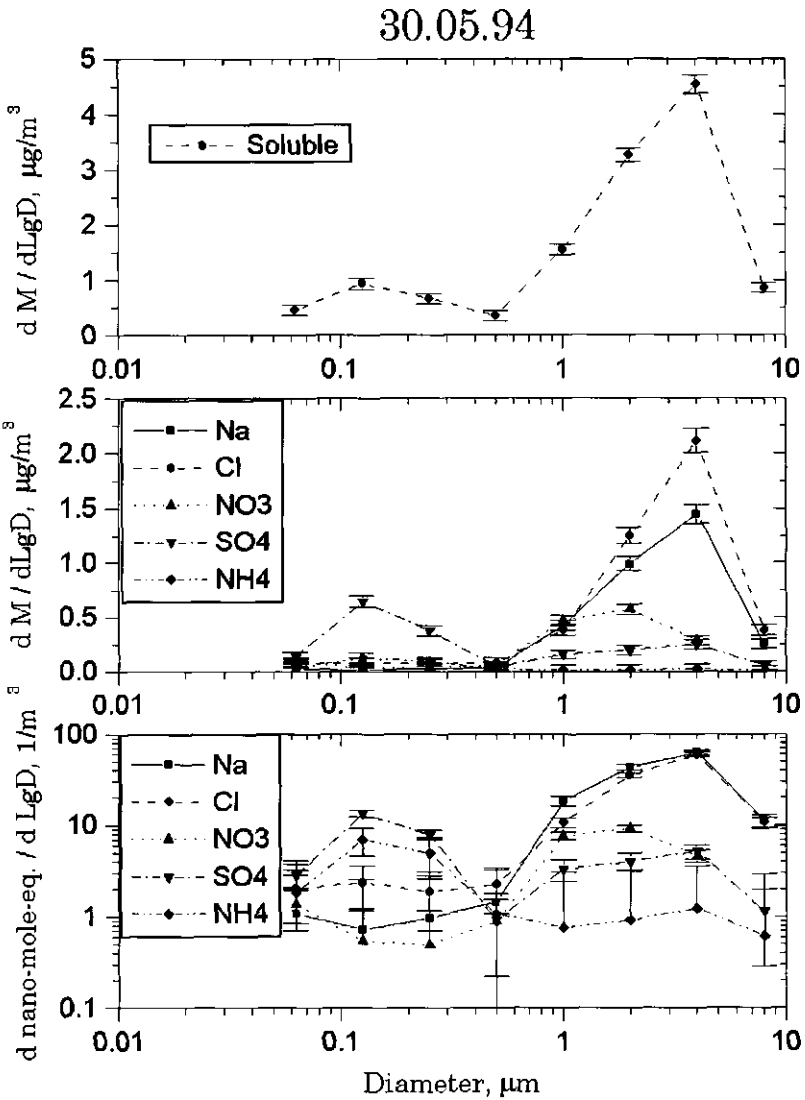
30.05.94
Soluble
d M / dLgD, µg/m3
Na
Cl
NO3
SO4
NH4
d nano-mole-eq. / d LgD, 1/m3
Diameter, µm

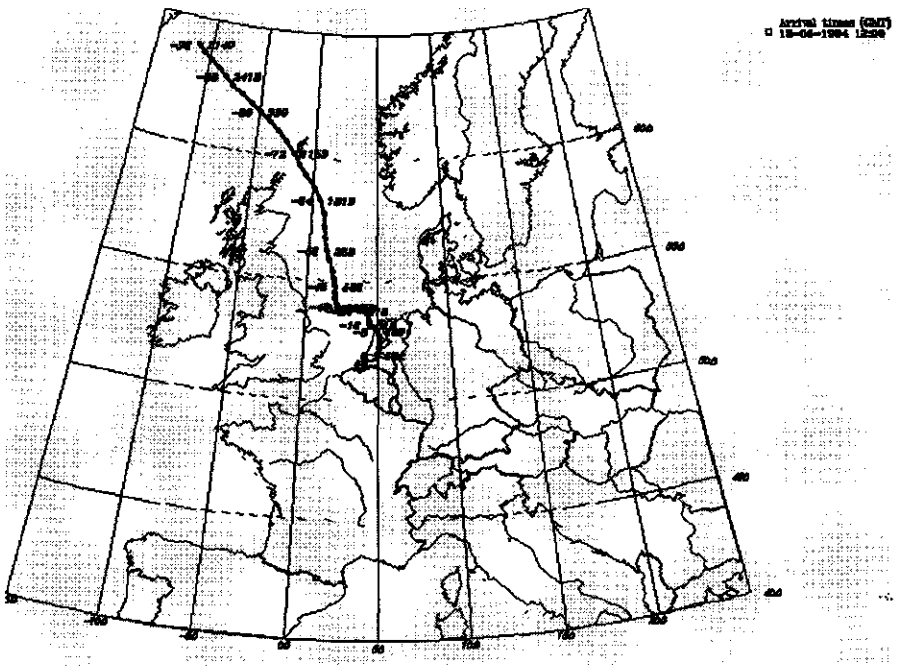

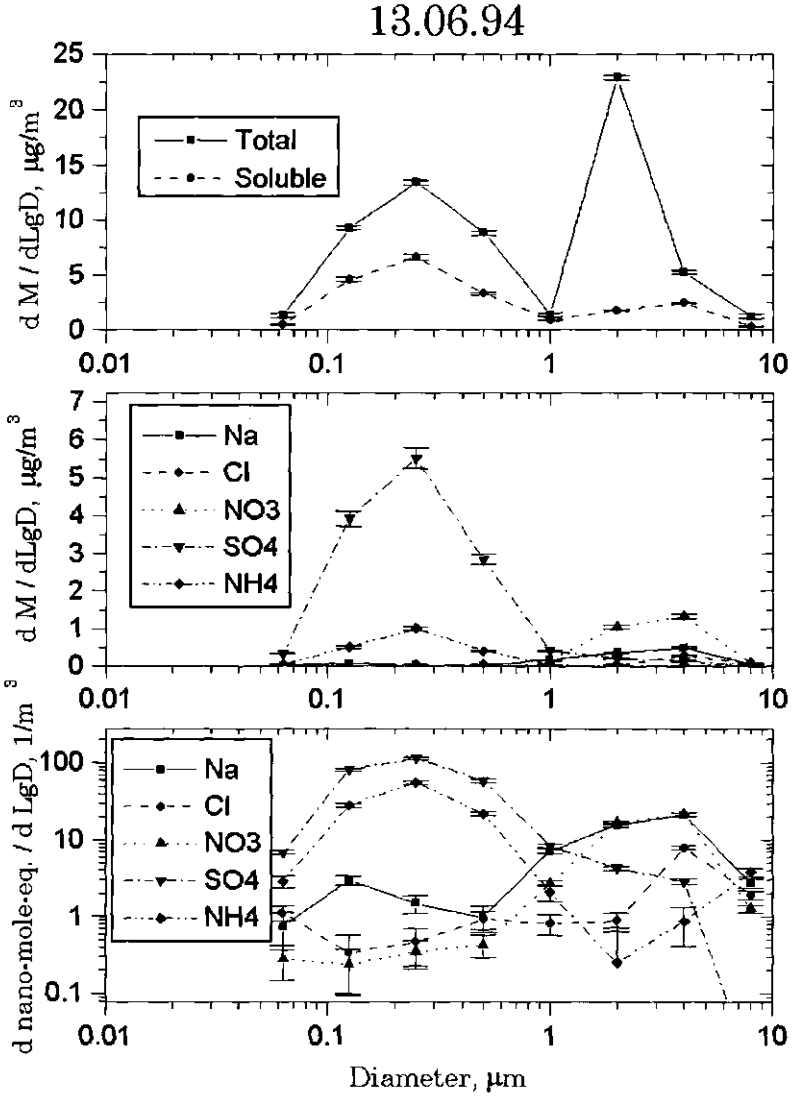
13.06.94
d M / dLgD, µg/m3
Total
Soluble
Na
Cl
NO3
SO4
NH4
d nano-mole-eq. / d LgD, 1/m3
Diameter, µm

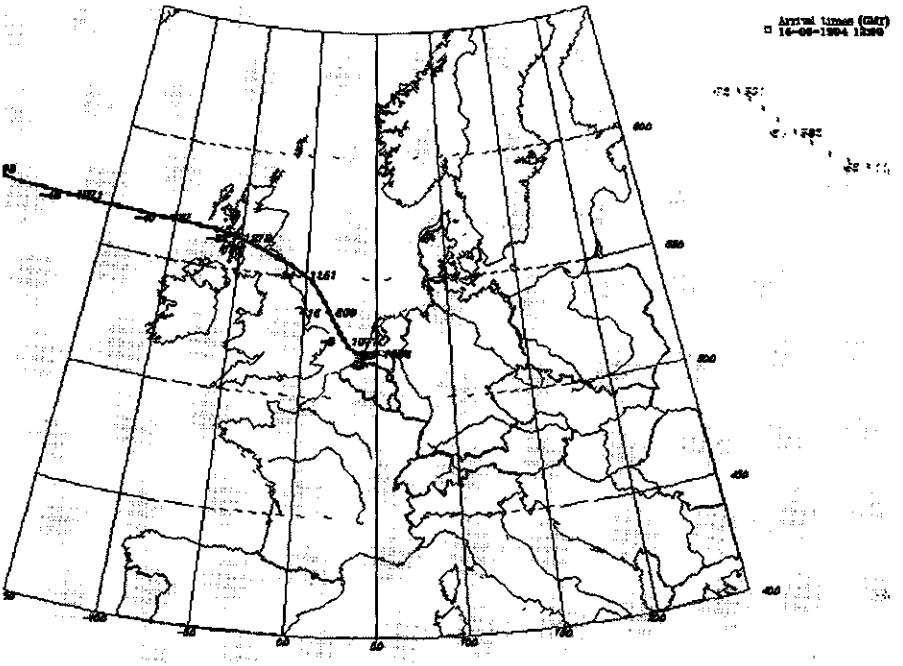

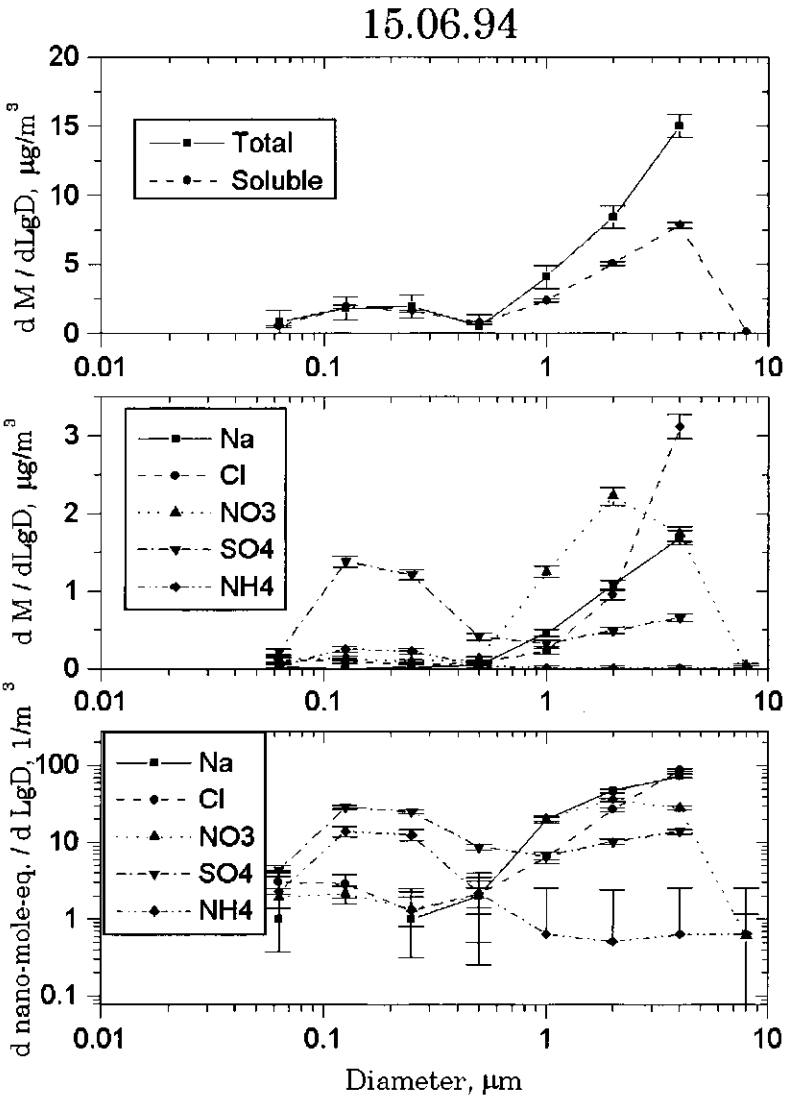
15.06.94
d M / dLgD, µg/m3
Total
Soluble
Na
Cl
NO3
SO4
NH4
d nano-mole-eq. / d LgD, 1/m3
Diameter, µm

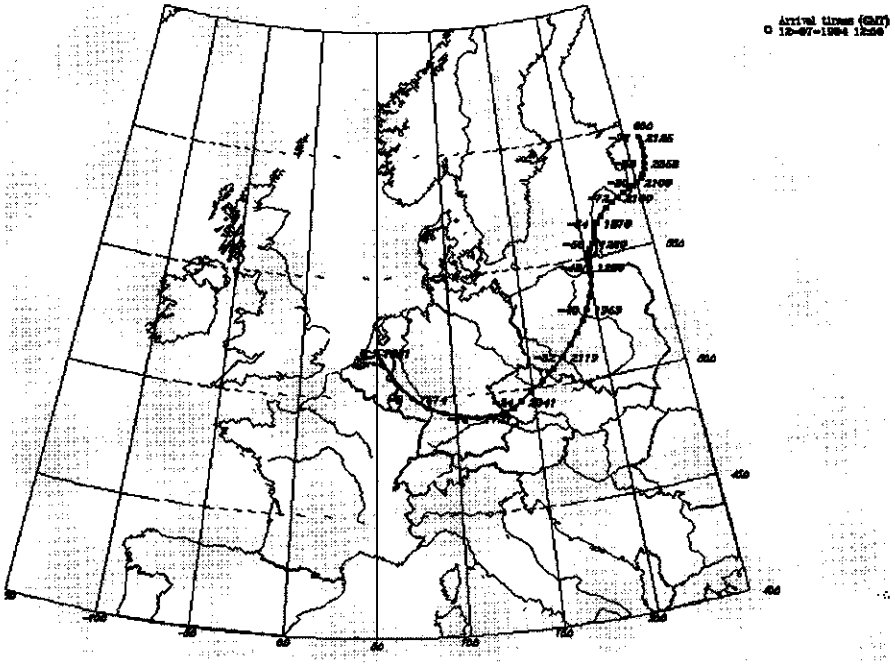
Arrival times (GMT)
0 12-07-1984 12:50

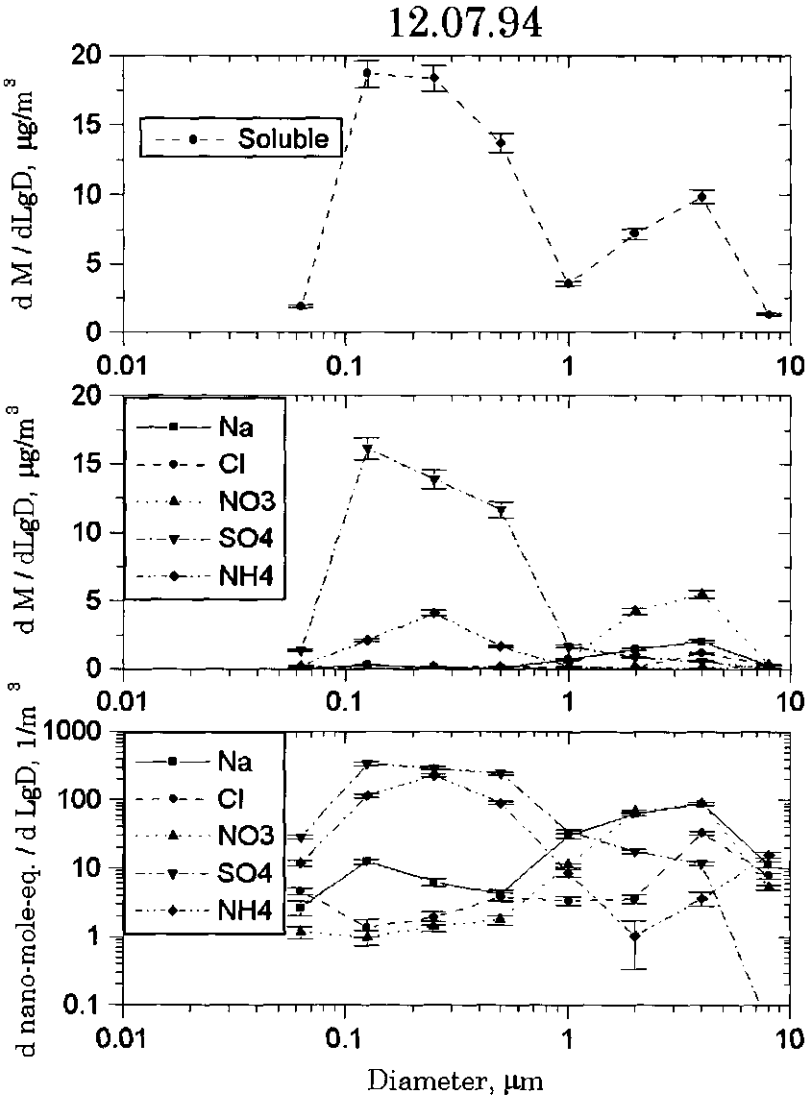
12.07.94
d M / dLgD, µg/m³
Soluble
Na
Cl
NO3
SO4
NH4
d nano-mole-eq. / d LgD, 1/m³
Diameter, µm

Appendix 2

Effect of latent heat transfer on radius change rate

In the case of steady-state mass and heat transfer to a growing (or evaporating) droplet the radius change rate, $y = dr/dt$, is:

$$y = \frac{D_v M_w}{r \rho R}\left(\frac{p_\infty}{T_\infty} - \frac{p_r(y)}{T_r(y)}\right) \qquad \text{A2.1}$$

in which r is the droplet radius, D_v is the diffusion coefficient of water vapor, ρ and M_w are the (liquid) density and the molecular weight of water. R is the gas constant, p is the vapor pressure and T is temperature. The subscripts r and ∞ denote parameters describing the droplet and the environment, respectively. The dependence of the vapor pressure, p_r, at the droplet surface on the radius change rate, y, comes from its dependence on temperature, which is [*Pruppacher and Klett*, 1978]:

$$T_r = T_\infty + \frac{L_h \rho r}{k} y \qquad \text{A2.2}$$

in which L_h is the latent heat and k is the thermal conductivity of moist air.

Applying of Eq.A2.1 for calculations of steady-state radius change rate is probleamtic because this equation is implicit for y. A number of approximate analytical solutions of Eq.A2.1 were reported in the literature [*Mason*, 1971; *Pruppacher and Klett*, 1978; *Hänel*, 1987;

Rogers and Yau, 1989]. These approximate solutions are based on applying the Clausius-Claypeiron equation to express the vapor pressure at the droplet surface, $p_r(T(y_0))$, in terms of vapor pressure above the droplet surface at the temperature of the environment, T, with the consequent linearization of the dependence of the saturated vapor pressure on temperature [*Pruppacher and Klett*, 1978]:

$$p_r(T(y_0)) = p_r(T_0) \exp\left(\frac{L_h M_w}{R} \frac{(T(y_0) - T_0)}{T_0 T(y_0)}\right) \approx$$

$$\approx p_r(T_0)\left(1 + \frac{L_h M_w}{R} \frac{L_h \rho r}{k} \frac{y}{T_0^2}\right) \qquad \text{A2.3}$$

in which T_0 is the temperature of the environment.

Here it will be shown, using the same approximations as used in the above mentioned approximate solutions of Eq.A2.1, that the radius change rate in the case of coupled mass and heat transfer is slowed by a constant factor relatively to the radius change rate, y_0, which is calculated without accounting for the heat transfer.

The growth rate is found by searching zeroes of a function derived from equation A2.1:

$$f(y) = y - \frac{D_v M_w}{r \rho R}\left(\frac{p_\infty}{T_\infty} - \frac{p_r(y)}{T_r(y)}\right) \qquad \text{A2.4}$$

This function is fairly linear at small y (when the pressure difference between the droplet surface and the environment is small, the assumption which is required for the linearization used in Eq.A2.3), which can be shown using the same linearization as in Eq.A2.3:

$$f(y) \approx y - \frac{D_v M_w}{r \rho R}\left[\frac{p_0}{T_0} - \frac{p_r(T_0)}{T_0}\left(1 + \frac{L_h M_w}{R} \frac{L_h \rho r}{k} \frac{y}{T_0^2}\right)\right] \qquad \text{A2.5}$$

Here, similarly to Eq.A2.3, an approximation $T_r(y) \approx T_0$ was done. After simple arithmetics Eq.A2.5 becomes:

$$f(y) \approx A\,y - y_0 \qquad \text{A2.6}$$

in which y_0 is the radius change rate if there is no latent heat transfer:

$$y_0 = \frac{D_v M_w}{r \rho R}\left(\frac{p_0}{T_0} - \frac{p_r(T_0)}{T_0}\right) \qquad \text{A2.7}$$

A is a constant which depends on ambient temperature and the saturation ratio above the particle surface, s_r:

$$A = 1 + s_r \frac{D_v M_w^2 L_h^2 p_{sat}(T_o)}{k R^2 T_0^3} \qquad \text{A2.8}$$

The actual radius change rate with the latent heat transfer accounted for is found by serching zeroes of Eq.A2.6. Sinse this equation is linear, the solution is straightforward:

$$y = \frac{y_0}{1 + s_r C} \qquad \text{A2.9}$$

in which C is a constant that depends only on the temperature of the environment:

$$C = \frac{D_v M_w^2 L_h^2 p_{sat}(T_o)}{k R^2 T_0^3} \qquad \text{A2.10}$$

Equation A2.9 implies that the radius change rate of a particle of any size at a given relative humidity is slowed down due to the latent heat transfer by a constant factor, which depends only on the temperature of the environment. At 0°C the coefficient C in Eq.A2.9 is about 0.7, at 10°C -- 1.2 and at 20°C it is 2.1.

Appendix 3

Weather maps

Weather maps for the days on which cloud activation experiments were carried out were provided by the Royal Dutch Meteorological Institute (KNMI).

VRIJDAG 26 JUNI 1992 1200 UTC.

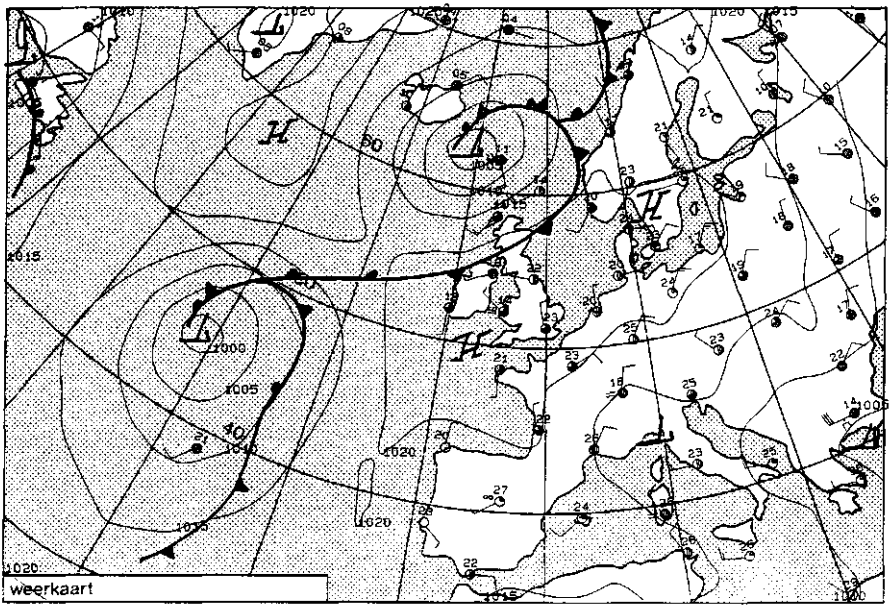

MAANDAG 29 JUNI 1992 1200 UTC.

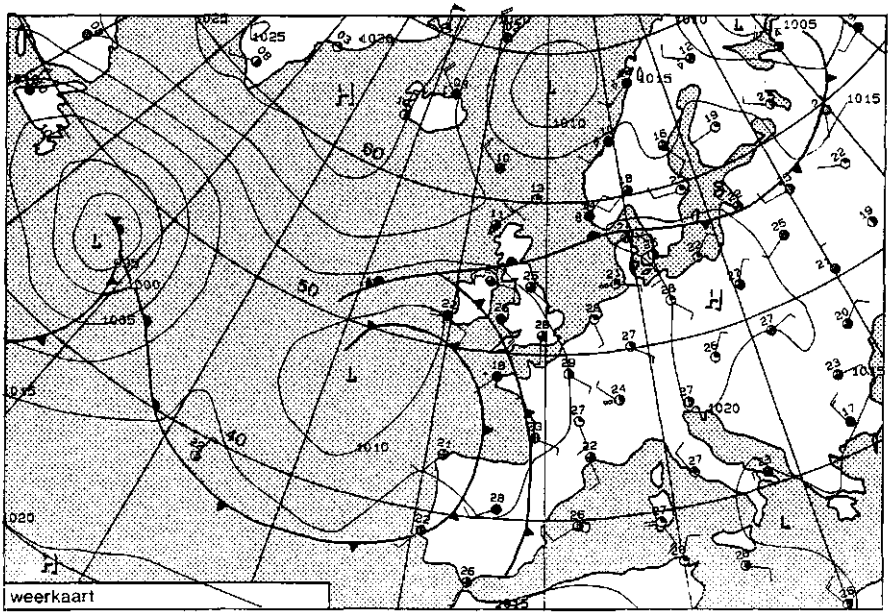

DINSDAG 30 JUNI 1992 1200 UTC.

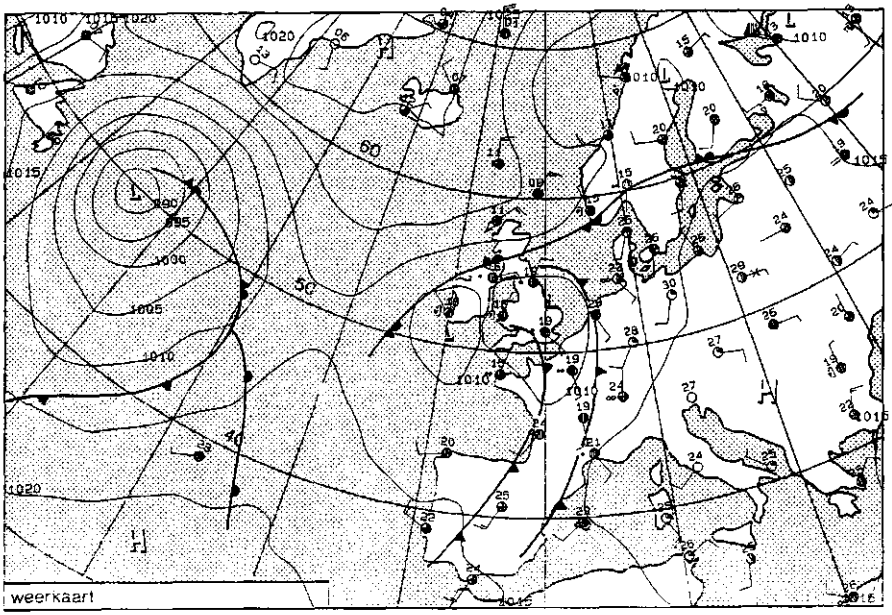

WOENSDAG 1 JULI 1992 1200 UTC.

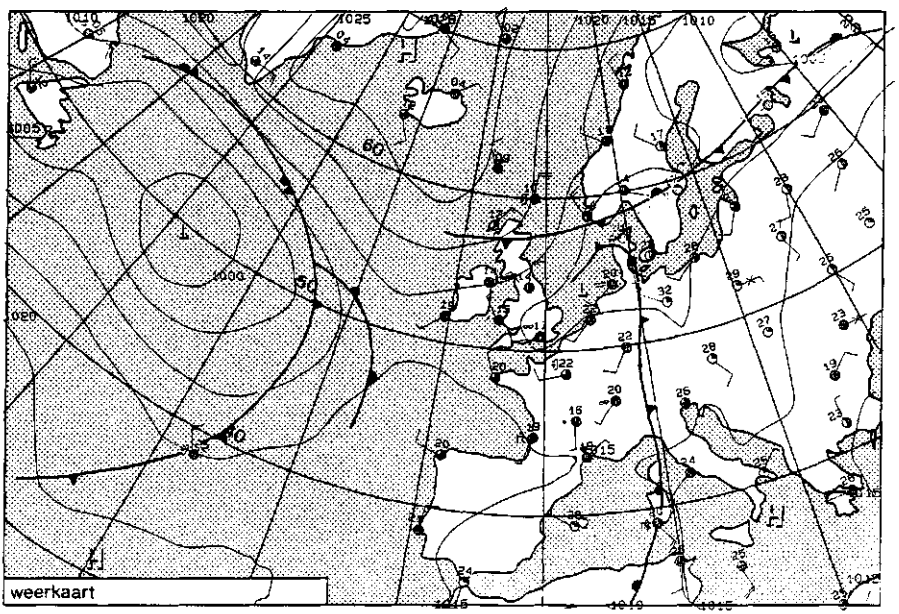

DONDERDAG 02 JULI 1992 1200 UTC.

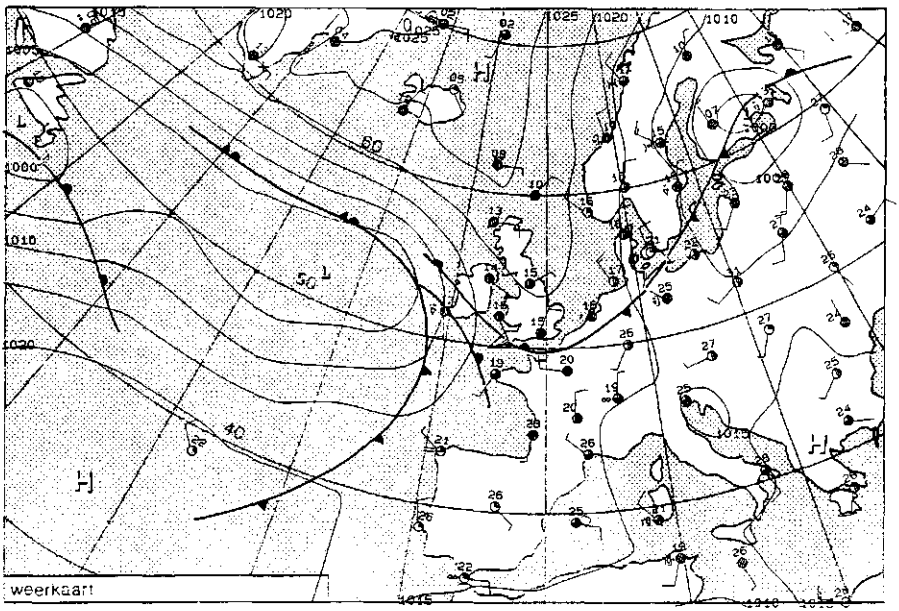

VRIJDAG 3 JULI 1992 1200 UTC.

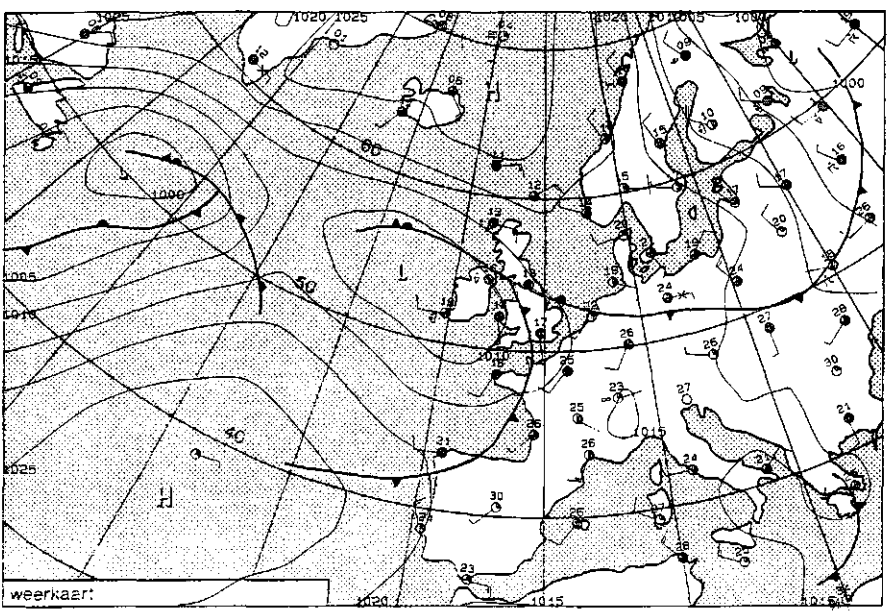

MAANDAG 6 JULI 1992 1200 UTC

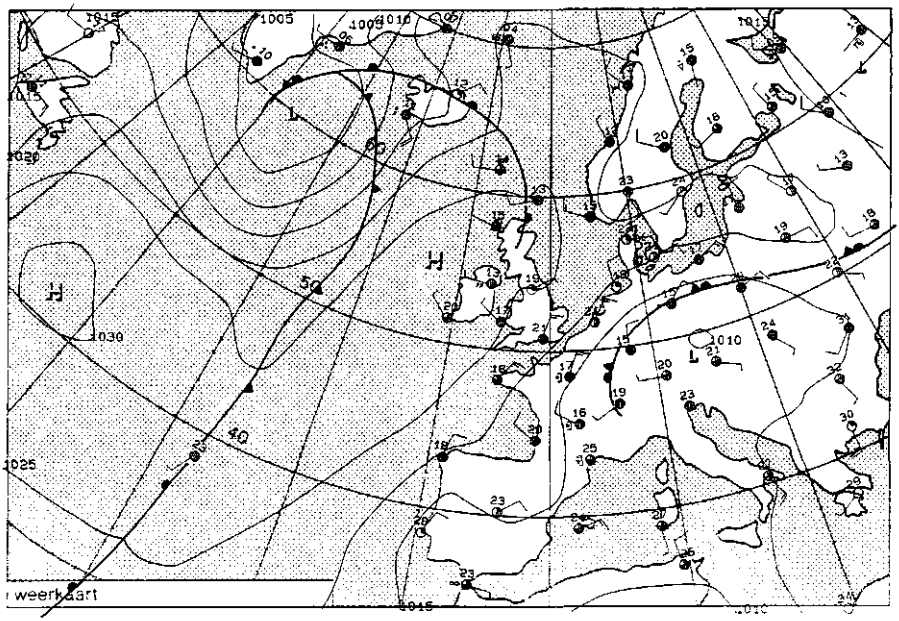

MAANDAG 5 JULI 1993 1200 UTC

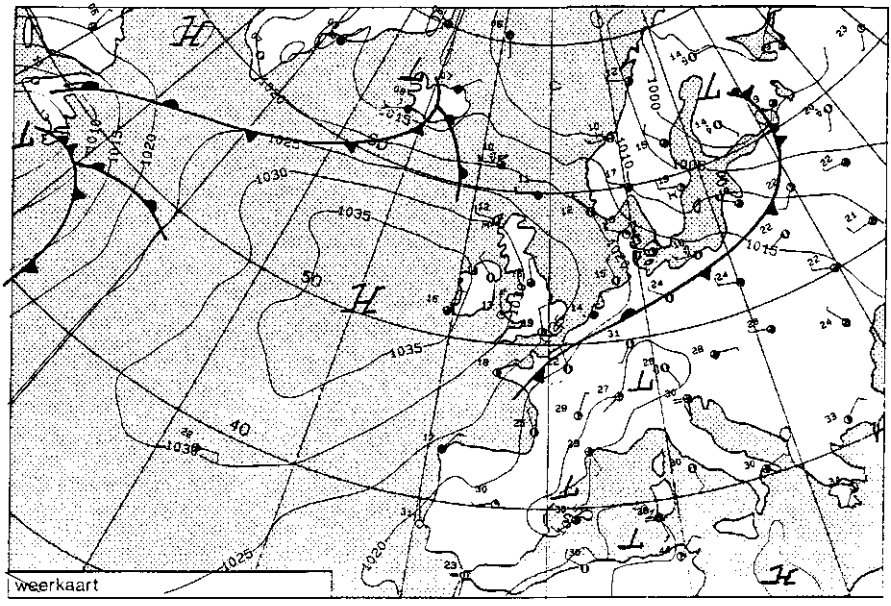

DINSDAG 6 JULI 1993 1200 UTC

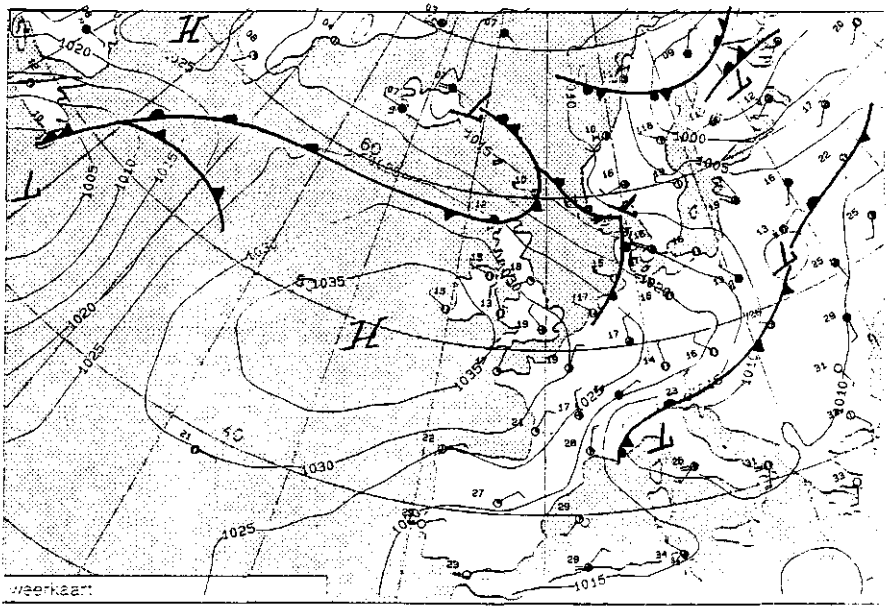

DONDERDAG 8 JULI 1993 1200 UTC

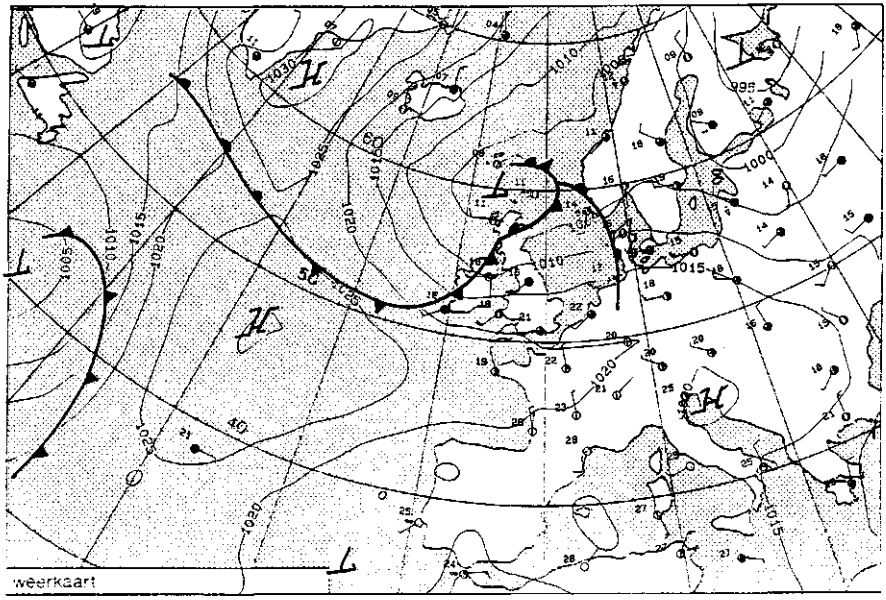

DINSDAG 12 APRIL 1994 1200 UTC.

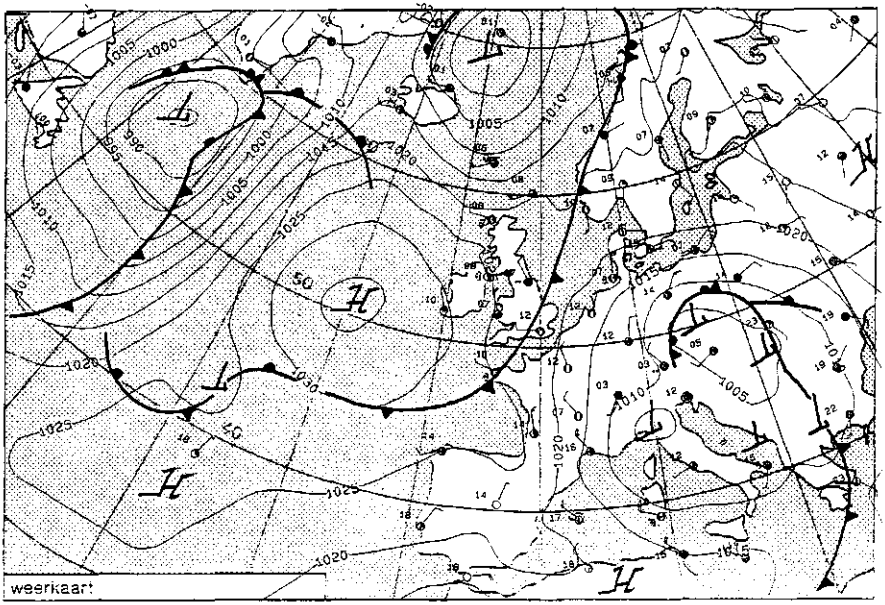

WOENSDAG 13 APRIL 1994 1200 UTC.

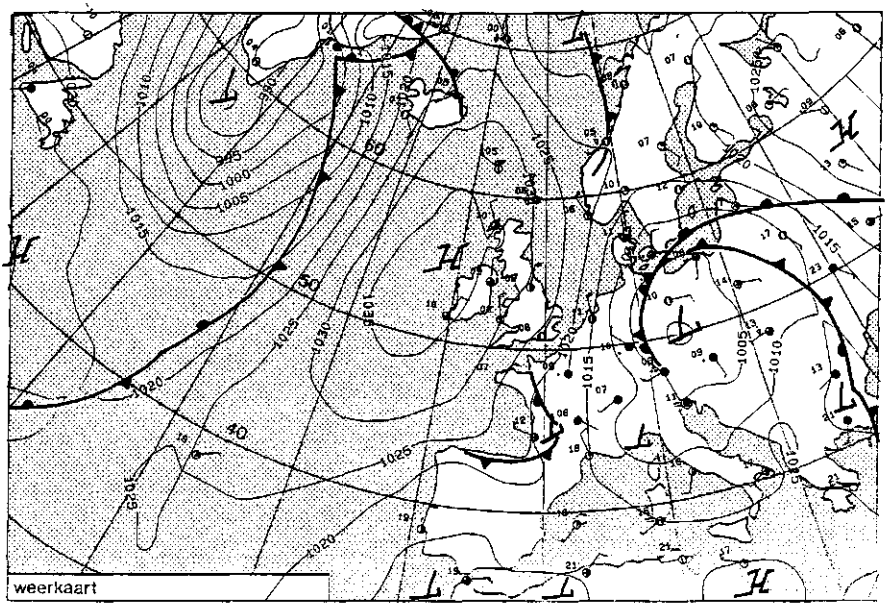

DONDERDAG 14 APRIL 1994 1200 UTC

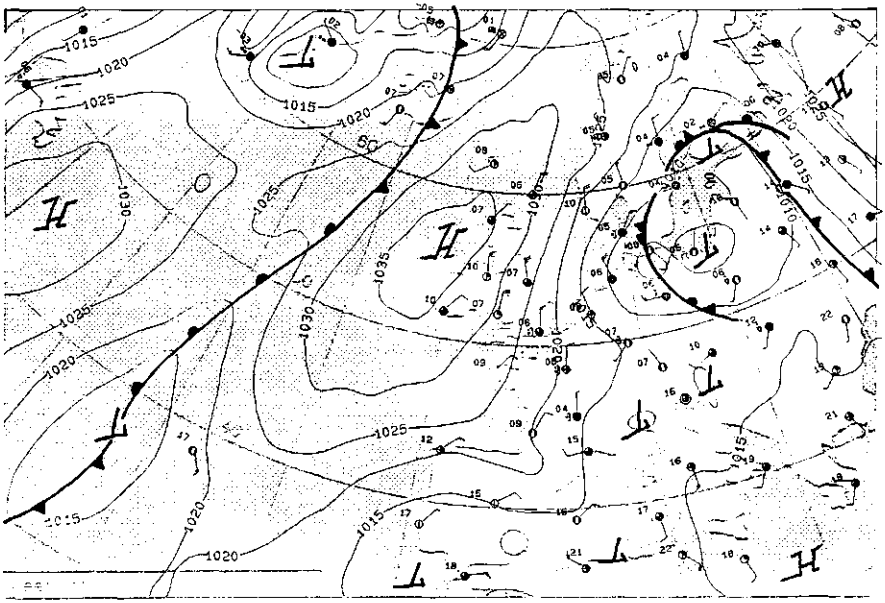

VRIJDAG 15 APRIL 1994 1200 UTC

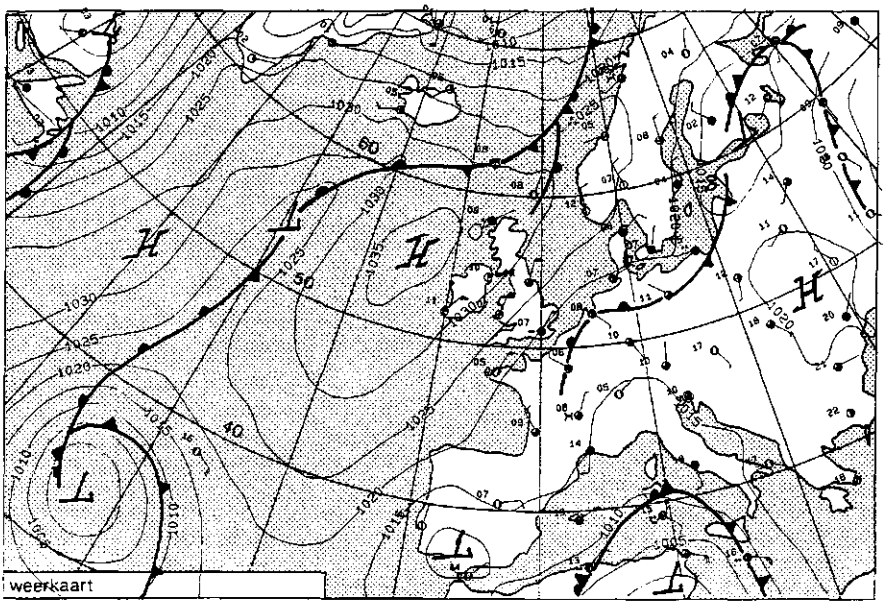

VRIJDAG 10 JUNI 1994 1200 UTC

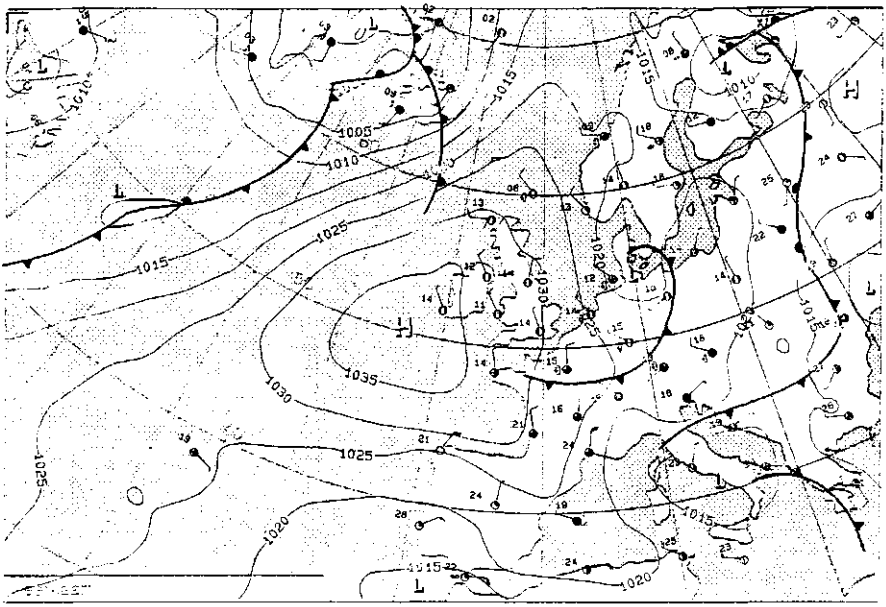

WOENSDAG 5 OKTOBER 1994 1200 UTC

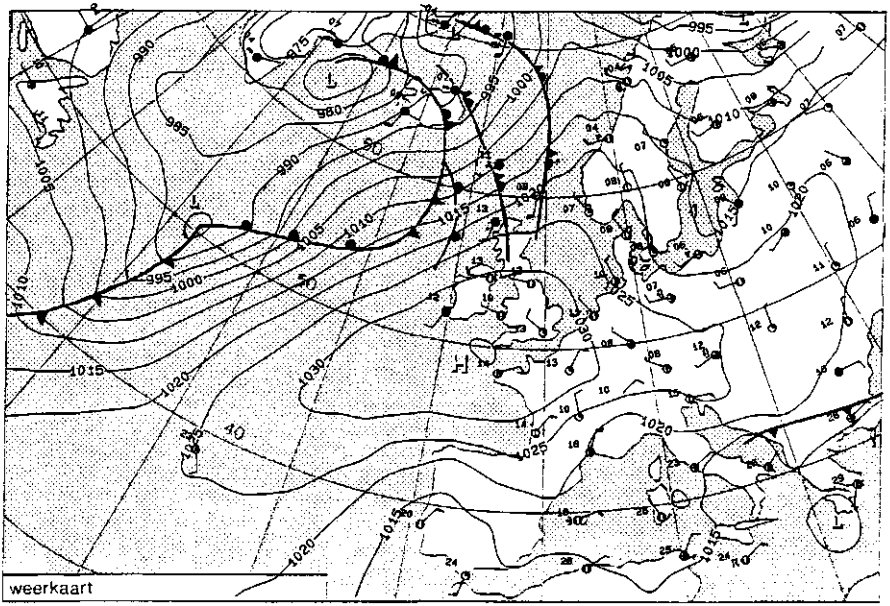

Acknowledgments

The work on this thesis would have never been possible without the help of numerous people all of whom I wish to thank here for their valuable support. My special thanks go to my co-promotor and direct supervisor Harry ten Brink who learned me how to approach scientific problems, to carry out and report the research in the best possible way. I also wish to thank my promotor Sjaak Slanina for the numerous discussions and advise to address the scientific issues from a broader perspective, all of which helped me to shape up this thesis to its present form. I am very grateful to Stephen Schwartz for the very valuable comments and suggestions to the thesis and the advise on how to improve my writing style. The success of the cloud chamber measurements would not have been possible without the practical assistance from Gerard Kos, who has also provided a large part of the impactor data summarized in this thesis. I am grateful to Axel Berner and Christian Kruisz for performing impactor measurements during cloud chamber experiments with ambient aerosol. I am very thankful to Paul Wyers, René Otjes, Anita Wayers-IJpelaan, Piet Jongejan, Pauline Dougle and Pavel Mikuska for their contribution to the development and testing of the SJAC. I wish to thank Alex Vermeulen for his help to solve my programming questions and maintaining the operating system on my PC. I would like to thank the whole of the Environmental Research group for the very friendly atmosphere which made my work here a very pleasant experience.

I am very grateful to my parents, my wife Irina and our children, Nikita and Katja for their love, support and help in everyday life.

Curriculum vitae

5 October 1968	born in Novokuznetsk
June 1985	graduated form the Novosibirsk physics and mathematics high school
1985 - 1992	study at the Novosibirsk State University at the Natural Sciences Department (chemistry and biology)
1987 - 1989	military service
1992	diploma cum laude M.Sc. in chemistry with physical chemistry as a main subject
1991 - present	Netherlands Energy Research Foundation (ECN).